

**SYMBIOTIC HOLLOW FIBER MEMBRANE  
PHOTOBIOREACTOR FOR MICROALGAL GROWTH  
AND ACTIVATED SLUDGE WASTEWATER  
TREATMENT**

**VU TRAN KHANH LINH**

*(M. Eng., Ho Chi Minh City University of Technology, Viet Nam)*

**A THESIS SUBMITTED**

**FOR THE DEGREE OF DOCTOR OF PHILOSOPHY**

**DEPARTMENT OF CHEMICAL AND BIOMOLECULAR ENGINEERING**

**NATIONAL UNIVERSITY OF SINGAPORE**

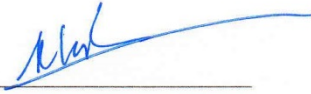
**2014**



## **DECLARATION**

I hereby declare that the work presented in this thesis is my own and it has been written by me in its entirety. Where information has been derived from other sources, I confirm that this has been indicated in the thesis.

This thesis has not been submitted for any degree in any university previously.

A handwritten signature in blue ink, appearing to read 'Vu Tran Khanh Linh', is written over a horizontal line.

Vu Tran Khanh Linh

December 1, 2014

## **ACKNOWLEDGEMENTS**

It is a pleasure to thank the many people who made this thesis possible. First and foremost, I would like to express my sincere appreciation to my supervisor, Professor Loh Kai-Chee for his gracious guidance, strong encouragement and consistent support throughout the course of my research. His constructive criticisms, data interpretations skills and detailed recommendations have always inspired and enriched my growth as a student and as a researcher.

I am thankful to Professor Chung Tai-Shung Neal for his kind support and encouragement to my work. I also gratefully acknowledge Professor Ting Yen Peng and Dr. Qiu Guanglei for their kind support, advice and fruitful discussions when I got my first-hand experience in dealing with activated sludge.

I am thankful to my former colleagues, Dr. Karthiga Nagarajan, Dr. Vivek Vasudevan, Dr. Satyen Gautam, Ms. Phay Jia-Jia and Dr. Cheng Xiyu for their help and support during my PhD study. My special thanks to my current lab mates and friends, Dr. Prashant Praveen and Ms. Nguyen Thi Thuy Duong for their support, encouragement, helpful discussions, assistance to my work as well as for all the unforgettable moments we had together throughout the past 5 years.

I thank laboratory staffs Ms. Tay Kaisi Alyssa, Mr. Ang Wee Siong, Ms. Xu Yanfang, Mr. Tan Evan Stephen, Ms. Ng Sook Poh and Mr. Ng Kim Poi for all the help, assistance and support.

I am especially grateful my parents, my parents - in - law, my brother and his family for their love and support. I am eternally thankful to my loving husband for his unconditional love, support, encouragement and for always being by my side throughout this tough Ph.D life. Without him, I might not be able to complete the thesis. Not to forget are my dear Vietnamese friends, especially Ms. Le Ngoc Lieu for being a wonderful friend on whom I can always count.

Finally, I want to thank NUS and AUN/Seed-Net program for the research scholarship provided to me.

# TABLE OF CONTENTS

ACKNOWLEDGEMENTS .....	i
TABLE OF CONTENTS.....	iii
SUMMARY .....	vii
LIST OF TABLES .....	xi
LIST OF FIGURES .....	xiii
LIST OF ABBREVIATIONS AND SYMBOLS .....	xv
Chapter 1 .....	1
Introduction.....	1
1.1 Research Background and Motivations.....	1
1.2 Research Objectives .....	9
1.3 Scope .....	10
1.4 Thesis Organization.....	11
Chapter 2.....	12
Literature Review.....	12
2.1 Microalgae.....	12
2.1.1 Cultivation of microalgae .....	13
2.1.2 Application areas of microalgal technology.....	15
2.2 Activated Sludge Process .....	20
2.2.1 Process description .....	20
2.2.2 Process microbiology .....	21
2.2.3 Oxygen requirements and transfer.....	23
2.2.4 Effluent quality .....	24
2.2.5 Nitrogen and phosphorus removal.....	24
2.3 Symbiotic Microalgal-Bacterial Process for Wastewater Treatment.....	25
2.3.1 Applications.....	26
2.3.2 Limitations of current symbiotic microalgal – bacterial processes.....	29
2.4 Hollow Fiber Membrane Bioreactors for Microalgae Cultivation and Wastewater Treatment.....	32

2.4.1 Microalgae cultivation.....	32
2.4.2 Wastewater treatment .....	35
Chapter 3.....	40
General Materials and Methods .....	40
3.1 Microorganisms, Culture Conditions, and Chemicals .....	40
3.1.1 Microalgae .....	40
3.1.2 Bacteria.....	41
3.1.3 Activated sludge .....	42
3.1.4 Chemicals .....	43
3.2 Membrane Contactor and Fiber Bundle Fabrication.....	43
3.2.1 Gas exchange hollow fiber membrane .....	43
3.2.2. Hollow fiber membrane contactor.....	44
3.2.3 Fiber bundle.....	45
3.3. Sterilization of Membrane Contactor and Fiber Bundle .....	45
3.4. Experimental Setup .....	46
3.5. Contamination Test for <i>C. vulgaris</i> Culture.....	46
3.6. Analytical Methods .....	47
Chapter 4.....	49
Baseline Studies for <i>C. vulgaris</i> and <i>P. putida</i> .....	49
4.1 Introduction .....	49
4.2 Materials and Methods .....	51
4.2.1 Baseline studies on <i>C. vulgaris</i> growth .....	51
4.2.2 Baseline studies on <i>P. putida</i> growth .....	52
4.3 Results and Discussion.....	53
4.3.1 Baseline studies on <i>C. vulgaris</i> growth .....	53
4.3.2 Baseline studies on <i>P. putida</i> growth .....	64
4.4 Concluding Remarks .....	68
Chapter 5.....	69
Symbiotic Hollow Fiber Membrane Photobioreactor for Microalgal Growth and Bacterial Wastewater Treatment.....	69
5.1 Introduction .....	69

5.2 Materials and Methods .....	70
5.2.1 Abiotic study.....	70
5.2.2 Symbiotic HFMP operation.....	71
5.3 Results and Discussion.....	75
5.3.1 Abiotic study.....	75
5.3.2 Proof – of – Concept.....	77
5.3.3 Effects of flow orientation.....	85
5.3.4 Effects of flow velocities.....	90
5.3.5 Effects of number of fibers.....	104
5.4 Concluding Remarks .....	107
Chapter 6.....	109
Submerged Hollow Fiber Membrane Photobioreactor for Retrofitting Existing Activated Sludge Tank .....	109
6.1 Introduction .....	109
6.2 Materials and Methods .....	112
6.2.1 SHFMP setup.....	112
6.2.2 Batch operation of SHFMP .....	113
6.2.3 Continuous operation of SHFMP .....	114
6.3 Results and Discussion.....	116
6.3.1 Batch operation of SHFMP .....	116
6.3.2 Continuous operation of SHFMP .....	125
6.3.3 Retrofitting existing activated sludge tank using SHFMP .....	144
6.4. Concluding Remarks .....	146
Chapter 7.....	147
Coupling the Submerged Hollow Fiber Membrane Photobioreactor to Activated Sludge Wastewater Treatment Process .....	147
7.1 Introduction .....	147
7.2 Materials and Methods .....	149
7.2.1 AS-SHFMP setup .....	149
7.2.2 Performance of the AS-SHFMP at different HRTs.....	151
7.2.3 Long-term operation of the AS-SHFMP .....	152



7.3 Results and Discussion.....	153
7.3.1 Performance of the AS-SHFMP at different HRTs.....	153
7.3.2 Long-term operation of the AS-SHFMP .....	175
7.3.3 Comparison between AS-SHFMP and current co-culture symbiotic wastewater treatment processes .....	181
7.4 Concluding Remarks .....	185
Chapter 8.....	187
Conclusions and Recommendations for Future Work .....	187
8.1 Conclusions .....	187
8.2 Recommendations for Future Works .....	190
REFERENCES .....	192
LIST OF CONFERENCE PRESENTATIONS .....	202
LIST OF PUBLICATIONS .....	202

## SUMMARY

Photosynthetic oxygenation is a plausible approach to reduce the energy cost of mechanical aeration in the activated sludge wastewater treatment process. However, this method has faced some problems such as the unexpected interactions between microalgae and bacteria, the high sensitivity of microalgae to toxic pollutants and the contaminations of microalgal biomass by bacteria and toxic pollutants. To overcome these limitations, this study aimed to develop hollow fiber membrane photobioreactors for symbiotic activated sludge wastewater treatment and microalgal biomass production.

In the first part, a symbiotic hollow fiber membrane photobioreactor (HFMP) resembling a shell and tube dialysis module was developed to physically separate microalgal and bacterial cultures, and solely facilitate the intertransfer of CO<sub>2</sub> and O<sub>2</sub> through concentration gradient as the driving force. *Chlorella vulgaris* and *Pseudomonas putida* were chosen as microbial models to elucidate the concept, with *C. vulgaris* culture was circulated in one side of the membrane contactor and *P. putida* culture was circulated in the other side. Results supported the hypothesis that a symbiotic relationship exists between microalgal and bacterial cultures in the HFMP, reflecting by the photo-autotrophic growth of *C. vulgaris* using the CO<sub>2</sub> supply from *P. putida* and the complete biodegradation of 500 mg/L glucose in synthetic wastewater by *P. putida* using photosynthetic oxygen produced by *C. vulgaris*. The effects of other operating parameters such as flow orientation, flow velocities of microalgal and bacterial cultures, and the number of fibers on the symbiotic HFMP performance were also investigated. It was found that the

performance of the symbiotic HFMP was significantly enhanced when circulating microalgal culture in the lumen side, and bacterial culture in the shell side of the membrane contactor. Using this flow orientation, the average percentage of glucose degraded per 8 – hour cycle was as high as 98% and microalgal biomass productivity was increased by 69% compared to the other orientation. The flow velocity at 3 cm/s in both the lumen and shell sides was demonstrated to be the most suitable for the operation of the symbiotic HFMP. The increase in the interfacial area remarkably enhanced glucose biodegradation rate, however, it had no significant effect on improving *C. vulgaris* growth.

In the second part of this research, the HFMP was modified to retrofit existing activated sludge tank to solve the available space problem in current existing wastewater treatment plants. In this design, called submerged hollow fiber membrane photobioreactor (SHFMP), the microalgae tank could be built close to or on top of an activated sludge tank whenever land area is insufficient. Hollow fiber membranes were directly submerged in the activated sludge tank and the microalgal culture was circulated through the lumen of the hollow fibers to perform CO<sub>2</sub> and O<sub>2</sub> exchange. In the SHFMP, the microalgal culture volume was minimized to enhance the practical application and light penetration. Results showed that even at the volume ratio of microalgal culture to bacterial culture of 1 : 2.4, the microalgae could generate sufficient oxygen to support efficient glucose biodegradation during the batch operation. Especially, continuous operation of the SHFMP was also successfully accomplished. At a hydraulic retention time of 10.6 hours, *P. putida* completely biodegraded 500 mg/L glucose

in the influent using the sole oxygen supply from *C. vulgaris* photosynthesis. The feasibility of the continuous operation of the SHFMP enhances its applicability as the influent wastewater stream in wastewater treatment plant is normally in continuous mode.

The idea of second part was further examined by coupling the SHFMP to the activated sludge process (AS-SHFMP) for the treatment of synthetic domestic wastewater. With the support from photosynthetic oxygenation, the AS-SHFMP successfully removed 98% COD, 63%  $\text{NH}_4^+ - \text{N}$  and 60%  $\text{PO}_4^{3-} - \text{P}$  at a hydraulic retention time of 10 hours. These results were comparable to those obtained in the conventional activated sludge process as well as other symbiotic microalgal-bacterial processes in treating domestic or municipal wastewater. In addition, the stability of the AS-SHFMP was also evaluated by a 17-day continuous operation. The repeatability of AS-SHFMP was demonstrated to be feasible when a fed-batch strategy was used to resupply the nutrients for microalgae, and the fiber bundles were exchanged every 4 days to ensure good gaseous exchange performance. The periodical substitution of fiber bundles also benefits the reusability and the life span of the fibers.

Another important advantage of the symbiotic hollow fiber membrane photobioreactor configurations in this research was the generation of clean *C. vulgaris* biomass. The microalgal biomass productivities obtained in the symbiotic HFMP and SHFMP systems ranged from 0.294 g/L.day to 0.709 g/L.day, which were comparable to those obtained in other photobioreactors reported in literature. The *C. vulgaris* concentration in the AS-SHFMP can be as high as 2.5 g/L,

significantly higher than the microalgae concentration in the high rate algal pond (HRAP) systems.

In conclusion, this study has facilitated the development of symbiotic hollow fiber membrane photobioreactor configurations for simultaneous activated sludge wastewater treatment and microalgal biomass production, opening up an avenue for the application of the novel designs in practice to reduce the energy cost for mechanical aeration, convert the emitted CO<sub>2</sub> to clean and high quality microalgal biomass for extracting other high-value added products. The SHFMP configuration also provides a new solution for coupling existing activated sludge process with the microalgal biomass production. The benefits of this coupling are: (i) less or no space would be required for the construction of hollow fiber membrane contactor and microalgae photobioreactor, (ii) the two cultures (the microalgal culture and the mixed liquor) could be manipulated independently and flexibly.

## LIST OF TABLES

<b>Table 2.1.</b> General composition of different human food sources and algae (% of dry matter) (Becker 2004).....	17
<b>Table 2.2.</b> Organic pollutants removal by algal-bacterial consortia.....	29
<b>Table 3.1.</b> Composition of BBM .....	41
<b>Table 3.2.</b> Composition of MM (Loh and Wang 1998).....	42
<b>Table 3.3.</b> Composition of synthetic wastewater (Qiu and Ting 2013).....	43
<b>Table 3.4</b> Specifications for the hollow fiber membranes .....	44
<b>Table 3.5</b> Characteristics of the membrane contactor .....	44
<b>Table 3.6</b> Analytical methods for the determination of some parameters .....	48
<b>Table 4.1.</b> Summary of the baseline studies for <i>C. vulgaris</i> .....	51
<b>Table 4.2.</b> Specific growth rate and biomass production of <i>C. vulgaris</i> at different concentrations of CO <sub>2</sub> aeration .....	54
<b>Table 4.3.</b> Specific growth rate and biomass production of <i>C. vulgaris</i> at different CO <sub>2</sub> aeration rates.....	59
<b>Table 4.4.</b> Specific growth rate and biomass production <i>C. vulgaris</i> at different light intensities .....	61
<b>Table 5.1.</b> Summary of experiments to investigate effects of operating conditions.....	74
<b>Table 5.2.</b> Summary of microalgal growth and glucose biodegradation under different experimental conditions .....	87
<b>Table 5.3.</b> Summary of microalgal growth and glucose biodegradation in experimental set A.....	92
<b>Table 5.4</b> Summary of microalgal growth and glucose biodegradation in experimental set B .....	98
<b>Table 5.5.</b> Biomass productivity of different microalgal species under different cultivation conditions.....	103
<b>Table 6.1.</b> Summary of the experiments to investigate the effects of VM/VB ratio on the SHFMP performance .....	114
<b>Table 6.2.</b> Summary of experimental run in the continuous operation of SHFMP and other control experiments.....	115
<b>Table 6.3.</b> Summary of microalgal growth and glucose biodegradation in experimental set E .....	119
<b>Table 6.4.</b> Effects of hydraulic retention time (HRT) on SHFMP performance at the VM/VB of 1 : 2.4.....	138
<b>Table 7.1.</b> Summary of the experimental runs in the AS-SHFMP and control experiments .....	151
<b>Table 7.2.</b> Summary of microalgal growth in experiment M1, N1 and Q.....	155

<b>Table 7.3.</b> Summary of nitrogen removal performance in experimental sets M and N.	162
<b>Table 7.4.</b> Summary of phosphorus removal performance in experimental sets M and N .....	167
<b>Table 7.5.</b> COD and nutrient removal performances of the AS-SHFMP, conventional activated sludge process and current symbiotic co-culture processes treating different types of wastewater.....	182

# LIST OF FIGURES

<b>Figure 3.1</b> Hollow fiber membrane contactor.....	44
<b>Figure 3.2.</b> Fiber bundle .....	45
<b>Figure 4.1.</b> Effects of CO <sub>2</sub> concentration on: (a) <i>C. vulgaris</i> growth, (b) NO <sub>3</sub> <sup>-</sup> – N consumption, (c) pH profile. ....	55
<b>Figure 4.2.</b> Effects of CO <sub>2</sub> aeration rate on: (a) <i>C. vulgaris</i> growth, (b) NO <sub>3</sub> <sup>-</sup> – N consumption.....	59
<b>Figure 4.3.</b> Effects of light intensity on: (a) <i>C. vulgaris</i> growth, (b) NO <sub>3</sub> <sup>-</sup> – N consumption.....	62
<b>Figure 4.4.</b> Temporal profiles of biomass and percentage of remaining glucose under aerated and non-aerated conditions. ....	64
<b>Figure 4.5.</b> Temporal profiles of effluent glucose and cell concentrations at D = 0.13 hr <sup>-1</sup> (HRT = 8 hours).....	66
<b>Figure 4.6.</b> Steady state biomass concentration, steady state effluent glucose concentration at different dilution rates.....	67
<b>Figure 5.1.</b> Schematic diagram of the symbiotic HFMP.....	71
<b>Figure 5.2.</b> Abiotic experiment: (a) dissolve oxygen (DO) and inorganic carbon (IC) concentration profiles in the shell-flask and lumen-flask. Error bars indicate standard deviation from the mean of triplicates.....	75
<b>Figure 5.3.</b> Temporal profiles of (a) <i>P. putida</i> biomass and glucose concentration, (b) <i>C. vulgaris</i> biomass and NO <sub>3</sub> <sup>-</sup> – N concentration, (c) pH in the symbiotic HFMP. Day 0 – 2: without <i>C. vulgaris</i> culture (square dot line); day 2 – 7: with the presence of <i>C. vulgaris</i> culture (solid line). ....	78
<b>Figure 5.4.</b> Membrane morphology of Acurrel ® 50/280 hollow fiber membrane: pristine and after 7-day operation. ....	82
<b>Figure 5.5.</b> Effects of flow orientation on: (a) <i>P. putida</i> growth and glucose biodegradation and (b) <i>C. vulgaris</i> growth and NO <sub>3</sub> <sup>-</sup> – N consumption. ....	86
<b>Figure 5.6.</b> Effects of lumen side flow velocity on glucose biodegradation and microalgal growth in the symbiotic HFMP: temporal profiles of (a) percentage of remaining glucose in A1 and A2, (b) percentage of remaining glucose in A2 and A3, (c) percentage of remaining glucose in A2 and A4; (d) <i>C. vulgaris</i> concentration. ....	94
<b>Figure 5.7.</b> Effects of shell side flow velocity on glucose biodegradation and microalgal growth in the symbiotic HFMP: temporal profiles of (a) <i>P. putida</i> concentration and percentage of remaining glucose in B1 and B2, (b) percentage of remaining glucose in B2 and B3; (c) <i>C. vulgaris</i> concentration.....	99
<b>Figure 5.8.</b> Effects of number of fibers on glucose biodegradation and microalgal growth in the symbiotic HFMP: (a) Temporal profiles of <i>P. putida</i> concentration and percentage of remaining glucose; (c) Temporal profiles of <i>C. vulgaris</i> concentration. D1: 100 fibers, D2: 200 fibers. ....	105
<b>Figure 6.1.</b> Schematic diagram of the SHFMP.....	113



<b>Figure 6.2.</b> Effects of VM/VB ratio on glucose biodegradation and microalgal growth in the SHFMP: (a) temporal profiles of <i>P. putida</i> concentration and percentage of remaining glucose; (b) temporal concentration profiles of <i>C. vulgaris</i> ; (c) temporal profiles of total microalgal cell mass.....	118
<b>Figure 6.3.</b> Temporal profiles of: (a) glucose concentration, (b) glucose removal efficiency, (c) <i>P. putida</i> concentration and (d) <i>C. vulgaris</i> and $\text{NO}_3^- - \text{N}$ concentrations in experiments F1 and F2, (e) DO concentrations of the effluent and <i>C. vulgaris</i> culture in experiments F1.....	127
<b>Figure 6.4.</b> Temporal profiles of: (a) glucose concentration and glucose removal efficiency, (b) <i>P. putida</i> concentration and <i>C. vulgaris</i> concentration in experiment G. The start of the feed is marked by the dotted lines. ....	133
<b>Figure 6.5.</b> Temporal profiles of: (a) effluent glucose concentration and glucose removal efficiency, (b) <i>C. vulgaris</i> concentration and effluent <i>P. putida</i> concentration in experiment H. The substitution of fiber bundles is marked by the dotted lines. ....	136
<b>Figure 6.6.</b> Temporal profiles of (a) effluent glucose concentrations in experiments K1 and K2, (b) effluent <i>P. putida</i> concentrations in experiments K1 and K2, (c) <i>C. vulgaris</i> and $\text{NO}_3^- - \text{N}$ concentrations in the microalgal cultures of experiment K1 and K3, and $\text{NH}_4^+ - \text{N}$ concentration in the autoclaved water of experiment K2.....	140
<b>Figure 7.1.</b> Experimental setup of the AS-SHFMP: (a) continuous operation setup, (b) submerged hollow fiber membranes in AS tank.....	150
<b>Figure 7.2.</b> Temporal concentration profiles of <i>C. vulgaris</i> and $\text{NO}_3^- - \text{N}$ in experiments M1, N1 and control experiment Q.....	154
<b>Figure 7.3.</b> Temporal profiles of (a) effluent COD concentration and COD removal efficiency in experimental set M (HRT = 8 hours), (b) effluent COD concentration and removal efficiency in experimental set N (HRT = 10 hours). ....	157
<b>Figure 7.4.</b> Temporal concentration profiles of $\text{NH}_4^+ - \text{N}$ in the lumen-water of M2 and N2, and $\text{NH}_4^+ - \text{N}$ , $\text{NO}_2^- - \text{N}$ , $\text{NO}_3^- - \text{N}$ , total nitrogen (TN) in the effluent of the AS-SHFMPs (M1, N1) and the control experiments (M2, M3, N2, N3). ....	161
<b>Figure 7.5.</b> Temporal concentration profiles of effluent $\text{PO}_4^{3-} - \text{P}$ in: (a) experimental set M, (b) experimental set N. ....	167
<b>Figure 7.6.</b> Hollow fiber membranes after 5-day run: (a) fibers in experiment N1 before washing, (b,c) fibers in experiment N2 before washing, (d) fibers in N1 after washing with 1M NaOH, (e) fibers in N2 after washing with 1M NaOH. ....	172
<b>Figure 7.7.</b> Long-term operation of the AS-SHFMP: temporal concentration profiles of (a1) <i>C. vulgaris</i> , (a2) $\text{NO}_3^- - \text{N}$ and $\text{PO}_4^{3-} - \text{P}$ in the microalgal culture; temporal concentration profiles of (b) COD, (c) $\text{NH}_4^+ - \text{N}$ , $\text{NO}_2^- - \text{N}$ , $\text{NO}_3^- - \text{N}$ and (d) $\text{PO}_4^{3-} - \text{P}$ in the effluent. ....	177
<b>Figure 7.8.</b> Nutrient agar plate of the <i>C. vulgaris</i> culture in the long-term operation experiment after one – week incubation at 30°C.....	180

## LIST OF ABBREVIATIONS

AS	Activated Sludge
AS-SHFMP	Activated Sludge-Submerged Hollow Fiber Membrane Photobioreactor
BBM	Bold's Basal Medium
BNR	Biological Nitrogen Removal
BOD	Biochemical Oxygen Demand
BOD <sub>5</sub>	5 – day Biochemical Oxygen Demand
COD	Chemical Oxygen Demand
CSLM	Confocal Scanning Laser Microscopy
DC	Degradation Capacity
DCW	Dry Cell Weight
DO	Dissolved Oxygen
EBPR	Enhanced Biological Phosphorus Removal
EDTA	Ethylenediaminetetraacetic acid
EPS	Extracellular Polymeric Substances
Expt.	Experiment
FESEM	Field-Emission Scanning Electron Microscopy
HFMP	Hollow Fiber Membrane Photobioreactor
HRAP	High Rate Algal Pond
HRT	Hydraulic Retention Time
IC	Inorganic Carbon
LED	Light-Emitting Diode

MBR	Membrane Bioreactor
MLSS	Mixed Liquor Suspended Solids
MLVSS	Mixed Liquor Volatile Suspended Solids
MM	Mineral Medium
OD	Optical Density
P	Phosphorus
PTFE	Polytetrafluoroethylene
RE	Removal Efficiency
SHFMP	Submerged Hollow Fiber Membrane Photobioreactor
TN	Total Nitrogen
VB	Volume of Bacterial Culture
VM	Volume of Microalgal Culture

# Chapter 1

## Introduction

### 1.1 Research Background and Motivations

Over the past century, human population has grown more than four-fold from 1.7 billion to 7.2 billion. This increasing growth has entailed a raising amount of wastewater worldwide. Being mainly composed of biodegradable organic compounds, volatile organic compounds, nutrients (nitrogen and phosphorus), recalcitrant xenobiotics, toxic metals, suspended solids, microbial pathogens and parasites (Bitton 2005b), the wastewater has been continuously endangering the environment, human community and economy. It is hence critical to treat wastewater before discharging it into receiving water bodies.

Activated sludge wastewater treatment is widely practiced industrially because of its high treatment rate and pollutant removal efficiency (Tamer *et al.* 2006). However, owing to the low aqueous solubility of oxygen, intense mechanical aeration is required to achieve the high pollutant removal rates. This results in high energy demand, typically 45% to 75% of the wastewater treatment plant energy consumption is ascribed to mechanical aeration (Reardon 1995). Furthermore, intense aeration also creates hazardous aerosols, which carry microorganisms and toxic organic compounds into the air (Brandi *et al.* 2000; Hamoda 2006). Carbon dioxide produced by microbial respiration is also released

to the atmosphere, contributing to the greenhouse effect of global warming (Keller and Hartley 2003; Monteith *et al.* 2005).

Photosynthetic oxygenation is a plausible approach proposed to overcome the abovementioned limitations (Muñoz and Guieysse 2006; Oswald *et al.* 1953). This exploits microalgae photosynthesis to provide sufficient O<sub>2</sub> that the heterotrophic bacteria require to degrade the organic pollutants; CO<sub>2</sub> released from bacterial respiration is then consumed by the microalgae during their photosynthesis. This symbiotic microalgal-bacterial process allows cost-effective aeration (as sunlight is the main energy source), limits the risk of pollutant volatilization and sequesters the greenhouse gas CO<sub>2</sub> to convert to microalgal biomass (Muñoz and Guieysse 2006; Oswald 1991).

Microalgae are used in photosynthetic aeration because they can generate oxygen at a high rate. The oxygen production rate of microalgae in a typical tubular photobioreactor may reach 10 g O<sub>2</sub>/m<sup>3</sup>.min under high irradiance condition (Chisti, 2007). Recently, microalgae have also become a potential candidate for biofuel production such as methane, biodiesel and hydrogen (Brennan and Owende 2010; Ghirardi *et al.* 2000; Sialve *et al.* 2009) because of the rapid depletion of fossil fuels and the severe effect of greenhouse gas emissions on the global climate change. Especially, owing to their chemical composition which gives microalgae interesting qualities, microalgal biomass has also been applied in the production of human and animal nutrition, cosmetics and other high-value added products (Lehr and Posten 2009; Spolaore *et al.* 2006), although the mass production of microalgae is still relatively expensive (Chisti 2007; Mata *et al.*

2010; Scott *et al.* 2010). One of the reasons of high microalgae production cost is the cost for CO<sub>2</sub> supply including CO<sub>2</sub> gas and power of CO<sub>2</sub> aeration. As analyzed and estimated by Acién and colleagues (2012), CO<sub>2</sub> is the most expensive consumable. The cost for CO<sub>2</sub> supply can account for 31 – 46% of raw materials and utilities cost. Hence, the integration of microalgae cultivation with wastewater treatment in the photosynthetic oxygenation could provide important benefits for both processes, because free CO<sub>2</sub> produced by microbial respiration will be provided for microalgal growth, resulting in reduction of the CO<sub>2</sub> supply cost for microalgal biomass production.

High-rate algal ponds (HRAPs) were first established by Oswald and his group in the early 1950s to treat domestic wastewater while producing microalgal biomass (Olguín 2012; Oswald 1962; Oswald and Gotaas 1957; Oswald *et al.* 1953). In a typical activated sludge process, the extended aeration system requires 0.4-1.1 kWh to introduce 1 kg of dissolved oxygen (Owen 1982). However, the electricity requirement for HRAPs operation is only 0.075 – 0.15 kWh/kg O<sub>2</sub> (Green *et al.* 1995). HRAPs are hence deemed promising low-cost wastewater treatment systems and have been used at several treatment plants around the world to treat a variety of organic wastes (Craggs *et al.* 2011). Besides HRAPs, recent studies have been conducted to treat other types of wastewater using photosynthetic oxygenation such as agro-industrial wastewater (Posadas *et al.* 2014), simulated sugar factory wastewater (Memon *et al.* 2014), and swine slurry (González-Fernández *et al.* 2011b). In addition, the symbiotic microalgal-bacterial consortia have also been applied for the safe and economical biodegradation of other

hazardous contaminants when the proper microalgal strains and process configuration are used (Borde *et al.* 2003; Muñoz *et al.* 2006; Muñoz *et al.* 2005b; Tang *et al.* 2010).

The association between the microalgae and the bacteria in the same bioreactor, however, poses several critical problems. The efficiency of HRAP treatment operated in open ponds decreases overtime when the light penetration through the pond declines when the microbial concentration increases. Under open ponds operation, variability of climatic conditions such as lighting, temperature, and the presence of predators like zooplankton and protozoa that feed on the microalgae also adversely affect the treatment efficacy (Rawat *et al.* 2011). Furthermore, compared to heterotrophic bacteria, microalgae grow at much slower rates and are more sensitive to the toxic pollutants present in the wastewater (Borde *et al.* 2003; Muñoz *et al.* 2006). In particular, heavy metals in the wastewater are potent inhibitors of microalgal photosynthesis because they can replace or block the prosthetic metal atoms in the active site of relevant photosynthetic enzymes (Kumar *et al.* 2010a). Hence, physical or chemical pretreatment steps are often needed to render the wastewater amenable to photosynthetic oxygenation treatment (Tamer *et al.* 2006). More often than not, specific microalgal strains that are resistant to the wastewater contaminants are sought for the process to be feasible (Safonova *et al.* 2004).

Another issue of concern is microbial interactions. When culturing microalgae and bacteria/activated sludge together, the microalgae might inhibit bacterial activity through the increased pH, a high inhibitory dissolved oxygen

concentration or by the production of inhibitory metabolites (Cole 1982; Muñoz and Guieysse 2006; Oswald 2003; Schumacher *et al.* 2003). On the other hand, there are also reports of aquatic bacteria and fungi that cause algal cells to lyse (Cole 1982). In some cases, the bacteria might also have detrimental effects on microalgal growth through the release of algicidal extracellular organic carbon (Cole 1982; Fukami *et al.* 1997). Therefore, selection and screening of compatible microalgal – bacterial consortia are crucial and fundamental in the photosynthetic oxygenation process design, rendering the process complicated and time-consuming.

In addition, harvesting the microalgae from the HRAPs is still challenging due to the small microalgal cell size (3 - 30  $\mu\text{m}$ ), the low biomass concentration (typically < 0.5 g dry weight/L), and the large volume of water to be treated (Craggs *et al.* 2011; Molina-Grima *et al.* 2003; Olguín 2012). Biofilm photobioreactors could offer an alternative approach to reduce biomass harvesting cost in the photosynthetic oxygenation process. In these systems, biofilm of microalgal-bacterial biomass was formed based on sole attachment of the biomass to photobioreactor walls, thus the microalgal-bacterial biomass was separated from the effluent and can be harvested by scraping the biofilm from the walls (de Godos *et al.* 2009; Muñoz *et al.* 2009; Posadas *et al.* 2013). Even then, with the contamination of bacteria and the presence of other potent contaminants in the wastewater such as heavy metals, recalcitrant organics, the harvested microalgal-bacterial biomass in the current co-culture symbiotic processes will seldom be suitable for the production of human nutrition or high-value added compounds



due to the high quality requirements and public acceptance of nutritional supplements (Muñoz and Guieysse 2006; Rawat *et al.* 2011).

In recent years, there has been a considerable interest in integrating hollow fiber membranes to photobioreactors to enhance gaseous transfer in microalgae cultivation (Cheng *et al.* 2006; Ferreira *et al.* 1998). Typically, the carbon source is provided by the bubbling of CO<sub>2</sub> enriched air into the microalgal culture using porous diffuser. However, this procedure leads to a considerable waste of CO<sub>2</sub> to the open atmosphere, adding to the operating cost (Carvalho *et al.* 2006; Ferreira *et al.* 1998; Kumar *et al.* 2010b). Although closed photobioreactors can offer higher gas transfer rates as compared to open pond systems, the accumulation of dissolved oxygen, a photosynthetic by-product, can inhibit the metabolic process (Kumar *et al.* 2010a). Hollow fiber membranes, on the contrary, can facilitate the gas exchange between the media inside and outside the fiber. Due to their high specific surface area, the interfacial area of contact between the gas and the culture increases, resulting in higher mass transfer rate (Carvalho *et al.* 2006; Kalontarov *et al.* 2014). Several studies have verified that the integration of hollow fiber membranes to photobioreactors improved microalgal biomass production, enhanced mass transfer and promoted CO<sub>2</sub> fixation (Carvalho and Malcata 2001; Cheng *et al.* 2006; Fan *et al.* 2008; Kalontarov *et al.* 2014; Kumar *et al.* 2010b). The dissolved oxygen concentration was also found to be lower than in the bubbling systems as this could be removed by the membranes (Carvalho *et al.* 2006; Cheng *et al.* 2006). Hollow fiber membrane bioreactor is hence a promising alternative for effective gaseous transfer, not only for

microalgae cultivation, but possibly also for bubble-free aeration in biological wastewater treatment. Apart from efficient gaseous exchange, the use of hollow fiber membranes also offers several advantages over mechanical aeration, such as minimizing the stripping of organic compounds or the formation of foaming, higher aeration rates, and higher efficiency of gas delivery to the active biomass in the membrane aerated biofilm reactor (Casey *et al.* 1999; Côté *et al.* 1989; Gabelman and Hwang 1999; Semmens 2008). The use of gas-permeable membranes for bubbleless aeration could also potentially reduce the energy cost associated with gas transfer, a major operating cost in biological wastewater treatment as indicated earlier (Semmens 2008).

To overcome the limitations highlighted for co-culture photosynthetic oxygenation, and to make possible the efficient use of microalgal biomass, the present study aimed to integrate two separate cultures of microalgae and bacteria/activated sludge in a closed system while still ensuring their symbiotic relationship with regards to aeration. To this end, a symbiotic hollow fiber membrane photobioreactor (HFMP) for simultaneous microalgal biomass production and bacterial wastewater treatment was developed. In this newly designed HFMP, a gas exchange membrane was used as a barrier, not only to physically separate the microalgal and bacterial cultures, but also to solely facilitate the intertransfer of CO<sub>2</sub> and O<sub>2</sub> through concentration gradient as the driving force. Through the use of suitable gas-exchange membranes in a symbiotic HFMP, higher CO<sub>2</sub> and O<sub>2</sub> mass transfer efficiencies can be achieved with minimal CO<sub>2</sub>/O<sub>2</sub> loss to the atmosphere. Moreover, the removal of O<sub>2</sub> from

the microalgal culture can alleviate the toxicity of O<sub>2</sub> build-up in the microalgal culture. By growing the microalgae and the bacteria on separate sides of the membrane, operation of the two cultures can be independently manipulated. Given that the microalgae is separated from the bacteria/activated sludge, the microalgal biomass, which is free of contaminants, can be easily harvested for various purposes such as for biodiesel production, food, feed and other high-value added chemicals production. By itself, the latter is ample benefit because the use of microalgal biomass for the production of healthy human nutrition, or as an ingredient in animal and aquaculture feed, is in fact a fast-growing market (Kumar *et al.* 2010a; Pulz and Gross 2004).

In consideration of the limited land area in current wastewater treatment plants, especially in a small country like Singapore, the symbiotic HFMP can be modified to a submerged hollow fiber membrane photobioreactor (SHFMP) to retrofit existing activated sludge treatment system. In this configuration, the hollow fiber membrane bundles can be directly submerged in the activated sludge tank, and the microalgal culture circulated through the lumen of the hollow fibers to perform CO<sub>2</sub> and O<sub>2</sub> exchange. The microalgae photobioreactor can be built closed to or on top of the activated sludge tank whenever land area is insufficient. With this design, additional land area required for hollow fiber membrane contactor can be minimized and the energy for intensive mechanical aeration can be reduced as a consequence of the photosynthetic oxygenation.

## 1.2 Research Objectives

The overall objective of this thesis was to apply hollow fiber membrane-based technology to design novel hollow fiber membrane photobioreactors to simultaneously perform aerobic wastewater treatment and microalgal biomass production. The specific research objectives included:

1. Establish baseline studies for the microbial models *Chlorella vulgaris* and *Pseudomonas putida* to understand cell growths and substrate removal potential prior to the design and operation of the symbiotic HFMP;
2. Demonstrate the concept of the symbiotic HFMP for simultaneous microalgal growth and bacterial wastewater treatment using *C. vulgaris* and *P. putida* as microbial models;
3. Investigate the effects of operating parameters on symbiotic HFMP performance to achieve better understanding as well as to optimize its operation;
4. Develop a submerged HFMP (SHFMP) to retrofit the existing activated sludge tank. Study batch and continuous operations of the SHFMP to evaluate the performance and applicability of the system;
5. Couple the SHFMP to the activated sludge process (AS-SHFMP) to investigate microalgal growth and COD/BOD<sub>5</sub> and nutrients biodegradation performance. Evaluate the stability of the AS-SHFMP system during continuous operation.

This program endeavored to develop novel symbiotic hollow fiber membrane photobioreactors to concomitantly treat wastewater and produce clean microalgae

biomass at the laboratory scale. Compared to current symbiotic microalgal-bacterial processes, there are two major contributions of this hybrid photobioreactor. One of these is the use of hollow fiber membranes to isolate the microbes in the activated sludge from the microalgae, and for gas exchanges between the microalgae and activated sludge growth. The other contribution is the compact footprint of the system, the practical application and scalability are hence feasible. The proposed symbiotic membrane photobioreactors also contribute toward the reduction of energy cost for mechanical aeration and the conversion of the CO<sub>2</sub> to clean microalgal biomass. The symbiotic microalgal – bacterial processes have been applied in wastewater treatment for more than 50 years, but the symbiotic hollow fiber membrane photobioreactor system examined here, to the best of the author’s knowledge, is the first design wherein microalgae and bacteria are separately cultured but still supporting each other in a closed system.

### **1.3 Scope**

It is understood that different types of pollutants exist in the real wastewater. However, this research only focused on using synthetic wastewater to demonstrate the concept and study the effects of operational parameters.

In addition, harvesting and usage of microalgal biomass were not included because the major scope of this thesis was to produce clean microalgal biomass using the developed symbiotic hollow fiber membrane photobioreactor.

## 1.4 Thesis Organization

This thesis comprises eight chapters. The first chapter briefly discusses the motivations for the development of novel symbiotic HFMP and SHFMP for activated sludge wastewater treatment and microalgal biomass production, and lists the overall and specific objectives of the research program. A detailed literature review focused on the activated sludge process, current studies and applications of symbiotic microalgal – bacterial processes, and applications of hollow fiber membrane contactors for microalgal biomass production and wastewater treatment is discussed in Chapter 2. Chapter 3 details the general materials and protocols used in the research. Chapter 4 summarizes the results obtained from the baseline studies on suspended cultures of *C. vulgaris* and *P. putida*. Chapter 5 presents the results on proof - of - concept of the symbiotic HFMP and an analysis of the effects of operating parameters on the symbiotic HFMP performance. Chapter 6 describes the glucose biodegradation performance and microalgal growth in the batch and continuous operations of the SHFMP. Results obtained from the coupling of activated sludge process with the submerged hollow fiber membrane photobioreactor are presented and discussed in Chapter 7. Finally, Chapter 8 summarizes the important contributions of this research program and also proposes several recommendations for future work.

## **Chapter 2**

### **Literature Review**

This chapter begins with an overview about microalgae and applications of microalgal technology in different fields, followed by a brief review of activated sludge process together with current problems of mechanical aeration. The concept and current studies of photosynthetic oxygenation are then presented. The applications of hollow fiber membrane contactors on microalgae cultivation and wastewater treatment are also highlighted. These provide the fundamentals on which to base the motivations of this research program.

#### **2.1 Microalgae**

Microalgae are found all over the world. They are microscopic microorganisms which can utilize light energy and inorganic nutrients (CO<sub>2</sub>, nitrogen, phosphorus etc.) to convert to their storage and structural compounds such as lipids, proteins, carbohydrates, pigments etc (Gouveia 2011; Markou and Nerantzis 2013). Owing to their photosynthetic capacity, chemical composition and ability to curb emerging environmental problems, microalgae have garnered the interest for various applications in different fields. The first part of this chapter discusses the cultivation of microalgae, the application of microalgal biomass in production of a variety of consumer products, as well as microalgae for environmental applications.

### **2.1.1 Cultivation of microalgae**

Microalgae can be cultivated using open ponds or photobioreactors.

#### ***2.1.1(a) Open ponds***

Algae cultivation in open ponds systems has been used since the 1950s. The most commonly used system is raceway pond which is typically made of concrete and the depth is ranging between 0.2 - 0.5m (Brennan and Owende 2010). An individual pond can be up to 1 ha in area. These ponds utilize paddle wheels with flow rate ranging from 10-30 cm/s to circulate the water to maintain adequate mixing and eliminate sedimentation. During daylight, feed is introduced continuously in front of the paddlewheel. Microalgae are harvested on the completion of the circulation loop just behind the paddlewheel (Chisti 2007; Harun *et al.* 2010).

Compared with closed systems, open ponds are significantly less expensive to build and simpler for construction and operation. In addition, sunlight is utilized for illumination, which helps decreasing energy cost for commercial algae production (Mata *et al.* 2010). However, open ponds still have some critical problems. It is difficult to keep the operating conditions constant such as evaporation losses, temperature and light intensity. Open ponds use CO<sub>2</sub> much less efficiently than photobioreactors due to losses to the atmosphere (Chisti 2007). Additionally, they occupy more extensive land area and are more susceptible to contamination from unwanted microalgae and other microorganisms that feed on microalgae (Mata *et al.* 2010). Especially, the



biomass density is relatively low (0.3 g DCW/L), increasing the cost for harvesting stage (Norsker *et al.* 2010).

To avoid microbial contamination in open pond systems, highly selective growth conditions have been used to guarantee the dominance of the selected strain such as *Dunaliella* in high saline medium, *Spirulina* at high alkalinity, and *Chlorella* at high nutritional condition (Lee 2001; Scott *et al.* 2010). However, such extreme conditions are not available for all microalgal species. Hence, apparently little room has left for further technological improvement to the open systems.

### **2.1.1(b) Photobioreactors**

To overcome the major problems associated with open culture systems, much attention has been paid to the development of closed photobioreactors for microalgal biomass production. Depends on their shape and design, photobioreactors could offer several advantages over open ponds such as offer better control of growth conditions (pH, temperature, mixing etc), reduce CO<sub>2</sub> loss, prevent contamination or minimize the invasion of competing microorganisms (Mata *et al.* 2010). The controlled environment in photobioreactors hence allows higher microalgae concentration (greater than 1 g/L) and volumetric biomass productivity, which could significantly reduce the harvesting cost (Brennan and Owende 2010). Different types of photobioreactors have been developed in the last three decades including column, flat-plate, tubular, column, and internally-illuminated photobioreactors (Pegallapati and Nirmalakhandan 2013; Wang *et al.* 2012).

Despite their advantages, the closed photobioreactors suffers from several drawbacks such as the accumulation of oxygen, the difficulty in scaling up and especially the high capital investment and production costs. One of the reasons of high microalgae production cost is the cost for CO<sub>2</sub> supply including CO<sub>2</sub> gas and power of CO<sub>2</sub> aeration. As analyzed and estimated by Acién and colleagues (2012), the cost for CO<sub>2</sub> supply can account for 31 – 46% of raw materials and utilities cost. Hence, the development of a cost-effective and high-efficiency microalgae cultivation system that could provide high – quality microalgal biomass needs considerable attention.

## **2.1.2 Application areas of microalgal technology**

### ***2.1.2(a) Biofuel production***

Because of increasing world population, rapid depletion of fossil fuels and the severe effects of greenhouse gas emission on the global climate change, it is critical to find new renewable resources for energy production. Microalgae have been suggested as a potential feedstock for the production of biofuels (Markou and Nerantzis 2013). This is because microalgae can accumulate large quantities of oil/neutral lipids (20 – 50%) which can be extracted and converted into biodiesels (Chisti 2007; Hu *et al.* 2008). In addition, microalgal biomass can also be used to provide other types of renewable biofuels such as methane produced by anaerobic digestion of biomass (Ras *et al.* 2011), bioethanol produced by fermentation of sugars extracted from microalgal biomass (Doan *et al.* 2012), and photobiologically produced biohydrogen (Rupprecht 2009). However, the cost of producing biodiesel from microalgal biomass is still high. It was estimated that oil

recovered from low cost microalgal biomass produced in photobioreactors can cost around \$2.8 /L, significantly higher than price of petrodiesel in 2006 (\$0.66 – \$0.79/L) (Chisti 2007). Hence, biotechnological improvements including strains, photobioreactors, harvesting, and the downstream technologies are needed to make price of microalgal biodiesel a feasible option (Acién Fernández *et al.* 2012; Chisti 2008).

### ***2.1.2(b) Microalgae in human and animal nutrition***

During the past few decades, an enormous amount of interest has been focused on the use of microalgae biomass for the production of human and animal nutrition, and other high-value added chemicals. This is because microalgae can accumulate lipid, protein, and carbohydrate with percentages are similar to those of human food sources as presented in Table 2.1. Microalgae also represent a valuable source of nearly all essential vitamins including A, B1, B2, B6, B12, C, E, nicotinate, biotin, folic acid, improving the nutritional value of microalgal biomass. The chemical composition of microalgae is not intrinsically constant, but varies from strain to strain, batch to batch, and mainly depends on the operational parameters such as temperature, illumination, pH value, CO<sub>2</sub> supply, mineral content of the medium, etc. (Becker 2004).

However, prior to their commercialization for human and animal nutrition, microalgal material must be analyzed for the presence of toxic components such as nucleic acids, toxins and heavy metals to prove their harmlessness (Reboloso Fuentes *et al.* 2000; Spolaore *et al.* 2006).

**Table 2.1.** General composition of different human food sources and algae (% of dry matter) (Becker 2004).

Commodity	Protein	Carbohydrate	Lipid
Bakers' yeast	39	38	1
Meat	43	1	34
Milk	26	38	28
Rice	8	77	2
Soybean	37	30	20
<i>Anabaena cylindrica</i>	43-56	25-30	4-7
<i>Chlamydomonas reinhardtii</i>	48	17	21
<i>Chlorella vulgaris</i>	51-58	12-17	14-22
<i>Dunaliella salina</i>	57	32	6
<i>Scenedesmus obliquus</i>	50-56	10-17	12-14
<i>Spirulina maxima</i>	60-71	13-16	6-7

### ***Human nutrition***

Recently, microalgal biomass has been predominantly exploited in the health food market. More than 75% of the annual biomass production has been being used for the manufacture of health foods in forms of powders, tablets, capsules and liquids (Pulz and Gross 2004; Spolaore *et al.* 2006). The dry biomass or extracts can also be incorporated into noodles, candies, snack foods, bread, tofu, etc. as flavors, nutritional supplements or natural food colorants (Spolaore *et al.* 2006; Yamaguchi 1996). *Chlorella*, *Arthrospira* (*Spirulina*), *D. salina* and *Aphanizomenon flos-aquae* are currently the four strains dominant the commercial applications in human nutrition (Pulz and Gross 2004; Spolaore *et al.* 2006).

### ***Animal nutrition and feed***

In addition to its application in human nutrition, microalgae can also be incorporated into the feed of aquaculture. For example, microalgae serve as a direct or indirect food source for larvae of many species such as mollusks,

crustaceans and fish. The most frequently used species in aquaculture are *Chlorella*, *Tetraselmis*, *Isochrysis*, *Pavlova*, *Phaeodactylum*, *Chaetoceros*, *Nannochloropsis*, *Skeletonema* and *Thalassiosira* (Apt and Behrens 1999; Spolaore et al. 2006; Yamaguchi 1996). Microalgal biomass is also proven its suitability as feed supplement for many types of animals such as cats, dogs, aquarium fish, ornamental birds, horses, cows and breeding bulls by providing natural vitamins, minerals, and essential fatty acids. *Arthrospira* and *Chlorella* are largely used in this domain (Spolaore et al. 2006).

#### **2.1.2(c) Microalgae in cosmetics**

Some microalgal species have been used in skin care market with the most common ones are *Arthrospira* and *Chlorella*. Their extracts can be found in such cosmetics products as anti-aging cream, refreshing or regenerant care products, emollient. For example, an extract from *Chlorella vulgaris* was found to stimulate the collagen synthesis in skin, thus supporting tissue regeneration and reducing the wrinkle (Spolaore et al. 2006).

#### **2.1.2(d) High-value added chemicals from microalgae**

In addition to the application in human and animal nutrition, some pure molecules can also be extracted from microalgal biomass to produce high – value added products such as: fatty acids, pigments and stable isotope biochemicals.

- Fatty acids: DHA ( $\omega$ 3 fatty acid) from *Cryptocodinium cohnii*, *Schizochytrium*, which can be added to infant milk formula.

- Pigments:  $\beta$  – carotene from *Dunaliella salina* for human use, chlorophyll from *Chlorella* species as source of pigments in cosmetics and food industries (Harun *et al.* 2010; Spolaore *et al.* 2006; Yen *et al.* 2013).
- Stable isotope biochemicals: microalgae are able to incorporate stable isotopes from inexpensive inorganic C-sources, H-sources and N-sources to more highly valued organic compounds such as amino acids, carbohydrates, lipids and nucleic acids. These stable isotope-labeled biochemicals can be used for scientific and clinical purposes (Apt and Behrens 1999; Pulz and Gross 2004; Spolaore *et al.* 2006).

To conclude, due to the valuable composition, microalgae have several applications from human and animal nutrients to cosmetics, and other high-value added substances. Microalgae production is mostly processed in outdoor cultivation. Closed system commercialization has also begun with *Chlorella* in Germany and with *Haematococcus* in Japan and Israel. Today the microalgal biomass for aquaculture and human consumption purposes are produced at a rate of 5 kt/year at a price of 250 €/kg. One of the reasons of this high price is because pure CO<sub>2</sub> is strictly required for biomass cultivation to ensure the quality of the biomass produced for human consumption (Acién Fernández *et al.* 2012). Hence microalgae production systems need to be further improved so that the price of microalgal biomass becomes more competitive and more economically feasible.

#### ***2.1.2(e) Microalgae for environmental applications***

Due to the ability to photosynthetically assimilate CO<sub>2</sub>, microalgae – based system has been considered as one of the most promising tools for CO<sub>2</sub> capture

from flue gases, mitigating the greenhouse emissions (de Godos *et al.* 2010a; Yoo *et al.* 2010). Microalgae also serve as an oxygenator to supply oxygen in aerobic treatment of different types of wastewater (Subashchandrabose *et al.* 2011). Some phenol resistant microalgae such as *Ankistrodesmus braunii* and *Scenedesmus quadricauda* were capable of removing phenols from the wastewater (Pinto *et al.* 2003). Cell walls of microalgae are composed of polysaccharides and carbohydrates that have negatively-charged groups (amino, carboxyl, hydroxyl or sulfide). Most metals are bound to these negatively-charged ligand groups, hence microalgae can also be used for removing heavy metals in industrial wastewater (Harun *et al.* 2010; Muñoz *et al.* 2006; Subashchandrabose *et al.* 2011). However, heavy metals in the wastewater are potent inhibitors of microalgal photosynthesis because they can replace or block the prosthetic metal atoms in the active site of relevant photosynthetic enzymes (Kumar *et al.* 2010a; Subashchandrabose *et al.* 2011).

## **2.2 Activated Sludge Process**

### **2.2.1 Process description**

Wastewater, originating from residences, institutions, offices and industries, mainly composed of biodegradable organic compounds, volatile organic compounds, nutrients (nitrogen and phosphorus), recalcitrant xenobiotics, toxic metals, suspended solids, and microbial pathogens and parasites (Bitton 2005b; Comeau 2008). Hence, not treating wastewater before it is discharged into receiving water bodies results in severe environmental and human health effects

such as the depletion of dissolved oxygen, the generation of odours, and the release of nutrients, toxic contaminants and pathogens (Comeau 2008).

Activated sludge wastewater treatment is by far the most common biological treatment method used for treating domestic and industrial wastewater. Since its first establishment in 1914, the treatment process has been widely adopted and well developed all over the world because of its low construction cost and ability to produce high quality effluents for a reasonable operating and maintenance cost compared to other technologies. In this process, wastewater discharged from the primary clarifier is introduced to an aeration basin into which a complex microbial population (referred to as activated sludge) is mixed. The activated sludge is capable of aerobically degrading organic matters, converting them to CO<sub>2</sub>, water, new cell biomass and other end products (Shieh and Nguyen 1999a).

After a period contact between the wastewater and the activated sludge, the mixed liquor (mixture of wastewater and microbial mass) is separated from sludge in a secondary clarifier. Clarified effluent is produced for discharge while a portion of settled sludge is recycled back to the aeration tank to maintain the required sludge concentration.

### **2.2.2 Process microbiology**

The basic operation unit of the activated sludge is the floc (EPA 1997). The activated sludge floc consists mostly of bacteria and other microorganisms (protozoa, yeast, fungi, and worms), particles, impurities and coagulants coming together to form a mass (EPA 1997). AS flocs are irregular in shape and their size varies between  $< 1$  to  $\geq 1000$   $\mu\text{m}$ . AS flocs helps to collect both organic and



inorganic pollutants in the wastewater by adsorption, absorption or entrapment (Bitton 2005a; EPA 1997).

In the activated sludge process, bacteria are the most important microorganisms in decomposing the organic materials in the influent. The group of bacteria in activated sludge primarily belongs to the Gram-negative species, including carbon oxidizers and nitrogen oxidizers, floc-formers and nonfloc-formers, and aerobes and facultative anaerobes. In general, the bacteria in the activated sludge process are from the major genera such as *Pseudomonas*, *Zoogloea*, *Achromobacter*, *Flavobacterium*, *Nocardia*, *Bdellovibrio*, *Mycobacterium*, *Nitrosomonas*, and *Nitrobacter* (Bitton 2005a; Shieh and Nguyen 1999a). *Nitrosomonas* and *Nitrobacter* are nitrifying bacteria (nitrifiers) and they are slow growing species. Hence, it is necessary to maintain an adequate population of nitrifying bacteria to ensure that they are not washed out (Shieh and Nguyen 1999a).

During the aerobic treatment, in addition to energy, microorganisms in the activated sludge requires sources of organic and inorganic compounds to synthesis their cellular components. Hence a portion of organic materials and nutrients in the wastewater is converted into new cell mass. Only a portion of the original waste is oxidized to low-energy compounds such as nitrate, sulfate and CO<sub>2</sub>. Additionally, many intermediate products are also form before the end products (Comeau 2008; Shieh and Nguyen 1999a). The carbon, nitrogen and phosphorus requirements for cell growth can be evaluated by considering that they constitute 50%, 12 – 14% and 1.0 – 3.0%, respectively, of the volatile fraction of the biomass produced (MLVSS) (Comeau 2008; Gerardi 2006a;

Gerardi 2006f). Empirical formulae for active biomass found in wastewater treatment processes can also be proposed as  $C_5H_7O_2NP_{1/12}$  (Comeau 2008).

### **2.2.3 Oxygen requirements and transfer**

In the activated sludge process, aeration is strictly required as it has duals function:

- to supply oxygen to the aerobic microorganisms for their respiration; and
- to maintain the activated sludge flocs in suspension, ensuring maximum contact between the surface of the flocs and the wastewater (Scholz 2006).

Too much or too little oxygen is undesirable to the process because too much oxygen increases the power cost, while too little oxygen decreases the metabolism activity of the microorganisms as well as the efficiency of the process. The dissolved oxygen (DO) in the mixed liquor should be maintained between 1 and 2 mg/L (EPA 1997). Mechanical aeration can be achieved by the use of surface aerators, coarse-bubble systems, and fine-bubble systems (Stenstrom and Rosso 2008).

However, the use of mechanical aeration in activated sludge process results in high energy input demand, generally accounting for 45 – 75% of the plant energy consumption (Reardon 1995). Intensive aeration can also generate aerosols containing microorganisms and toxic organic compounds, hazardous for exposed subjects (Brandi *et al.* 2000; Hamoda 2006). In addition, the emission of CO<sub>2</sub> during the aerobic treatment of wastewater negatively contributes to the green – house effect (Keller and Hartley 2003; Monteith *et al.* 2005).

#### **2.2.4 Effluent quality**

The objectives of conventional activated sludge process are to decompose the organic matters, remove carbonaceous BOD, coagulate and remove non-settleable colloidal solids, stabilize the organic matters and if necessary, remove nutrients such as nitrogen and phosphorus. For municipal wastewater, activated sludge treatment removes the following major pollutants: > 90% BOD<sub>5</sub>, >70% COD, 90% suspended solids, > 30% P (phosphorus) and 35% N (nitrogen) (Shieh and Nguyen 1999a; Shieh and Nguyen 1999b).

#### **2.2.5 Nitrogen and phosphorus removal**

The conventional activated sludge process does not facilitate biological nutrient (nitrogen and phosphorus) removal (Reuter 1999). For example, in Singapore the original conventional activated sludge process could not completely remove ammonia, and effluent ammonia concentration is usually in the range of 20 - 25 mg/L or higher (Cao *et al.* 2008).

Currently special attention is given to nutrient removal because an excessive increase in quantities of nitrogen and phosphorus in the aquatic environment will cause the growth of cyanobacteria and microalgae in lakes, rivers and the sea, disturbing the ecological balance (eutrophication) (Wiesmann *et al.* 2007). Therefore, biological nutrient removal has been being widely adopted and developed in wastewater treatment plants in Europe and North America since the early 1980s to prevent eutrophication. However, most of Asia countries except Japan still have not paid enough focus on biological nutrient removal (Cao 2011a).

To enhance the nutrient removal, Biological Nitrogen Removal (BNR) and Enhanced Biological Phosphorus Removal (EBPR) processes can be incorporated into the existing activated sludge process. The principles of BNR and EBPR have been well documented in literature (Ekama and Wentzel 2008; EPA 1997; Hong and Holbrook 1999; Loosdrecht 2008; Wentzel *et al.* 2008). In recent years, comprehensive investigations have been also conducted to accommodate nitrogen and phosphorus removals in the existing activated sludge process in Singapore's Water Reclamation Plants (Cao 2011a; Cao *et al.* 2008).

### **2.3 Symbiotic Microalgal-Bacterial Process for Wastewater Treatment**

The photosynthetic oxygenation or symbiotic microalgal – bacterial process was proposed in 1950s and has been widely adopted to overcome the limitations of mechanical aeration in the activated sludge process (Muñoz and Guieysse 2006; Oswald *et al.* 1953). In the symbiotic microalgal – bacterial process, bacteria and microalgae are cultured together in the wastewater in the presence of light. Aerobic bacteria break down the organic compounds in the wastewater to CO<sub>2</sub> and other nutrients which are then employed by microalgae for their photosynthesis. O<sub>2</sub> liberated in the photosynthesis is in turn used by aerobic bacteria to oxidize the organic compounds (Muñoz and Guieysse 2006; Oswald 1962). This symbiotic microalgal-bacterial process hence allows cost-effective aeration (as sunlight is the main energy source), limits the risk of pollutant or aerosol release and converts the green-house gas CO<sub>2</sub> to microalgal biomass (Muñoz and Guieysse 2006; Oswald 1991).

### **2.3.1 Applications**

#### ***2.3.1(a) Wastewater treatments***

High rate algal ponds (HRAPs) were the first microalgae-based systems pioneered and developed by Oswald and co-workers in the 1950s for domestic wastewater treatment and resource recovery (Craggs *et al.* 2011; Green *et al.* 1995; Oswald 1991; Oswald *et al.* 1953). These open, paddlewheel – mixed, shallow raceway ponds are designed to promote algae growth. The hydraulic retention time of HRAPs ranges from 3 – 10 days, thereby allowing sufficient aeration for BOD removal in the wastewater (Muñoz and Guieysse 2006; Rawat *et al.* 2011). Typically, 0.4 – 1.1 kWh is required to deliver 1 kg of dissolved oxygen in activated sludge process and extended aeration system (Owen 1982). However, the electricity requirement for HRAPs operation is only 0.075 – 0.15 kWh/kg O<sub>2</sub> (Green *et al.* 1995). HRAPs hence are promising cost effective wastewater treatment systems and are used at several treatment plants around the world to oxidize organic matter and remove soluble nutrients in a variety of wastewaters such as anaerobic pond effluents, domestic wastewater, agricultural wastewaters, etc (Craggs *et al.* 2011). Microalgae growing in the wastewater assimilate nutrients (nitrogen and phosphorus), and hence subsequent harvest of the microalgal biomass recovers the nutrients from the wastewater (Park *et al.* 2011). Many attempts have also been made to further improve the performance of the HRAPs. Park and Craggs (2011) suggested that the addition of CO<sub>2</sub> to the HRAPs stimulated the microalgal growth, enhancing nitrogen removal efficiency to 83.3%. Santiago *et al.* (2013) pre – disinfected the wastewater by UV lamps prior

to the HRAP treatment to reduce the loads of bacteria and protozoa which can negatively affect microalgae growth rate by competing for space and nutrients. Removal efficiencies of  $\text{NH}_4^+ - \text{N}$  and solute phosphorus were improved from 71% and 14% to 74% and 19%, respectively, with the pre-disinfection by UV radiation. Sutherland and colleagues (2014b) reported that increased pond depth could improve overall microalgal productivity and nutrient removal in the HRAPs. However, maximum removal efficiencies of  $\text{NH}_4^+ - \text{N}$  and dissolved reactive phosphorus were 77.4 % and 34.3%, respectively. Hence, in spite of the long hydraulic retention time used (3 – 7 days) and technical solutions applied to enhance the HRAP performance, complete nutrient removal in most of the reported HRAP treatments still could not be obtained.

In addition to the HRAPs, recent studies have also been conducted in lab-scale to treat other types of wastewater using photosynthetic oxygenation such as agro-industrial wastewater (Posadas *et al.* 2014), simulated sugar factory wastewater (Memon *et al.* 2014), and swine slurry (González-Fernández *et al.* 2011a; González-Fernández *et al.* 2011b). To reduce the cost of biomass harvesting, biofilm photobioreactors were also developed (de Godos *et al.* 2009; Muñoz *et al.* 2009; Posadas *et al.* 2013). Biofilm of microalgal-bacterial biomass in these systems was formed based on sole attachment of the biomass to the reactor walls, making harvesting much easier than in suspended systems. The biomass can be easily harvested by scraping the biofilm from the reactor walls (Boelee *et al.* 2011). Removal efficiencies of up to 75% COD, 86%  $\text{PO}_4^{3-} - \text{P}$ , 99%  $\text{NH}_4^+ - \text{N}$  were achieved by the *C. sorokiniana* mixed with bacterial culture from the

activated sludge process in the tubular biofilm photobioreactor (González *et al.* 2008).

### ***2.3.1(b) Biodegradation of organic pollutants***

Not only being used for treating various types of wastewaters, the symbiotic microalgal-bacterial consortia were also applied for the safe and economical biodegradation of hazardous pollutants when proper algal strains were used. Table 2.2 summarizes the findings of the some organic pollutants removal performance by symbiotic microalgal-bacterial processes reported in literature.

As presented in the table, the microalgal – bacterial consortium comprising of salicylate – degrading *Ralstonia basilensis*, phenol degrading - *Acinetobacter haemolyticus* and phenanthrene – degrading *Pseudomonas migulae* and *Sphingomonas yanoikuyae*, and the green microalga *Chlorella sorokiniana* was able to remove up to 85% of these three pollutants under continuous lighting condition (Borde *et al.* 2003). The consortium *C. sorokiniana* and *R. basilensis* was found to biodegrade salicylate with a subsequent removal of heavy metals from the solutions (Muñoz *et al.* 2006). Chavan and Mukherji (2008) used consortium of oil tolerant microalgae and oil degrading bacterium to treat hydrocarbon-rich wastewater.

**Table 2.2.** Organic pollutants removal by algal-bacterial consortia

Compound	Experimental system	Microalga / Bacterium	Removal efficiency*	Reference
Phenanthrene	50 mL glass tube with silicone oil at 20%	<i>Chlorella sorokiniana</i> / <i>Pseudomonas migulae</i>	24.2 g/m <sup>3</sup> .h (200 – 500 mg/L)	(Muñoz <i>et al.</i> 2003a)
Sodium salicylate	155 mL flask seal with rubber septa	<i>C. sorokiniana</i> / <i>R. basilensis</i>	100% (5 mM)	(Borde <i>et al.</i> 2003)
Sodium salicylate		<i>C. sorokiniana</i> / <i>Ralstonia</i> sp.	19 mg/L.h (800 mg/L)	(Muñoz <i>et al.</i> 2003b)
Sodium salicylate	600 mL continuous stirred tank reactor	<i>C. sorokiniana</i> / <i>R. basilensis</i>	87 mg/L.h (1 g/L)	(Muñoz <i>et al.</i> 2004)
Phenol		<i>C. sorokiniana</i> / <i>Acinetobacter haemolyticus</i>	89% (4.25 mM)	(Borde <i>et al.</i> 2003)
Acetonitrile	600 mL Stirred tank Reactor (STR)	<i>C. sorokiniana</i> / bacterial consortium	12.8 mg/L.h (1 g/L)	(Muñoz <i>et al.</i> 2005a)
Sodium salicylate		<i>Chlorella vulgaris</i> / <i>R. basilensis</i>	14 mg/L.h (800 mg/L)	(Muñoz <i>et al.</i> 2003b)
Phenol, oil	100 L tank	<i>Chorella</i> sp., <i>Scenedesmus obliquus</i> , <i>Stichococcus</i> sp. <i>Phormidium</i> sp. / <i>Rhodococcus</i> , <i>Kibdelosporangium aridum</i>	85% phenol (0.48 mg/L) 96% oil (40 mg/L)	(Safonova <i>et al.</i> 2004)
Diesel		<i>Phormidium</i> sp., <i>Oscillatoria</i> sp., <i>Chroococcus</i> sp. / <i>Burkholderia cepacia</i>	99.5% (0.6% v/v)	(Chavan and Mukherji 2008)
Total petroleum hydrocarbon		<i>Phormidium</i> sp., <i>Oscillatoria</i> sp., <i>Chroococcus</i> sp. / <i>Burkholderia cepacia</i>	99% (0.6% v/v diesel)	(Chavan and Mukherji 2010)
Methyl tert-butyl ether	100 mL seal bottle	<i>Chlorella ellipsoidea</i> / <i>Methylibium petroleiphilum</i> <i>PM1</i>	8.808 mg/L.day (62 mg/L)	(Zhong <i>et al.</i> 2011)

\*Values in parentheses are the initial concentrations of the organic pollutants added

### 2.3.2 Limitations of current symbiotic microalgal – bacterial processes

Despite the advantages in energy saving for mechanical aeration, the current symbiotic microalgal – bacterial processes still have several limitations. HRAPs



are opened algae-based systems, hence there are a number of issues which could adversely affect photosynthetic oxygenation such as the decline in light penetration when the cell density in HRAPs increases, the instability of climate conditions (i.e. lighting, temperature), and the presence of predators like zooplankton and protozoa that graze on microalgae and can reduce microalgal growth within a few days (Rawat *et al.* 2011). Besides, compared to heterotrophic bacteria, microalgae grow at much slower rates and have higher sensitivity to toxic pollutants presented in the wastewater, which may lead to process failure (Borde *et al.* 2003; Muñoz *et al.* 2006). Heavy metals in the wastewater are also potent inhibitors for microalgal photosynthesis because they can block or replace the prosthetic metal atoms in the active site of relevant enzymes (Kumar *et al.* 2010a). To prevent such problems, physical or chemical pretreatment steps for wastewater are often needed to disinfect or detoxify the wastewater prior its treatment with an algal-bacterial consortium (Santiago *et al.* 2013; Tamer *et al.* 2006). The detection of microalgal strains resistant to the wastewater or pollutants is also required for a successful process. For example, Tamer and colleagues (2006) detoxified the wastewater by activated carbon adsorption and UV(A-B)-irradiation prior to its biological treatment using microalgal-bacteria consortium. In order to use photosynthetic oxygenation in the treatment of industrial wastewater, intensive work had also been done to screen for the algal strains *Chlorella* sp. ES-13, *Chlorella* sp. ES-30, *Scenedesmus obliquus* ES-55, *Stichococcus* because they were resistant to the industrial wastewater (Safonova *et al.* 2004). These pretreatment and screening steps thus can help to minimize the

failure in photosynthetic oxygenation. However they may be costly and very time-consuming.

Another issue in current symbiotic microalgal-bacterial processes is the microbial interaction. When culturing microalgae and bacteria or activated sludge together, microalgae might inhibit bacterial activity by increasing the pH, the dissolved oxygen concentration of the culture or by producing inhibitory substances (Cole 1982; Muñoz and Guieysse 2006; Oswald 2003; Schumacher *et al.* 2003). On the contrary, some aquatic bacteria and fungi were reported to cause algal lysis (Cole 1982). Bacteria can also have a detrimental effect on microalgae by releasing algicidal extracellular metabolites (Cole 1982; Fukami *et al.* 1997). Hence to avoid such unexpected interactions, the selection and screening of compatible microalgae – bacteria consortium are crucial and fundamental in the self – oxygenation process design, but again they might be complicated and time-consuming.

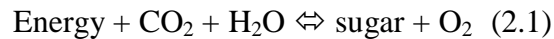
In addition, the harvest of microalgal biomass from the photosynthetically oxygenated systems has encountered some challenges due to the small microalgal cell size (3 - 30  $\mu\text{m}$ ), the low biomass concentration (typically < 0.5 g dry weight/L), and the large volume of water being harvested, and more importantly the contaminated from bacteria (Craggs *et al.* 2011; Molina-Grima *et al.* 2003; Olguín 2012). Although biofilm photobioreactors could offer an alternative approach to reduce biomass harvesting cost in the photosynthetic oxygenation process, the contamination from bacteria is unavoidable. Additionally, the microalgal biomass might also contain other potent pollutants in the wastewater

such as toxin, heavy metals and recalcitrant organics. Hence, the harvested microalgal-bacterial biomass will seldom be suitable for the production of human nutrition or high value compounds due to the regulatory requirements and public acceptance (Muñoz and Guieysse 2006; Oswald 1962; Spolaore *et al.* 2006). The best option to use the microalgal – bacterial biomass is for biogas production by anaerobic digestion (Muñoz and Guieysse 2006).

## **2.4 Hollow Fiber Membrane Bioreactors for Microalgae Cultivation and Wastewater Treatment**

### **2.4.1 Microalgae cultivation**

During photosynthesis, microalgae sequester CO<sub>2</sub> and generate O<sub>2</sub> as can be simply presented in equation (2.1):



If oxygen buildup occurs, the reversible reaction (2.1) is shifted to the left, decreasing photosynthetic efficiency. Therefore, CO<sub>2</sub> supply and O<sub>2</sub> removal in a photobioreactor must be controlled to obtain high biomass productivity.

Currently, bubbling CO<sub>2</sub>-enriched air into the photobioreactor using diffusers has been the most common approach. However a limitation of this method is that most of the supplied CO<sub>2</sub> is lost to the atmosphere, adding to the operational cost (Kumar *et al.* 2010b). Using closed photobioreactors can offer higher gas transfer rates and higher photosynthetic efficiency than open ponds. However, the accumulation of dissolved oxygen (DO), a by-product of photosynthesis, much greater than the air saturation values can inhibit photosynthesis (Chisti 2007;

Molina *et al.* 2001; Peng *et al.* 2013). For example, in the pond used by Jiménez and colleagues (2003) to study the growth of *Spirulina platensis*, the DO concentration in culture can reach 30 mg/L in summer, and a clear decrease in biomass concentration was observed when the DO concentration was larger than 25 mg/L. Additionally, a high DO concentration combining with intense sunlight can produce photooxidative damage to algal cells (Chisti 2007). Molina and colleagues (2001) reported that the DO concentration in the tubular photobioreactor used for cultivating *Phaeodactylum tricornutum* under outdoor condition can reach up to 24 mg/L. Consequently, the culture was damaged due to the photooxidation induced by high concentration of oxygen combines with intense irradiance.

One solution to increase mass transfer rate of CO<sub>2</sub> to the culture broth is increasing the interfacial areas between the gas and the culture medium. This can be obtained by using permeable membranes through which gas diffuses into the culture. The permeable membrane can be either microporous or made of material possessing high gas permeability (e.g. silicone). Carvalho and colleagues (2006) concluded that hollow fiber membrane systems theoretically offered several advantages over bubbling system such as minimization of CO<sub>2</sub> loss to atmosphere, possibility to accurately control CO<sub>2</sub> transfer rates. It is also possible to operate at low gas pressures because it is unnecessary to counterbalance hydrostatic heads (Carvalho and Malcata 2001).

Several studies were conducted to compare the mass transfer rates obtained under bubbling condition and by diffusion through hollow fiber membranes. It was

demonstrated that  $k_La$  values (overall volumetric transfer coefficient for CO<sub>2</sub> transfer) were higher in the latter case. For instance,  $k_La$  value of hydrophobic membrane was found at  $1.48 \times 10^{-2} \text{ min}^{-1}$ , significantly higher than  $k_La$  value of plain bubbling ( $7.0 \times 10^{-3} \text{ min}^{-1}$ ) (Carvalho and Malcata 2001). Similarly, Fan *et al.* (2007) investigated the CO<sub>2</sub> fixation efficiency by *C. vulgaris* cultivated in a polyvinylidene fluoride (PVDF) hollow fiber membrane photobioreactor and concluded that the CO<sub>2</sub> fixation rate in the membrane photobioreactor was 2.15 and 1.95 times higher than those in bubble column and airlift photobioreactor.

As for O<sub>2</sub> removal, the most commonly used solution is the usage of a degasser when the reactor configuration does not have an interface between culture and surrounding atmosphere (for instance, tubular or flat plate photobioreactors) (Carvalho *et al.* 2006). However, to obtain effective O<sub>2</sub> separation the distance between entrance and exit of the degasser should be long enough so that the smallest bubbles can have enough time to disengage from the liquid phase before they leave the unit (Carvalho *et al.* 2006). On the other hand, in stirred tanks and bubbling-type reactors, oxygen leaves the microalgal culture when it reaches the surface, hence allowing degassing of the whole culture. Interestingly, when using hollow fiber membrane contactors, the content of DO was found to be lower than that in the bubbling systems as oxygen was removed through the membranes (Carvalho *et al.* 2006; Kumar *et al.* 2010b). Thus, hollow fiber membrane bioreactor is a promising alternative for effective gaseous transfer for microalgae cultivation.

### 2.4.2 Wastewater treatment

Apart from application in microalgae cultivation, hollow fiber membranes are also used for bubble-free aeration in biological wastewater treatment. This method actually offers several advantages over mechanical aeration, such as minimizing the stripping of organic compounds or the formation of foaming, offering higher aeration rates, and higher efficiency of gas delivery to the active biomass in the membrane aerated biofilm reactor (Casey *et al.* 1999; Côté *et al.* 1989; Gabelman and Hwang 1999; Semmens 2008). The use of gas-permeable membranes for bubbleless aeration could also potentially reduce the energy cost associated with gas transfer, a major operating cost in biological wastewater treatment as indicated earlier (Semmens 2008).

Besides bubbleless aeration, membrane bioreactors (MBR) have also been increasingly used as filters to replace the secondary sedimentation. MBRs combine biological treatment by activated sludge and liquid/solid separation by porous membrane to effectively remove contaminants from wastewaters (Bérubé 2010; Le-Clech 2010). Today, several thousand of MRBs have been commissioned worldwide due to the significant advantages that they can convey: the small footprint for the construction of new treatment system, the stringent regulations imposed for treated water discharge, and the reduction in membrane cost.

One main problem emerging during the operation of MBR is that the materials that are retained by the membrane can deposit and accumulate, forming fouling on membrane surface, resulting in a decrease in membrane performance. In the

case of gas-permeable membranes for bubbleless aeration, there is no flux across the membrane, hence solids do not tend to accumulate on the membrane surface (Semmens 2008). However, biofouling from microorganisms still can occur. These problems should be addressed to make the practical application of membrane reactors more feasible. Currently, significant progress has been made to provide effective strategies for fouling mitigation (Kraume and Drews 2010).

## **2.5. Symbiotic HFMP for simultaneous microalgal biomass production and bacterial wastewater treatment**

As mentioned above, the conventional symbiotic microalgal-bacterial process has provided the solutions for the cost-effective aeration as well as resource recovery. However, several limitations still remain such as the negative interactions between microalgae and bacteria, the low microalgal biomass concentration, the contamination of microalgal biomass. Recently hollow fiber membrane technology has gained increasing attention due to its high efficiency and small foot print, making it a promising option of choice for wastewater treatment. This study hence aimed to utilize hollow fiber membrane – based technology to develop a novel symbiotic hollow fiber membrane photobioreactor for microalgal growth and activated sludge wastewater treatment which can mitigate those limitations. In this newly designed HFMP, a gas exchange membrane was used as a barrier, not only to physically separate the microalgal and bacterial cultures, but also to solely facilitate the intertransfer of CO<sub>2</sub> and O<sub>2</sub> through concentration gradient as the driving force. Through the use of suitable gas-exchange membranes in a symbiotic HFMP, higher CO<sub>2</sub> and O<sub>2</sub> mass transfer efficiencies

can be achieved. By growing the microalgae and the bacteria on separate sides of the membrane, operation of the two cultures can be independently manipulated. Given that the microalgae is separated from the bacteria/activated sludge, the microalgal biomass, which is free of contaminants, can be easily harvested for various purposes.

The operation of the symbiotic HFMP configurations needs the intertransfer of CO<sub>2</sub> and O<sub>2</sub> through the membrane. Such transport processes depend on following conditions:

### **2.5.1. Mixing condition**

Mixing is required to keep good dispersion of solid components and ensure the homogenous condition for the two cultures. For microalgae, efficient mixing should be provided to not only produce a uniform dispersion of microalgal cells within the culture medium, but also to expose the cells periodically to light, eliminate the gradients of nutrient concentration (including CO<sub>2</sub>) and temperature. Mixing is also essential for gaseous exchange in the symbiotic HFMP system.

Mixing should be supplied to proper extents. Inadequate mixing will lead to the clumping of cells, resulting in a development of the three-phase system (gas/liquid/solid) inside the system and hence decreasing the mass transfer rate. On the other hand, high mixing rates may induce shear stress, hampering the cells' viability (Carvalho *et al.* 2006). In the proposed symbiotic HFMP, the circulation of the cultures through the shell and lumen sides of the fibers helped to mix the cultures. In addition, the external stirring was also applied in the culture tanks to ensure good mixing condition for the two cultures.



### **2.5.2 Membrane characteristics**

In order to provide a good performance for the symbiotic HFMP system, the membrane should have following properties:

- Large surface area to provide high gas transport through it. In this study, the hollow fiber configuration was employed because its surface area was reported to be much higher than the flat-sheet configuration.
- Small pore size to prevent the immobilization of microalgal and bacterial cells into the pore of the fibers and prevent the cross contamination of the cultures across the fibers.
- High hydrophobicity to restrict the permeation of the two aqueous media across the membrane, high mechanical strength to physically separate the two cultures, and good chemical resistance to survive when being in contact with washing solutions.

### **2.5.3 Viscosity**

Viscosity is governed by the formation of the cultures. It will affect the mass transfer of nutrients into cells and gas transfer through the membrane. In this study, aqueous media were used in the symbiotic HFMP. Hence their viscosity was relatively low (about 0.001 kg/m.s).

### **2.5.4. Flow velocity**

The flow velocities of the microalgal and bacterial cultures are also important for the mass transfer of CO<sub>2</sub> and O<sub>2</sub>. It should be high enough to reduce mass transfer resistance in the aqueous boundary layer at the inner and outer sides of the fiber.

However, too high flow velocity corresponds directly to higher energy costs for pumping. It may also induce shear stress and hence hamper the cells' viability. The effects of flow velocity were hence also investigated in the study.

## Chapter 3

### General Materials and Methods

#### 3.1 Microorganisms, Culture Conditions, and Chemicals

##### 3.1.1 Microalgae

*Chlorella vulgaris* ATCC 13482 was purchased from The American Type Culture Collection. *C. vulgaris* was cultivated in Bold's Basal Medium (BBM) (Andersen *et al.* 2005). The composition of BBM is listed on Table 3.1. *C. vulgaris* stock cultures were maintained on BBM agar plates and were stored at 4°C. To furnish microalgal inoculum, the cells were transferred from the agar plate to 500 – mL Erlenmeyer flask containing 250 mL of BBM. A 5% CO<sub>2</sub> - enriched air stream which had been filtered using sterilized filters (0.2 μm, Millipore) and saturated with water was bubbled into the culture flask at a flow rate of 0.5 vvm. The culture was agitated with a magnetic stirrer at room temperature (25 ± 1°C). Continuous light intensity using Light-Emitting diodes (LEDs) was provided at 200 μmol photo/m<sup>2</sup>.s (Quantum meter, Apogee Instruments) at the flask surface. The microalgal cells were cultivated for 4-5 days before being harvested for inoculation.

All media and apparatus such as pipette tips, Erlenmeyer flasks fitted with silicone bungs, Erlenmeyer flask containing ultrapure water, magnetic stirrer bars, filters and tubing used for *C. vulgaris* culturing were autoclaved at 121 °C for 20 min before use.

**Table 3.1.** Composition of BBM

Component	Concentration (mg/L)
NaNO <sub>3</sub>	250
CaCl <sub>2</sub> .2H <sub>2</sub> O	25
MgSO <sub>4</sub> .7H <sub>2</sub> O	75
K <sub>2</sub> HPO <sub>4</sub>	75
KH <sub>2</sub> PO <sub>4</sub>	175
NaCl	25
EDTA	50
KOH	31
FeSO <sub>4</sub> .7H <sub>2</sub> O	4.98
H <sub>2</sub> SO <sub>4</sub> (concentrated)	1.84
H <sub>3</sub> BO <sub>3</sub>	11.42
ZnSO <sub>4</sub> .7H <sub>2</sub> O	8.82
MnCl <sub>2</sub> .4H <sub>2</sub> O	1.44
Na <sub>2</sub> MoO <sub>4</sub> .2H <sub>2</sub> O	1.19
CuSO <sub>4</sub> .5H <sub>2</sub> O	1.57
Co(NO <sub>3</sub> ) <sub>2</sub> .6H <sub>2</sub> O	0.49

\*Note that the final pH of BBM should be 6.6

### 3.1.2 Bacteria

*Pseudomonas putida* ATTC 11172 was purchased from The American Type Culture Collection. Stock cultures were maintained on nutrient agar (Oxoid, Hampshire, UK) plates and were stored at 4°C. *P. putida* cells were grown in a chemically defined mineral medium (MM) supplemented with glucose. The composition of MM is listed in Table 3.2.

Prior to inoculation, bacterial cells were induced by transferring stock culture from the agar plate to 5 mL of MM containing 300 mg/L glucose and incubated in a water bath shaker at 30°C and at 140 rpm (GFL 1092, Burgwedel, Germany). After 8 hours, 4 mL of this pre-culture was transferred to 250 mL of MM containing 500 mg/L glucose and the contents were agitated at 140 rpm, at 30°C

using a water bath shaker. Activated cells at the exponential growth phase were then harvested for the inoculation.

**Table 3.2.** Composition of MM (Loh and Wang 1998)

Component	Concentration (mg/L)
K <sub>2</sub> HPO <sub>4</sub>	650
KH <sub>2</sub> PO <sub>4</sub>	190
NaNO <sub>3</sub>	500
MgSO <sub>4</sub> .7H <sub>2</sub> O	100
FeSO <sub>4</sub> .7H <sub>2</sub> O	5.56
(NH <sub>4</sub> ) <sub>2</sub> SO <sub>4</sub>	500
(CH <sub>2</sub> ) <sub>3</sub> N(COOH) <sub>3</sub>	15
MnSO <sub>4</sub> .H <sub>2</sub> O	5
CoCl <sub>2</sub> .6H <sub>2</sub> O	1
CaCl <sub>2</sub>	1
ZnSO <sub>4</sub> .7H <sub>2</sub> O	1
CuSO <sub>4</sub> .5H <sub>2</sub> O	0.1
H <sub>3</sub> BO <sub>3</sub>	0.1
Na <sub>2</sub> MoO <sub>4</sub> .2H <sub>2</sub> O	0.1

All media and apparatus such as pipette tips, Erlenmeyer flasks fitted with cotton plugs or silicone bungs, magnetic stirrer bars, filters and tubing that used for *P. putida* culturing were autoclaved at 121 °C for 20 min before use.

### 3.1.3 Activated sludge

Activated sludge was originally collected from Ulu Pandan MBR plant in Singapore. The activated sludge was cultivated using synthetic wastewater containing around 600 mg/L COD, 40 mg/L NH<sub>4</sub><sup>+</sup> – N and 8 mg/L PO<sub>4</sub><sup>3-</sup> – P. The composition of the synthetic wastewater is listed in Table 3.3. During the cultivation, the mixed liquor was continuously aerated at a flow rate of 0.5 vvm

and 2% of sludge was wasted per day (sludge retention time of 50 days). The pH of the mixed liquor was maintained within the range of 7.0 – 8.0.

**Table 3.3.** Composition of synthetic wastewater (Qiu and Ting 2013)

Component	Concentration (mg/L)
Glucose	600
NH <sub>4</sub> Cl	151.4
KH <sub>2</sub> PO <sub>4</sub>	35.12
CaCl <sub>2</sub> ·2H <sub>2</sub> O	19.3
MgSO <sub>4</sub> ·7H <sub>2</sub> O	71
FeSO <sub>4</sub> ·7H <sub>2</sub> O	17.4
CuCl <sub>2</sub> ·2H <sub>2</sub> O	0.07
MnCl <sub>2</sub> ·4H <sub>2</sub> O	0.13
ZnSO <sub>4</sub> ·7H <sub>2</sub> O	0.13
Na <sub>2</sub> MoO <sub>4</sub> ·2H <sub>2</sub> O	0.03
H <sub>3</sub> BO <sub>3</sub>	0.025
KI	0.033
NaHCO <sub>3</sub>	1000

### 3.1.4 Chemicals

All the chemicals used in this research were of analytical grade and purchased either from Sigma-Aldrich (St. Louis, United States) or Merck (Darmstadt, Germany).

## 3.2 Membrane Contactor and Fiber Bundle Fabrication

### 3.2.1 Gas exchange hollow fiber membrane

Hydrophobic microporous polypropylene hollow fiber membrane Accurel<sup>®</sup> PP 50/280 purchase from Membrana GmbH, Germany was used throughout the research program it possess all these properties mentioned in Section 2.5.2. Specifications for the hollow fiber membranes are given in Table 3.4.

**Table 3.4** Specifications for the hollow fiber membranes

Membrane characteristics	Values
Internal diameter ( $\mu\text{m}$ )	280
Wall thickness ( $\mu\text{m}$ )	$50 \pm 10$
Outer diameter ( $\mu\text{m}$ )	$380 \pm 35$
Average pore diameter ( $\mu\text{m}$ )	0.1
Porosity	0.6

### 3.2.2. Hollow fiber membrane contactor

The hollow fiber membrane contactor used to set up the symbiotic HFMP was fabricated by inserting the cluster of 100 hollow fiber membranes into a glass shell and sealing them on both ends of the shell with epoxy resin (Araldite, England). Specifications for the membrane contactor are given in Table 3.5. A diagram of membrane contactor is shown in Figure 3.1.

**Table 3.5** Characteristics of the membrane contactor

Characteristics	Values
Shell internal diameter	0.8 cm
Shell outer diameter	1 cm
Number of fibers	100
Effective fiber length	30 cm

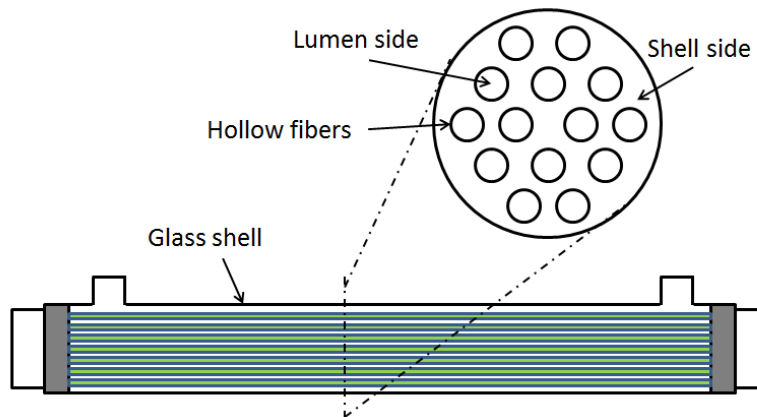


**Figure 3.1** Hollow fiber membrane contactor

### 3.2.3 Fiber bundle

The hollow fiber membrane bundles were used in the SHFMP and AS-SHFMP configurations. Bundle of 100 fibers (effective length of 9 cm) was sealed at both ends using epoxy. These two ends were then inserted into two plastic shells (inner diameter = 0.8 cm, outer diameter = 0.9 cm, length = 2 cm) to support the membranes. These shells were also sealed to bundle-ends by epoxy. A diagram of fiber bundle is shown in Figure 3.2.

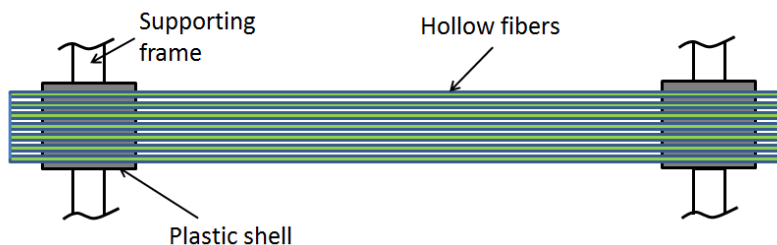


Figure 3.2. Fiber bundle

### 3.3. Sterilization of Membrane Contactor and Fiber Bundle

The membrane contactors and fiber bundles could not be sterilized by autoclaving because the epoxy layers between the fibers and the glass wall or plastic shell are easily damaged by the high temperature, and could result in a leakage during the experiment. Therefore the membrane contactors and fiber bundles were sterilized by washing the shell side and lumen side with 1M NaOH for 6 – 8 hours, followed by at least 4 times washing with autoclaved ultrapure water to flush out any remaining sodium hydroxide inside and outside the fibers. After that the membrane contactors and fiber bundles were dried in the oven (without the presence of light) at 30°C – 40°C for a few days to prevent recontamination and promote drying. This sterilization technique was effective, and no contamination



was observed in the lumen side and shell side during the operation of the symbiotic HFMP, SHFMP and in the lumen side during the operation of the AS-SHFMP.

At the end of each run in these configurations, the lumen side and shell side were again washed with 1M NaOH for 8 hours to remove the loosely attached cells on the fibers, glass shell and tubings. This was also followed by 4 - 5 times washing with autoclaved ultrapure water until the pH dropped below 7. This washing was also for re-sterilizing the contactors or bundles so that they were ready to use for the subsequent experiments.

### **3.4. Experimental Setup**

The detailed experimental setups of the baseline studies, symbiotic HFMP, SHFMP and AS-SHFMP operations were explained in the corresponding chapters. Each experiment was performed in triplicates (error bars indicates standard deviation) and duplicates (error bars were calculated as the variation of mean value between the low and high values of data points at each time point) for reproducibility.

### **3.5. Contamination Test for *C. vulgaris* Culture**

After each baseline study for suspended culture and each hollow fiber membrane photobioreactor run, the *C. vulgaris* culture was always tested for contamination by streak plate method. One loop of the microalgal culture was streaked on nutrient agar plates and the plates were then incubated at 30°C for at least 3 days to observe the presence of colonies from other microorganisms. The *C. vulgaris*

culture was axenic if no colonies of other microorganisms were found after the incubation.

### 3.6. Analytical Methods

*C. vulgaris* concentration was monitored by measuring the optical density (OD) at a wavelength of 540 nm using an ultraviolet-visible spectrophotometer (UV-1800, Shimadzu, Japan). Prior to the OD measurement, microalgal samples were diluted to an appropriate concentration so that the OD<sub>540</sub> value was within a range of 0.1 - 0.8. Microalgal biomass at different OD values was also harvested, dried and weighed. The dry cell weight (DCW) corresponded to the OD<sub>540</sub> value by a regression equation: DCW (g/L) = 0.4268 x OD<sub>540</sub> (R<sup>2</sup> = 0.9754). The daily biomass productivity was calculated by using the equation: P (g/L.day) = (X<sub>t</sub> - X<sub>0</sub>)/(t-t<sub>0</sub>), where X<sub>t</sub> and X<sub>0</sub> are the final and initial biomass concentrations (g/L) (Rodolfi *et al.* 2009).

*P. putida* growth was monitored by OD measurement at 600 nm using an ultraviolet-visible spectrophotometer (UV-1800, Shimadzu, Japan). Harvested bacterial biomass at different OD values was dried and weighed. The OD<sub>600</sub> was used to compute the biomass concentration by the formula: DCW (g/L) = 0.3815 x OD<sub>600</sub> (R<sup>2</sup> = 0.9975).

Light intensity was measured using Quantum meter (Apogee Instruments) with intensity fluctuation was less than 5%.

Dissolved oxygen (DO) concentrations (mg/L) and pH were measured using Orion 4 Star pH/DO meter couple with Orion DO probe and Orion pH probe

(Thermo Scientific). Small pH electrode (Orion, Thermo Scientific) was also used for small volume of samples.

The inner and outer surfaces of the membrane were observed by using a JSM-6700P field emission scanning electron microscope (FESEM). The protocols of removing moisture from the membrane samples and fixing the immobilized cells have been described in previous study (Li and Loh 2006).

Glucose concentrations during the experiments were measured using the Biochemistry Analyser (YSI 2700 Select, YSI (UK) Ltd).

BOD was measured using BOD sensors (VELP, Scientifica). The MLSS, COD,  $\text{PO}_4^{3-} - \text{P}$ ,  $\text{NH}_4^+ - \text{N}$ ,  $\text{NO}_2^- - \text{N}$ , and  $\text{NO}_3^- - \text{N}$  concentrations were measured according to standard methods (APHA 2012). A summary of the analytical methods is presented in Table 3.6.

**Table 3.6** Analytical methods for the determination of some parameters

Parameter	Method (APHA 2012)	Sample volume (mL)	Number of samples
MLSS	2540 B. Total Solids Dried at 103–105°C	25	3
COD	5220 D. Closed Reflux, Colorimetric Method	2.5	2
$\text{PO}_4^{3-} - \text{P}$	4500-P E. Ascorbic Acid Method	2	2
$\text{NH}_4^+ - \text{N}$	4500-NH <sub>3</sub> F. Phenate Method	2.5	2
$\text{NO}_2^- - \text{N}$	4500-NO <sub>2</sub> <sup>-</sup> B. Colorimetric method	2	2
$\text{NO}_3^- - \text{N}$	4500-NO <sub>3</sub> <sup>-</sup> B. Ultraviolet Spectrophotometric Method	2	2

## Chapter 4

### Baseline Studies for *C. vulgaris* and *P. putida*

#### 4.1 Introduction

The operation of the symbiotic HFMP involved the growth of heterotrophic and photoautotrophic microorganisms; bacterium *Pseudomonas putida* and microalga *Chlorella vulgaris* were chosen as the microbial models for the research program. *P. putida* was used because it is a harmless obligate aerobe, and it can consume sugars and other organic compounds for its growth (Memon *et al.* 2014). Due to the ability to degrade a large variety of substrates, *Pseudomonas* has become one of the major genera in activated sludge and they are present in large numbers in most wastewater treatment plants (Bitton 2005a; Gerardi 2006d).

Microalga *C. vulgaris* was selected since *Chlorella* species has been extensively studied due to its fast growth rate and easy cultivation (Illman *et al.* 2000; Liu *et al.* 2008). Moreover, the *Chlorella* biomass and its extracts have been used diversely for the production of human nutrition, animal nutrition and feed, skin care products and other high – value added chemicals as reviewed in Section 2.1.2. *Chlorella* is also credited as a potential candidate for biodiesel production because of their ability to synthesize high lipid content under certain culturing conditions (Brennan and Owende 2010). In addition, *Chlorella* sp. is commonly used in wastewater treatment applications because of its high removal capacity of such nutrients as ammonia nitrogen, nitrate nitrogen and phosphorus from many types of wastewater (Johnson and Wen 2009; Wang *et al.* 2009). *Chlorella* hence

has been evaluated as one of the most important species in the microalgal industry (Tomaselli 2004).

Prior to the design and operation of the HFMP to study the symbiotic relationship of *C. vulgaris* and *P. putida* in the HFMP, the suspension studies of *C. vulgaris* and *P. putida* were first carried out to understand the cell growths and substrate removal trends. The specific objectives of this research were:

1. For microalgae: investigate the effects of CO<sub>2</sub> concentration, CO<sub>2</sub> aeration rate and light intensity on *C. vulgaris* growth.
2. For bacteria:
  - a. Investigate the effects of oxygen supply on growth and glucose biodegradation performance of *P. putida* in batch culture.
  - b. Study the effects of different dilution rates on glucose biodegradability of *P. putida* in continuous culture.

Bubbling of CO<sub>2</sub> enriched air is a typical technology to supply CO<sub>2</sub> for microalgal photosynthesis. A series of experiments were hence conducted to determine the most suitable CO<sub>2</sub> aeration condition for *C. vulgaris* ATCC 13482. Effects of light intensity on microalgal growth were also investigated. In addition, baseline studies for suspended cultures of *P. putida* were conducted to understand their glucose biodegradation performance under batch and continuous operations. The results from microalgae and bacteria baseline studies were useful for designing the experiments during the symbiotic HFMP and SHFMP operations, and were subsequently used for the comparison with the results obtained in those systems.

## 4.2 Materials and Methods

### 4.2.1 Baseline studies on *C. vulgaris* growth

*C. vulgaris* cells were inoculated at a concentration of 60 mg/L in a 500 – mL Erlenmeyer flask containing 260 mL of BBM. The composition of BBM is listed in Table 3.1. All the microalgal cultures were cultivated at room temperature ( $25 \pm 1^\circ\text{C}$ ) under continuous stirring condition (200 rpm) and continuous illumination using LEDs. Light intensity was measured at the surface of the flask. Table 4.1 summarizes the experiments conducted to investigate the effects of different cultivation conditions on *C. vulgaris* growth. Under headspace condition (Table 4.1), there was no external aeration. In this case the microalgae-flask was fitted with the cotton plug; the microalgal culture solely relied on the atmospheric  $\text{CO}_2$  that diffused through the cotton plug for growth. Under  $\text{CO}_2$  enriched air sparging conditions,  $\text{CO}_2$  and air streams, which had been filtered, were blended to provide desired  $\text{CO}_2$  concentration (1%, 5% or 10%). The  $\text{CO}_2$  enriched air stream was then saturated with autoclaved water and bubbled into the culture flask.

**Table 4.1.** Summary of the baseline studies for *C. vulgaris*

Experiment	$\text{CO}_2$ concentration in air (%)	$\text{CO}_2$ aeration rate (vvm)	Light intensity ( $\mu\text{mol photon/m}^2.\text{s}$ )
Effects of $\text{CO}_2$ concentration	Headspace	0	200
	1%	0.5	200
	5%	0.5	200
	10%	0.5	200
Effects of $\text{CO}_2$ aeration rate	5%	0.3	200
	5%	0.5	200
	5%	0.75	200
Effects of light intensity	5%	0.5	100
	5%	0.5	200
	5%	0.5	300

Each batch culture of *C. vulgaris* was carried out for 5 days. Each experiment was performed in triplicates and duplicates (for Headspace conditions) for reproducibility. Specific growth rate ( $\mu$ , day<sup>-1</sup>) was calculated from biomass increased per unit time (Becker 1994):

$$\mu = \frac{\ln(X_1/X_0)}{t_1 - t_0}$$

where  $X_0$  and  $X_1$  are cell biomass (mg/L) at beginning ( $t_0$ ) and at end ( $t_1$ ) of selected time interval during incubation.

#### **4.2.2 Baseline studies on *P. putida* growth**

##### **4.2.2(a) Batch culture**

*P. putida* was inoculated at an initial cell concentration of 8 mg/L into 260 mL of synthetic wastewater. Synthetic wastewater was made from mineral medium (MM) supplemented with 500 mg/L glucose. The composition of MM is listed in Table 3.2. The cell cultures were agitated at 140 rpm, at 30°C using a water bath shaker. *P. putida* was grown under 2 conditions: non-aerated and aerated condition. Under non-aerated condition, 260 mL of bacterial culture was contained in a 250 – mL Erlenmeyer flask fitted with a silicone bung in order limit the diffusion of oxygen from the surrounding environment into the culture. It should be noticed that 250 – mL Erlenmeyer flask can contain maximum 300 mL of water (up to the brim). The volume of bacterial culture was chosen at 260 mL to minimize the available headspace in the 250-mL Erlenmeyer flask. On the other hand, under aerated condition, bacterial culture was contained in a 500 – mL flask and purified air was continuously sparged into the content at the flow rate of

0.5vvm. Each experiment was performed in duplicates for reproducibility (the results in duplicated did not differ by more than 10%).

#### **4.2.2(b) Continuous culture**

*P. putida* culture was operated under single-stage chemostat mode. Bacterial cells were inoculated at an initial cell concentration of 8 mg/L in a 500 – mL Erlenmeyer flask containing 240 mL of synthetic wastewater (MM supplemented with 500 mg/L glucose). The bacterial culture was agitated with a magnetic stirrer at a speed of around 200 rpm at room temperature ( $25 \pm 1^\circ\text{C}$ ) and was aerated at a flow rate of 0.5vvm. Feed was also prepared from the same synthetic wastewater (pH value was always 7). The feed stream was continuously supplied into bacteria culture using peristaltic pump (Masterflex, USA). Feed tank was stirred at room temperature ( $25 \pm 1^\circ\text{C}$ ) without aeration. The feed flow rate was adjusted to obtain desired dilution rates (D) of: 0.13, 0.17, 0.25, 0.32 and  $0.46 \text{ hr}^{-1}$ . Corresponding hydraulic retention times (HRTs) were 8.0, 5.9, 4.1, 3.1 and 2.2 hours. Batch culture of *P. putida* under the same conditions was also carried out to determine its specific growth rate at dilution rate  $D = 0$ . Each experiment was performed in duplicates for reproducibility.

### **4.3 Results and Discussion**

#### **4.3.1 Baseline studies on *C. vulgaris* growth**

##### **4.3.1(a) Effects of $\text{CO}_2$ concentration**

Carbon dioxide is one the major raw materials for the microalgal photosynthesis. Insufficient  $\text{CO}_2$  supply will cause slow microalgal growth rate, and an excess



supply of CO<sub>2</sub> may be harmful to microalgal cells. Hence, effects of different CO<sub>2</sub> concentrations on the growth of *C. vulgaris* strain used in this research were investigated. Figure 4.1 shows the temporal profiles of *C. vulgaris* growth, the depletion of NO<sub>3</sub><sup>-</sup> – N concentration, and pH change under different CO<sub>2</sub> concentrations. Table 4.2 summarizes the specific growth rate and biomass productivity of *C. vulgaris*.

**Table 4.2.** Specific growth rate and biomass production of *C. vulgaris* at different concentrations of CO<sub>2</sub> aeration

CO <sub>2</sub> concentration (%)	Specific growth rate (day <sup>-1</sup> ) *	Final biomass concentration (g/L)	Biomass productivity (g/L.day)
Headspace	0.04	0.074	0.003
1	1.07	1.05	0.198
5	1.08	1.25	0.237
10	0.87	0.89	0.165

\*Calculated from day 0 – day 1.5 (1% and 5% CO<sub>2</sub>) or from day 0 – day 2 (10% CO<sub>2</sub>)

As can be seen in Figure 4.1a, there was a significant difference in the microalgae concentration between the cultures. After 5 days of cultivation, the biomass concentration under headspace condition was only 0.074 g/L, slightly increased as compared to initial concentration (0.06 g/L). It is hence certain that atmospheric CO<sub>2</sub> in the headspace of the flask, approximately 0.0387%, was not sufficient to support the high microalgal growth rate.

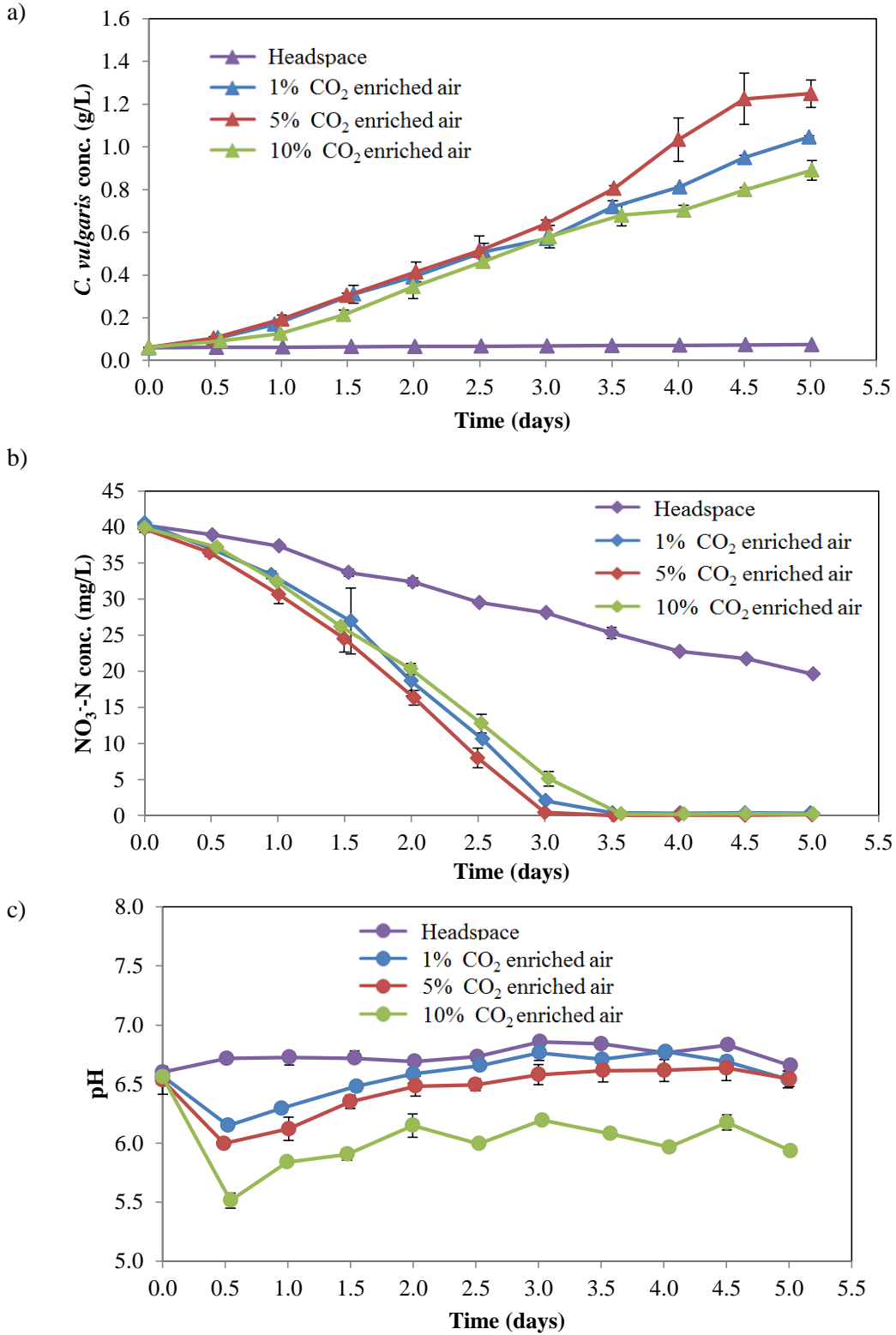
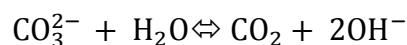
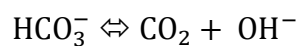
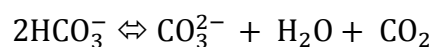


**Figure 4.1.** Effects of CO<sub>2</sub> concentration on: (a) *C. vulgaris* growth, (b) NO<sub>3</sub><sup>-</sup> – N consumption, (c) pH profile.

Microalgal growth rate was significantly improved under CO<sub>2</sub> aeration condition. Under the air streams containing 1% and 5% CO<sub>2</sub>, the microalgal growth trends were similar in the first 2.5 days, resulting in similar specific growth rates (Figure 4.1a, Table 4.2). After that, the microalgae concentration under 5% CO<sub>2</sub> enriched air sparging, however, accelerated and reached a final concentration of 1.25 g /L, significantly higher than that of 1% CO<sub>2</sub> aeration (1.05 g/L). This implied that 1% CO<sub>2</sub> in air may not provide sufficient CO<sub>2</sub> for *C. vulgaris* cells to grow. As the CO<sub>2</sub> concentration was further increased to 10%, specific growth rate and biomass concentration were significantly lower than those of 5% and 1% CO<sub>2</sub> aeration conditions (Table 4.2). Biomass productivity obtained was only 0.165 g/L.day, 30% and 17% lower than those under 5% and 1% CO<sub>2</sub> aeration conditions, respectively. The drastic decrease in microalgal growth could be due to the low culture pH under 10% CO<sub>2</sub> aeration (Figure 4.1c). When CO<sub>2</sub> is supplied to the medium, the bicarbonate-carbonate buffer system will develop to provide CO<sub>2</sub> for photosynthesis through these following reactions (Grobbelaar 2004):



These reactions suggest that during photosynthetic CO<sub>2</sub> fixation, OH<sup>-</sup> is accumulated in the growth culture, which will lead to a gradual rise in pH (Grobbelaar 2004). As shown in Figure 4.1c, under headspace condition, pH of cell culture slightly increased from 6.6 to 6.88 over the 5 days. This was due to a very small amount of CO<sub>2</sub> was assimilated during the photosynthesis. On the

other hand, the pH values of 1%, 5% and 10% CO<sub>2</sub> aeration conditions during 5 days were always maintained below pH 7 (Figure 4.1c). This was because the three cultures were continuously acidified by the CO<sub>2</sub> enriched air streams. Especially, the culture pH values under 10% CO<sub>2</sub> aeration was significant lower than those in the other two cases. This suggested that if the CO<sub>2</sub> concentration was too high, pH of the culture decreased and could cause an adverse effect on microalgal physiology (Kumar *et al.* 2010a; Kunjapur and Eldridge 2010). As a consequence, specific growth rate and biomass productivity were significantly decreased as elucidated in the case of 10% CO<sub>2</sub> aeration. The results are consistent with those reported in the literature where *C. vulgaris* were cultivated under high CO<sub>2</sub> concentrations (Chiu *et al.* 2008; Lv *et al.* 2010).

In addition to carbon source, nitrogen and phosphorus sources also play important roles in microalgal growth. Because the phosphate phosphorus (PO<sub>4</sub><sup>3-</sup> – P) concentration in BBM was provided in excess, only the nitrate nitrogen (NO<sub>3</sub><sup>-</sup> – N) concentration during the cultivation was measured. The NO<sub>3</sub><sup>-</sup> – N consumption trends were in accordance with the microalgal growth trend. As can be seen in Figure 4.1b, under headspace condition where microalgal growth rate was the slowest, only 50% of NO<sub>3</sub><sup>-</sup> – N was consumed after 5 days. On the other hand, the NO<sub>3</sub><sup>-</sup> – N concentration under 5% CO<sub>2</sub> aeration was quickly depleted after 3 days, approximately half day earlier than those under 1% and 10% CO<sub>2</sub>. It should be noted that the microalgal growth rate was reduced after 1.5 days (for 1% CO<sub>2</sub> and 5% CO<sub>2</sub>) or 2 days (10% CO<sub>2</sub>) of cultivation. This could be due to the reduction

in the  $\text{NO}_3^- - \text{N}$  concentration in the cultures. The phenomenon coincided with the results reported in literature (Aguirre and Bassi 2013; Li *et al.* 2008).

Results also show that although the  $\text{NO}_3^- - \text{N}$  concentration was depleted, microalgae under  $\text{CO}_2$  aeration condition still continued to grow. As suggested by Li *et al.* (2008), when the nitrogen source was exhausted, the microalgal cells would consume intracellular nitrogen pools such as chlorophyll molecules, proteins, nucleic acid to further support their growth.

In brief, increasing  $\text{CO}_2$  concentration can lead to higher biomass concentration, but can also result in low culture pH, which may adversely affect microalgal growth. Results obtained in this part showed that 5%  $\text{CO}_2$  in air yielded highest specific growth rate and biomass productivity (0.237 g/L.day). This  $\text{CO}_2$  concentration was hence chosen to study the effects of  $\text{CO}_2$  aeration rate and light intensity in subsequent experiments.

#### **4.3.1(b) Effects of $\text{CO}_2$ aeration rate**

Aeration rate is also an important factor to the microalgal growth. Increasing aeration rate can improve the  $\text{CO}_2$  supply, resulting in higher productivity. Besides, it can enhance internal mixing to homogenize the culture medium, promote the exposure of microalgal cells to light, remove accumulated dissolved oxygen to eliminate its toxicity to microalgae (Anjos *et al.* 2013; Zhang *et al.* 2002). The effects of aeration rate on the growth of *C. vulgaris* were investigated to determine the optimal aeration rate supporting microalgal growth. This was conducted by sparging 5%  $\text{CO}_2$ -enriched air to the microalgal culture at aeration rate of 0.3 vvm, 0.5 vvm and 0.75 vvm. Figure 4.2 shows the temporal profiles of

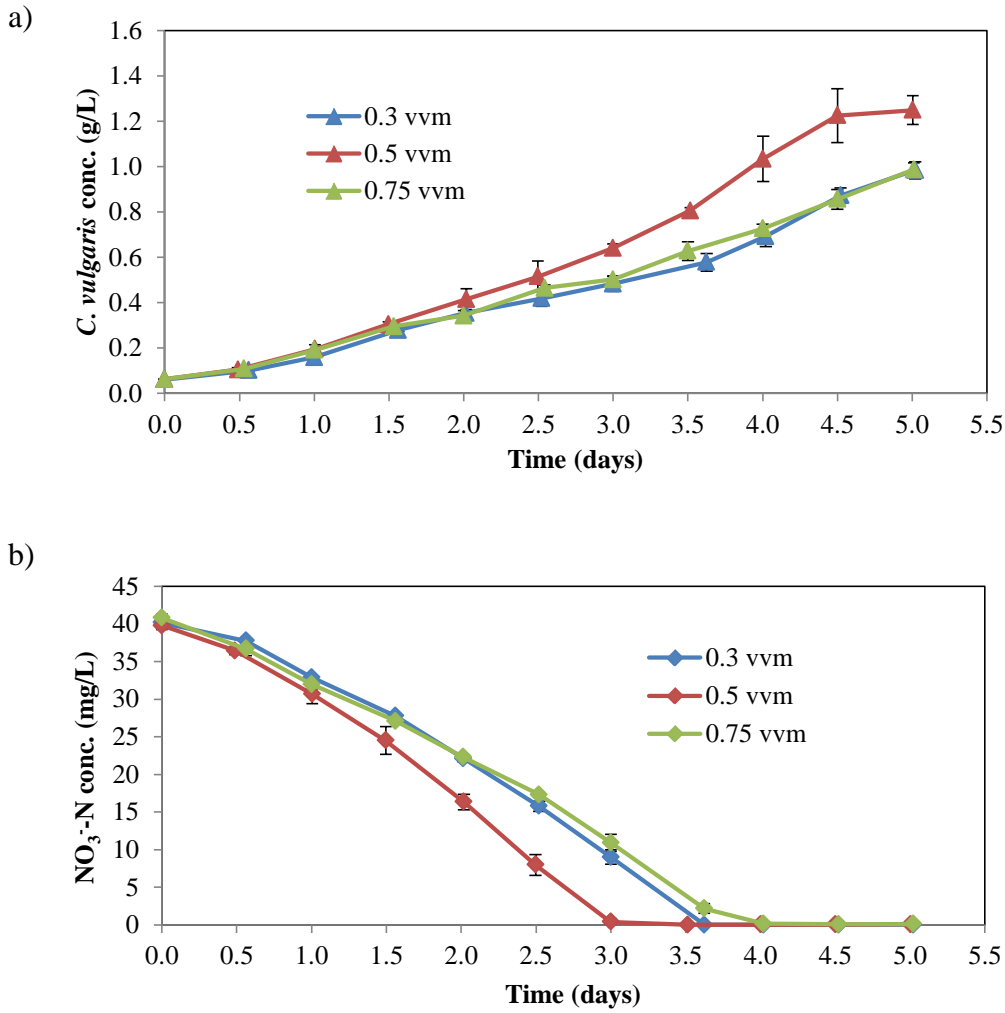
microalgae and  $\text{NO}_3^- - \text{N}$  concentrations under different  $\text{CO}_2$  aeration rates.

Table 4.3 summarizes the specific growth rate and biomass productivity of *C. vulgaris*.

**Table 4.3.** Specific growth rate and biomass production of *C. vulgaris* at different  $\text{CO}_2$  aeration rates

$\text{CO}_2$ aeration rate (vvm)	Specific growth rate ( $\text{day}^{-1}$ ) *	Biomass (g/L)	Productivity (g/L.day)
0.3	0.98	0.98	0.184
0.5	1.08	1.25	0.237
0.75	1.04	0.99	0.185

\*Calculated from day 0 – day 1.5



**Figure 4.2.** Effects of  $\text{CO}_2$  aeration rate on: (a) *C. vulgaris* growth, (b)  $\text{NO}_3^- - \text{N}$  consumption.

As shown in Figure 4.2 and Table 4.3, microalgae concentration and specific growth rate were significantly improved when the aeration rate increased from 0.3 vvm to 0.5 vvm. The  $\text{NO}_3^- - \text{N}$  consumption rate of microalgal cells under 0.5 vvm was also faster than those under 0.3 vvm. One explanation could be that the increase in aeration flow rate would increase the gas-liquid mass transfer coefficient. Moreover, higher aeration rate resulted in the higher turbulent motion of liquid, increasing the movement of cells to the region adjacent to the flask wall where the light intensity was maximum. The enhancements in light usage and gas-liquid mass transfer resulted in higher microalgae concentration and biomass productivity. However, an increase of 5%  $\text{CO}_2$  aeration rate to 0.75 vvm resulted in significantly lower biomass concentration (0.99 g/L versus 1.25 g/L) and  $\text{NO}_3^- - \text{N}$  consumption rate (Figure 4.2b). This occurred because when aeration rate was further increased to 0.75 vvm, the  $\text{CO}_2$  retention time inside the flask was reduced, the gas mixture was quickly escaped from the flask before an efficient mixing occurred. As a consequence, overall biomass productivity in the case of 0.75 vvm was significantly reduced because the majority of the supplied  $\text{CO}_2$  might not be efficiently used by microalgal cells. The results were in agreement with previous studies (Anjos *et al.* 2013; Fan *et al.* 2007).

To sum up, taking into consideration of specific growth rate and biomass productivity, the aeration rate at 0.5 vvm was the most appropriate among the aeration rates studied, and hence was selected for the next experiments.

#### 4.3.1(c) Effects of light intensity

In addition to CO<sub>2</sub> and nutrients, light intensity is another important factor for microalgal photosynthesis. Microalgal growth is limited by too low light intensity, but too much light can also be deleterious to the microalgal cells (Behrens 2005; Carvalho *et al.* 2011). Thus, it is necessary to examine the effects of light intensity on *C. vulgaris* growth. The experiment was operated in accordance with the conditions described in Table 4.1. Three microalgal cultures were continuously illuminated at different light intensities of 100, 200 and 300  $\mu\text{mol photon/m}^2\cdot\text{s}$ . In all cultures, 5% CO<sub>2</sub> enriched air was continuously sparged at aeration rate of 0.5 vvm. Figure 4.3 shows the temporal profiles of microalgae and NO<sub>3</sub><sup>-</sup> – N concentrations under different light intensity. Table 4.4 also summarizes the specific growth rate and biomass productivity of *C. vulgaris* under studied conditions.

**Table 4.4.** Specific growth rate and biomass production *C. vulgaris* at different light intensities

Light intensity ( $\mu\text{mol photon/m}^2\cdot\text{s}$ )	Specific growth rate ( $\text{day}^{-1}$ ) *	Biomass (g/L)	Productivity (g/L.day)
100	0.73	0.58	0.105
200	1.08	1.25	0.237
300	1.35	1.22	0.233

\*Calculated from day 0 – day 1.5 (200 and 300  $\mu\text{mol photon/m}^2\cdot\text{s}$ ) or from day 0 – day 2 (100  $\mu\text{mol photon/m}^2\cdot\text{s}$ )



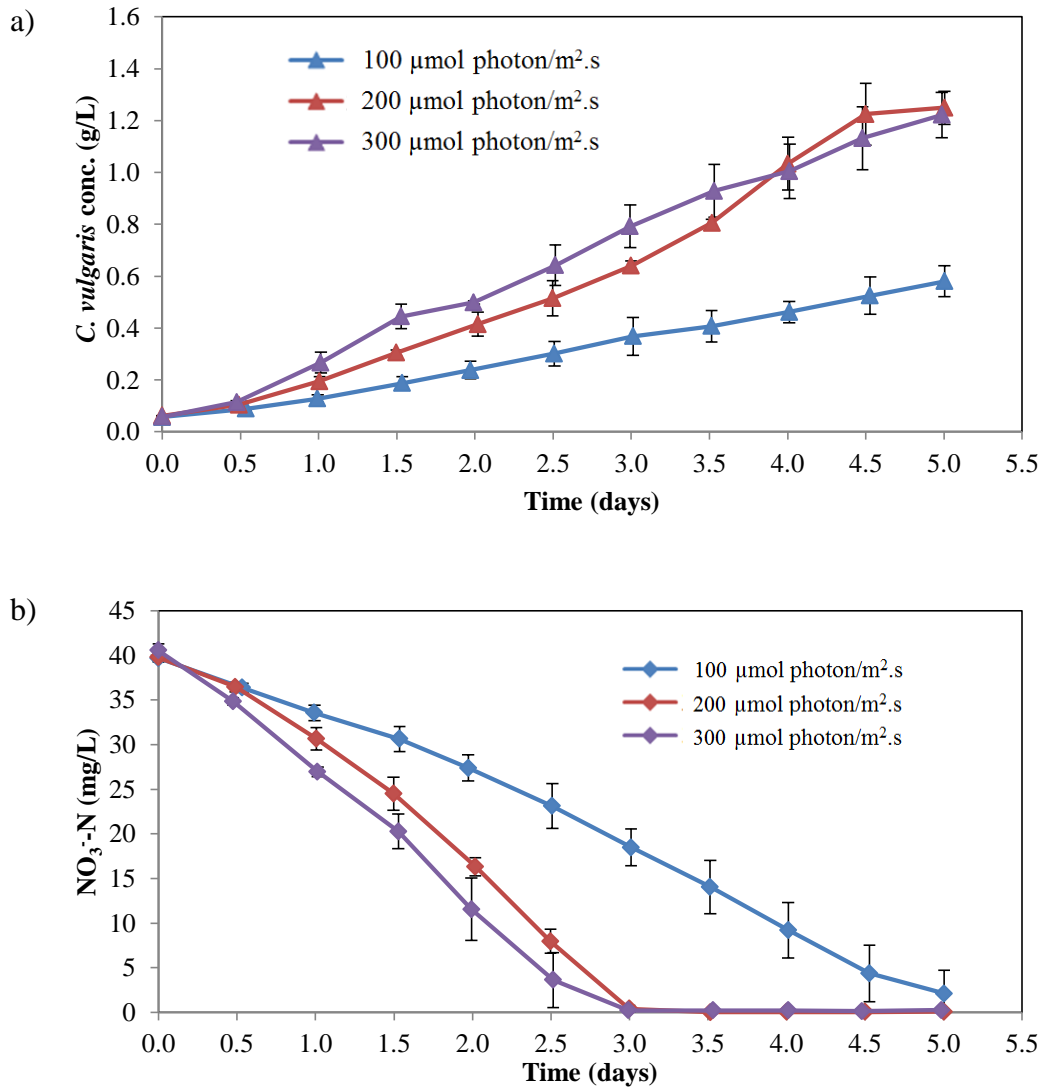


**Figure 4.3.** Effects of light intensity on: (a) *C. vulgaris* growth, (b)  $\text{NO}_3^-$ -N consumption.

As shown in Figure 4.3 and Table 4.4, light intensity at 100  $\mu\text{mol photon/m}^2\cdot\text{s}$  was not sufficient for *C. vulgaris* photosynthesis: the specific growth rate was found to be the slowest ( $0.73 \text{ day}^{-1}$ ) and biomass concentration after 5 days was only 0.58 g/L. When the light intensity increased to 200  $\mu\text{mol photon/m}^2\cdot\text{s}$ , microalgae grew at much faster growth rate ( $1.08 \text{ day}^{-1}$  versus  $0.73 \text{ day}^{-1}$ ), and final biomass concentration was improved by 116%. With the further increase in

light intensity to 300  $\mu\text{mol photon/m}^2\cdot\text{s}$  the cell growth was slightly faster in the first 1.5 days of cultivation. After that, microalgal growth rate decelerated from day 1.5 to day 5, and final biomass concentration was similar to that of 200  $\mu\text{mol photon/m}^2\cdot\text{s}$  condition (1.22 g/L). The depletion of  $\text{NO}_3^- - \text{N}$  concentration was also in accordance with the microalgal growth trend. The  $\text{NO}_3^- - \text{N}$  consumption rate under 300  $\mu\text{mol photon/m}^2\cdot\text{s}$  condition was slightly faster than that of 200  $\mu\text{mol photon/m}^2\cdot\text{s}$  condition although the  $\text{NO}_3^- - \text{N}$  concentrations in these two experiments were both depleted after 3 days. On the other hand, the  $\text{NO}_3^- - \text{N}$  content under 100  $\mu\text{mol photon/m}^2\cdot\text{s}$  condition was degraded with much slower rate and was only depleted in the 5<sup>th</sup> day of cultivation.

The results suggested that with the same  $\text{CO}_2$  supply, the increase in light intensity from 100  $\mu\text{mol photon/m}^2\cdot\text{s}$  to 200  $\mu\text{mol photon/m}^2\cdot\text{s}$  significantly enhanced microalgal growth rate and biomass productivity. The further increase to 300  $\mu\text{mol photon/m}^2\cdot\text{s}$  enhanced microalgal growth rate in the first 1.5 days, resulting in faster consumption rate of nutrients and minerals in the culture as compared to that of 200  $\mu\text{mol photon/m}^2\cdot\text{s}$ . However, after 1.5 days, the earlier exhaustion in  $\text{NO}_3^- - \text{N}$  and other minerals may induce the deceleration of microalgal growth under 300  $\mu\text{mol photon/m}^2\cdot\text{s}$  as compared to that that of 200  $\mu\text{mol photon/m}^2\cdot\text{s}$ . As a result, similar biomass productivities were obtained after 5 days of operation (0.237 g/L.day and 0.233 g/L.day, Table 4.4). Taking into consideration of operating cost for maintaining the light source at a higher intensity, and the biomass productivity, the light intensity of 200  $\mu\text{mol}$

photon/m<sup>2</sup>.s was chosen for *C. vulgaris* culture in subsequent studies in Chapter 5, Chapter 6 and Chapter 7.

### 4.3.2 Baseline studies on *P. putida* growth

#### 4.3.2(a) Batch culture

In the research program, glucose was used as an organic carbon source in the synthetic wastewater to elucidate the performance of the symbiotic HFMP. The batch culture of *P. putida* under aerated and non-aerated conditions was conducted to show the effect of the oxygen supply on the growth and glucose biodegradation potential of *P. putida*. The protocol of the experiment was described in Section 4.2.2. Glucose concentration at 500 mg/L was chosen because this concentration will be used in the operation of the symbiotic HFMP and SHFMP to emulate the BOD concentration in domestic wastewater. Figure 4.4 shows the temporal profiles of *P. putida* growth and percentage of remaining glucose under aerated and non-aerated conditions.

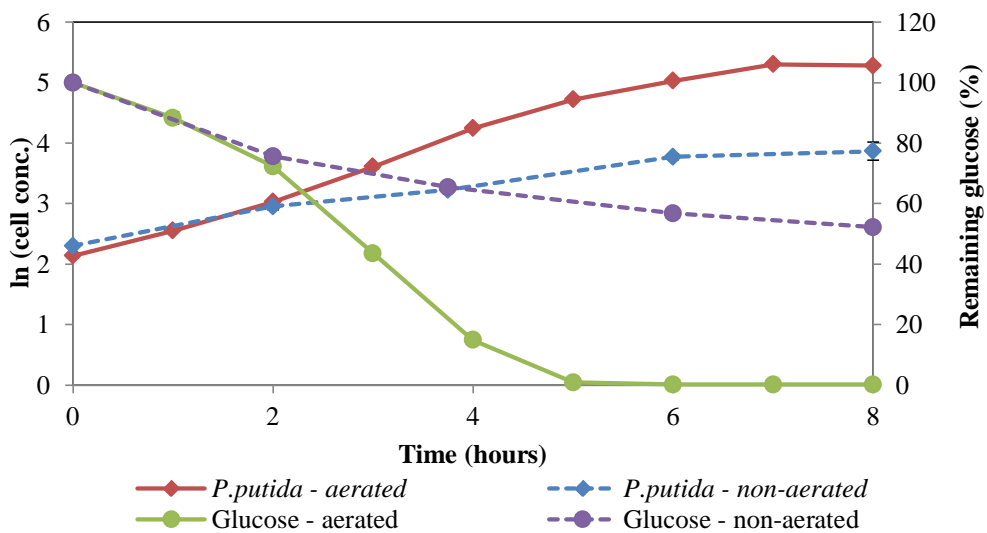


**Figure 4.4.** Temporal profiles of biomass and percentage of remaining glucose under aerated and non-aerated conditions.

As shown in Figure 4.4, in the absence of sparged oxygen, glucose biodegradation was incomplete – only 48% of glucose provided was depleted by bacteria after 8 hours. It was likely that glucose biodegradation proceeded because of the limited atmospheric oxygen available in the headspace of the flask. *P. putida* growth was also limited as a result of the incomplete glucose biodegradation. The specific growth rate of *P. putida* under non-aerated condition was only  $0.24 \text{ hr}^{-1}$ . On the contrary, when oxygen was provided in excess (aerated condition), the glucose uptake rate of *P. putida* was much improved – complete glucose degraded was achieved after 5 hours. Concomitant with the increased glucose biodegradation, specific growth rate of *P. putida* was also much higher ( $0.53 \text{ hr}^{-1}$ ). It should be noted that, after 5 hours *P. putida* continued to grow at much slower rate and eventually approached stationary phase with the highest biomass concentration at around  $0.2 \text{ g/L}$ . This was because the amount of organic carbon available for bacterial growth had been depleted, decelerating the growth of bacteria and eventually halting it.

The obtained results clearly indicated that *P. putida* ATCC 11172 is a chemoheterotrophic bacterium because it requires both oxygen and an organic carbon source in order to survive and grow. Even at low glucose concentration of  $500 \text{ mg/L}$ , sufficient oxygen supply was required to achieve complete glucose biodegradation.

#### ***4.3.2(b) Continuous culture***

As is well known, the ability of continuous operation of a bioreactor is crucial for its practical applications, especially in wastewater treatment where the feed might

be a continuous wastewater stream. Hence, prior to design the experiments for continuous operation of the SHFMP (Chapter 6), it is necessary to investigate the continuous operation of the suspended *P. putida* culture to understand the bacterial growth and glucose biodegradation potential. The study was operated in accordance with the protocol described in Section 4.2.2.

At dilution rate  $D = 0$  (batch culture), the maximum specific growth rate of *P. putida* was at  $0.45 \text{ hr}^{-1}$  (at  $25^\circ\text{C}$ ) and final biomass concentration was around  $188 \text{ mg/L}$ . Hence, single-stage chemostat culture of *P. putida* was performed at dilution rates ranged from  $0$  to  $0.46 \text{ hr}^{-1}$  to understand the bacterial growth as well as glucose consumption performance. Figure 4.5 shows an example of the effluent biomass and glucose concentration at dilution rate of  $0.13 \text{ hr}^{-1}$  (corresponding HRT of 8 hours). Figure 4.6 presents the steady state biomass concentration, glucose concentration in the effluent at different dilution rates.

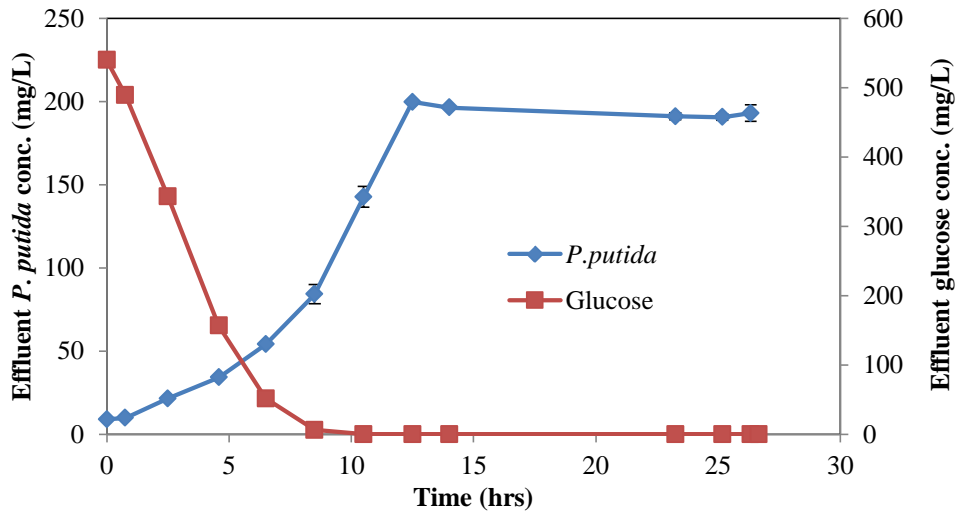


**Figure 4.5.** Temporal profiles of effluent glucose and cell concentrations at  $D = 0.13 \text{ hr}^{-1}$  (HRT = 8 hours).

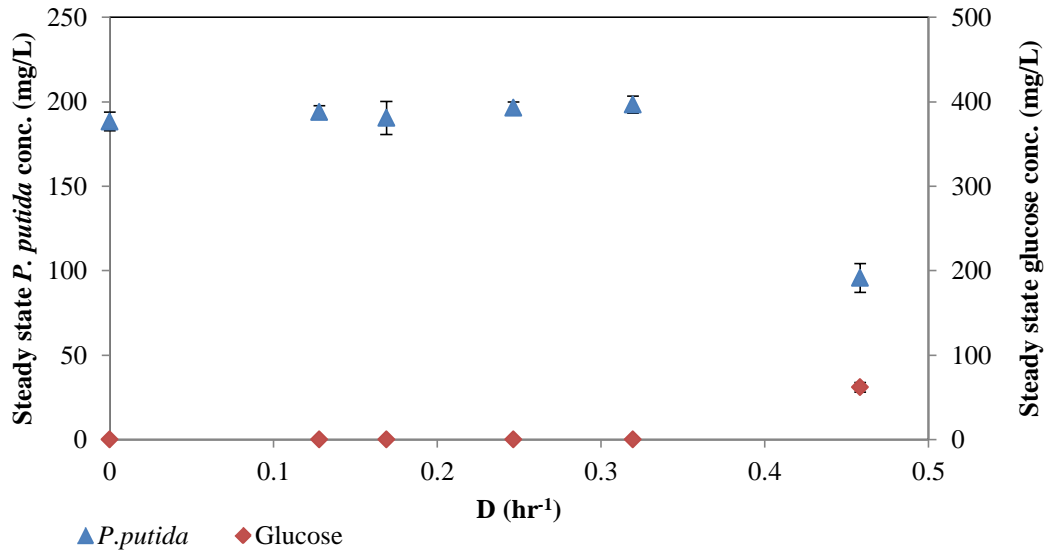


**Figure 4.6.** Steady state biomass concentration, steady state effluent glucose concentration at different dilution rates.

Results in Figure 4.5 show that under fully aeration condition, at the dilution rate of  $0.13 \text{ hr}^{-1}$ , steady state was achieved after 9 hours: cell concentration in the effluent was  $194 \text{ mg/L}$  and glucose was completely removed.

When dilution rates increased from  $0.13 \text{ hr}^{-1}$  to  $0.16$ ,  $0.25$  and  $0.37 \text{ hr}^{-1}$ , similar trends in glucose biodegradation and cell concentration were observed. Steady state effluent glucose concentration was maintained at zero, and cell concentration was constant at around  $194 \text{ mg/L}$  (Figure 4.6). However, when dilution rate was increased to  $0.46 \text{ hr}^{-1}$ , effluent bacterial concentration drastically dropped to  $96.57 \text{ mg/L}$  and steady state effluent glucose concentration significantly increased to  $61.9 \text{ mg/L}$ . This occurred because when the dilution rate was set at a value greater than  $0.45 \text{ hr}^{-1}$  (specific growth rate), the bacterial culture cannot reproduce quickly enough to sustain itself in the bioreactor and was hence washed out. This suggested that under fully aeration condition, chemostat culture of *P. putida*

should be operated at dilution rate lower than  $0.4 \text{ hr}^{-1}$  so that the bacteria can grow in a physiological steady state and complete glucose removal can be obtained.

#### **4.4 Concluding Remarks**

Suspension studies of microalgae and bacteria were conducted to investigate cell growth and substrate biodegradability of *C. vulgaris* and *P. putida*. Among the conditions studied, the 5%  $\text{CO}_2$  aeration at the flow rate of 0.5 vvm and continuous light illumination at the intensity of  $200 \text{ umol photon/m}^2 \cdot \text{s}$  were found to be optimal for *C. vulgaris* ATCC 13482 photosynthesis. The growth of *C. vulgaris* under this condition was hence used to compare with the microalgal growth in the symbiotic HFMP.

Batch culture of *P. putida* indicated that  $\text{O}_2$  plays an important role in glucose biodegradability of bacteria even at low glucose concentration (500 mg/L). Under fully aeration condition, single-stage chemostat culture of *P. putida* were able to degraded 100% of glucose in the influent when it was operated at dilution rate lower than  $0.4 \text{ hr}^{-1}$ . This result was used as a reference to design the experiments for the SHFMP in Chapter 6. Mineral medium (MM) supplemented with 500 mg/L of glucose was also used as synthetic wastewater in Chapter 5 and Chapter 6 because the glucose concentration of 500 mg/L was representative for the BOD concentration in domestic wastewater.

## Chapter 5

# Symbiotic Hollow Fiber Membrane Photobioreactor for Microalgal Growth and Bacterial Wastewater Treatment

### 5.1 Introduction

The overall objective of this part of the research program was to demonstrate the concept of the symbiotic HFMP for simultaneous microalgal growth and bacterial wastewater treatment using *Chlorella vulgaris* and *Pseudomonas putida* as microbial models. The specific objectives of this research were:

1. Investigate the feasibility of polypropylene hollow fiber membranes to perform simultaneous O<sub>2</sub> and CO<sub>2</sub> exchange (abiotic study);
2. Demonstrate the proof – of – concept for the symbiotic HFMP for simultaneous microalgal growth and bacterial wastewater treatment (biotic study); and
3. Investigate the effects of operating parameters to better understand and optimize the operation of the symbiotic HFMP performance; namely
  - (a) Effects of flow orientation;
  - (b) Effects of circulation flow velocities of microalgal culture and bacterial culture; and
  - (c) Effects of number of fibers.



## 5.2 Materials and Methods

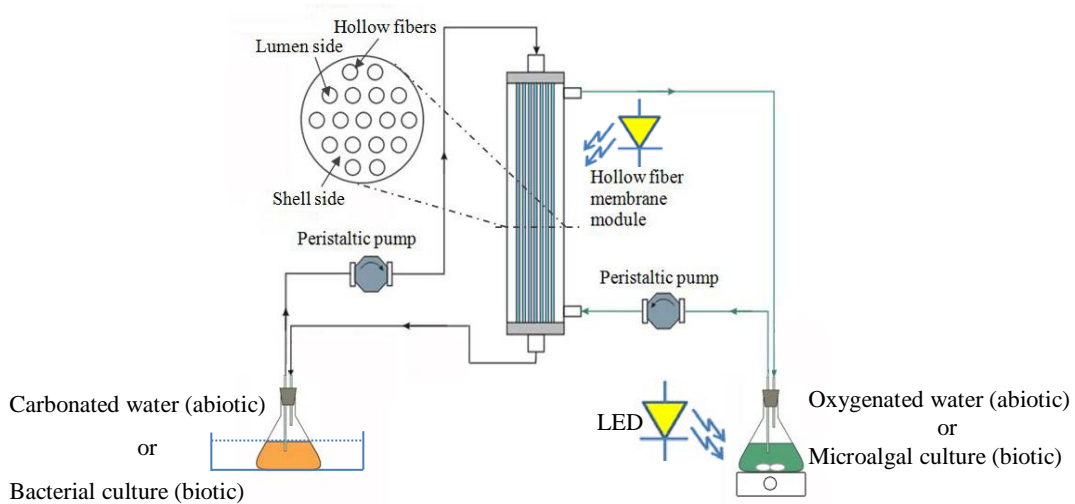
### 5.2.1 Abiotic study

Figure 5.1 shows a schematic diagram of the experimental setup for both the abiotic and biotic studies. The HFMP contactor was constructed to resemble shell – and – tube heat exchanger. Specifications for the hollow fiber membranes and the contactor are given in Table 3.4 and Table 3.5.

For abiotic experiments, the flasks (250 – mL Erlenmeyer flasks) feeding the lumen side and shell side were filled with 260 mL ultrapure water and the water in each flask was well mixed using magnetic stirrers (RC-2, Eyela, Japan). Water in the lumen-flask was continuously sparged with pure CO<sub>2</sub>, while water in the shell-flask was continuously sparged with pure O<sub>2</sub>. pH and dissolved oxygen (DO) electrodes were inserted into the two flasks. When the pH value in the lumen-flask reached pH 3.9 and DO concentration in the shell-flask reached 37 mg/L, both CO<sub>2</sub> and O<sub>2</sub> sparging were halted and the gas inlets and outlets in the two flasks were clamped. The liquid in the two flasks were then circulated through the membrane contactor for 1 hr at velocity of 3 cm/s in both the lumen and shell sides using two peristaltic pumps (BT100-2J and BT600-2J, Longerpump). The flow direction of oxygenated water and carbonated water was operated in countercurrent mode as shown in Figure 5.1. The temporal profiles of DO concentration and pH in the two flasks were recorded. The pH values were used to estimate the dissolved inorganic carbon (IC) concentration (mmol/L) in abiotic experiment based on carbonate equilibrium chemistry. The equilibrium

and the equilibrium constants values used in this study have been described elsewhere (Valdés *et al.* 2012). The experiment was performed in triplicates.

### 5.2.2 Symbiotic HFMP operation



**Figure 5.1.** Schematic diagram of the symbiotic HFMP

In the case of the proof – of – concept (biotic) study, the flow direction of microalgal culture and bacterial culture was first operated in countercurrent mode as shown in Figure 5.1.

The microalgal culture was circulated at 3 cm/s, in the shell side of the membrane contactor to reduce its travelling time in the light deficient zone. The microalgal cells were inoculated at a concentration of 60 mg/L in a 250-mL Erlenmeyer flask containing 260 mL of BBM, and agitated at a speed of around 200 rpm with a magnetic stirrer at room temperature ( $25 \pm 1^\circ\text{C}$ ). Continuous light intensity using LEDs was provided at  $200 \mu\text{mol photon/m}^2.\text{s}$  around the flask surface and along the HFMP module. Microalgal samples were collected daily for the determination of cell concentration.

The flask feeding the lumen side contained 260 mL of synthetic wastewater inoculated with 8 mg/L *P. putida*. The contents were agitated at 140 rpm, at 30°C using a water bath shaker. Mineral medium (MM) supplemented with 500 mg/L of glucose (corresponding to  $BOD_5 = 330 \pm 8.3$  mg O<sub>2</sub>/L based on *P. putida*) was used as synthetic wastewater. Bacterial culture was circulated through the lumen side of the contactor at a superficial velocity of 3 cm/s. Bacterial samples were periodically collected to determine the bacteria concentration and glucose concentration. Every 8 hours, the spent bacterial culture in the lumen side was withdrawn and replaced with 260 mL of fresh synthetic wastewater. Bacteria that remained in the reactor (tubing, fibers) served as the inoculum for subsequent cycles. All shell side and lumen side connections were made using polytetrafluoroethylene (PTFE) tubing as PTFE is not permeable to O<sub>2</sub> and CO<sub>2</sub>. The reactor run was conducted for 5 days.

It should be noticed that 250 – mL Erlenmeyer flask can contain maximum 300 mL of water (up to the brim). The volumes of microalgal culture and bacterial culture were chosen at 260 mL to minimize the available headspace in the 250-mL Erlenmeyer flasks. The inoculum sizes of microalgae and bacteria were chosen so that the initial inoculum ratio was 7.5 (DCW:DCW) based on the study of Muñoz *et al.* (2003a). After every 8 hour when the old bacterial culture was replaced with fresh synthetic wastewater, this inoculum ratio would change because of the increase in microalgae concentration and the changes in the initial suspended bacteria concentration.

Specific growth rate of microalgae was calculated from the exponential growth phase over the first 1.5 – 2 days. The pH of bacterial and microalgal cultures was monitored periodically but was not adjusted during the run because they were all within acceptable ranges for microbial growth. For instance, the pH of *P. putida* culture ranged between 6 – 7, while that of *C. vulgaris* varied from 6.5 – 8.0.

### **5.2.2 (a) Proof – of – concept (PoC) experiment**

To demonstrate the proof – of – concept of the symbiotic HFMP, for the first 2 days, 260 mL of autoclaved water in the shell-flask was circulated through the shell side of the module at a superficial velocity of 3 cm/s to examine glucose biodegradation by *P. putida* in the absence of photosynthetic oxygenation. Thereafter, the autoclaved water was replaced with 260 mL of *C. vulgaris* culture at 60 mg/L inoculum size. Continuous light intensity using LEDs was provided at 200  $\mu\text{mol photon/m}^2\cdot\text{s}$  around the flask surface and along the HFMP module. The HFMP was then operated for the next 5 days.

### **5.2.2 (b) Effects of flow orientation**

The operation of the symbiotic HFMP was examined in 2 different flow orientations:

Configuration 1 (C1): microalgal culture was circulated in the shell side at superficial velocity at 3 cm/s (corresponding flow rate was 70 mL/min) and bacterial culture was circulated in the lumen side at superficial velocity of 3 cm/s (corresponding flow rate was 11 mL/min). Continuous light intensity using LEDs

was provided at 200  $\mu\text{mol photon/m}^2\cdot\text{s}$  around the flask surface and along the HFMP module.

Configuration 2 (C2): microalgal culture was circulated in the lumen side at superficial velocity of 3 cm/s (corresponding flow rate was 11 mL/min), and bacterial culture was circulated in the shell side at superficial velocity at 3 cm/s (corresponding flow rate was 70 mL/min). Continuous light intensity using LEDs was provided at 200  $\mu\text{mol photon/m}^2\cdot\text{s}$  around the flask surface.

### 5.2.2 (c) Effects of operating parameters

Table 5.1 summarizes the experiments conducted to investigate the effects of operating parameters on the performance of the HFMP setup. Experimental sets A, B and D were conducted using the C2 orientation.

**Table 5.1.** Summary of experiments to investigate effects of operating conditions

Experimental set	Number of fibers	Flow velocity (cm/s)		Study the effects of
		Shell side	Lumen Side	
A1	100	3	2	Lumen side flow velocity
A2	100	3	3	
A3	100	3	4	
A4	100	3	6	
B1	100	2	3	Shell side flow velocity
B2	100	3	3	
B3	100	4	3	
D1	100	3	3	Number of fibers
D2	200	3	3	

Each experimental run in HFMP was carried out in triplicates for reproducibility.

## 5.3 Results and Discussion

### 5.3.1 Abiotic study

In the symbiotic HFMP, the hollow fiber membranes should not only allow gas exchange between the cultures, but they should also serve to physically separate the microalgal culture and the bacteria culture. The HFMP was fabricated using polypropylene Accurel<sup>®</sup> PP 50/280 membranes, chosen for 2 reasons apart from gas exchange functionality: (1) the pore size of 0.1  $\mu\text{m}$  prevents the immobilization of microalgal and bacterial cells into the pores of the fibers and prevents the cross contamination of the cultures across the fibers, and (2) the hydrophobicity of the fibers restricts the permeation of the two aqueous media across the membranes.

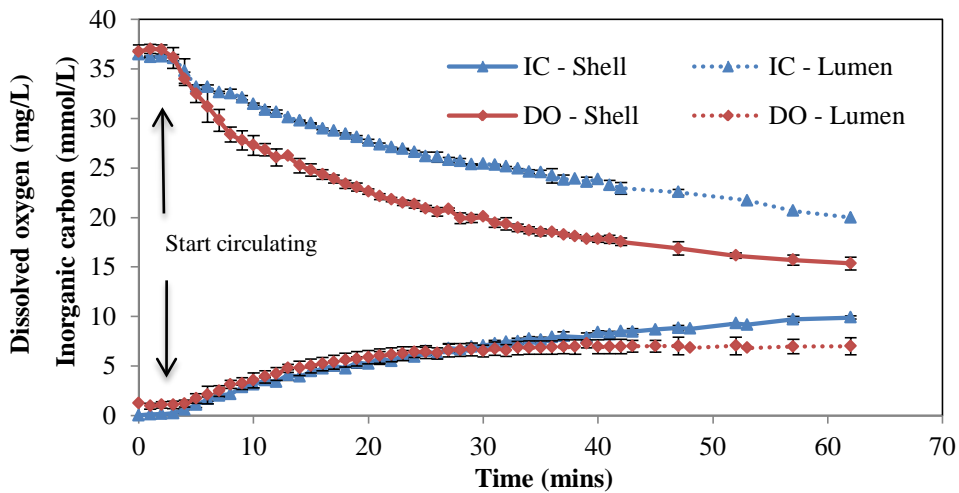


**Figure 5.2.** Abiotic experiment: (a) dissolve oxygen (DO) and inorganic carbon (IC) concentration profiles in the shell-flask and lumen-flask. Error bars indicate standard deviation from the mean of triplicates.

In this abiotic study, the HFMP was tested for its simultaneous  $\text{CO}_2$  and  $\text{O}_2$  exchange. Figure 5.2 shows the dissolved oxygen (DO) and inorganic carbon (IC)

concentration profiles over time. IC concentration was used as an indication of the amount of dissolved CO<sub>2</sub> in water, which was present as H<sub>2</sub>CO<sub>3</sub>, HCO<sub>3</sub><sup>-</sup> and CO<sub>3</sub><sup>2-</sup> species. Before circulation, water in lumen side flask was saturated at an IC concentration of 36.3 mmol/L and DO concentration of 1.07 mg/L. The amount of DO (1.07 mg/L) was much lower than the saturated DO concentration of 7 – 8 mg/L at 1 atm and 25°C because of the CO<sub>2</sub> sparging into the water, stripping much of the DO. In the shell-flask, the saturated concentration of DO was around 37 mg/L and IC concentration was about 0.14 mmol/L. It can be seen from Figure 5.2 that upon circulation of the water from both flasks through the HFMP, both IC and DO in the lumen flask and shell flask, respectively, quickly decreased. During the first 15 minutes of circulation, when the concentration gradients across the hollow fiber membrane were the greatest, IC concentration in the lumen-flask decreased from 36.3 mmol/L to 28.8 mmol/L at an average rate of 0.5 mmol/L.min while the IC concentration in the shell-flask increased from 0.14 mmol/L to 5.0 mmol/L at an average rate of 0.33 mmol/L.min. In the shell-flask, DO decreased from 37 mg/L to 23.9 mg/L at an average rate of 0.87 mg/L.min, while the DO in the lumen-flask increased from the initial 1.07 mg/L to 5.39 mg/L at an average rate of 0.29 mg/L.min. Subsequently, the decrease in IC and DO in both flasks was slower as the concentration gradients across the membranes decreased. At steady state after 1 hr of circulation, concentrations in both flasks stabilized. In the shell flask, DO stabilized at 15.5 mg/L and IC was increased to 9.88 mmol/L. In the lumen-flask, IC stabilized at 20 mmol/L and DO was increased to 7 mg/L. It is clear that the polypropylene hollow fiber

membranes used facilitated simultaneous gas exchange of O<sub>2</sub> and CO<sub>2</sub> as a result of concentration gradients across the membranes.

Since *C. vulgaris* could also grow heterotrophically on organic carbon sources such as glucose and glycerol, the HFMP was also tested for the glucose diffusion from the lumen to the shell side. Water containing glucose (at 500 and 1000 mg/L) was circulated through the lumen, and pure water was circulated through the shell side of the HFMP. It was found that the glucose concentration in lumen-flask remained unchanged at both tested glucose concentrations and there was no glucose in the shell-flask (data not shown), confirming there was no glucose penetration through the polypropylene membranes, as a result of the hydrophobicity of the membranes.

### **5.3.2 Proof – of – Concept**

The HFMP was operated in accordance with the protocol described in Section 5.2.2 to demonstrate the feasibility of photosynthetic oxygenation and the existence of symbiotic relationship between *P. putida* and *C. vulgaris*. The HFMP was initially operated for 6 eight-hour cycles, during which 500 mg/L glucose was circulated through the lumen and only water circulated in the shell side. This was conducted to show the effect of the lack of photosynthetic oxygenation on the growth and biodegradation potential of *P. putida*. From the 7<sup>th</sup> cycle onwards (up to 21 cycles), the shell side was circulated with *C. vulgaris* inoculated BBM solution. During these cycles, oxygen was not provided to the *P. putida* side, and carbon dioxide was not provided to the *C. vulgaris* side. Glucose solution was replaced every 8 hours in the lumen side, while *C. vulgaris* was continuously



circulated through the shell side without replacement. Figure 5.3 shows the temporal profiles of the experimental data obtained.

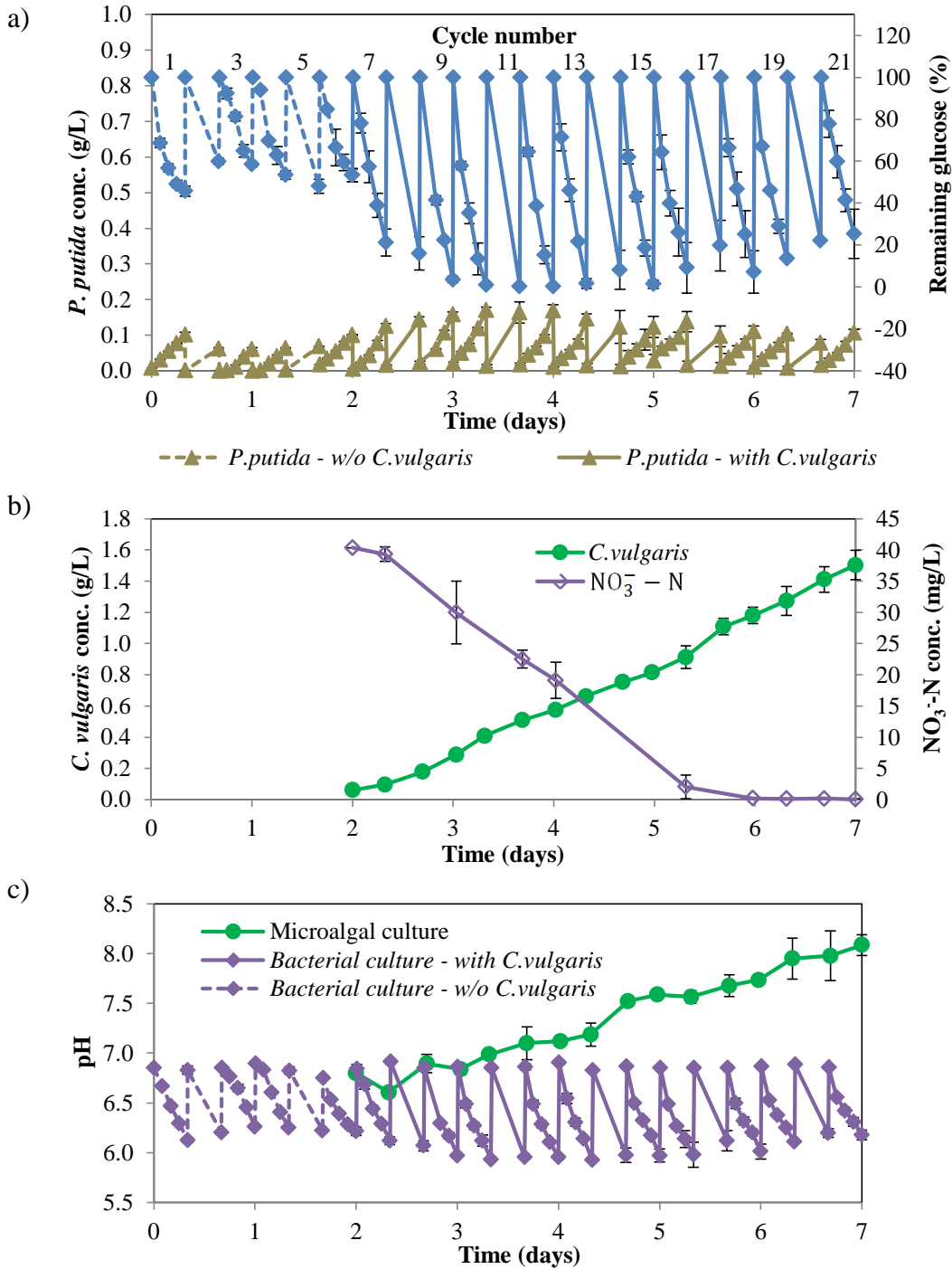


**Figure 5.3.** Temporal profiles of (a) *P. putida* biomass and glucose concentration, (b) *C. vulgaris* biomass and  $\text{NO}_3^- - \text{N}$  concentration, (c) pH in the symbiotic HFMP. Day 0 – 2: without *C. vulgaris* culture (square dot line); day 2 – 7: with the presence of *C. vulgaris* culture (solid line).

Figure 5.3a shows the biodegradation of glucose, as well as the accumulation of *P. putida* during each cycle. During the first 6 cycles, in the absence of sparged oxygen and photosynthetic oxygenation, glucose biodegradation was incomplete - only 40 to 54% of the glucose provided was depleted by the bacteria. It was likely that glucose biodegradation proceeded because of the limited oxygen available from the headspace of the lumen-flask. *P. putida* growth was also limited as a result of the incomplete glucose biodegradation.

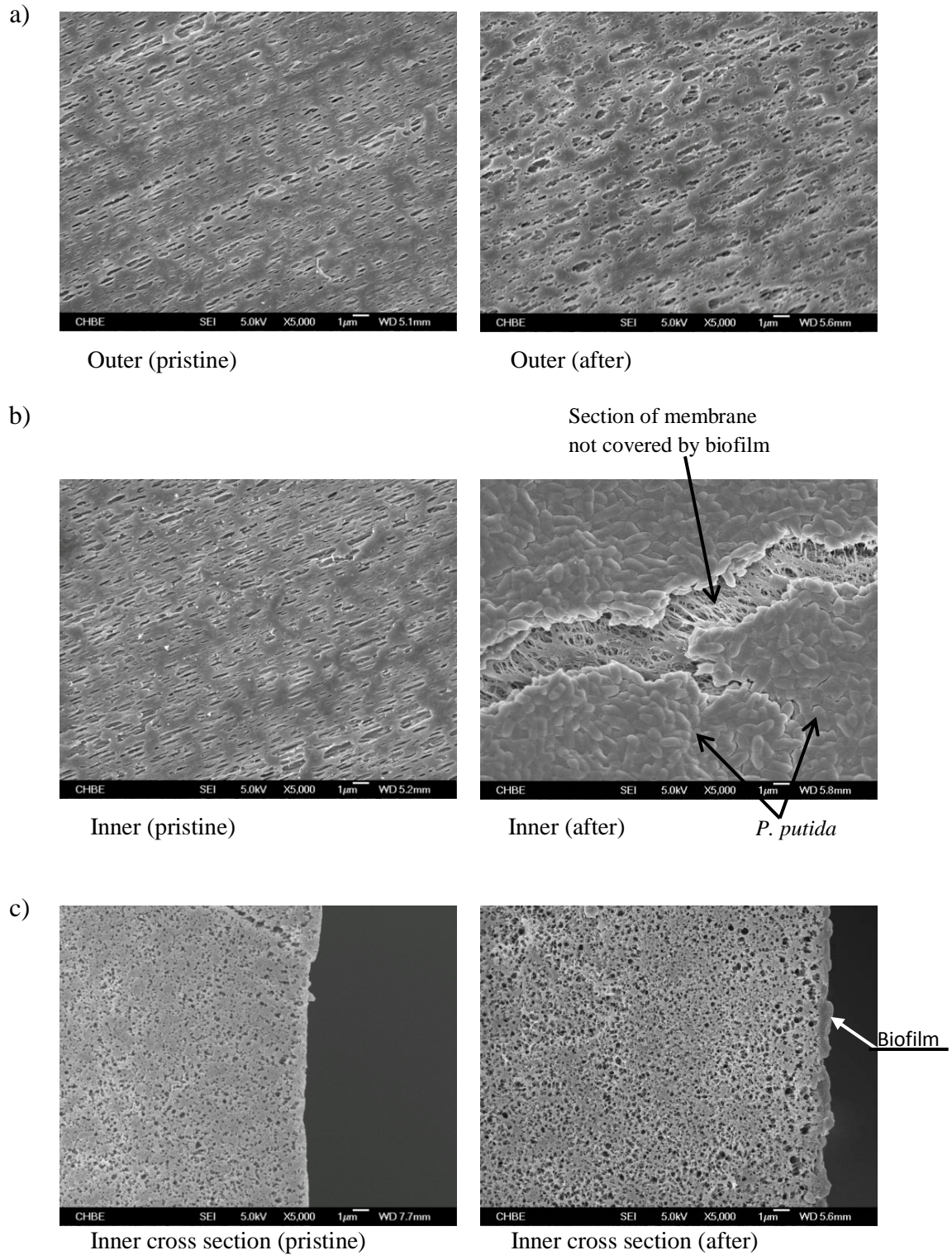
These results are consistent with the baseline studies discussed in Section 4.3.2, in which the non-aerated batch culture of *P. putida* could only biodegrade 48% of the glucose fed. Figure 5.3c, pH in the lumen-flask decreased from an initial value of 6.9 to about 6.2 during the first 6 cycles, the decrease of which was not deemed detrimental to *P. putida* growth. pH decrease during glucose biodegradation by *P. putida* has been well documented (Loh and Wang 1998). From cycle 7 onwards, when *C. vulgaris* was circulated through the shell side of the HFMP, Figure 5.3a shows that the amount of glucose biodegradation increased from 79% in cycle 7 to 100% in cycle 10. From cycles 10 to 15, complete glucose biodegradation was achieved. Concomitant with the increased glucose biodegradation, *P. putida* growth was also much higher in each cycle from 7 to 15. During these cycles, pH decreased from 6.9 to about 6 (Figure 5.3c). Given that there was no external supply of oxygen to the system, complete glucose biodegradation and consequential bacterial growth could only have resulted from photosynthetic oxygenation provided by the shell side *C. vulgaris*.

Figure 5.3b shows the temporal profiles of *C. vulgaris* growth and the depletion of  $\text{NO}_3^- - \text{N}$  concentration in the shell-flask. It can be seen that there was gradual growth of the microalgae from cycle 7 onwards. *C. vulgaris* grew with a specific growth rate of  $1.48 \text{ day}^{-1}$  and reached a final biomass concentration of  $1.5 \text{ g/L}$  after the 5 days of circulation.  $\text{NO}_3^- - \text{N}$  concentration was completely depleted after about 3.5 days of circulation. Since there was no external supply of  $\text{CO}_2$ , and glucose could not permeate the polypropylene membranes, carbon needed for microalgae growth must have been sequestered from the lumen side, i.e.  $\text{CO}_2$  generated by *P. putida* during glucose biodegradation. By comparing the amount of microalgae grown in this study against the baseline studies described in Section 4.3.1, it is clear that *C. vulgaris* growth here was not due to  $\text{CO}_2$  sequestered from the headspace of the shell-flask. With reference to Figure 4.1, the profile of *C. vulgaris* growth in this study better matched that for batch cultivation under continuous sparging of 5%  $\text{CO}_2$  enriched air. In fact, *C. vulgaris* growth was better in the HFMP than in the batch culture at the same inoculum size and the same provision of light irradiation. *C. vulgaris* growth had approached stationary phase after 4.5 days despite continuous air sparging, while the microalgae continued to grow up to the 5<sup>th</sup> day of operation. In using the HFMP, much of the  $\text{CO}_2$  present in the system was available to the microalgae, while in the case of air sparging, much of the supplied  $\text{CO}_2$  could have vented and lost to the atmosphere. Figure 5.3c shows the pH change in the shell-flask during *C. vulgaris* growth. It can be seen that the pH increased from 6.5 to about 8 over the 5 days. This occurred because of the accumulation of hydroxyl ions ( $\text{OH}^-$ ) during

photosynthetic CO<sub>2</sub> fixation. The increase in pH in the HFMP was more drastic than that under CO<sub>2</sub> aeration (Figure 4.1c) possibly because the amount of CO<sub>2</sub> received from the lumen was not enough to acidify the microalgal culture.

It is interesting to note glucose biodegradation and bacterial growth during cycles 16 – 21. Right up to cycle 15, glucose biodegradation was complete at 100%. However, from cycle 16 to 21, glucose biodegradation decreased from 91 to 75%. As a consequence, the amount of bacteria biomass accumulation during those cycles also dropped. We suspected that biofilm formation could have something to do with this decrease in biodegradation efficiency. It is to be noted that biofilm formation is inevitable in membrane bioreactors. To investigate the reason for this apparent decrease, the Field-Emission Scanning Electron Microscopy (FESEM) pictures were taken of the inner cross-sections, inner and outer surfaces of the hollow fiber membranes pristine, and at the end of the last cycle (cycle 21).

Figure 5.4 shows the FESEM pictures obtained. It can be seen that the microporous structure of the Accurel<sup>®</sup> 50/280 membranes used is generally uniform throughout the membrane thickness, and the inner and outer surfaces of the membranes were similar in structure when pristine. At the end of cycle 21, the outer surfaces of the membranes remained relatively clean (Figure 5.4a) suggesting that *C. vulgaris* did not form biofilm to adhere to the outer surfaces.



**Figure 5.4.** Membrane morphology of Acurrel® 50/280 hollow fiber membrane: pristine and after 7-day operation.

Although *Chlorella* species have been reported to be anchorage-dependent under certain conditions (Irving and Allen 2011; Johnson and Wen 2010), *C. vulgaris* used in this study remained largely in suspension (planktonic) with adequate mixing. In addition, EDTA in the BBM medium might have also prevented the attachment of the microalgae since EDTA has been reported to cause bacterial cell dispersion from biofilm (Banin *et al.* 2006) and EDTA is also one of the recommended cleaning agents for membranes (Nguyen *et al.* 2012).

On the other hand, it can be seen that *P. putida* had formed significant biofilms on the hydrophobic membrane surfaces, possibly due to hydrophobic interactions, as well as the excretion of extracellular polymeric substances (EPS) that enhanced biofilm formation (Jahn *et al.* 1999). Figure 5.4b and 5.4c clearly show that the biofilm of *P. putida* had covered the inner surface of the membranes. It should be noted that the thickness of the biofilm shown in the pictures did not reflect the actual biofilm thickness because before FESEM scanning, chemical fixation and dehydration had been performed, and that significantly reduced the biofilm thickness. A more suitable method to visualize actual biofilm thickness could be the use of Confocal Scanning Laser Microscopy (CSLM) as this allows a non-destructive visualization of the fully hydrated microbial biofilm without the need for harsh chemical fixation or embedding techniques (Costerton *et al.* 1995; Lawrence *et al.* 1991). Using CSLM, it has been reported that biofilms are typically highly hydrated, open structures composed of a high fraction of EPS and spaces (Lawrence *et al.* 1991; Moller *et al.* 1996). The large void spaces and channels present in the biofilm structure increase the influx of substrate and

nutrient to the inner parts of the biofilm and facilitate the efflux of wastes (Tolker-Nielsen and Molin 2000). It was anticipated that the initial formation of the *P. putida* biofilm on the inner membrane surfaces could have been advantageous because the bacteria could immediately consume oxygen that had permeated through for the biodegradation of glucose. This consequently resulted in a steeper concentration gradient that accelerated the oxygen transfer from the shell side to the lumen side. After each cycle when the spent glucose medium was removed, the attached biofilm served as the inoculum for the next cycle. This inoculum size increased over subsequent cycles as the biofilm buildup increased. The combination of increased O<sub>2</sub> supply from the microalgae (due to increased microalgae concentration in the shell side), the increase of inoculum (biofilm thickness), with consequential accelerated O<sub>2</sub> transfer contributed to the enhanced glucose biodegradation rates during cycles 7 to 15. However, as the biofilm thickness increased further, and cells aged within the biofilm, an increasing fraction of the biofilm cells could become non-viable (Tresse *et al.* 2003). As the fraction of these non-viable cells became a significant composition of the biofilm, the EPS components also became more cross-linked and tighter (Hwang *et al.* 2008). When this happened, the biofilm became a mass transfer barrier, impeding the mass transfer fluxes of both CO<sub>2</sub> and O<sub>2</sub>. Concomitant with this, glucose biodegradation potential decreased, as observed from cycles 16 to 21. It is expected that some form of membranes washing will have to be performed during repeated cycles of the HFMP. More details of this membrane washing regime will be discussed in Section 5.3.4 of this thesis.

Notwithstanding, results of the operation of the HFMP indicated that there is a clear symbiotic relationship between the bacterial and the microalgal cultures in which photosynthetic activity has provided sufficient oxygen for glucose biodegradation and at the same time, carbon dioxide resulting from the latter was made available for microalgae photosynthesis. Glucose biodegradation and microalgal growth had been achieved in the absence of external supply of O<sub>2</sub> and CO<sub>2</sub>. Proof –of – concept has been demonstrated and the next few sections sought to optimize the operation of this HFMP with regards to a number of operating and bioreactor characteristics.

### **5.3.3 Effects of flow orientation**

Since the symbiotic HFMP was developed based on the symbiotic relationship between two different microbial cultures, the flow orientation could also critically affect the HFMP performance. Therefore, the effects of flow orientation were investigated via two configurations (C1 and C2) described in Section 5.2.2. Figure 5.5 shows the temporal profiles of *C. vulgaris* and *P. putida* growths, and the depletions of glucose and NO<sub>3</sub><sup>-</sup> – N concentrations in these two configurations. Table 5.2 presents a summary of microalgal growth and glucose biodegradation in experiments C1, C2 and PoC.

Figure 5.5a shows the biodegradation of glucose and the concentration of *P. putida* during each cycle of C1. In this configuration, microalgal culture was circulated in the shell side at flow velocity of 3 cm/s and bacterial culture was circulated in the lumen side at flow velocity of 3 cm/s.



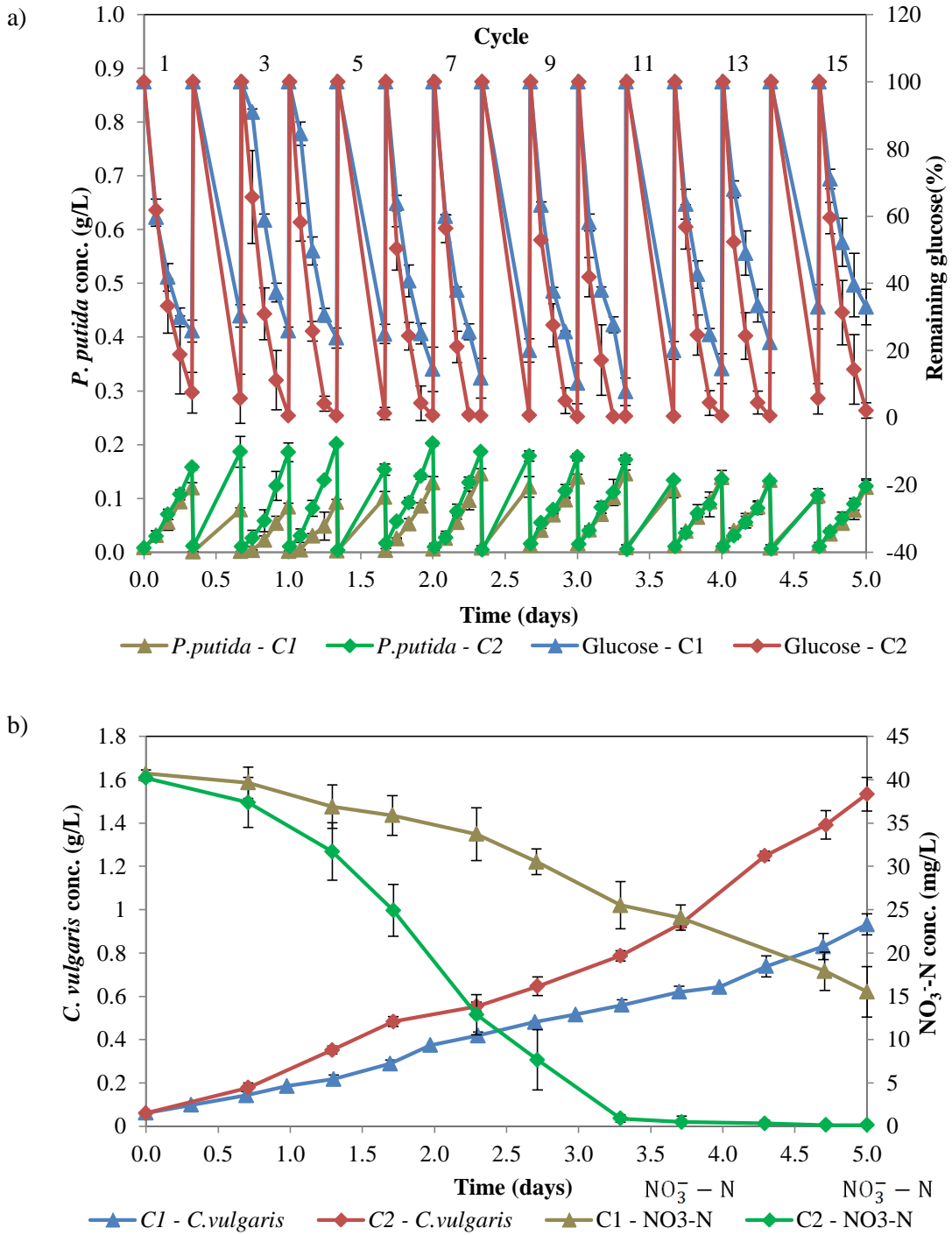


**Table 5.2.** Summary of microalgal growth and glucose biodegradation under different experimental conditions

	Experiment		
	PoC	C1	C2
<b>Final microalgae concentration (g/L)</b>	1.50	0.93	1.54
<b>Microalgal biomass productivity (g/L.day)</b>	0.289	0.174	0.294
<b>Average percentage of glucose degraded (per 8-hour cycle) (%)</b>	90*	79	98

\*Calculated from day 2 to day 7

Results show that *P. putida* degraded 70 – 76% of glucose content in the first 5 cycles. From cycle 6 – 10, the percentage of glucose degraded in C1 was increased and reached highest removal efficiency at cycle 9 (90%) and cycle 10 (92%), consistent with the increase of the bacterial growth. In the last 5 cycles, the glucose biodegradation severely decreased from 85% to 67%. As a consequence, the amount of bacterial biomass accumulation during those cycles also dropped. This was likely due to the formation of biofilm on the inner surface of the fibers.

The average percentage of glucose degraded per 8-hour cycle in C1 was just 79%, much lower than that of PoC (90%, Table 5.2). This low glucose biodegradation affected *C. vulgaris* growth. After 5 day, the final microalgae concentration was only 0.93 g/L, biomass productivity was 0.174 g/L.day, around 60% of biomass productivity in PoC. Although the bacterial cultures were both circulated in the lumen side in experiments C1 and PoC, the performance of the symbiotic HFMP in experiment PoC was better. Possible explanations could be: firstly, *P. putida* cells in experiment PoC had been accumulated in the HFMP for 6 successive

cycles in the first 2 days (Figure 5.3a), hence when *C. vulgaris* culture was introduced at the beginning of cycle 7, the initial bacteria concentration in this cycle should be higher than that in cycle 1 of C1. Secondly, as being circulated in the lumen side for 2 days prior to the introduction of *C. vulgaris* culture, *P. putida* cells in PoC were probably acclimatized to the new growth condition in the symbiotic HFMP. Hence, in the symbiosis with *C. vulgaris* from day 3 onward, they could have become more active than those in experiment C1.

In C2, microalgal culture was circulated in the lumen side, and bacterial culture was circulated in the shell side with the same superficial velocities as in C1. Light was only provided around the microalgae flask. As revealed in Figure 5.5a, significant improvement in glucose biodegradation was obtained. Except the first two cycles where 94% of glucose was degraded, the glucose content in subsequent cycles 3 – 13 was completely removed. Even in the last 2 cycles, the percentage of glucose degraded was just slightly dropped to 94% and 98%. The average percentage of glucose degraded per 8-hour cycle was 98% (Table 5.2), significantly higher than those of C1 and PoC. Concomitant with the increased glucose biodegradation, *P. putida* growth in C2 was also much higher than in C1 in each cycle from 1 – 10. However, the *P. putida* growth in C2 from cycles 11 - 15 decreased although glucose was completely degraded in these cycles. The glucose biodegradation rate in each cycle of C2 was significantly higher than that of C1 because when circulating bacteria in the shell side of contactor, the outer surface of hollow fiber membrane provided a larger surface area for the bacterial attachment (358 cm<sup>2</sup> versus 263.8 cm<sup>2</sup>). Since more bacteria would attach on the

outer surface as compared to the inner surface, the instantaneous consumption of the  $O_2$  on the surface would be enhanced, creating a much steeper  $O_2$  concentration gradient across the membranes, and consequently accelerating the mass transfer of  $O_2$  from the lumen side more efficiently, as mentioned in part 5.3.2.

Obviously, the attachment of bacteria on the outer surface of the fiber would result in the formation of biofilm and eventually act as a mass transfer resistance to the  $O_2$  and  $CO_2$  exchange. However, the negative effect of biofilm formation on the outer surface could be less serious than on the inner surface. It was reported that the thickness of biofilm formed by *P. putida* R1 on polyvinyl difluoride cubes was around 30  $\mu m$  after 5 days of cultivation, and increased up to 120  $\mu m$  after 12 days (Pedersen *et al.* 1997), thick enough to narrow the inner diameter of the hollow fiber membranes in this study or partially block it. Hence, circulate bacteria in the shell side would not only benefit the system performance but also the life span of the hollow fibers. Results from Figure 5.5a shows that the adhesion of bacteria onto the hydrophobic membranes occurred in C2 since cycle 11, reflecting by the reduction of bacterial biomass accumulation during cycles 11 – 15. However, the negative effect of the biofilm on glucose biodegradation rate was not obvious until the last cycle of C2.

*C. vulgaris* growth in C2 was also remarkably improved as compared to that of C1. As can be seen in Figure 5.5b and Table 5.2, the biomass productivity in C2 was 0.294 g/L.day, 69% higher than that of C1. The  $NO_3^- - N$  consumption trend of microalgae was also in accordance with the microalgal growth. Results show

that the  $\text{NO}_3^- - \text{N}$  concentration in C2 was completely depleted after 3.3 days, while due to slower microalgal growth rate, 15.5 mg/L  $\text{NO}_3^- - \text{N}$  was still remained in the microalgal culture of C1 after 5 days. The higher *C. vulgaris* growth in C2 could be attributed to the higher amount of  $\text{CO}_2$  obtained from the shell side. This better photosynthesis capacity resulted in higher  $\text{O}_2$  production, which in turn induced the faster glucose uptake rate of *P. putida*.

Another advantage of flow orientation in C2 is that *C. vulgaris* did not form the biofilm to adhere to the inner surface of the membranes, the negative effects of biofilm formation in the lumen side hence can be avoided. Besides, although being circulated in the lumen of the fibers where the light illumination was limited, *C. vulgaris* growth in C2 was similar to that of PoC and remarkably outperformed that of C1, suggesting that the travelling time of microalgal cells inside the hollow fibers (or in the dark zone) may not significantly affect their growth.

The results obtained in this study showed that circulating microalgal culture in the lumen side and bacterial culture in the shell side significantly improved the symbiotic HFMP performance in terms of glucose biodegradation as well as microalgal growth. The negative effect of bacterial biofilm was also minimized. Hence, the flow orientation of microalgal and bacterial cultures as in configuration 2 was used in subsequent studies.

#### **5.3.4 Effects of flow velocities**

In the symbiotic HFMP,  $\text{CO}_2$  and  $\text{O}_2$  were produced by bacteria and microalgae, and were then transferred to the other side of the membrane. The mass transfer

involves 3 sequential steps: first, the CO<sub>2</sub>/O<sub>2</sub> diffuses out of the liquid to the membrane surface. Second, it diffuses into the gas-filled pores in the walls of the hydrophobic hollow fibers. And third, when the CO<sub>2</sub>/O<sub>2</sub> reaches the other wall of the fibers, it diffuses into the surrounding liquid in the other side (Yang and Cussler 1986). Thus, the moving of CO<sub>2</sub> from the shell side to lumen side (and vice versa for O<sub>2</sub>) through a hydrophobic membrane encounters 3 individual resistances in series: the two aqueous phase boundary layers at the two sides of the membrane, and the gas-filled membrane (Ferreira *et al.* 1998; Gabelman and Hwang 1999). At increasing flow velocities, the thickness of boundary layer is reduced, resulting in lower mass transfer resistance and hence higher gas transfer rates to the liquid (Kumar *et al.* 2010b; Yang and Cussler 1986).

Since the amount of O<sub>2</sub> and CO<sub>2</sub> produced by microorganisms in the symbiotic HFMP was not abundant as in the continuous air sparging systems, sufficient flow velocities for lumen side and shell side need to be determined to ensure adequate transfer of O<sub>2</sub> and CO<sub>2</sub> to support microbial growths as well as minimum pumping energy. To investigate the effects of flow velocities on the glucose biodegradation kinetics and microalgal growth in the symbiotic HFMP, experimental sets A and B were conducted (Table 5.1). For experiments A1 – A4, the shell side superficial velocity was kept constant at 3 cm/s (70 mL/min) while the lumen side superficial velocity ranged from 2 cm/s (7.5 mL/min) to 6 cm/s (22 mL/min) to determine the suitable flow velocity in the lumen side. Similarly, for experiments B1 – B3 the shell side flow velocity was varied from 2 cm/s to 4

cm/s (47 mL/min to 93.5 mL/min) while maintaining the flow in the lumen side at the velocity determined in experimental set A.

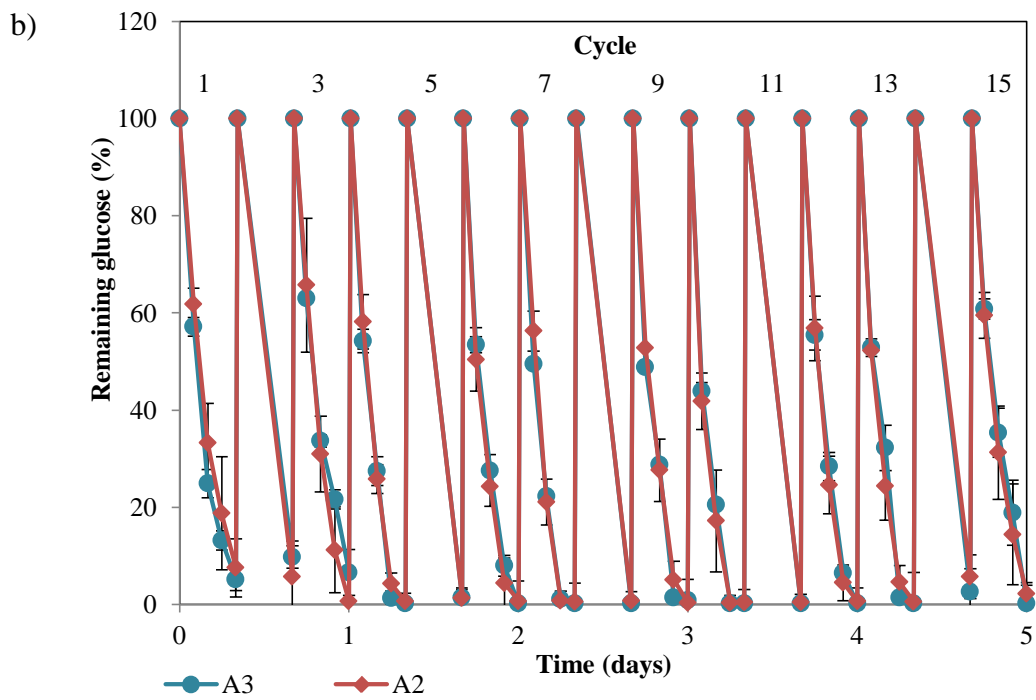
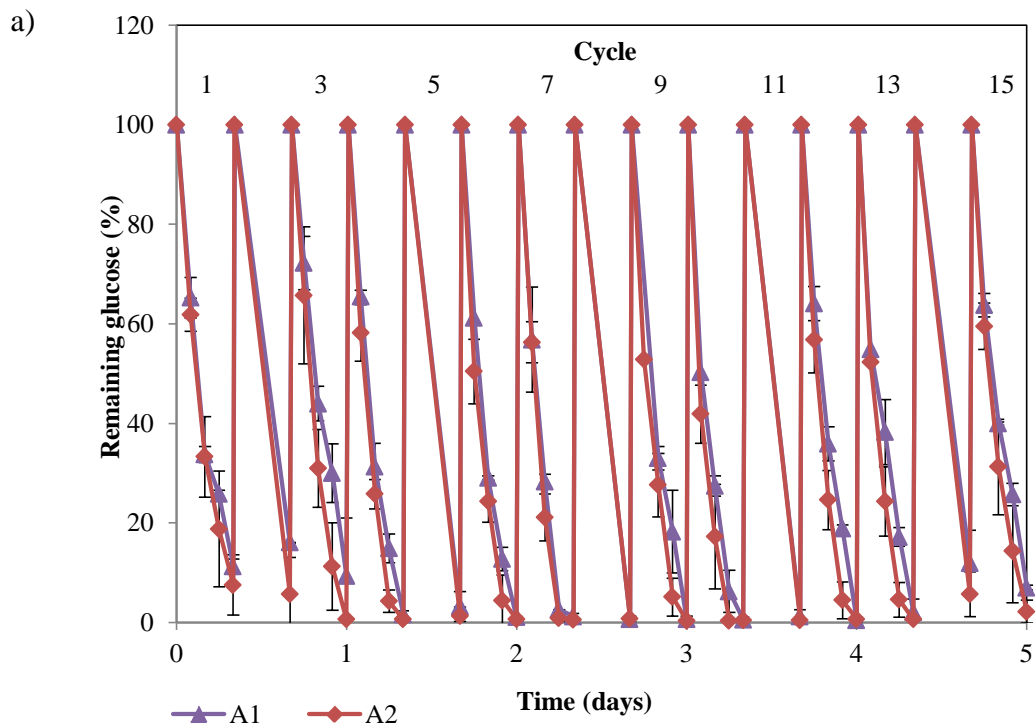
### 5.3.4(a) Effects of lumen side flow velocity

The effects of changes in the lumen side flow velocity on glucose biodegradation and microalgal growth are shown in Figure 5.6 and Table 5.3.

**Table 5.3.** Summary of microalgal growth and glucose biodegradation in experimental set A

	Experiment			
	A1	A2	A3	A4
<b>Specific growth rate of microalgae (day<sup>-1</sup>)</b>	1.05	1.22	1.11	1.25
<b>Final microalgae concentration (g/L)</b>	1.41	1.54	1.51	1.51
<b>Microalgal biomass productivity (g/L.day)</b>	0.268	0.294	0.289	0.289
<b>Number of cycles with complete glucose degradation*</b>	9	12	11	15
<b>Average percentage of glucose degraded (per 8-hour cycle) (%)</b>	95.5	98	98	99

\* Cycle with complete glucose degradation was defined when 98 – 100% of the supplied glucose was removed





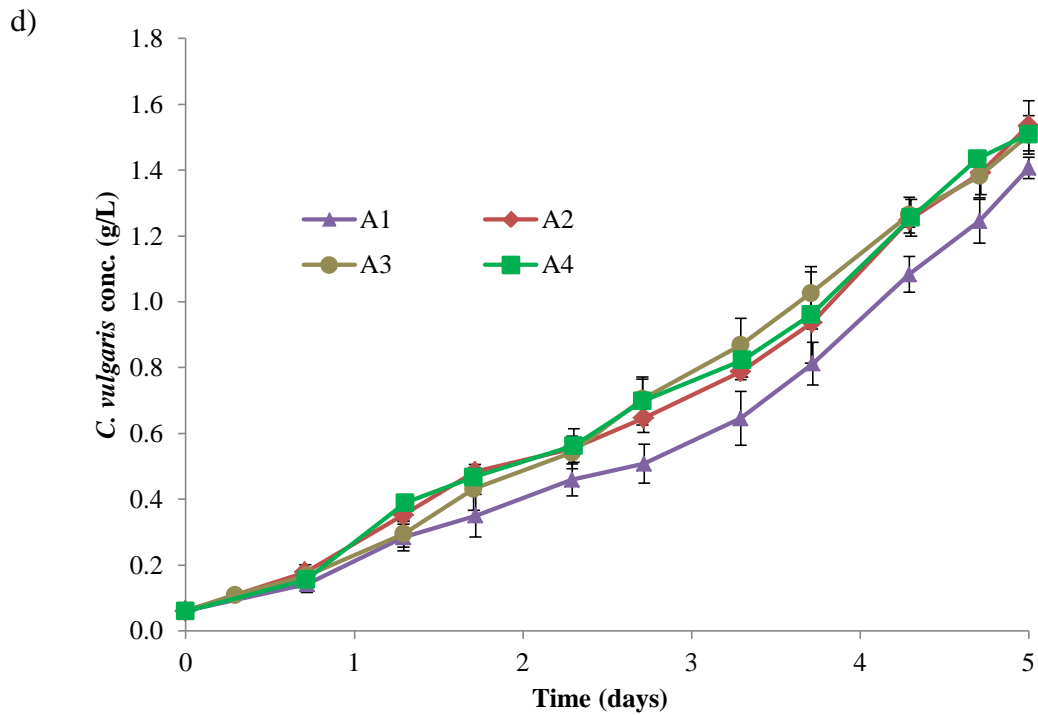
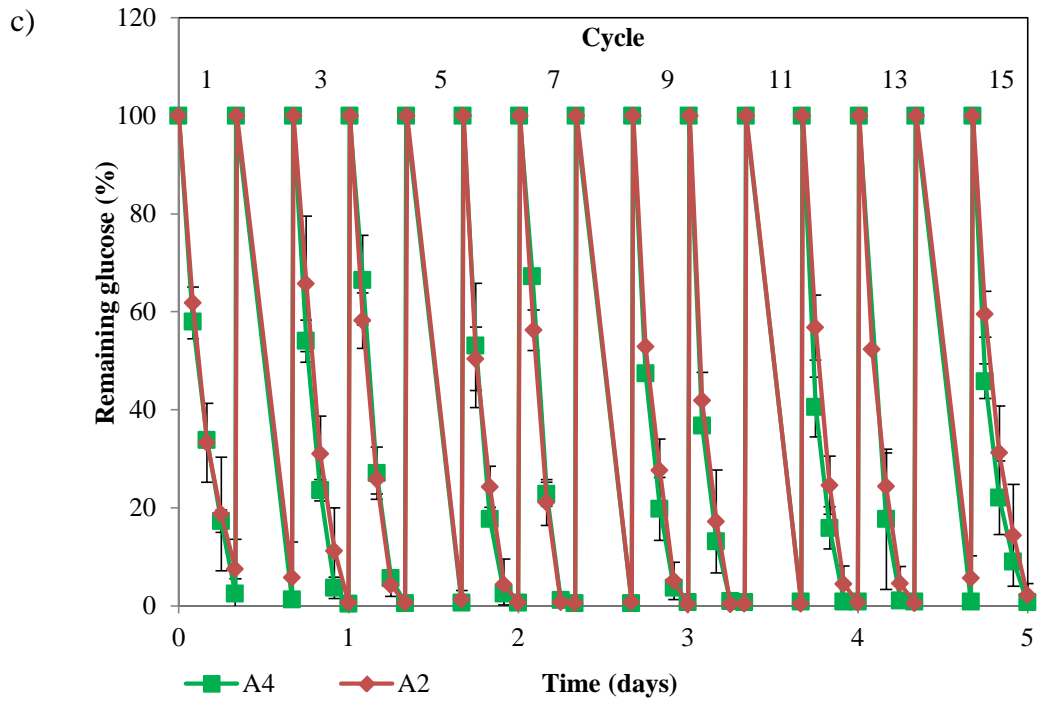


**Figure 5.6.** Effects of lumen side flow velocity on glucose biodegradation and microalgal growth in the symbiotic HFMP: temporal profiles of (a) percentage of remaining glucose in A1 and A2, (b) percentage of remaining glucose in A2 and A3, (c) percentage of remaining glucose in A2 and A4; (d) *C. vulgaris* concentration.

### *A1 and A2 comparison*

As can be seen in Figure 5.6a, A1 had 9 cycles whose glucose was completely depleted within 8 hours (cycles 4 – 13 except cycle 5). However, the glucose uptake rates of A2 were significantly faster than A1 in several cycles such as 2 – 4, 9 – 15. Especially, at the 6<sup>th</sup> hour in cycle 3, 4, 6, 9, 12, 13, *P. putida* in A2 consumed more than 90% of glucose fed while around 13 – 30% of supplied glucose was still remained in A1's corresponding cycles ( $p < 0.05$ ). In addition, glucose biodegradation in A1 dropped to 88 – 93% in the last two cycles. This suggested that the decrease of lumen side flow velocity to 2 cm/s compromised the mass transfer, decelerating the glucose biodegradation rate. As a result, the number of cycles with complete glucose degradation was only 9, and average percentage of glucose degraded per 8-hour cycle was just 95.5%, lower than those of A2 (12 cycles and 98%, Table 5.3).

In addition, due to the slower lumen side velocity in A1, the diffusion of CO<sub>2</sub> from the inner membrane surface to the lumen side liquid was also affected, resulting in significantly lower specific growth rate and final *C. vulgaris* concentration as compared to those of A2 (Figure 5.6d and Table 5.3). As shown in Figure 5.6d, after the 1<sup>st</sup> day, the difference in microalgae concentration between A1 and A2 was quite significant and consistent until the 5<sup>th</sup> day. The microalgal growth trends were also similar to those reported in the membrane carbonation photobioreactor (Kim *et al.* 2011). It was concluded that when the circulation flow rate of microalgal culture through the membrane module

increased, delivery rate of Ci (inorganic carbon including  $\text{CO}_{2(\text{aq})}$ ,  $\text{HCO}_3^-$ , and  $\text{CO}_3^{2-}$ ) were enhanced, resulting in higher biomass concentration.

#### *A2 and A3 comparison*

When the lumen side velocity increased from 3 cm/s to 4 cm/s, there was no significant difference in glucose consumption trends between A2 and A3 (Figure 5.6b), resulting in the identical average percentage of glucose degraded per 8-hour cycle (Table 5.3). *C. vulgaris* growth trends in A2 and A3 were also similar as shown in Figure 5.6d and Table 5.3.

#### *A2 and A4 comparison*

In experiment A4, the lumen side velocity was further increased to 6 cm/s. As can be seen in Figure 5.6c, glucose biodegradation in cycles 1, 2 and 14 of A4 was slightly higher than that in A2's corresponding cycles. This resulted in 15 cycles with complete glucose degradation and slightly higher average percentage of glucose degraded per 8-hour cycle (99% in A4 versus 98% in A2 and A3, Table 5.3). However, the microalgal growth trend in A4 did not differ from that of A2 and A3. In fact, the final microalgal biomass concentrations and biomass productivities in experiments A2, A3 and A4 were similar (Table 5.3).

In short, the increase in lumen side velocity resulted in a lower mass transfer resistance in the aqueous boundary layer at the inner side of the fiber. This shortened the diffusion period of  $\text{O}_2$  from the lumen side liquid to the membrane surface and also accelerated the diffusion of  $\text{CO}_2$  from the membrane surface to the lumen side liquid. As a result, the glucose uptake rates and *C. vulgaris*

growths in A2, A3 and A4 were improved as compared to those in A1. However, there were no significant differences in glucose biodegradation rates and microalgal growth trends when the lumen side velocity increased from 3 cm/s to 4cm/s and 6 cm/s. Lumen side flow velocity at 3 cm/s was hence chosen because it was high enough to ensure high microalgal growth as well as complete removal of 500 mg/L glucose in the synthetic wastewater.

#### ***5.3.4(b) Effects of shell side flow velocity***

The effects of changes in the shell side flow velocity on glucose biodegradation and microalgal growth are shown in Figure 5.7 and Table 5.4.

##### ***B1 and B2 comparison***

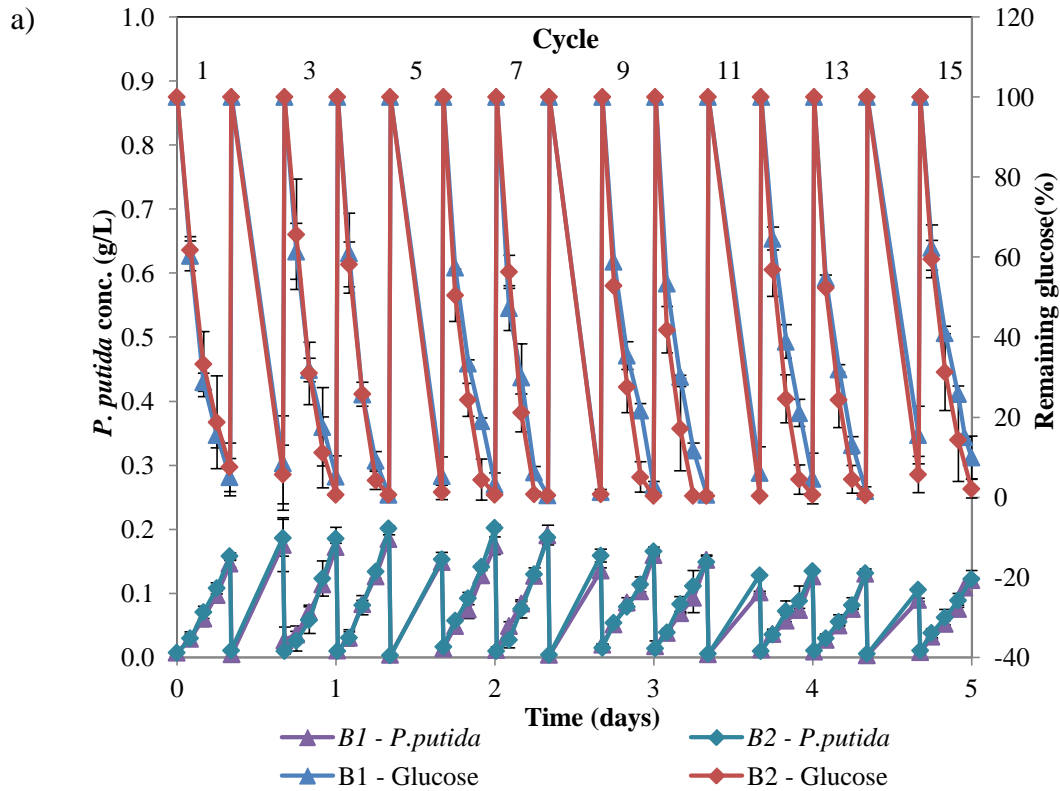
As can be seen in Figure 5.7a, glucose biodegradation trends in the first 8 cycles of B1 and B2 were quite identical. However, from cycle 9 (day 2.7) onwards, the glucose uptake rates in B1 were slower than B2. Results showed that during cycles 9 – 14, after 6 hours, more than 95% of glucose had been degraded in each cycle of B2, while 12 – 22% of glucose was still remained in those of B1.

Similar trend was also observed for microalgae growth in B1 and B2. As can be seen in Figure 5.7c, the two microalgal growth curves were overlapped each other from day 0 to day 2.3. After this point, they started diverging and final *C. vulgaris* concentration of B2 was 1.54 g/L, significantly higher than that of B1 (1.4 g/L, Table 5.4). It should be noted that the amount of bacterial biomass accumulation was decreased from cycle 8 in both B1 and B2 (Figure 5.7a), inferring the formation bacterial biofilm on the outer surface of hollow fiber membranes.

**Table 5.4** Summary of microalgal growth and glucose biodegradation in experimental set B

	Experiment		
	B1	B2	B3
Final microalgae concentration (g/L)	1.40	1.54	1.26
Microalgal biomass productivity (g/L.day)	0.267	0.294	0.240
Number of cycles with complete glucose degradation*	6	12	12
Average percentage of glucose degraded (per 8-hour cycle) (%)	95	98	97

\* Cycle with complete glucose degradation was defined when 98 – 100% of the supplied glucose was removed



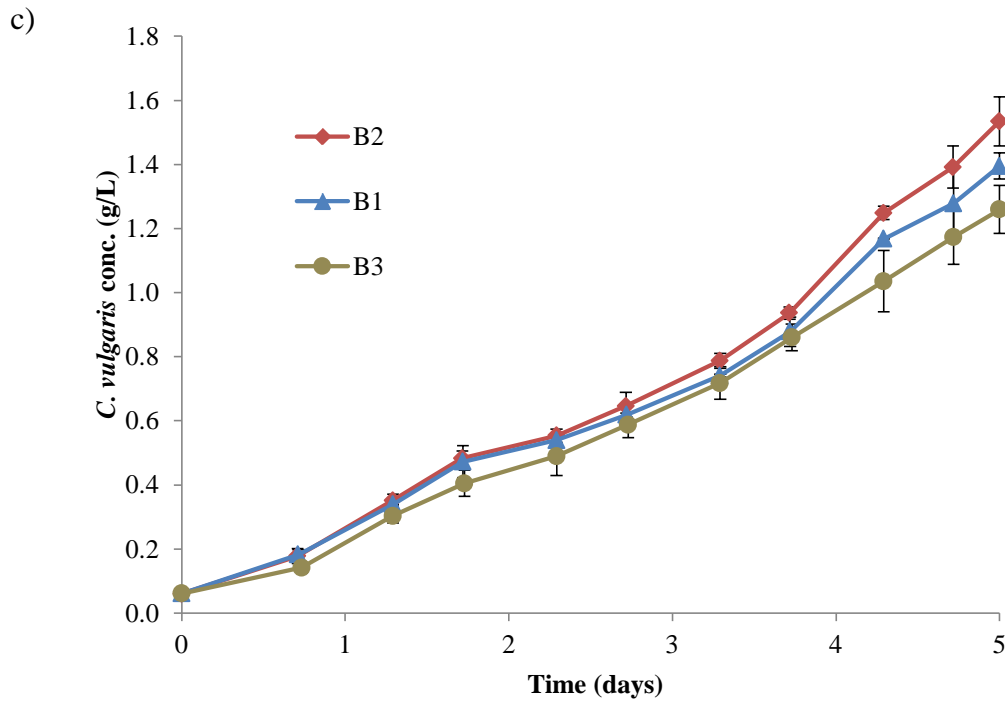
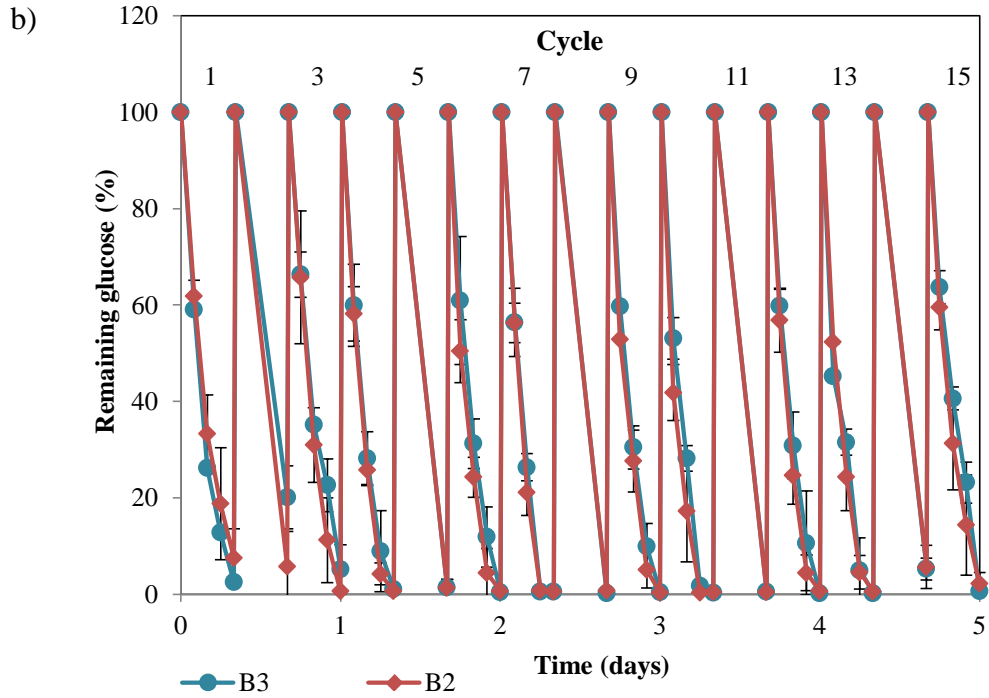


**Figure 5.7.** Effects of shell side flow velocity on glucose biodegradation and microalgal growth in the symbiotic HFMP: temporal profiles of (a) *P. putida* concentration and percentage of remaining glucose in B1 and B2, (b) percentage of remaining glucose in B2 and B3; (c) *C. vulgaris* concentration.

Results obtained during the first 2 days of B1 implied that flow velocity at 2 cm/s could be good enough for the O<sub>2</sub> and CO<sub>2</sub> exchanges. However, after 2 days when the bacterial biofilm might start to act as a barrier for mass transfer, velocity at 2 cm/s might not be high enough to accelerate the mass transfer of O<sub>2</sub> from the outer surface of the membrane and the biofilm layer to the shell side aqueous phase. This led to the slower glucose biodegradation rates during cycles 9 – 14 as compared to those of B2. The slower glucose biodegradation rate of bacteria resulted in slower CO<sub>2</sub> production rate, and together with slower shell side velocity (2 cm/s) the mass transfer of CO<sub>2</sub> to the lumen side would be reduced. As a consequence, from day 2.3 onwards, *C. vulgaris* growth in B1 was slower than that of B2.

#### *B2 and B3 comparison*

As can be seen in Figure 5.7b, the temporal profiles of glucose biodegradation in experiments B2 and B3 were identical. The number of cycles with complete glucose degradation in B2 and B3 was 12, twice as many as in B1 (Table 5.4). Hence, it can be ascertained that when the shell side flow velocity increased from 2 cm/s to 3 cm/s and 4 cm/s, the diffusivity of O<sub>2</sub> from the outer wall of the membrane to the shell side aqueous phase was improved. As a result, glucose biodegradation rates in B2 and B3 were faster than that of B1. However, the microalgal growth rate in B3 was not improved, and even worsened than that in B1 (Figure 5.7c). Final *C. vulgaris* concentration and biomass productivity in B3 were 1.26 g/L and 0.24 g/L.day, respectively, significantly lower than those in B2 (1.45 g/L and 0.294 g/L.day, Table 5.4). The possible reasons may be due to the

slower diffusion rate of CO<sub>2</sub> across the membrane. To understand why there was an opposite effect of the shell side flow velocity on the diffusivity of O<sub>2</sub> and CO<sub>2</sub>, their mass transfer resistances across the membrane and the biofilm formed on the membrane surface should be taken into account. Since CO<sub>2</sub> and O<sub>2</sub> have similar kinetic diameters, 3.3 Å and 3.46 Å (Duan *et al.* 2014), and there is no interaction between both of them with the polypropylene membrane, the membrane should provide an equal resistance towards their transportation. As a result, their mass resistance comparison was governed by the biofilm. It was reported that under laminar regime, more exopolysaccharides were produced by the bacteria in biofilm when subjected to higher flow velocities (Brading *et al.* 1995). Hence, when the shell side flow velocity increased from 3 cm/s to 4 cm/s, the biofilm in B3 (4 cm/s) could become more resistant due to more EPS produced. Such resistance was more critical for CO<sub>2</sub> than O<sub>2</sub>. As mentioned in Section 5.3.2, *P. putida* cells inside the biofilm can consume O<sub>2</sub> and hence leading to steeper O<sub>2</sub> concentration gradient between the biofilm and the lumen side which improved its diffusion. On contrary, *P. putida* cells inside the biofilm were unable to ingest CO<sub>2</sub> and hence the increased EPS would inhibit the CO<sub>2</sub> transfer. As a result, the transport of CO<sub>2</sub> produced from the bulk liquid (bacterial culture) and from the biofilm surface contacting with aqueous phase to the lumen side could be more unfavorable. In addition, too high shell side velocity could also reduce the contact time between the CO<sub>2</sub> in the bulk liquid and the biofilm surface, decelerating the diffusion of CO<sub>2</sub> across the membrane. Summarily, the biofilm formation with a higher amount of EPS at higher shell side flow velocity could induce more



resistance towards the transport of CO<sub>2</sub> than that of O<sub>2</sub>. As a consequent, the microalgal growth rate in B3 was remarkably affected, biomass productivity was only 82% of B2.

To sum up, the increase in shell side velocity from 2 cm/s to 3 cm/s resulted in higher glucose uptake and microalgal biomass productivity. But shell side flow velocity at 4 cm/s did not favor CO<sub>2</sub> transfer, resulting in much lower final *C. vulgaris* concentration. Shell side flow velocity at 3 cm/s was hence chosen in this course of study.

Among the conditions studied, the operation of the symbiotic HFMP using flow orientation depicted in configuration 2 with lumen side and shell side flow velocities at 3 cm/s resulted in highest glucose removal rate and microalgal biomass production. Table 5.5 summarizes the biomass productivity of different microalgal species under different cultivation conditions. The biomass productivity of *C. vulgaris* attained in the symbiotic HFMP was higher than or at least comparable to those obtained in typical photobioreactors and other membrane photobioreactors reported in literature. Especially, compared to microalgal biomass concentration in the HRAPs, which is typically less than 0.5 g/L (Craggs *et al.* 2011), the microalgal biomass concentration attained in this symbiotic HFMP (1.5 g/L) was much higher.

**Table 5.5.** Biomass productivity of different microalgal species under different cultivation conditions

Reactor type	Microalgae	Biomass productivity (g/L.day)	Reference
Symbiotic HFMP	<i>C. vulgaris</i>	0.294	This work
Photobioreactors	<i>C. vulgaris</i> (FACHB1068)	0.21 - 0.35	(Feng <i>et al.</i> 2011)
	<i>C. vulgaris</i> KCTC AG10032	0.105	(Yoo <i>et al.</i> 2010)
	<i>Chlorella</i> sp.	0.33 - 0.61	(Chiu <i>et al.</i> 2009)
	<i>C. vulgaris</i> CCAP 211/11b	0.17	(Rodolfi <i>et al.</i> 2009)
	<i>C. vulgaris</i> F&M-M49	0.2	(Rodolfi <i>et al.</i> 2009)
	<i>C. vulgaris</i> CCAP 211/11B	0.037 - 0.041	(Illman <i>et al.</i> 2000)
Membrane photobioreactors*	<i>Synechocystis</i> sp. PCC6803	0.084 – 0.1	(Kim <i>et al.</i> 2011)
	<i>Spirulina platensis</i>	0.072 – 0.427	(Kumar <i>et al.</i> 2010b)
	<i>C. vulgaris</i>	0.077 – 0.12	(Fan <i>et al.</i> 2008)
	<i>C. vulgaris</i>	0.08	(Ferreira <i>et al.</i> 1998)

\* Hollow fiber membranes were used for gas transfer in the photobioreactors

As is well known, bacterial biofilm formation on hydrophobic hollow fiber membrane is unavoidable. For the symbiotic HFMP using the flow orientation as in configuration 2, the biofilm formation did not adversely affect the HFMP performance until day 5. However, as the run prolongs, the biofilm would impede the mass transfer of O<sub>2</sub> and CO<sub>2</sub>, and the symbiotic HFMP performance cannot be sustained. Hence, controlling the biofilms was crucial for achieving high performance. Therefore, a washing strategy was applied after every 5-day operation to remove the attached cells. The membrane contactor was first cleaned by 1M NaOH for a few hours. After that it was washed with autoclaved pure water until the pH dropped below 7. As such the HFMP contactor could be reused and enhanced biodegradation performance was resumed.

### 5.3.5 Effects of number of fibers

One of the advantages of hollow fiber membrane contactor is that it provides more interfacial area for mass transfer (Carvalho and Malcata 2001). As aforementioned, the glucose biodegradation performance and microalgal growth in symbiotic HFMP are critically related to the mass transfer rates of O<sub>2</sub> and CO<sub>2</sub> between the two cell cultures. Hence, another approach to enhance the mass transfer flux in symbiotic HFMP is to enhance the interfacial area between the two aqueous phases. The effects of interfacial area on symbiotic HFMP performance were investigated by increasing the number of fibers (experiments D1 and D2). Under the same growth conditions, the HFMP in Figure 5.1 was modified by connecting another identical membrane contactor in parallel with the existing unit. The number of fibers in experiment D2 was hence doubled. Figure 5.8 shows the temporal profiles of the experimental data obtained.

Figure 5.8a shows the biodegradation of glucose, as well as the accumulation of *P. putida* during each cycle. During the first 4 days of operation, the glucose biodegradation rate in D2 showed a significant increase as compared to D1: the glucose fed was completely degraded in 6 hours (cycle 1-6) or even 4 hours (cycle 7-12). This inferred that the diffusivity of O<sub>2</sub> through the membrane had been improved due to larger surface area.

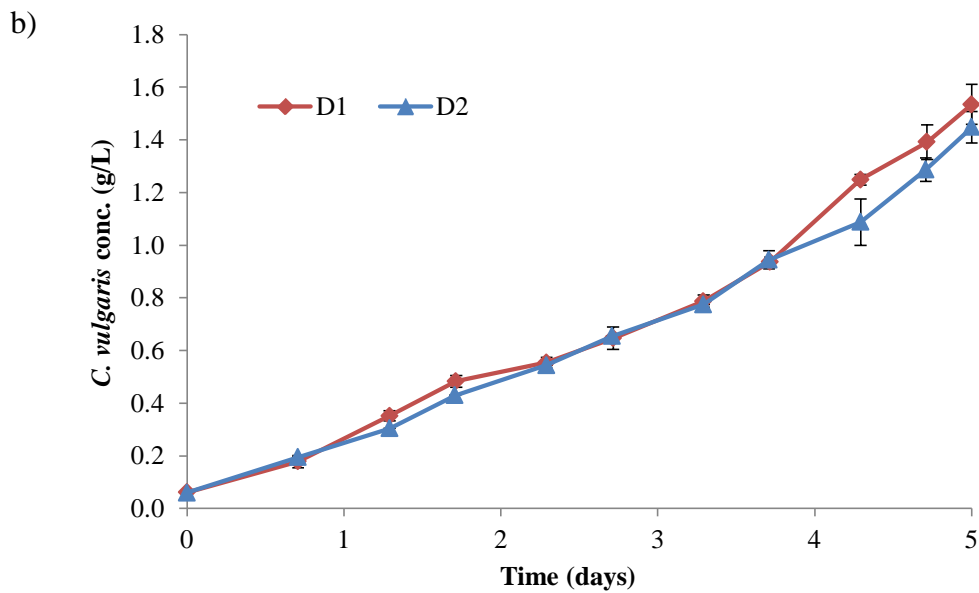
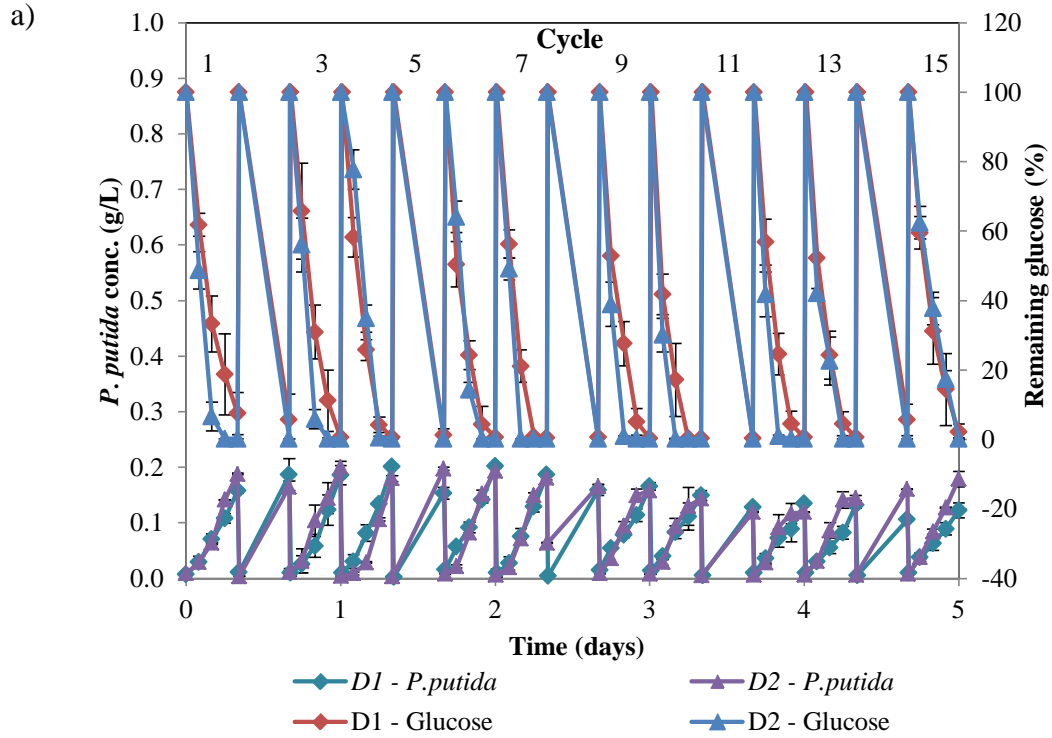


**Figure 5.8.** Effects of number of fibers on glucose biodegradation and microalgal growth in the symbiotic HFMP: (a) Temporal profiles of *P. putida* concentration and percentage of remaining glucose; (c) Temporal profiles of *C. vulgaris* concentration. D1: 100 fibers, D2: 200 fibers.

In addition, since more bacterial cells would attach on the outer surface of D2 as compared to that of D1, the intermediate consumption of the  $O_2$  on the surface was enhanced, creating a much steeper  $O_2$  gradient concentration and consequently accelerating the mass transfer of  $O_2$  from the lumen side to the shell side more effectively. Hence, the glucose fed in D2 was degraded more quickly from the beginning. Especially, in cycles 7 – 12, the glucose biodegradation time in D2 was shortened by 33% as compared to that of D1. However, from day 4 onwards (the last 3 cycles), the two bioreactors behaved similarly. This was attributed to the fact that the bacteria biofilms started impeding the mass transfer of  $O_2$ , thus decelerating the glucose biodegradation rates although glucose fed was still completely depleted within 8 hours. The amount of suspended bacterial biomass accumulation during cycles 8 - 15 dropped (Figure 5.8b), clearly indicating the presence the biofilms on the outer surface of the membrane.

Although glucose uptake rate of bacteria was significantly enhanced when the number of fibers was doubled, the microalgal growth trends in the two reactor systems were similar (Figure 5.8b). This suggested that a fixed amount of  $CO_2$  had been consumed by microalgae regardless the mass transfer rate and the amount of  $CO_2$  transferred to the microalgae side in each cycle could be larger due to higher surface area in experiment D2. Hence, this could be explained by the slow growth rate nature of the used microalgal strain.

From these results it can be concluded that higher interfacial mass transfer area significantly improved the  $O_2$  mass transfer rate, leading to higher glucose

removal rate and shorter biodegradation time. However, the increased interfacial area in the symbiotic HFMP did not enhance *C. vulgaris* growth.

#### **5.4 Concluding Remarks**

The concept of using symbiotic HFMP for microalgal growth and bacterial wastewater treatment has been successfully proved. In an enclosed system, *P. putida* aerobically degraded all of the glucose provided using the O<sub>2</sub> supply from the oxygenator *C. vulgaris*, while the microalgae grew photo-autotrophically using the CO<sub>2</sub> produced by the bacteria. The two configurations (C1 and C2) of the symbiotic HFMPs were illustrated to be feasible, with configuration 2 was superior to configuration 1 in terms of glucose biodegradation rate, microalgal biomass production and repeatability. With the flow orientation as in configuration 2, the flow velocity at 3 cm/s in both the lumen and shell sides was proved to be the most suitable for the operation of the symbiotic HFMP. In addition, increasing the interfacial area did enhance glucose biodegradation rate, however it had no significant effect on improving *C. vulgaris* growth.

To our best knowledge, the symbiotic HFMP in this study is the first design where microalgae culture and bacteria culture were separated but still supporting each other in a closed system. Compared to conventional symbiotic microalgal-bacterial processes, there are two major enhancements in the development of this hybrid photobioreactor. One of these lies in the compact footprint of the HFMP module. As a result, it is relatively easy to couple the photobioreactor to the wastewater treatment process. The photobioreactor is also scalable either through increasing the size of the shell or the number of the bioreactor modules. The other

enhancement in this symbiotic HFMP is the use of hollow fiber membranes to isolate the microbes in the activated sludge from the microalgae, and for gas exchanges in both the microalgal and activated sludge growth. Because the two cultures are separated, better control for microalgal and bacterial growth conditions can be achieved. Pre-processing steps such as isolating microalgal strains resistant to the wastewater, screening for a compatible microalgal-bacterial consortium could be avoided. The concept of using hollow fiber membranes for symbiotic wastewater treatment and microalgal growth hence will be further applied and developed in submerged hollow fiber membrane photobioreactor (SFHMP) for microalgal growth and bacterial wastewater treatment which will be discussed in Chapter 6.

## **Chapter 6**

# **Submerged Hollow Fiber Membrane Photobioreactor for Retrofitting Existing Activated Sludge Tank**

### **6.1 Introduction**

The membrane bioreactor (MBR) process is generally described as the combination of biodegradation treatment by activated sludge with liquid/solid separation by porous membranes (Le-Clech 2010). Since 1990s, MBRs have been installed to treat domestic wastewater in UK and increasingly developed in many countries, especially in the United State and Europe (Kraume and Drews 2010). By 2008, more than 200 municipal MBR plants with capacity greater than 100 m<sup>3</sup>/day and near 600 industrial MBR plants were in operation in Europe only (Kraume and Drews 2010). The reasons for this fast and large development are their unique advantages like: superb and hygienic effluent, reduced footprint and controlled biomass retention.

Due to these advantages, membrane technology is garnering the interest in both conventional plants and the construction of new treatment systems, especially in existing wastewater treatment plants where the demands for increasing the capacity and effluent quality are concerned (Kraume and Drews 2010). Instead of building a whole new treatment plant, the retrofitting of MBR to the existing systems could be a much more cost-effective solution because of the significant reduction of the capital and operation cost. This dual-configuration could be



achieved by directly installing the submerged membrane modules inside the bioreactor. Although the MBR systems encounter the unwanted deposition of materials on the membrane surface, results from advanced studies in membrane fouling have provided effective strategies for fouling mitigation (reviewed in Kraume and Drews 2010). Besides, a good mixing regime could provide higher shear rate, resulting in the reduction in the fouling layers on the membrane surface (Bérubé *et al.* 2006).

Inspired by the attractive idea of integrating submerged membrane to biological wastewater treatment, this study attempted to make contributions toward the retrofitting of the symbiotic HFMP to existing activated sludge process. Given the constraints of the limited or compact land area in current wastewater treatment plants, especially in a small country like Singapore, the application of submerged HFPM to existing activated sludge process might be a potential solution. In this new configuration, the hollow fiber membrane bundles were directly submerged in the activated sludge tank, and the microalgal culture was circulated through the hollow fibers to perform CO<sub>2</sub> and O<sub>2</sub> exchange. The microalgae photobioreactor can be built closed to or on top of the activated sludge tank whenever the land area is insufficient. With this design, photosynthetic oxygenation still can be performed to reduce the energy for extensive mechanical aeration while additional land area required for hollow fiber membrane contactor can be minimized. The energy that is used for pumping the wastewater through the contactor is also eliminated. Essentially, the clean and high-quality microalgal biomass can be harvested from the process.

In this chapter, a lab-scale submerged hollow fiber membrane photobioreactor (SHFMP) for symbiotic bacterial wastewater treatment and microalgal growth was developed. The specific objectives of this research were:

1. Examine the batch operation of the SHFMP at different volume ratios of microalgal culture to bacteria culture.
2. Investigate the feasibility of operating the SHFMP in continuous mode

As studied in Chapter 5, the volume of microalgal culture and bacterial culture were fixed equally at 260 mL to minimize the available headspace in the flasks, supporting the proof – of – concept of the symbiotic HFMP. In SHFMP, with the direct and better mixing in the shell side of the hollow fiber membranes, the required working volume of microalgal culture can be reduced while good glucose biodegradation performance can still be guaranteed. The lower the volume of microalgal culture, the smaller the land area needed for the construction of microalgae photobioreactor, and the better the light penetration. Hence the effects of decreasing volume ratio of microalgal culture to bacterial culture (VM/VB ratio) on glucose biodegradation performance were first examined in batch operation of SHFMP. Results obtained in this part were fundamental for the operation of SHFMP in continuous mode.

As is well known, the ability of continuous operation of a bioreactor is crucial for its practical applications, especially in wastewater treatment where the feed might be a continuous wastewater stream. It is hence essential to investigate the performance of symbiotic SHFMP in continuous mode. In this setting, the bacterial culture was operated in single-stage chemostat mode, while the

microalgal culture was processed in batch mode. Being relied on photosynthetic oxygenation, the continuous operation of SHFMP is challenging because it could face such problems as oxygen limitation, low glucose degradation rate, and biofouling. Therefore, pertinent issues including the effects VM/VB ratio, the startup period, the feed rate were investigated.

## **6.2 Materials and Methods**

### **6.2.1 SHFMP setup**

A schematic diagram of the SHFMP setup is shown in Figure 6.1. The system consists of two separate compartments, one for an axenic *P. putida* culture (bacteria tank) and the other for an axenic *C. vulgaris* culture (photobioreactor). The dimensions of the bacteria tank are Length x Width x Depth = 10 cm x 5.5 cm x 4.5cm. Three 100-fiber bundles of polypropylene hollow fiber membranes (effective length of 9 cm) were submerged in the bacteria tank. The fabrication of fiber bundle is described in Section 3.2.2. Synthetic wastewater was made from mineral medium (MM) supplemented with 500 mg/L glucose. The working volume of bacteria culture was 240 mL. This volume was used to maximize the tank volume, leaving minimal headspace. Bacterial culture was agitated with a magnetic stirrer at 200 rpm and at room temperature ( $25 \pm 1^\circ\text{C}$ ).

The microalgal culture was contained in Erlenmeyer flasks of different volumes depending on the microalgal culture volume used so that the available headspace in the flask was minimized. For example, at microalgal culture volume of 200 mL and 150 mL, 250-mL Erlenmeyer flask was used. At low culture volumes of 100 mL and 50 mL, 100-mL and 50-mL Erlenmeyer flasks were used, respectively.

The *C. vulgaris* culture was agitated with a magnetic stirrer at 200 rpm and at room temperature ( $25\pm 1^\circ\text{C}$ ). Continuous light intensity using LEDs was provided at  $200\ \mu\text{mol photon/m}^2\cdot\text{s}$  around the flask surface. Based on the results obtained in Chapter 5, *C. vulgaris* culture was circulated through the lumen side of the fibers at flow velocity of 3cm/s using peristaltic pump (WT600-1F, Longerpump). All lumen side connections were made using PTFE tubing as it is not permeable to  $\text{O}_2$  and  $\text{CO}_2$ .

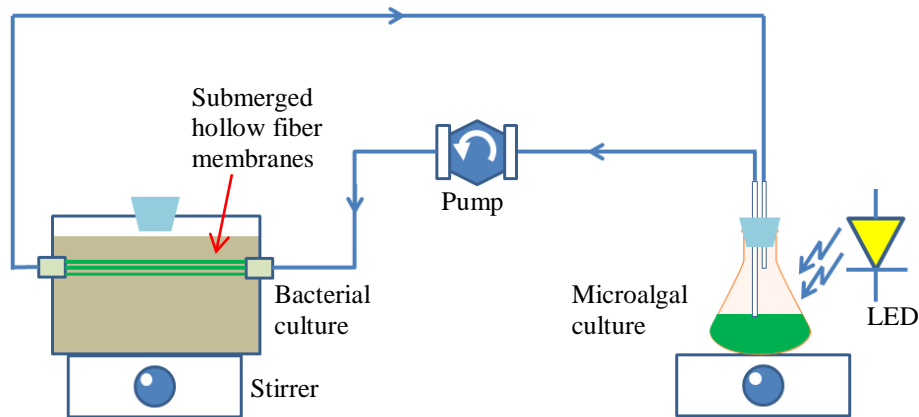


**Figure 6.1.** Schematic diagram of the SHFMP

### 6.2.2 Batch operation of SHFMP

Synthetic wastewater was inoculated with 8 mg/L *P. putida*. Bacterial samples were periodically collected to determine the bacteria concentration and glucose concentration. Every 8 hours, the spent bacterial culture in the bacteria tank was withdrawn and replaced with 240 mL of fresh synthetic wastewater. Bacteria that remained in the tank served as the inoculum for subsequent cycles.

*C. vulgaris* was cultured in BBM without organic or inorganic carbon supply. The initial concentration of microalgae was fixed at 60 mg/L, while the culture

volume was varied from 200 mL to 50 mL. This directly correlated with different initial microalgal cell mass in photobioreactor. Table 6.1 summarizes the experiments conducted in the batch operation of the SHFMP.

**Table 6.1.** Summary of the experiments to investigate the effects of VM/VB ratio on the SHFMP performance

Experiment	VM (mL)*	Initial microalgal cell mass (mg)	VB (mL)*	VM/VB ratio
E1	200	12	240	1 : 1.2
E2	150	9	240	1 : 1.6
E3	100	6	240	1 : 2.4
E4	50	3	240	1 : 4.8

\* VM: volume of microalgal culture (mL); VB: volume of bacterial culture (mL)

The total microalgal cell mass at time (t) =  $X_t \times V$ ; where  $X_t$  is microalgal biomass concentration at time t (g/L), V is the volume of microalgal culture (L).

### 6.2.3 Continuous operation of SHFMP

The experimental setup for continuous operation of the SHFMP was similar to that of batch operation (Figure 6.1) with the feed stream (influent) was continuously supplied into bacteria tank using peristaltic pump (Masterflex, USA). Feed was also prepared from the same synthetic wastewater (MM supplemented with 500 mg/L glucose) and pH value was 7. Feed tank was stirred at room temperature ( $25 \pm 1^\circ\text{C}$ ) without aeration. Feed flow rate (Q, mL/hr) was adjusted to obtain desired hydraulic retention time (HRT). The SHFMP was operated under different operating conditions as summarized in Table 6.2. Control experiments F2 and K2 were conducted where only water was circulated in the lumen side.

**Table 6.2.** Summary of experimental run in the continuous operation of SHFMP and other control experiments

Expt.	VM/VB ratio	Initial microalgae conc. (mg/L)	Initial bacteria conc. (mg/L)	HRT (hours)	Duration (days)	Study
F1	1 : 4.8	120	8	8	5	Continuous operation at VM/VB = 1 : 4.8
F2	1 : 4.8 *	0	8	8	5	
G	1 : 2.4	200	8	Q = 0 ***	0.37	Continuous operation at VM/VB = 1 : 2.4
				8	3.63	
				10.6	3.1	
H	1 : 2.4	500	157	11.4	2	Effects of the HRT
				10.6	1.3	
				9.7	1.8	
K1	1 : 2.4	500	157	11.4	2	Stability of continuous operation of the SHFMP
				10.6	4	
K2	1 : 2.4 **	0	157	11.4	2	
				10.6	4	

\* 50 mL of autoclaved ultrapure water was used in place of microalgal culture, \*\* 100 mL of autoclaved ultrapure water was used in place of microalgal culture

\*\*\* Feed flow rate  $Q = 0$  (batch mode)

Control experiment K3 for batch culture of microalgae was also conducted. In this experiment, *C. vulgaris* cells were inoculated at a concentration of 500 mg/L in a 250 - mL Erlenmeyer flask containing 100 mL of BBM. The culture was continuously sparged with 5% CO<sub>2</sub> enriched air at flow rate of 0.5 vvm and was continuously irradiated at a light intensity of 200  $\mu\text{mol photon/m}^2.\text{s}$  around the flask surface. The microalgal culture was agitated with a magnetic stirrer at room temperature ( $25 \pm 1^\circ\text{C}$ ).

During the reactor operation, bacterial samples were taken from the effluent to determine the suspension cell concentration, glucose concentration, pH and dissolved oxygen (DO) concentration. During the operation, the pH in the bacteria

tank was not controlled because the effluent pH never dropped below 6. The glucose removal efficiency (RE, %) and degradation capacity (DC, mg/L.hr) were calculated according equations (6.1) and (6.2):

$$RE = \frac{(C_{in} - C_{out})}{C_{in}} \cdot 100 \quad (6.1)$$

$$DC = \frac{Q}{V_R} (C_{in} - C_{out}) \quad (6.2)$$

where  $C_{in}$  and  $C_{out}$  are the influent and effluent glucose concentrations (mg/L);  $Q$  corresponds the feed flow rate (mL/hr);  $V_R$  is the working volume of bacterial culture (mL).

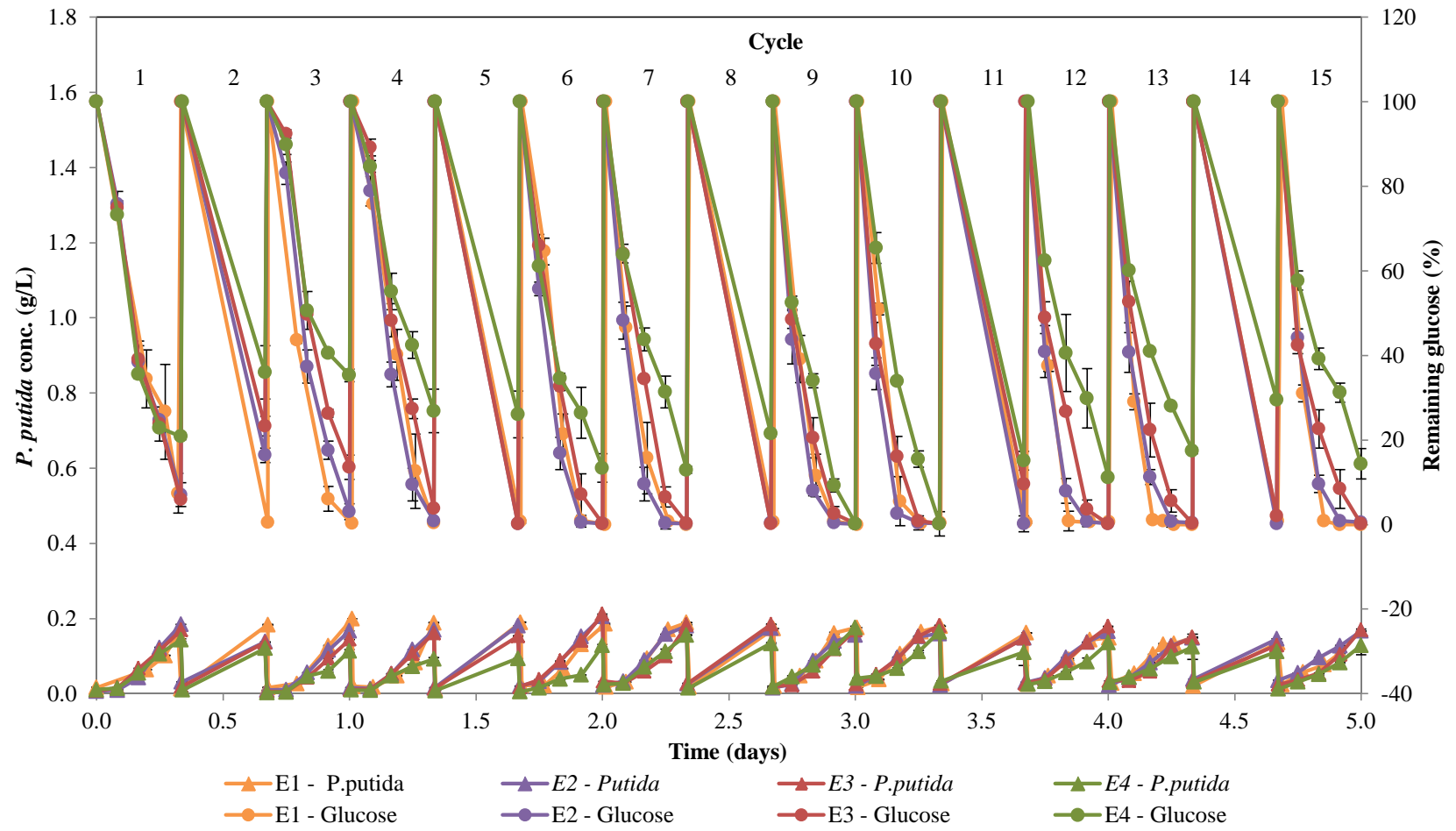
Microalgal samples were taken daily to measure the cell concentration,  $\text{NO}_3^- - \text{N}$  concentration and pH. In experiment F2 and K2, the water sample was taken to determine  $\text{NH}_4^+ - \text{N}$  and  $\text{PO}_4^{3-} - \text{P}$  concentrations.

## 6.3 Results and Discussion

### 6.3.1 Batch operation of SHFMP

The batch operation of the SHFMP was operated in accordance with the protocol described in Section 6.2.2 to investigate the effects of VM/VB ratio on *C. vulgaris* growth and glucose biodegradation performance of the SHFMP. At the same initial microalgae concentration of 60 mg/L, the volume of *C. vulgaris* culture decreasing from 200 mL to 50 mL while the volume of *P. putida* culture was fixed at 240 mL, and thus the VM/VB ratio of the SHFMP varied from 1 : 1.2 to 1 : 4.8. The temporal profiles and summary of the experimental data obtained are shown in Figure 6.2 and Table 6.3, respectively.

a)





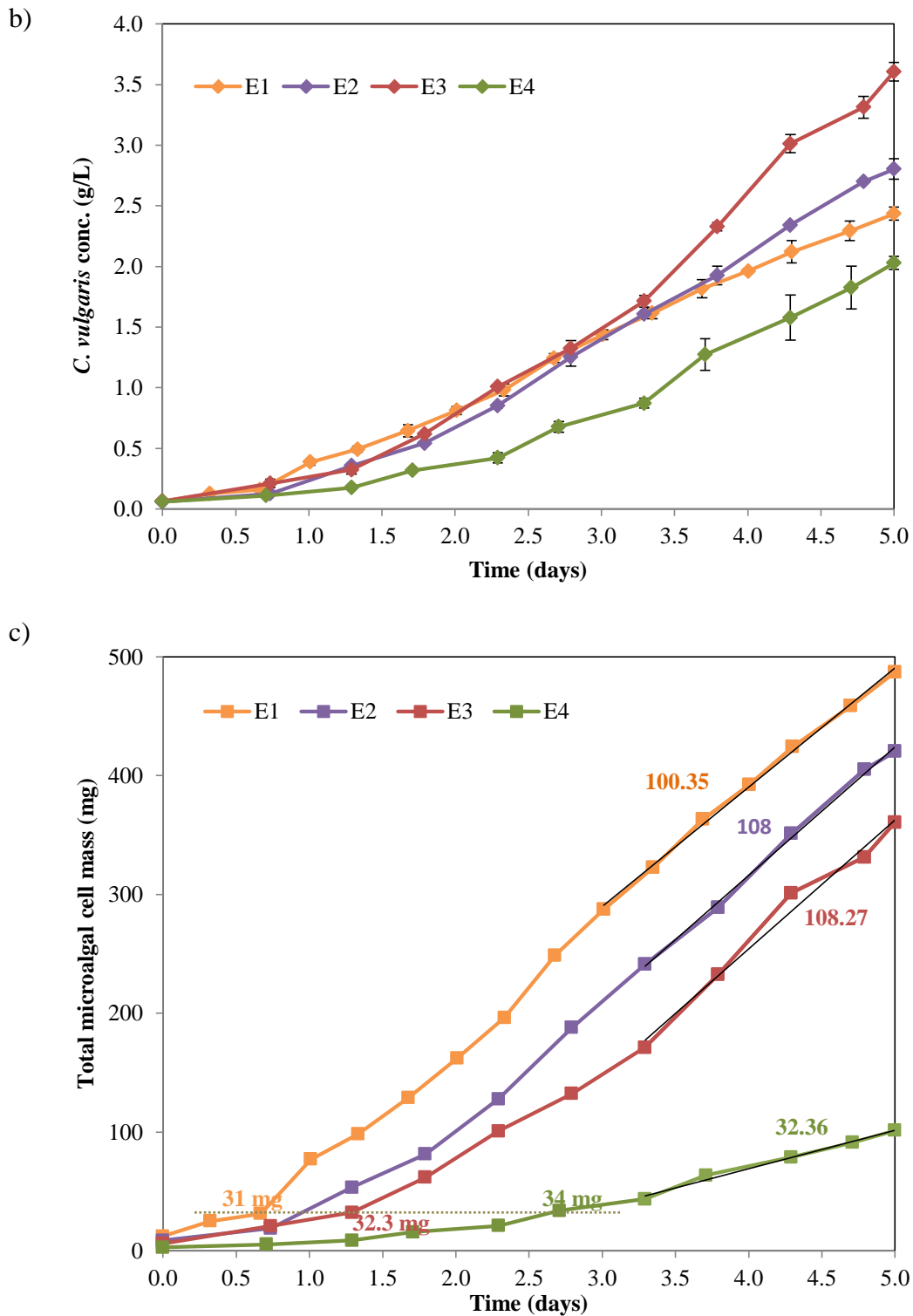


**Figure 6.2.** Effects of VM/VB ratio on glucose biodegradation and microalgal growth in the SHFMP: (a) temporal profiles of *P. putida* concentration and percentage of remaining glucose; (b) temporal concentration profiles of *C. vulgaris*; (c) temporal profiles of total microalgal cell mass.

**Table 6.3.** Summary of microalgal growth and glucose biodegradation in experimental set E

	Experiment			
	E1	E2	E3	E4
<b>VM/VB ratio</b>	1 : 1.2	1 : 1.6	1 : 2.4	1 : 4.8
<b>Final biomass concentration (g/L)</b>	2.44	2.80	3.61	2.03
<b>Biomass productivity (g/L.day)</b>	0.475	0.549	0.709	0.394
<b>Final total microalgal cell mass (mg)</b>	487	420	361	101
<b>Number of cycles with complete glucose degradation *</b>	14	12	10	2
<b>Average percentage of glucose degraded (per 8-hour cycle) (%)</b>	99	98	96	81

\* Cycle with complete glucose degradation was defined when 98 – 100% of the supplied glucose was removed

Figure 6.2a shows the biodegradation of glucose, as well as the accumulation of *P. putida* during each cycle. It should be noted that all the experiments E1 to E4 showed better glucose biodegradation performance in the first cycle than in the second cycle. This behavior was likely due to the exposure of bacterial culture to the atmospheric O<sub>2</sub> during the startup of the reactor. From cycle 2 onwards, when only O<sub>2</sub> produced by the photosynthetic oxygenation was available, a positive correlation between the glucose biodegradation and the VM/VB ratio was observed. In general, as the VM/VB ratio decreased, the glucose biodegradation rate in each cycle decreased. The glucose biodegradation trends were concomitant with *P. putida* growth trends in each cycle. Complete glucose biodegradation was first achieved in the experiment E1 (in cycle 2), which had highest VM/VB ratio (1 : 1.2), earlier than in E2 (cycle 4), and E3 (cycle 5). At lowest VM/VB ratio (1

: 4.8), *P. putida* in the experiment E4 could not completely biodegrade the glucose fed until cycle 9. The positive association was also reflected by the number of cycles with complete glucose degradation, with 14 cycles in E1, 12 cycles in E2, 10 cycles in E3 and only 2 cycles in E4 (Table 6.3). The average percentage of glucose degraded per 8-hour cycle E1, E2 and E3 were 99%, 98% and 96%, respectively (Table 6.3). In detail:

- In the experiment E1, the glucose removal rate was quite fast from the beginning, and further improved in subsequent cycles. The time needed for bacteria to remove 500 mg/L glucose decreased from 8 hours (cycle 2 to 5) to 6 hours (cycle 6 to 11), and to only 4 hours in the last 4 cycles (Figure 6.2a). Results also showed that the glucose removal rates in some cycles of E1 such as 2, 3, 12-15 were significantly higher than those in E2, E3 and E4.
- As the VM/VB ratio was decreased to 1 : 1.6 (experiment E2), the glucose removal rates in cycles 2, 3 and 12 – 15 were significantly lower than those in E1's corresponding cycles. However, the glucose removal rates during cycles 4 – 11 of E2 were relatively similar to those of E1.
- When VM/VB ratio was reduced to 1 : 2.4, glucose removal rates of E3 were slower than those of E1 and E2 in most of the cycles.
- At VM/VB ratio = 1 : 4.8, the glucose biodegradation rate significantly dropped. The percentage of glucose removal in each cycle increased from 64% to 87% (cycle 2 to 8), and finally reached 100% in only 2 cycles (9 and 10). After cycle 10, the glucose removal performance of E4 suddenly decreased, the percentage of glucose remained ranged from 71% to 89%. The

drastic drop in glucose biodegradation performance from cycles 11 – 15 was suspected to link with the inadequate amount of O<sub>2</sub> produced by microalgae in this experiment.

These results indicated that the decrease in VM/VB ratio reduced the glucose biodegradation performance of SHFMP. At very low VM/VB ratio (1 : 4.8), the amount of O<sub>2</sub> produced was certainly not enough to support the complete glucose biodegradation in the first 8 cycles and the last 4 cycles. Consequently, the average percentage of glucose degraded in this case was only 81%. Given that there was no external supply of oxygen to the system, the positive association between the glucose biodegradation and the initial microalgal cell mass (or the VM/VB ratio) was expected since higher initial microalgal cell mass resulted in higher amount of O<sub>2</sub> produced, accelerating the glucose consumption rate.

Interestingly, the glucose biodegradation performance of SHFMPs in experiment E1, E2, E3 were indeed better or at least comparable to that of symbiotic HFMP (experiment B2, section 5.3.4). Results from Table 6.3 shows that, although VM/VB ratios of E1 to E3 were all lower than that of B2 (VM/VB = 1 : 1), average percentage of glucose degraded of E1 and E2 was comparable to that of B2 (98%, Table 5.4), while that of E3 was slightly lower (96% versus 98%). The possible reasons are: firstly, because the membranes were immersed inside the bacteria tank, O<sub>2</sub> obtained from the lumen side was directly and immediately used by the bacteria inside the tank to degrade glucose, instead of being travelled back to the bacteria-flask as in the symbiotic HFMP. The immediate consumption of the O<sub>2</sub> in the tank induced a steeper O<sub>2</sub> concentration gradient, and consequently

accelerating the mass transfer of O<sub>2</sub> from the lumen side, enhancing the glucose uptake rate in SHFMP. Secondly, the mixing in the bacteria tank increased the liquid turbulence around the fibers, the thickness of the liquid boundary layer at the outer membrane surface was reduced, resulting in the increase in the gas transfer rates. Besides, direct mixing could induce more shear forces at the membrane surface, thus reducing the extent of bio-fouling and increasing the mass transfer flux (Bérubé *et al.* 2006). As can be seen in Figure 6.2a, the reduction in amount of bacteria biomass accumulation during cycles 8 – 15 of experiment E1 – E3 was not as drastic as that of the symbiotic HFMP (Figure 5.7a).

Figure 6.2b and 6.2c shows the temporal profiles of *C. vulgaris* concentration and total microalgal cell mass, respectively, in the experiments E1 to E4. As can be seen in Figure 6.2b, the gradual increase of microalgal concentration during the first 3 days was similar among E1, E2 and E3. But from the 3<sup>rd</sup> day of operation, the microalgae concentrations in E3 rose rapidly and reached a final concentration of 3.61 g/L after 5 days, significant higher than in E2 (2.80 g/L) and E1 (2.44 g/L). This order was simply because of the lower volume of culture medium used in E2 and E3. At the lowest culture volume used, however, the microalgal biomass concentration in E4 was also the lowest (2.03 g/L). This was due to the poor glucose biodegradation performance of the SHFMP in E4, resulting significantly lower amount of CO<sub>2</sub> transferred to the *C. vulgaris* side. In addition, the limitation in the culture volume and other nutrients in microalgal culture may also contribute to the inferior photosynthesis capacity of *C. vulgaris* in this case.

It should be noticed that the microalgal biomass productivities obtained in E1, E2 and E3 were relatively high (Table 6.3). Especially, the biomass productivity in E3 was 0.709 g/L.day, significantly higher than those reported in literature (summarized in Table 5.5).

The temporal profiles of microalgal cell mass show a different order (Figure 6.2c). Concomitant with the glucose biodegradation, the total microalgal cell mass in experiment E1 to E3 increased slowly (less than 30 mg/day) at the beginning when the batch *P. putida* cultures could only remove part of the glucose fed, and accumulated at much higher rate (around 100 mg/day) when most of the glucose fed was consumed (> 95%). In detail, since glucose was first completely degraded in cycle 2 of E1, the total microalgal cell mass in this experiment quickly entered the rapid cell mass increase phase after 0.6 day and eventually reached highest cell mass (487 mg, Table 6.3) after 5 days of operation. Similarly, microalgae in E2 entered the rapid cell mass increase phase after 1 day (cycle 3 of E2) and reached total cell mass of 420 mg at the end of the operation. The total cell mass in E3 increased gradually until day 1.3 (cycle 4), after that it increased rapidly and achieved a final of cell mass of 361 mg. It is noted that the total microalgal cell mass in E1, E2 and E3 was around 30 mg right before the SHFMP first had its complete - glucose - degradation cycle (Figure 6.2a and 6.2c).

In E4, VM/VB ratio of 1 : 4.8, the initial total microalgal cell mass in the medium was clearly not enough for a complete glucose biodegradation in the first 8 cycles. During cycles 2 to 7, as the total microalgal cell mass increased, the glucose biodegradation rates were also improved. Up to cycle 9, the total

microalgal cell mass increased to around 34 mg (Figure 6.2c), the O<sub>2</sub> generated by microalgae was sufficient for a complete biodegradation in cycle 9. However, due to the fact that 50 mL of BBM did not contain enough nutrients to sustain microalgal growth, the complete depletion of glucose in E4 was not repeatable from cycle 11 – 15. The increases in total microalgal cell mass from day 3 to day 5 were slightly faster than from day 0 to day 3, however, still much slower as compared to those of E1 – E3 (33.36 mg/day as compared to 100 mg/day).

In short, the decrease of VM/VB ratio affected the glucose biodegradation performance of the SHFMP. However the SHFMP still performed efficiently at VM/VB ratio of 1 : 2.4 with the average percentage of glucose degraded per 8 – hour cycle of 96% and the final microalgal biomass concentration of 3.61 g/L. This biomass concentration is significantly higher than that obtained in the HRAP systems (typically < 0.5 g/L, (Craggs *et al.* 2011)). The lower volume of microalgal culture and higher cell density could offer big advantages in saving energy for mixing and during downstream processing (Posten 2009). Although the VM/VB ratio at 1 : 4.8 did not show a very high glucose removal performance, the complete glucose removal still can be achieved when sufficient microalgal biomass concentration was produced. The results obtained from this study hence suggested that it is feasible to operate the SHFMP at low VM/VB ratio for dual purposes: wastewater treatment and clean microalgal biomass production.

### **6.3.2 Continuous operation of SHFMP**

The batch operation of SHFMP at low VM/VB ratio was feasible with relatively high glucose removal capacity as well as high microalgal biomass productivity. In considering the practical application of the developed SHFMP for wastewater treatment, it is essential to investigate the feasibility of continuous operation of the SHFMP for biodegradation purpose.

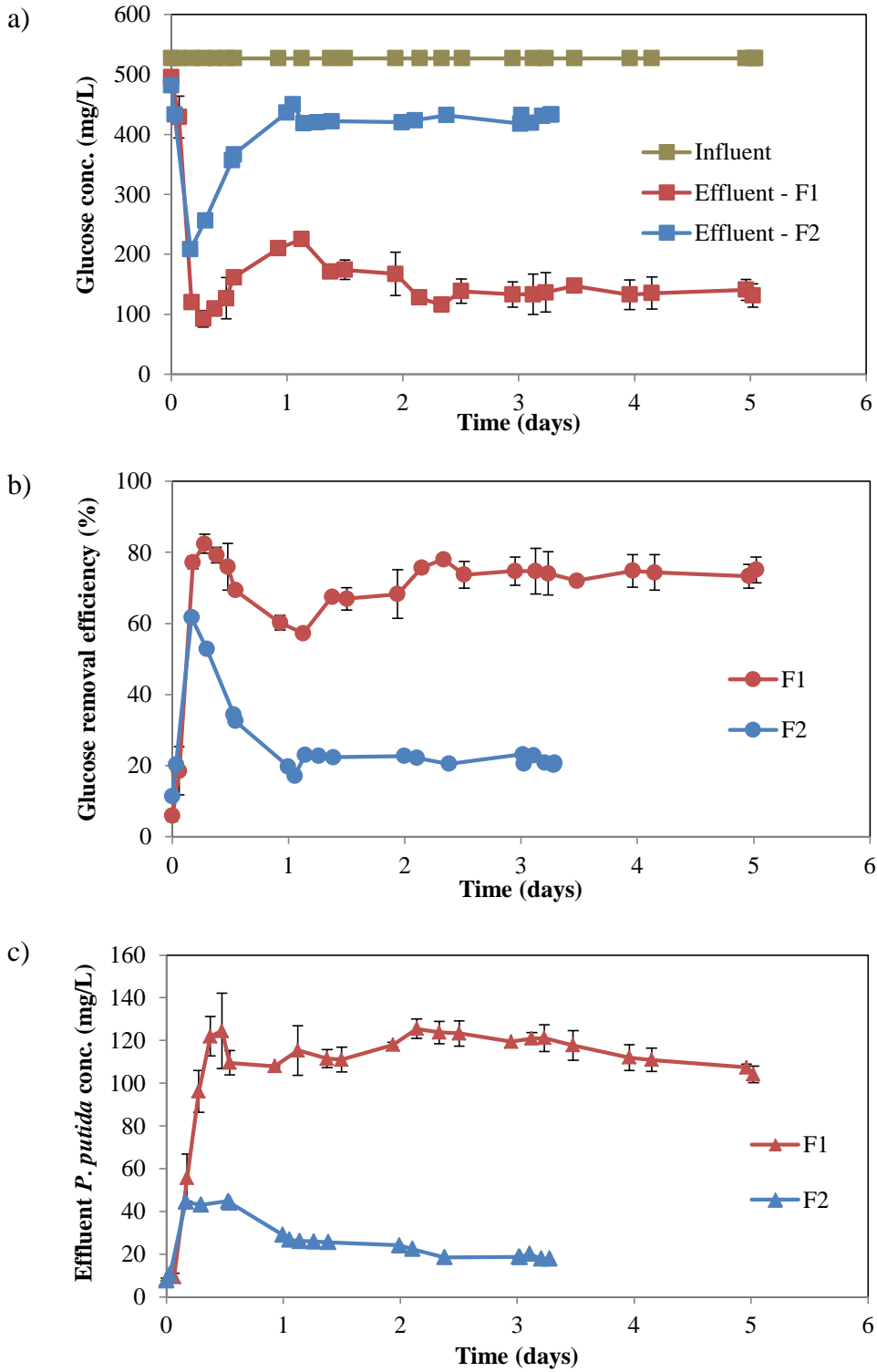
#### ***6.3.2(a) Continuous operation of SHFMP at VM/VB ratio of 1 : 4.8***

Results obtained in batch operation of SHFMP showed that at VM/VB = 1 : 4.8 (E4) the average percentage of glucose degraded per 8-hour cycle was just 81%. However there were two cycles wherein glucose was completely degraded. This VM/VB ratio hence could be considered as a bottom limit for the operation of the SHFMP. Experiment F1 was designed to investigate the continuous operation of SHFMP at VM/VB ratio = 1 : 4.8, establishing basic idea how the system would perform at the most unfavorable condition. HRT was chosen at 8 hours because 500 mg/L of glucose was observed to be depleted within 8-hour cycle in batch operation of the SHFMP. The corresponding dilution rate at this HRT was 0.14 hr<sup>-1</sup>, much lower than the upper limit of 0.4 hr<sup>-1</sup> as reported in Section 4.3.2, preventing the possibility of washout. The initial microalgae concentration was chosen at 120 mg/L to initiate the system, which can help to shorten the transient state (startup period) in order to reach steady state earlier.

Control experiment F2 was also carried out to evaluate the growth and glucose biodegradation potential of *P. putida* in the absence of photosynthetic oxygenation. In this control experiment, only sterilized water (50 mL) was



circulated in the lumen side. Figure 6.3 shows the temporal profiles of the experimental data obtained in experiments F1 and F2.



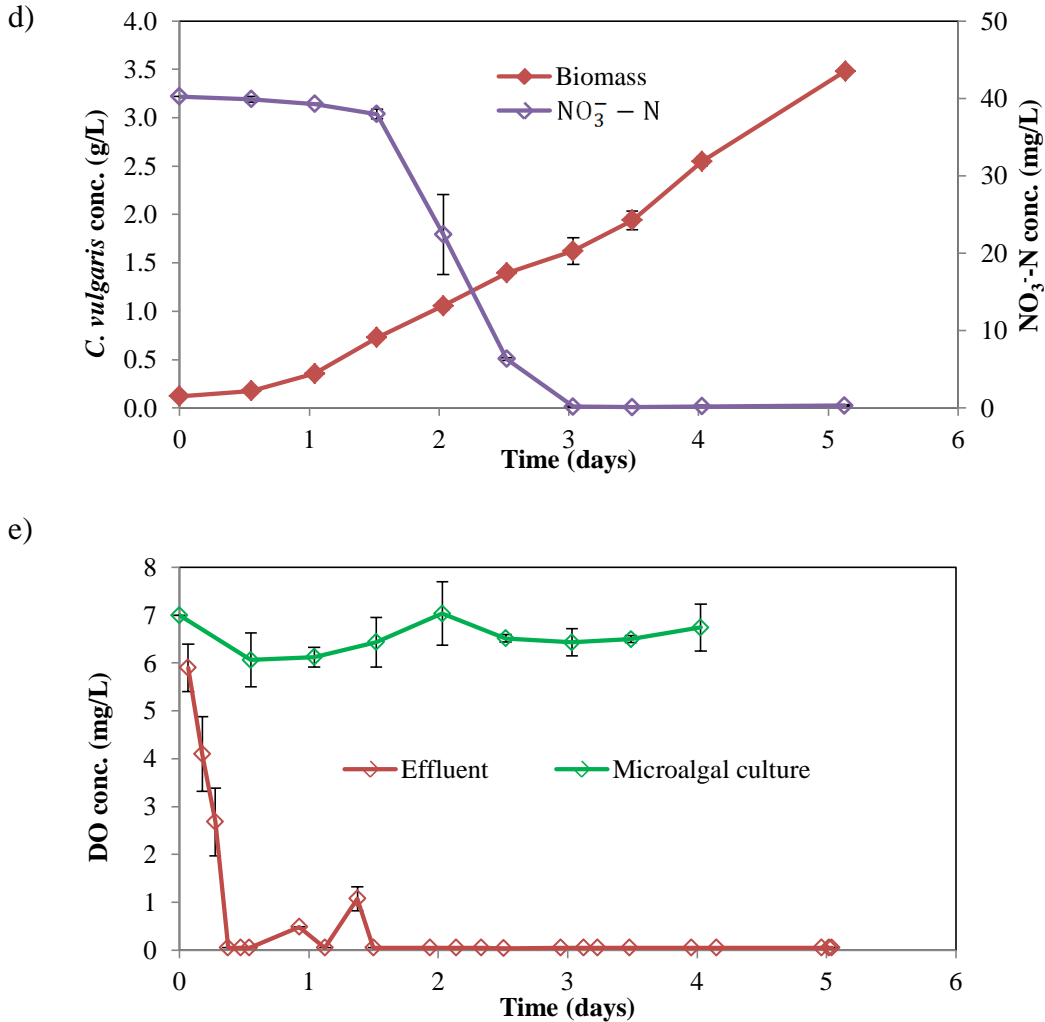


**Figure 6.3.** Temporal profiles of: (a) glucose concentration, (b) glucose removal efficiency, (c) *P. putida* concentration and (d) *C. vulgaris* and  $\text{NO}_3^- - \text{N}$  concentrations in experiments F1 and F2, (e) DO concentrations of the effluent and *C. vulgaris* culture in experiments F1.

### *Glucose removal and P. putida growth*

Figure 6.3a and 6.3b show temporal profiles of the glucose concentration and glucose removal efficiency in experiments F1 and F2. The symbiotic SHFMP in experiment F1 experienced a long startup phase, around 50 hours. As can be seen in Figure 6.3a glucose was quickly degraded to the concentration of 92 mg/L in the first 6.5 hours. After that the effluent glucose concentration increased and it

took about another 42 hours for the system to approach steady state. The steady state glucose concentration in effluent of F1 was around 136 mg/L, resulting in removal efficiency of 74% and degradation capacity of 49 mg/L.hr. In experiment F2, effluent glucose concentration trend was similar to that of F1 but the steady state was achieved one day earlier as compared to F1. However, only 22% of glucose was degraded in this case; the steady state effluent glucose concentration remained around 426 mg/L.

The bacteria concentration trends in the effluent (Figure 6.3c) were also correlated well with the glucose removal trends. Steady state *P. putida* concentration in the effluent of F1 was around 122 mg/L, significantly higher than that of F2 (21 mg/L). However the steady state *P. putida* concentration in F1 was still far from what obtained in the baseline study discussed in Section 4.3.2 (194 mg/L, Figure 4.5), which was due to the incomplete glucose biodegradation.

The results apparently indicated that, “oxygenator” *C. vulgaris* had provided O<sub>2</sub> for *P. putida* to remove more than 50% of glucose presented in the influent. However the photosynthetic O<sub>2</sub> evolved in experiment F1 was not enough to degrade 100% of glucose. The insufficiency in oxygen supply also resulted in the long startup period (transient state). As reported in Section 4.3.2, under fully aeration condition the continuous operation of the suspended bacterial culture at the same HRT and bacterial inoculum size reached steady state after only 9 hours (Figure 4.5).

### ***Microalgal growth and nitrogen consumption***

Figure 6.3d shows the temporal profiles of *C. vulgaris* growth and the depletion of  $\text{NO}_3^- - \text{N}$  concentration in the microalgae flask. *C. vulgaris* grew effectively in the symbiosis with *P. putida*. The biomass concentration gradually increased and reached a final concentration of 3.48 g/L after 5 days of operation, resulting in the biomass productivity of 0.655 g/L.day. It should be emphasized that the constant production of  $\text{O}_2$  by microalgae had supported the glucose biodegradation in continuous mode and the steady state operation was successfully achieved.

Figure 6.3d also shows that  $\text{NO}_3^- - \text{N}$  concentration in *C. vulgaris* culture was depleted after 3 days. As mentioned in Section 4.3.1, when the nitrogen source in microalgal culture was exhausted, the microalgal cells could consume their intracellular nitrogen pools to further support their growth. To verify whether *C. vulgaris* could rely on other nitrogen source beside their own intracellular nitrogen source, the sterilized ultrapure water in the lumen – flask of experiment F2 was examined for the presence of ammonium nitrogen ( $\text{NH}_4^+ - \text{N}$ ), one of the main nutrients in bacterial growth medium (MM), after the run was finished. Surprisingly, a concentration of 27.24 mg/L  $\text{NH}_4^+ - \text{N}$  was found in this water after 5 – day run although the lumen – water was not externally supplied with any nutrients during the experiment. This suggested that  $\text{NH}_4^+ - \text{N}$  of MM in the bacteria tank had transferred to the lumen side. It should be noticed that phosphate phosphorus ( $\text{PO}_4^{3-} - \text{P}$ ) is unable to diffuse across the membrane. Phosphate ion is generally hydrated in aqueous solution and its hydrated kinetic diameter is 0.8 nm (Liu and Huang 2000). Although its diameter is much smaller than the pore

size of the polypropylene membrane, its hydrated status prevents it from approaching the membrane surface because of the hydrophobicity of the membrane and hence its permeation through the membrane is restricted. The determination of  $\text{PO}_4^{3-} - \text{P}$  in the same lumen – water also confirmed no presence of this component during the reactor operation.

The principle of ammonia transfer through hydrophobic porous membrane has been discussed in literature (Semmens *et al.* 1990; Tan *et al.* 2006). In short, the ammonium equilibrium in aqueous solution can be described as following equation:



Because the polypropylene hollow fiber membranes are hydrophobic,  $\text{NH}_3$ , kinetic diameter is 0.26 nm (Kanezashi *et al.* 2010), can easily diffuse across the gas – filled pores in the fibers to the lumen side (Semmens *et al.* 1990). Although no trace of  $\text{NH}_4^+ - \text{N}$  was found in the *C. vulgaris* culture of F1, the presence of  $\text{NH}_4^+ - \text{N}$  the lumen side water of F2 suggested that *C. vulgaris* in F1 could also have consumed  $\text{NH}_4^+ - \text{N}$ , which was diffused from bacteria tank, to support their growth after the  $\text{NO}_3^- - \text{N}$  content had been depleted. This is actually another benefit of the SHFMP in practical applications because microalgae could help to degrade part of the  $\text{NH}_4^+ - \text{N}$  in the wastewater.

### ***Dissolved Oxygen (DO)***

Figure 6.3e shows the DO concentration profiles of the effluent and *C. vulgaris* culture in experiment F1. It can be seen that the DO concentration in *C. vulgaris*

culture ranged from 6 – 7 mg/L. On the other hand, the DO concentration in the effluent quickly dropped to zero after 0.4 day and remained around zero at the steady state from day 1.5 to day 5, although the glucose removal performance in F1 was much better than that in F2. This implied that bacteria had consumed all the O<sub>2</sub> released from the microalgal photosynthesis to biodegrade the glucose, hence the DO concentration in the effluent cannot be detected. The continuous removal of O<sub>2</sub> from the microalgal culture had helped to maintain its low DO concentration (6 – 7 mg/L), eliminating the toxicity of O<sub>2</sub> buildup on the photosynthesis.

To conclude, the continuous operation of the SHFMP at the VM/VB ratio of 1 : 4.8 and the HRT of 8 hours once again confirmed the important role of *C. vulgaris* culture in providing O<sub>2</sub> to support the aerobic glucose biodegradation. With the oxygen supply from the microalgae, steady state could be attained after 2 days of operation. However 26% of glucose was still remained in the effluent although *C. vulgaris* grew well and reached final concentration of 3.48 g/L. In comparison with experiment E4 where there were 2 cycles achieved complete glucose degradation when the microalgae concentration was high enough, the incomplete glucose biodegradation in experiment F1 suggested that the lack of O<sub>2</sub> was more obvious and impactful in continuous operation than in batch operation. The VM/VB ratio at 1 : 4.8 was certainly not sufficient to support a complete glucose removal in continuous operation of the SHFMP. Results obtained in experiment F1 were used as a reference to design the next experiment.

### ***6.3.2(b) Continuous operation of SHFMP at VM/VB ratio of 1 : 2.4***

Because the continuous operation of the symbiotic SHFMP at the VM/VB ratio of 1 : 4.8 could not achieve complete glucose removal, the VM/VB ratio was increased to 1 : 2.4 in this study.

When a bioreactor is operated in continuous mode, the startup phase is important because it involves the acclimatization of a new bioreactor system, the re-start of the system after cleanup or the maintenance (Li and Loh 2007). Since the startup phase of the SHFMP in experiment F1 was quite long (50 hours) and effluent glucose concentration was still high, an attempt was made to improve the startup phase. In experiment G, initial microalgae concentration was increased further to 200 mg/L. Initial bacteria concentration was kept at 8 mg/L, but the SHFMP was first run in batch mode for 9 hours until the glucose in bacteria tank was completely depleted and the concentration of bacteria in tank increased to 157 mg/L. After 9 hours of batch culture, the bacteria tank was continuously fed with 500 mg/L glucose at a flow rate maintained at 30 mL/hr (corresponding HRT = 8 hours). Figure 6.4 shows the temporal profiles of the experimental data obtained in experiment G.

As can be seen in Figure 6.4a, immediately after the start of the feed at day 0.37, glucose concentration in the effluent increased and reached steady state concentration after 22 hours (day 1.3). The steady state effluent concentration was about 98 mg/L, corresponding to removal efficiency of 82%.

In comparison to experiment F1, the increase in VM/VB ratio together with the modification in startup phase shortened the transient phase by 20 hours. At the

same HRT of 8 hours, the degradation capacity was improved from 49 mg/L.hr (F1) to 54 mg/L.hr (G). Glucose removal efficiency increased from 74% (F1) to 82% (G). Effluent bacteria concentration in G at the HRT of 8 hours was around 133 mg/L (Figure 6.4b), 9% higher than that of F1.

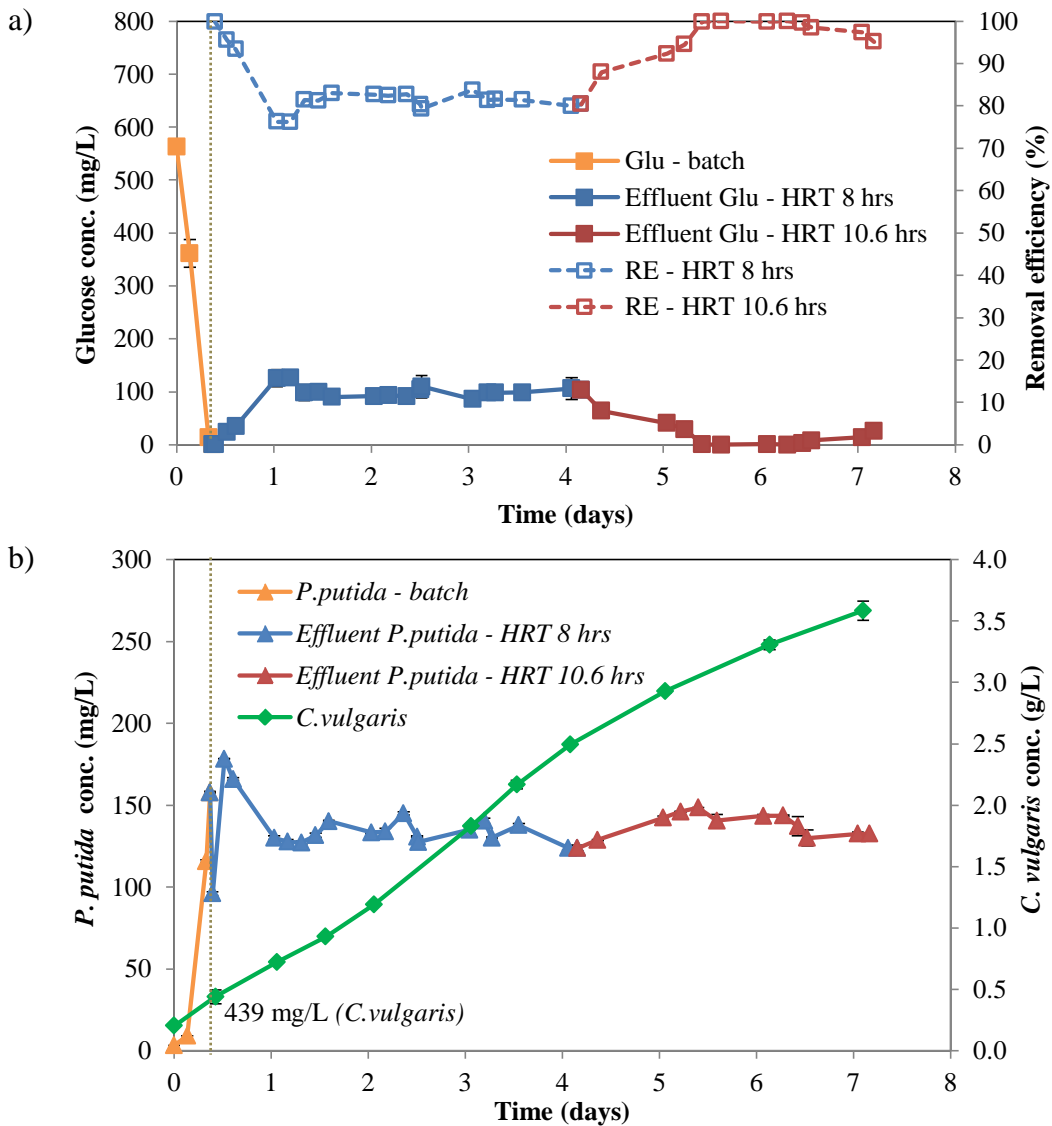


**Figure 6.4.** Temporal profiles of: (a) glucose concentration and glucose removal efficiency, (b) *P. putida* concentration and *C. vulgaris* concentration in experiment G. The start of the feed is marked by the dotted lines.

However, glucose biodegradation in experiment G at the HRT of 8 hours was not as effective as in experiment E3, where glucose could be completely removed in



8-hour cycle. The lower performance despite the same VM/VB ratio implied that the HRT of 8 hours may not be sufficient for *P. putida* to completely aerobically degrade glucose. In continuous process, hydraulic retention time is critical because the wastewater needs adequate contact time with the activated sludge in order to be degraded. Hence the HRT was increased to 10.6 hours on the 4<sup>th</sup> day of operation. As can be seen in Figure 6.4a, right after the HRT was changed to 10.6 hours, effluent glucose concentration dropped and effluent bacteria concentration slightly increased. After 30 hours (day 5.4), the effluent glucose concentration reached zero and effluent *P. putida* concentration was steady at around 141 mg/L. Results clearly indicated that a new steady state was re-established at the HRT of 10.6 hours and it prolonged for another 40 hours. It should be noted that at day 7 there was a slight increase in effluent glucose concentration to 14 – 25 mg/L, effluent bacteria concentration also dropped to 133 mg/L. It is suspected that the bacterial biofilm formation could have something to do with this slight decrease in glucose biodegradation efficiency.

Figure 6.4b also shows the temporal profile of *C. vulgaris* growth. When the SHFMP entered the continuous operation, the microalgae concentration was around 439 mg/L (day 0.43). During the operation of the SHFMP at the HRT of 8 hours, *C. vulgaris* grew effectively with an average biomass productivity of 0.562 g/L.day. During the period of the HRT at 10.6 hours (day 4.1 – 7.1), biomass productivity dropped to 0.361 g/L.day, which could be due to the depletion of nutrients and minerals in the *C. vulgaris* culture medium. Although the growth rate of microalgae was slower from day 5 – 7, glucose removal efficiency was

still at 100% in this period of time, suggesting that the HRT at 10.6 hours were sufficient for *P. putida* to degrade glucose using O<sub>2</sub> from microalgae, and in turn produce CO<sub>2</sub> to support the photosynthetic oxygenation. The final *C. vulgaris* concentration in experiment G was relatively high, around 3.59 g/L.

### **6.3.2(c) Effects of HRT**

Results obtained in experiment G suggested that continuous operation of the SHFMP with the VM/VB ratio of 1 : 2.4 can achieve 100% glucose removal efficiency at the HRT of 10.6 hours. In this study (experiment H), the effect of feed rate on glucose removal capacity was again verified; and further modification was also conducted for the startup phase so that complete glucose removal can be obtained from the beginning of the SHFMP operation.

According to experiment G, after the first 9 hours of batch culture, the glucose concentration in bacteria – tank dropped to zero, *P. putida* concentration increased to 157 mg/L and *C. vulgaris* concentration also increased to around 439 mg/L (Figure 6.4). To skip that 9-hour batch cycle, experiment H was started with very high microbial concentrations: the initial *P. putida* and *C. vulgaris* concentrations were inoculated at 157 and 500 mg/L, respectively. The bacteria tank was first continuously fed with 500 mg/L glucose at a flow rate maintained at 21 mL/hr (HRT = 11.4 hours). The temporal profiles of experimental data are depicted in Figure 6.5.

Figure 6.5a and 6.5b show the temporal profile of effluent glucose and *P. putida* concentrations. The bacteria concentration initially increased to 186 - 190 mg/L, concomitant with the exponential degradation of glucose. After 30 hours (day

1.2), the glucose concentration in the effluent was less than 5 mg/L; the removal efficiency was higher than 99% while effluent *P. putida* concentration was steady at about 155 mg/L. The system was clearly operating at steady state at this time. By starting – up in this manner, microalgae and bacteria had sufficient time to acclimatize to the new system as well as produce adequate O<sub>2</sub> and CO<sub>2</sub> to support the symbiosis, resulting in a complete glucose removal after 30 hours.

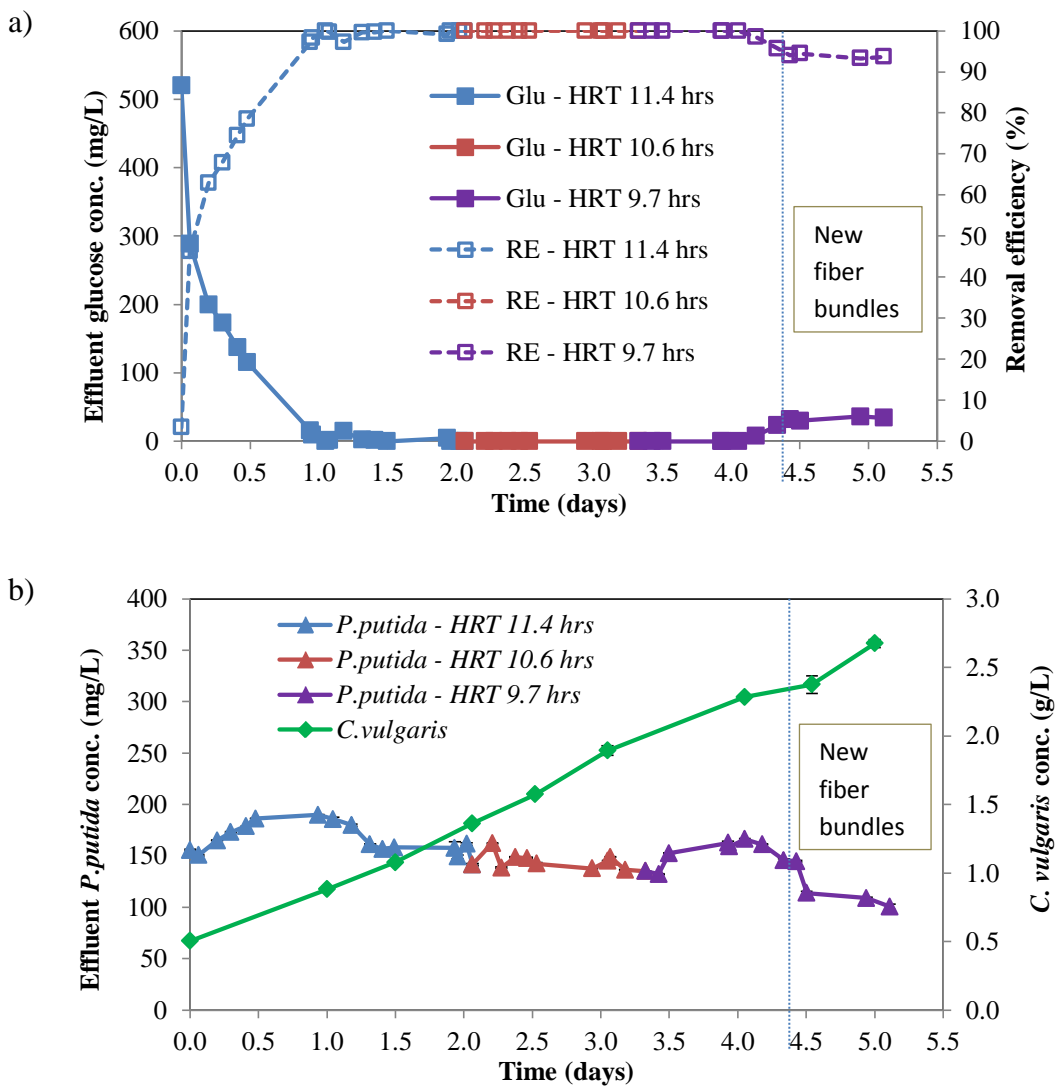


**Figure 6.5.** Temporal profiles of: (a) effluent glucose concentration and glucose removal efficiency, (b) *C. vulgaris* concentration and effluent *P. putida* concentration in experiment H. The substitution of fiber bundles is marked by the dotted lines.

Although complete glucose removal was attained at day 1.2, the SHFMP was still operated at the HRT of 11.4 hours for a further 19 hours to ensure the stability of the system. After that, it was subjected to higher glucose loading rate by increasing the feed flow rate to 22.6 mL/hr (corresponding HRT of 10.6 hours). As shown in Figure 6.5a, the performance of SHFMP was not affected and 100% removal of glucose was achieved for another 30 hours. The steady state concentration of *P. putida* in the effluent slightly reduced to about 144 mg/L during this period of HRT (Figure 6.5b).

As being steady at the HRT of 10.6 hours for 30 hours, a higher glucose loading rate was operated to investigate the glucose removal efficiency of the SHFMP. The feed flow rate was hence increased to 24.7 mL/hr (corresponding HRT of 9.7 hours). Right after the change in feed rate, the effluent bacteria concentration increased to 152 – 163 mg/L although effluent glucose concentration was still maintained at zero for another 17 hours. However, the effluent glucose concentration started increasing at day 4.18, suggesting that the bacterial biofilm on the outer surface of the fibers might have started to act as a barrier to the mass transfer flux of O<sub>2</sub>. Therefore, three new fiber bundles were used as a replacement for the old ones to eliminate the negative effects of the biofilm. The glucose concentration in the effluent did not decrease as expected, but was steady at around 33 mg/L, leading to glucose removal efficiency of 94%. Effluent bacteria concentration also dropped to 108 mg/L. Hence, it can be ascertained that HRT at 9.7 was not sufficient to obtain complete glucose removal. A longer contact time

is needed so that *P. putida* can capture photosynthetically generated O<sub>2</sub> to completely degrade glucose.

Figure 6.5b shows the temporal profile of *C. vulgaris* growth. Starting at high inoculum size (500 mg/L), *C. vulgaris* culture provided sufficient O<sub>2</sub> to support the complete glucose removal at the HRTs of 11.4 hours and 10.6 hours. The decrease in the HRT to 9.7 hours affected the glucose biodegradation efficiency, but it seemed not to significantly affect *C. vulgaris* growth rate. The final microalgae concentration at day 5 was 2.67 g/L, corresponding biomass productivity was 0.434 g/L.day.

Table 6.4 summarizes the removal efficiency, degradation capacity and steady state effluent glucose concentration at different HRTs in the continuous operation of SHFMP at the VM/VB ratio of 1 : 2.4.

**Table 6.4.** Effects of hydraulic retention time (HRT) on SHFMP performance at the VM/VB of 1 : 2.4

<b>Hydraulic retention time (hours)</b>	8*	9.7	10.6	11.4
<b>Removal efficiency (%)</b>	82	94	100	100
<b>Degradation capacity (mg/L.hr)</b>	54	52	51	47
<b>Steady state effluent glucose concentration (mg/L)</b>	98	34	0.59	1.09

\* *Experiment G*

At the HRT of 8 hours, the degradation capacity was as high as 54 mg/L.hr; however 98 mg/L of glucose still remained in the effluent, resulting in removal efficiency of 82%. Compared to this, HRTs of 9.7 hours and 10.6 hours showed higher removal efficiencies, but complete glucose biodegradation was only

achieved at the latter HRT. Therefore the HRT of 10.6 hours was more applicable for the continuous operation of SHFMP. Complete glucose removal was also obtained at 11.4 hours, however degradation capacity was quite low (47 mg/L.hr). This HRT is more suitable for the startup period of the SHFMP.

#### **6.3.2(d) Stability of continuous operation of SHFMP**

Results from experiments G and H showed that at the HRT of 10.6 hours complete glucose removal was achieved at steady state. To further investigate the stability of continuous operation of the symbiotic SHFMP for biological wastewater treatment and microalgal biomass production at the HRT of 10.6 hours, experiment K1 was conducted. Based on the results of previous experiments, the inoculum sizes for *P. putida* and *C. vulgaris* were set at 157 mg/L and 500 mg/L, respectively. The bacteria tank was continuously fed with 500 mg/L glucose at a hydraulic retention time of 11.4 hours for 49 hours. After that the HRT was decreased to 10.6 hours.

Control experiments K2 and K3 were operated in accordance with the protocol described in Section 6.2.3 to compare the microbial growths and their biodegradation performances with those in the SHFMP. All the conditions in experiment K2 were identical with those of K1, except the microalgal culture was replaced by 100 mL of sterilized ultrapure water in order to verify the vital role of photosynthetic oxygenation in glucose biodegradability of the SHFMP. In experiment K3, batch cultivation of microalgae under 5% CO<sub>2</sub> enriched air sparging was carried out to evaluate the microalgal growth and biomass

productivity. Figure 6.6 shows the temporal profiles of the experimental data obtained in experiment K1, K2 and K3.

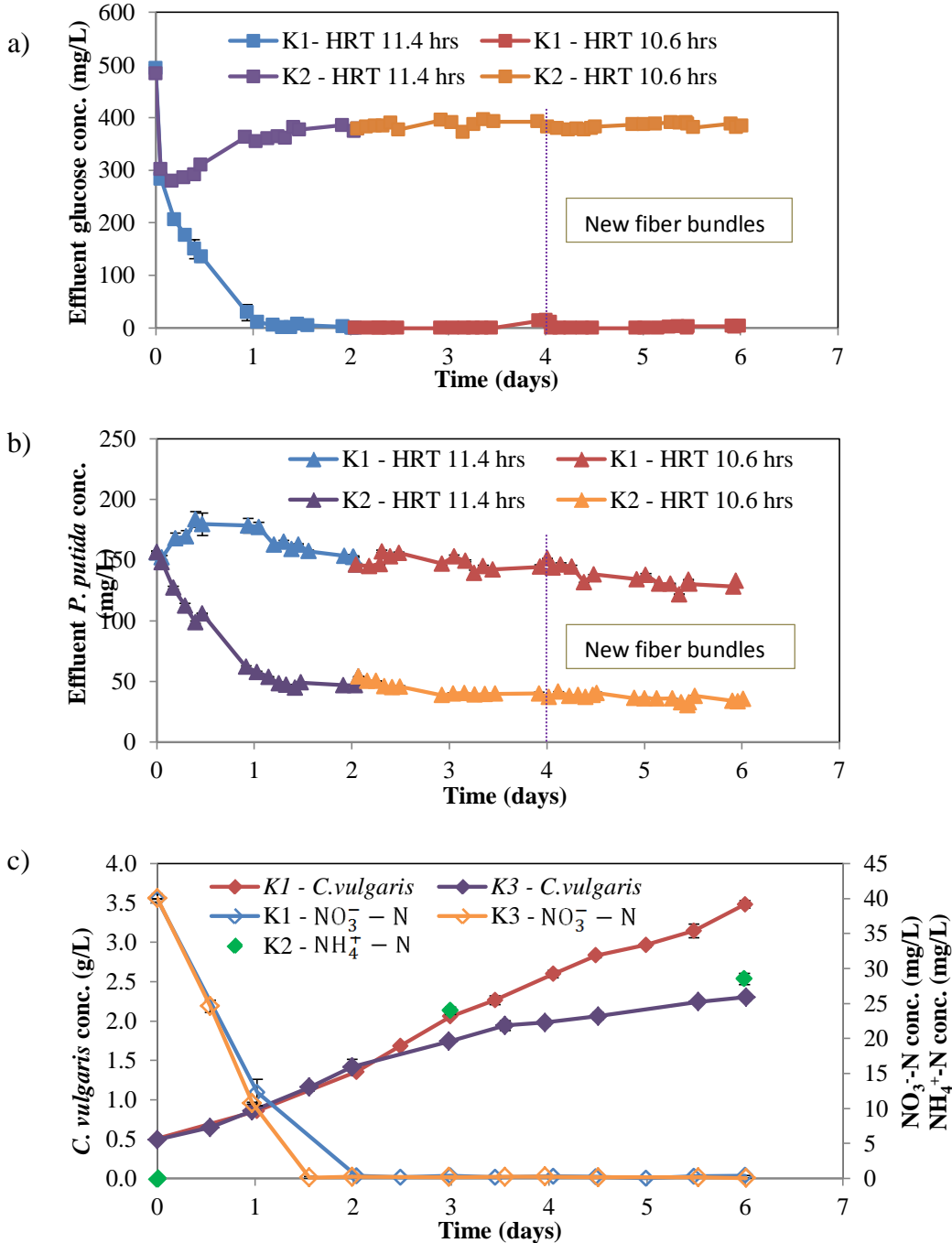


**Figure 6.6.** Temporal profiles of (a) effluent glucose concentrations in experiments K1 and K2, (b) effluent *P. putida* concentrations in experiments K1 and K2, (c) *C. vulgaris* and NO<sub>3</sub><sup>-</sup>-N concentrations in the microalgal cultures of experiment K1 and K3, and NH<sub>4</sub><sup>+</sup>-N concentration in the autoclaved water of experiment K2.

### ***Glucose biodegradation and bacterial growth***

Figure 6.6a shows the temporal profiles of effluent glucose concentrations of experiment K1 and K2. Similar to experiment H, in the presence of photosynthetic oxygenation (K1), the effluent glucose concentration drop to zero after 30 hours. When the SHFMP was operated at the HRT of 10.6 hours, the glucose removal efficiency was effectively maintained at 100%. It should be noticed that at the end of day 4, the effluent glucose concentration was slightly increased to 11 – 14.7 mg/L. This was likely caused by the biofilm because the effluent glucose concentration immediately returned to the steady state value of zero when the three old fiber bundles were replaced by the new ones, resuming 100% of glucose removal efficiency.

Regarding experiment K2, the effluent glucose concentration quickly dropped to 279 mg/L in the first 4 hours by consuming the available oxygen in the medium. After that, in the absence of photosynthetic oxygenation, the effluent glucose concentration started increasing and eventually reached steady state concentration of 379 mg/L. As the HRT decreased to 10.6 hours, steady state glucose concentration in the effluent also increased to 385 mg/L, resulting in removal efficiency of 27%. Degradation capacity at HRT of 10.6 hours was only 13.2 mg/L.hr, 74% lower than that of K1 (51 mg/L.hr).

The effluent bacteria concentrations also correlated well with the glucose biodegradation (Figure 6.6b). Although the control experiment K2 was started at a high *P. putida* concentration, the effluent bacteria concentration in K2 kept decreasing and eventually reached a steady state concentration at around 38 mg/L



(at HRT of 10.6 hours). This apparently indicated the lack of oxygen supply in experiment K2. With the support from photosynthetic oxygenation, the steady state effluent bacteria concentration in K1 was around 141 mg/L, 2.7 times higher than that of K2.

### ***Microalgal growth and nitrogen consumption***

Figure 6.6c shows the temporal profiles of *C. vulgaris* growth and the depletion of  $\text{NO}_3^- - \text{N}$  concentration in K1 and K3. With the  $\text{CO}_2$  supply from *P. putida* (K1), *C. vulgaris* growth in the SHFMP was sustained and attained a biomass concentration of 3.48 mg/L after 6 days of operation. It should be noticed that the concentration of *C. vulgaris* on the 5<sup>th</sup> day was 2.97 g/L, slightly higher than that obtained in experiment H (2.67 g/L on the 5<sup>th</sup> day, Figure 6.5b).

Under 5%  $\text{CO}_2$  enriched air sparging condition (K3), the growth trend of *C. vulgaris* in the first 2 days was identical with that of K1, however it was slower from day 3 onwards and the final biomass concentration was just 2.3 g/L. Thus, at the same inoculum size (0.5 g/L) and same provision of light irradiation, *C. vulgaris* growth was better in the SHFMP than in the batch cultivation under continuous sparging of 5%  $\text{CO}_2$  enriched air. The biomass productivity in K1 was 0.496 g/L.day, 65% higher than that of K3.

The  $\text{NO}_3^- - \text{N}$  content in microalgal cultures of K1 and K3 were quickly consumed after 1.5 - 2 days, around one day faster compared to experiment F1 due to the higher *C. vulgaris* inoculum size used. After the  $\text{NO}_3^- - \text{N}$  source was depleted the growth rate of microalgae in K1 was still maintained, while the microalgal growth in K3 was slowed down. It is worth noticing that the  $\text{NH}_4^+ - \text{N}$

content was found in the lumen - water of experiment K2 although the ultrapure water was used in the first place (Figure 6.6c). From zero the  $\text{NH}_4^+ - \text{N}$  concentration increased to 24 mg/L on day 3 and was measured at a concentration of 28.5 mg/L on day 6, suggesting the diffusion of  $\text{NH}_4^+ - \text{N}$  from the shell side to the lumen side as discussed in Section 6.3.2(a). Hence, the linear growth of *C. vulgaris* in K1 after the  $\text{NO}_3^- - \text{N}$  source in BBM was exhausted implied that the microalgae could have consumed their own intracellular nitrogen pools and  $\text{NH}_4^+ - \text{N}$  diffused from the bacteria side to further support their growth. The slower growth rate of microalgae in K3 could be attributed to the insufficiency in the nitrogen source. Taken altogether, it can be concluded that the microalgae cultivation in the SHFMP was more effective than that under bubbling condition.

To sum up, the continuous operation of the SHFMP for bacterial wastewater treatment and microalgal growth was feasible at the HRT of 10.6 hours. With the support of photosynthetic oxygenation, complete glucose removal was successfully attained. In reverse, the  $\text{CO}_2$  and  $\text{NH}_4^+ - \text{N}$  supplies from bacterial culture effectively supported the microalgal photosynthesis, resulting in the constant  $\text{O}_2$  production for bacteria and relatively high microalgal biomass productivity.

In the symbiotic microalgal – bacterial processes, the HRAPs are traditionally operated at 4 – 10 days HRT depending on the climatic condition (Sutherland *et al.* 2014a). Long HRTs have also been reported in enclosed photobioreactor when treating the phenolic wastewater (HRT of 3.6 – 6 days) (Tamer *et al.* 2006) or salicylate containing wastewater (HRT of 0.8 – 1.5 days) (Muñoz *et al.* 2004).

Hence, the HRT of 10.6 hours in this study is acceptable because it is within the HRT range of conventional wastewater treatment and much lower than that of other symbiotic microalgal-bacterial processes.

As mentioned in Chapter 5, the formation of bacterial biofilm on the hollow fiber membrane surface is unavoidable. In the continuous operation of SHFMP in experiment K1, where the steady state concentration of bacteria was relatively high, the adverse effects of biofilm on glucose removal performance occurred at the end of day 4. However, this problem could be solved by replacing the used membrane bundles with new ones on the 4<sup>th</sup> day so that the continuous operation of the SHFMP can be resumed and sustained. The used hollow fiber membrane bundles were immediately washed with 1M NaOH to remove the microbial cells and the biofilm, and the membranes can be reused in the subsequent operations.

### **6.3.3 Retrofitting existing activated sludge tank using SHFMP**

Based on the results obtained from batch operation and continuous operation of SHFMP, it can be ascertained that the SHFMP system is feasible for retrofitting existing activated sludge tank to aerobically treat the wastewater, reducing the energy required for mechanical aeration. Results showed that the operation of SHFMP was sustainable at the VM/VB ratio of 1 : 2.4. Currently a normal activated sludge tank has a depth of 4 – 5 m; the tank hence can be separated into 2 parts with the bottom part for the wastewater and top part for microalgal culture in order to utilize the energy of sunlight. With this design, 1.25 m height of microalgal culture can treat 3 m depth of wastewater. Although the volume of wastewater treated will be reduced, this configuration could assure sufficient light

penetration for the photosynthetic oxygenation (Park *et al.* 2011) and provide clean microalgal biomass. The height of microalgal culture can be increased to treat larger volume of wastewater with the help of artificial light such as LEDs. Over the past two decades, LED has been used as a light source for photobioreactor for cultivation of photosynthetic microorganism due to several advantages: (i) it provides higher energy efficiency than common light sources such as halogen lamps and fluorescent tubes, resulting in significant decrease in electricity consumption; (ii) it emits narrow wavelength spectra, appropriate for microalgal photosynthesis; (iii) LED has no emission in infrared range, generating low heat to the irradiated cultures; (iv) LED setup is light and small, convenient to fit any photobioreactor configuration; and (v) LED has a long lifespan, reducing the maintenance/replacement cost (Olivieri *et al.* 2014). According to Blanken and colleagues (2013), microalgae cultivation solely using LEDs will incite an acceptable electricity costs of 16.1 \$/kg-DCW. This cost could be reduced to 10.7 \$/kg-DCW in the future with the improvement of LED technology. The combination of artificial light and sunlight hence could further lessen the energy bill, especially in a tropical country like Singapore. Besides, this combination is more advantageous than solely exploiting sunlight since it can eliminate the effects of day/night cycles, changing weather conditions and seasonal changes. Additionally, the use of artificial light could result in the increased productivity of microalgal biomass, and hence high nutrient removal efficiency can be assured.

## 6.4. Concluding Remarks

A SHFMP was developed for simultaneous wastewater treatment and microalgal biomass production. Results suggested that a small VM/VB ratio ranging from 1 : 1.2 to 1 : 2.4 can be used to efficiently biodegrade glucose in batch operation. Especially, continuous glucose biodegradation was also accomplished in the SHFMP. Results showed that VM/VB ratio at 1 : 2.4 could be used to ensure high glucose removal efficiency. The SHFMP startup phase was short and steady state was accomplished within 30 hours. Complete glucose removal was attained at the HRT of 10.6 hours. Long-term sustainable continuous operation of SHFMP can be obtained if the fibers are changed every 4 days to eliminate the negative effects of biofilms.

The important contribution of this developed SHFMP is that it can be used to retrofit existing activated tank to economically treat the wastewater while minimizing the land area requirement for the construction of hollow fiber membrane contactor and microalgae tank, mitigating the greenhouse gas emission to convert to biomass resource in the form of clean microalgal biomass. The feasibility to operate SHFMP continuously is also validated, thus it is even more promising and applicable to the wastewater treatment process where the feed might be a continuous wastewater stream.

## Chapter 7

# Coupling the Submerged Hollow Fiber Membrane Photobioreactor to Activated Sludge Wastewater Treatment Process

### 7.1 Introduction

In previous chapter, a symbiotic SHFMP was developed for retrofitting existing activated sludge tank so that the energy required for the mechanical aeration can be reduced while minimizing the land area needed for the construction of microalgae tank. It was demonstrated that the SHFMP was capable of operating in continuous mode for symbiotic bacterial wastewater treatment and microalgal biomass production. Using monoculture of *P. putida* as a wastewater culture model, complete glucose removal was obtained at the HRT of 10.6 hours. These results demonstrated promising potential of the SHFMP. However, the coupling of the SHFMP model to the real activated sludge process is more challenging due to the following reasons:

- The activated sludge process involves activities of a mixed population of microorganisms. Among these microorganisms, bacteria, including carbon oxidizers and nitrogen oxidizers, floc-formers and nonfloc-formers and aerobes and facultative anaerobes, constitute the major component of activated sludge (AS) flocs and they are the most important microorganisms in decomposing the organic matters and nutrients in the wastewater (Bitton 2005a; Shieh and Nguyen 1999a). Interaction and competition between these

groups of bacteria largely affect the performance of the AS process. For example, the organisms in the activated sludge process work mostly side – by – side: nitrifying bacteria oxidize nitrogen components while carbon oxidizers consume BOD, and heterotrophic bacteria oxidize BOD while biological phosphorus removal occurs (Gerardi 2006d). The BOD and nutrients biodegradation performance of the AS flocs hence strongly depend on the availability of oxygen. As a result, the whole system performance will significantly rely on whether the microalgal photosynthesis could produce sufficient oxygen to support the simultaneous removals of carbonaceous materials and nutrients.

- The activated sludge contains such group of bacteria as heterotrophs and autotrophs. While the heterotrophs decompose the organic compounds and release CO<sub>2</sub>, the autotrophs (for e.g. nitrifying bacteria) obtain their carbon source for cellular synthesis by consuming inorganic carbon such as CO<sub>2</sub> (Gerardi 2006e). Therefore, the amount of CO<sub>2</sub> produced by the microorganisms in the activated sludge might be changed, directly affecting the microalgal photosynthesis. As a consequence, waste removal performance might also be impacted.

Owing to mentioned reasons, the symbiotic relationship between activated sludge and microalgae is more complicated and need to be investigated. In this research the activated sludge process was integrated with the microalgal culture in a SHFMP system called AS-SHFMP to investigate the COD/BOD<sub>5</sub> biodegradation performance in continuous mode. Nitrogen and phosphorus removal capacities

were also taken into consideration and were compared with the effluent quality of conventional activated sludge process. Besides, the stability of the AS-SHFMP during continuous operation was also demonstrated in a long-term experiment.

## **7.2 Materials and Methods**

### **7.2.1 AS-SHFMP setup**

The AS-SHFMP setup is shown in Figure 7.1. The system consists of two separate compartments: activated sludge tank (AS tank) and microalgae tank. The AS tank (10 cm length x 8 cm width x 5 cm height) had a working volume of 350 mL of mixed liquor. Four 100-fiber bundles of polypropylene hollow fiber membranes with effective length of 9 cm were submerged in the activated sludge tank. Mixed liquor was agitated with a magnetic stirrer at room temperature ( $25 \pm 1^\circ\text{C}$ ).

In all AS-SHFMP experiments, the synthetic wastewater used for startup and feed had the composition similar to that presented in Table 3.3 except the glucose concentration used in this study was 400 mg/L, giving concentration values around 430 mg/L COD ( $\text{BOD}_5 = 283 \pm 4 \text{ mg/L}$ ), 40 mg/L  $\text{NH}_4^+ - \text{N}$  and 8 mg/L  $\text{PO}_4^{3-} - \text{P}$ , respectively. This composition was chosen to represent the daily load of a conventional wastewater treatment plant with reference to the characteristics of domestic wastewater influent provided by Metcalf and Eddy (1991), Henze and Comeau (2008) and Cao (2011b). For startup, the cultivated activated sludge was added in the AS tank to a final MLSS concentration of about 2.5 g/L. During the AS-SHFMP operation, due to the small working volume in the AS tank the



activated sludge was not recycled but was kept inside the tank by a filter inserted at the outlet of effluent. The sludge retention time was fixed at 15 days by daily withdrawing around 23 mL of mixed liquor from the AS tank.

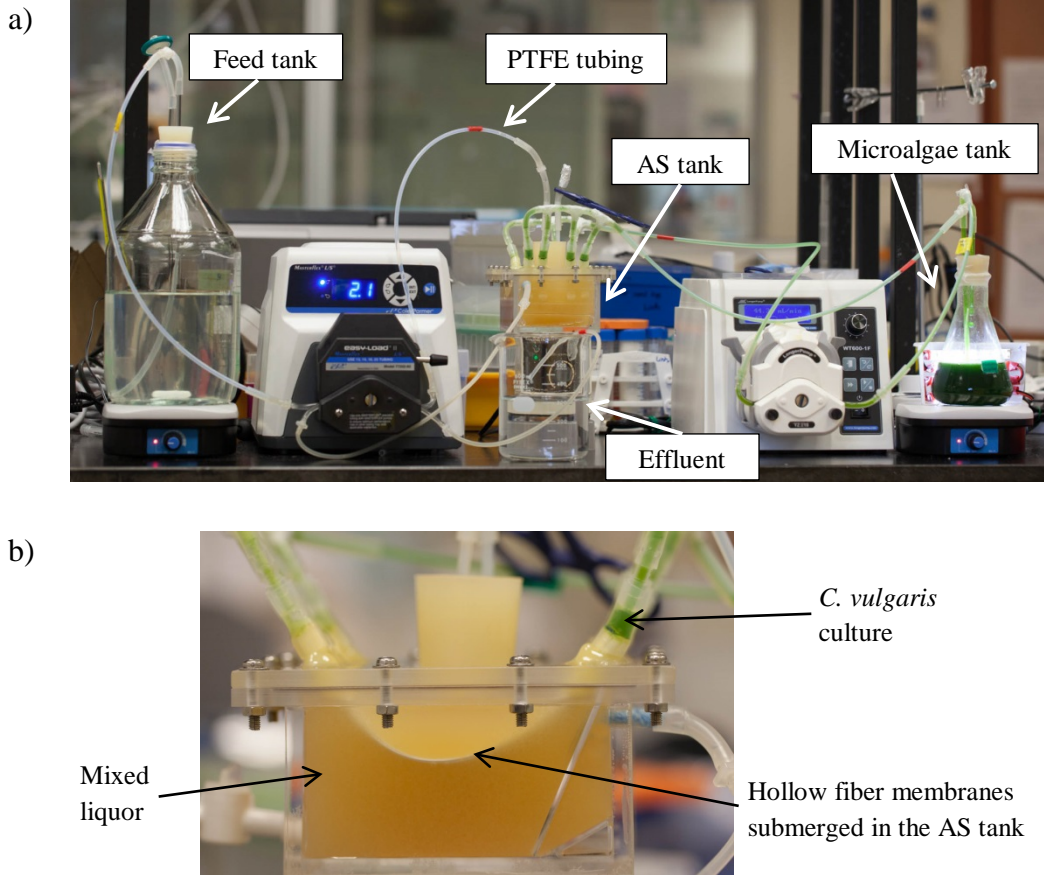


**Figure 7.1.** Experimental setup of the AS-SHFMP: (a) continuous operation setup, (b) submerged hollow fiber membranes in AS tank.

To prevent the feed from being contaminated by microorganisms during the experimental runs, feed was always prepared from autoclaved ultrapure water and stock solutions which had been filtered using sterile syringe filters (Millex® Syringe Unit, Millipore). Feed tank was stirred at room temperature ( $25 \pm 1^\circ\text{C}$ ) without aeration (Figure 7.1a).

The microalgal culture was contained in a 250-mL Erlenmeyer flask. Based on the results obtained in Chapter 6, volume of *C. vulgaris* culture was chosen at 150 mL to obtain the volume ratio of microalgal culture to mixed liquor of 1 : 2.4. *C.vulgaris* was inoculated into BBM (without organic or inorganic carbon source) at initial concentration of 500 mg/L. The microalgal culture was agitated with a magnetic stirrer at 200 rpm and at room temperature ( $25\pm 1^{\circ}\text{C}$ ). Continuous light intensity using LEDs was provided at  $200\ \mu\text{mol photon/m}^2\cdot\text{s}$  around the flask surface. The microalgal culture was circulated through the lumen side at flow velocity of 3 cm/s using peristaltic pump (WT600-1F, Longerpump). Lumen side connections were made using PTFE tubing as it is not permeable to  $\text{O}_2$  and  $\text{CO}_2$ .

### 7.2.2 Performance of the AS-SHFMP at different HRTs

Feed rate flow rate was adjusted to obtain desired HRT of 8 hours and 10 hours. A summary of all experiments performed in the AS-SHFMP is presented in Table 7.1.

**Table 7.1.** Summary of the experimental runs in the AS-SHFMP and control experiments

Experiment	HRT (hours)	Microalgal culture	Mixed liquor	Aeration in AS tank	5% $\text{CO}_2$ aeration
M1	8	+	+	-	-
M2	8	-	+	-	-
M3	8	-	+	+	-
N1	10	+	+	-	-
N2	10	-	+	-	-
N3	10	-	+	+	-
Q	-	+	-	-	+

- Experiments M1 and N1 performed continuous operation of the AS-SHFMP at the HRTs of 8 hours and 10 hours.

- Control experiments M2 and N2: continuous operation of the activated sludge process at the HRTs of 8 hours and 10 hours in the absence of photosynthetic oxygenation and external aeration. Only autoclaved ultrapure water was circulated in the lumen side.
- Control experiment M3 and N3: continuous operation of the activated sludge process at the HRTs of 8 hours and 10 hours under fully aeration condition. The mixed liquor was continuously aerated at a flow rate of 0.35 L/min (1vvm) to provide the oxygen to the activated sludge.
- Experiment Q: batch culture of *C.vulgaris* under 5% CO<sub>2</sub> enriched air sparging. The aeration rate was at 0.5 vvm. Working volume of the *C.vulgaris* culture, inoculum size, stirring condition and light intensity in this experiment were identical with those of microalgal cultures in the AS-SHFMP.

### **7.2.3 Long-term operation of the AS-SHFMP**

Continuous operation of AS-SHFMP was conducted at HRT of 10 hours for 17 days. On day 7 and day 12, 50 mL of microalgal culture (one-third of culture volume) was withdrawn and replaced by 50 mL of fresh BBM. To avoid the biofilm problems, the four fiber bundles were replaced every 4 days. When the experiment was stopped on day 17, the *C. vulgaris* culture was tested for contamination by streak plate method as described in Section 3.5.

During the AS-SHFMP operation, effluent samples were taken periodically and feed samples were taken every 2 days to determine the COD, NH<sub>4</sub><sup>+</sup> – N, PO<sub>4</sub><sup>3-</sup> – P, NO<sub>2</sub><sup>-</sup> – N, and NO<sub>3</sub><sup>-</sup> – N concentrations. The mixed liquor pH was not

controlled because it never dropped below 7 during the experimental runs. For instance, effluent pH ranged from 7.4 – 7.9 in experiments M1, N1 and long-term experiment, 7.1 – 7.8 in M2 and N2, and 7.9 – 8.3 in M3 and N3. The removal efficiency (RE, %) of component *i* (component *i* can be COD, NH<sub>4</sub><sup>+</sup> – N, PO<sub>4</sub><sup>3-</sup> – P and total nitrogen) was calculated according to equations (7.1):

$$RE = \frac{(C_{in,i} - C_{out,i})}{C_{in,i}} \cdot 100 \quad (7.1)$$

where  $C_{in,i}$  and  $C_{out,i}$  are the influent and effluent concentrations (mg/L) of component *i*.

## 7.3 Results and Discussion

### 7.3.1 Performance of the AS-SHFMP at different HRTs

The AS-SHFMP performance involved the symbiotic relationship between the activated sludge and the microalgae. The AS-SHFMP was operated in accordance with the protocol described in Section 7.2.2 to evaluate *C. vulgaris* growth, and COD and nutrient removals in the continuous operation of the AS-SHFMP at two HRTs of 8 hours and 10 hours.

Control experiments N2 and M2 were conducted to show the effect of lack of photosynthetic oxygenation and external aeration on biodegradation potential of the activated sludge. Control experiments M3 and N3 were carried out to examine the effect of external aeration on biodegradation potential of activated sludge, and subsequently to compare with the effect of photosynthetic oxygenation in the AS-SHFMP. Control experiment Q was conducted to compare the amount of

microalgae grown under continuous sparging of 5% CO<sub>2</sub> enriched air with the one grown in the AS-SHFMP. The temporal profiles of the experimental data are depicted in Figure 7.2 to 7.5.

### 7.3.1(a) Microalgal growth

Figure 7.2 shows the temporal profiles of *C. vulgaris* growth and the depletion of NO<sub>3</sub><sup>-</sup> - N concentration in the microalgae-flask of the AS-SHFMP at the HRTs of 8 hours (M1), 10 hours (N1) and in control experiment Q. The specific growth rate and biomass productivity of microalgae in the experiments were summarized in Table 7.2.

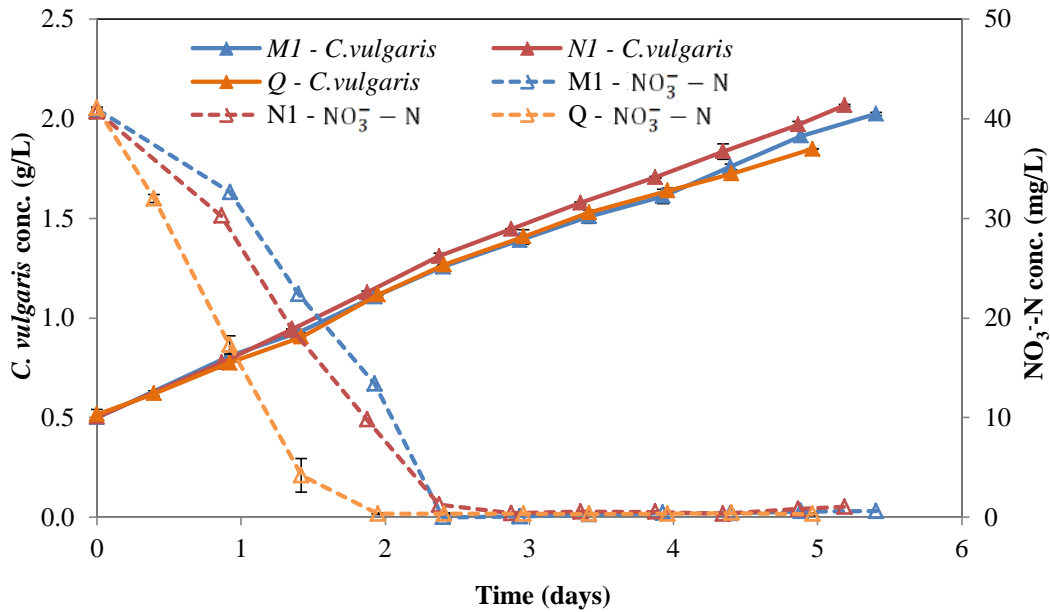


**Figure 7.2.** Temporal concentration profiles of *C. vulgaris* and NO<sub>3</sub><sup>-</sup> - N in experiments M1, N1 and control experiment Q.

**Table 7.2.** Summary of microalgal growth in experiment M1, N1 and Q

Experiment	Specific growth rate (day <sup>-1</sup> ) *	Biomass productivity (g/L.day)
M1	0.41	0.282
N1	0.43	0.302
Q	0.39	0.268

\*Calculated from day 0 – day 2

Similar to the results obtained in Chapter 6, the *C. vulgaris* concentrations in the AS-SHFMPs increased linearly. As can be seen, microalgal growth rate in N1 was slightly improved as compared to that of M1, resulting in higher biomass productivity (0.302 g/L.day versus 0.282 g/L.day). The NO<sub>3</sub><sup>-</sup> – N consumption trend in N1 was also faster than that of M1 although the NO<sub>3</sub><sup>-</sup> – N contents in two cases were both depleted in 2.4 days. The results suggested that at 10-hour HRT, the contact time between the nutrients in the wastewater and activated sludge was longer and hence more CO<sub>2</sub> could be produced and transferred to microalgae side to support the microalgal photosynthesis. However due to the slow growth rate nature of microalgae, the biomass productivity in experiment N1 was only 7% higher than that of M1. The biomass productivity in the AS-SHFMP is quite comparable to those obtained in other photobioreactors in the literatures (Table 5.5). It is noted that the specific growth rates of microalgae in experiment M1, N1 and Q were all lower than those in the symbiotic HFMP (Table 5.3). This was because of the high initial microalgae concentration used in these experiments (500 mg/L versus 60 mg/L).

Under CO<sub>2</sub> aeration condition, although the NO<sub>3</sub><sup>-</sup> – N consumption of microalgae in experiment Q was faster, the microalgal growth rate and biomass productivity

were lower than those of M1 and N1. This result once again verified that the microalgae cultivation in the AS-SHFMP was more efficient than in bubbling system in terms of the CO<sub>2</sub> conversion efficiency and the minimization of CO<sub>2</sub> loss.

### ***7.3.1(b) COD removal***

Due to the limitation in the sample volume and the long measuring time for BOD<sub>5</sub>, the COD concentration in the effluent was determined instead. It should be noted that the feed was prepared from autoclaved ultrapure water and sterilized stock solutions and was kept under sterile condition during the operation so that the influent COD concentration was constant around 426 – 435 mg/L during the all experimental runs. Figure 7.3 shows the temporal profiles of effluent COD concentration and COD removal efficiency in experimental sets M and N.

In the first 4.5 hours effluent COD concentrations in experimental sets M and N were quickly decreased. This was because the solute carbonaceous substrates such as glucose were rapidly absorbed and assimilated by the organisms in the activated sludge for biomass production.

Under fully aeration condition (experiments M3 and N3), the steady states were quickly achieved after 4.5 hours. The steady state effluent COD concentrations at the HRTs of 8 hours and 10 hours remained below 10 mg/L, resulting in removal efficiencies greater than 98%.

With the support of photosynthetic oxygenation in the AS-SHFMP (experiments M1 and N1), the steady state effluent COD concentration trends were identical

with those under aeration condition. The steady state effluent COD concentrations at the HRTs of 8 hours and 10 hours were less than 16 mg/L and 12 mg/L respectively, resulting in removal efficiencies around 98%.

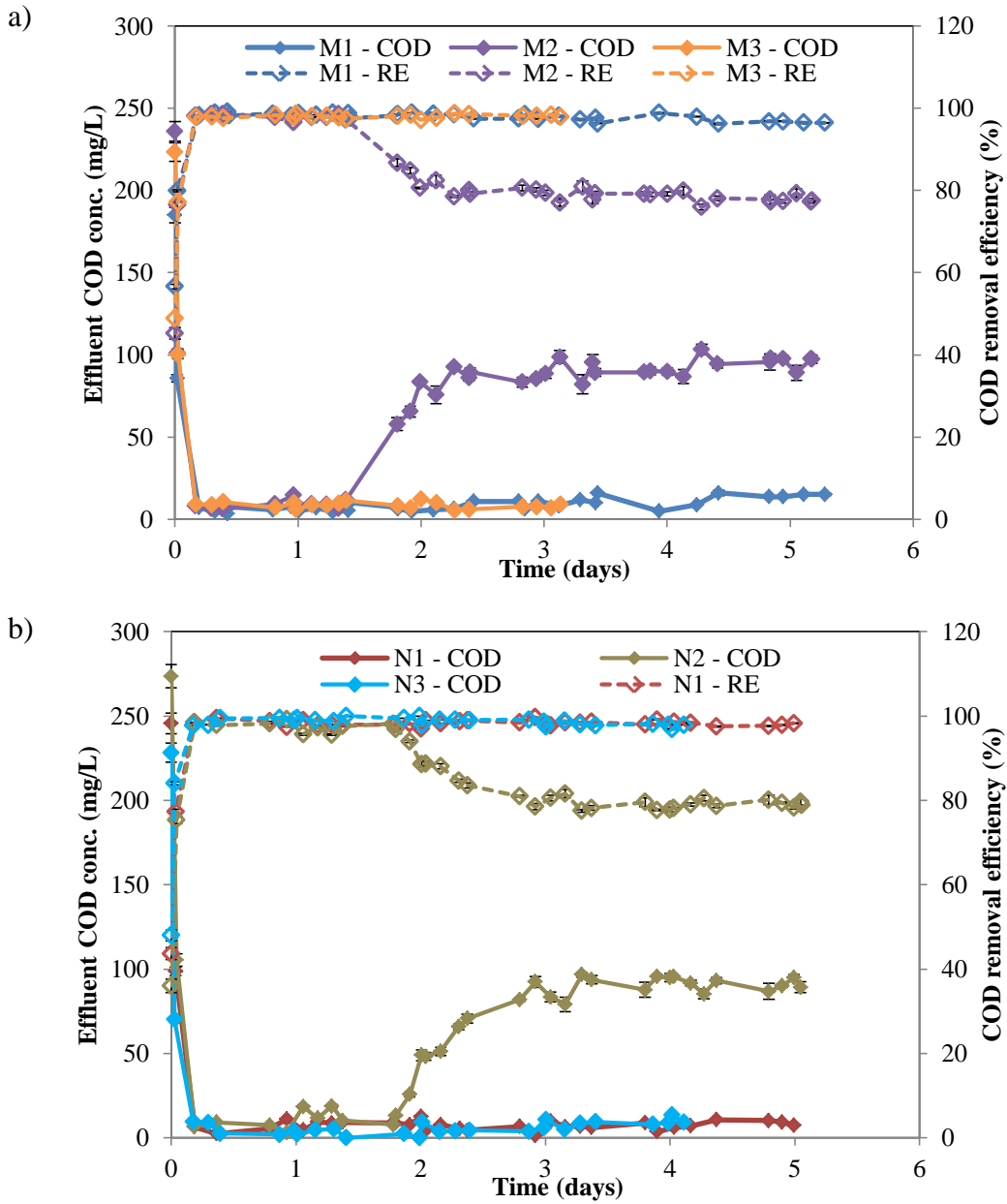


**Figure 7.3.** Temporal profiles of (a) effluent COD concentration and COD removal efficiency in experimental set M (HRT = 8 hours), (b) effluent COD concentration and removal efficiency in experimental set N (HRT = 10 hours).



In the absence of photosynthetic oxygenation and external aeration, the effluent COD concentrations in M2 and N2 still remained below 18 mg/L and 14 mg/L from day 0.18 – 1.39 and day 0.18 – 1.8, respectively. This was because the AS flocs comprise of both aerobes and facultative anaerobes, and the facultative anaerobe can degrade the organic compounds in the absence of free molecular oxygen (Gerardi 2006a). Besides, the microorganisms in the AS flocs could also have obtained the initial DO in the wastewater during the startup to degrade the organic matters. Hence, the fast initial oxidization of the organic compounds in M2 and N2 was likely for cell growth. However, after day 1.39 (M2) and day 1.8 (N2), the effluent COD concentrations in both cases started increasing and remained steady at round 92 – 100 mg/L. The remaining COD could be attributed to: (i) the accumulation of organic matters such as the metabolic products and intermediates generated by the microorganism in the activated sludge, or the lysis products from death bacteria, and (ii) the lack of dissolved oxygen to completely degrade those organic matters. As a result, the COD removal efficiencies in the oxygen-deficient condition were only 79%.

During the activated sludge process, only part of the organic matters, including metabolic products produced by the microorganisms and the lysis products from death cells, can be used by the bacteria as a carbon and energy source. Hence, the BOD<sub>5</sub> is always lower than the COD (Wiesmann *et al.* 2007). A successful activated sludge process should yield effluent containing an average of 20 mg/L of BOD<sub>5</sub> (Shieh and Nguyen 1999a). It was reported that the BOD<sub>5</sub>/COD ratio for domestic wastewater ranged from 0.2 – 0.6 (Bitton 2005b). Based on this, the

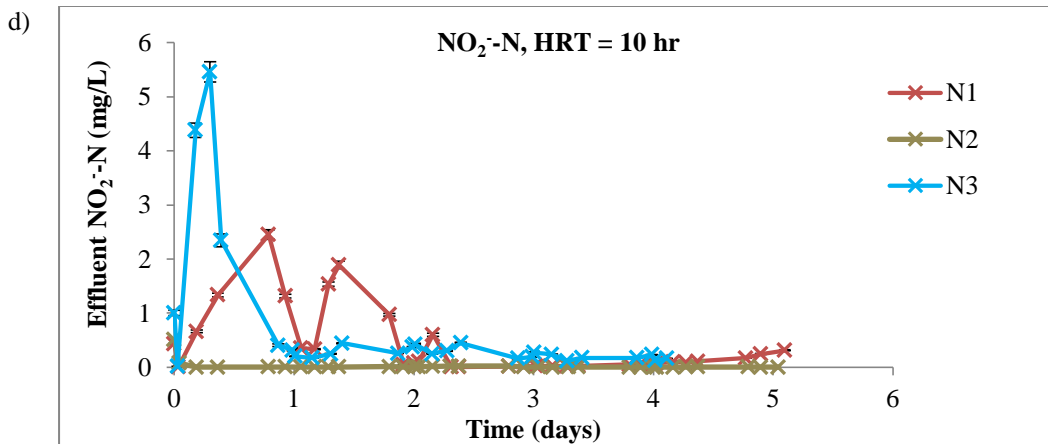
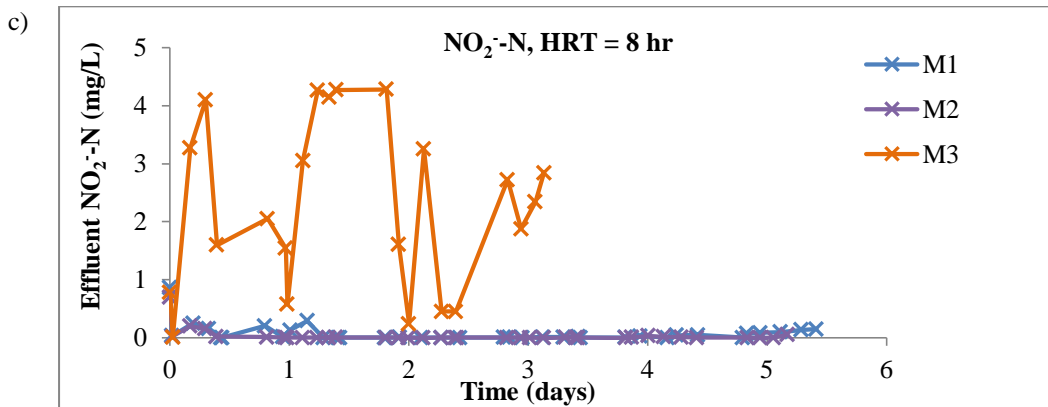
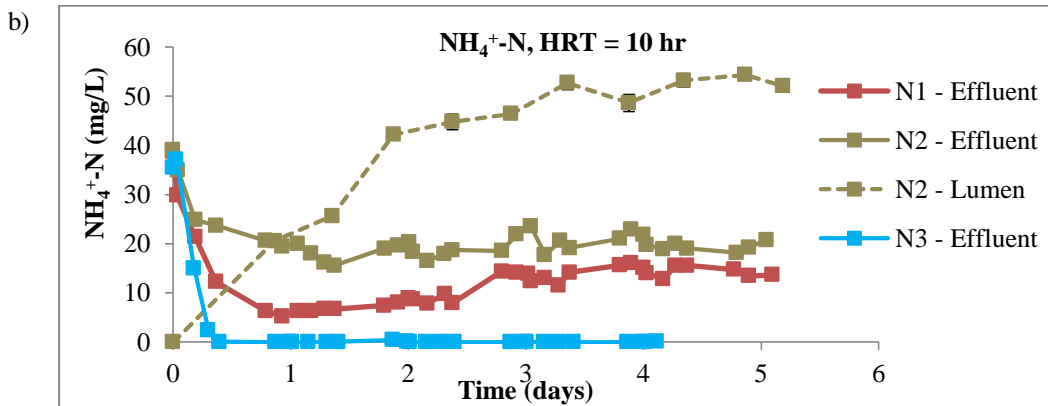
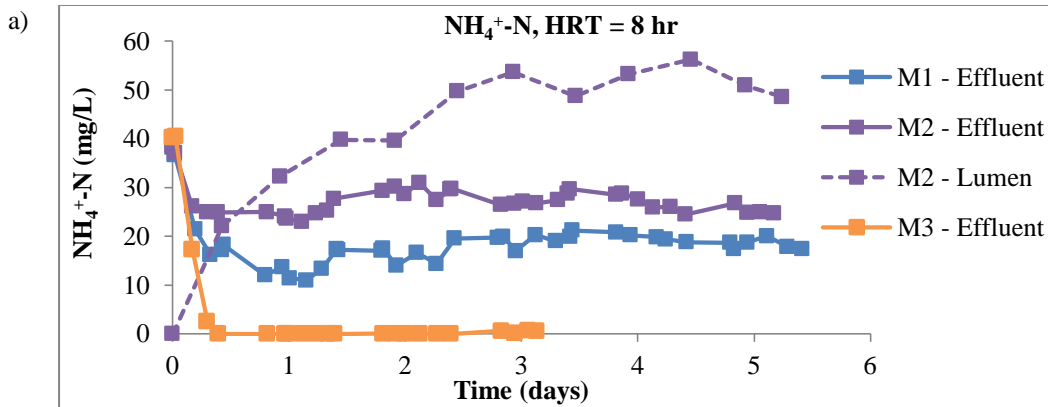
estimated steady state effluent BOD<sub>5</sub> concentrations in the symbiotic AS-SHFMP systems (M1 and N1) were less than 9.6 mg/L, which would definitely meet the desired BOD<sub>5</sub> for such a discharge. However, without the photosynthetic aeration or external aeration (experiments M2 and N2), a relatively high content of COD was still remained in the effluent (92 – 100 mg/L), indicating that a certain content of BOD<sub>5</sub>, from 60 – 18.4 mg/L, would still be present in the effluent. Hence the discharge of this effluent water could not be guaranteed.

To conclude, the photosynthetic oxygenation in the continuous operation of the AS-SHFMP successfully supported a complete COD removal, and hence a resultant complete BOD<sub>5</sub> removal at both HRTs. Without photosynthetic oxygenation as well as mechanical aeration, around 21% of influent COD still remained in the effluent.

### ***7.3.1(c) Nutrient removal***

#### ***Nitrogen removal***

The contribution of photosynthetic oxygenation to the nitrogen removal in the AS-SHFMPs operated with different HRTs was investigated. Figure 7.4 shows the temporal profiles of effluent NH<sub>4</sub><sup>+</sup> – N, NO<sub>2</sub><sup>-</sup> – N, NO<sub>3</sub><sup>-</sup> – N and total nitrogen (TN) concentrations in experimental sets M and N. Table 7.3 summarizes the nitrogen removal performance in experimental sets M and N.



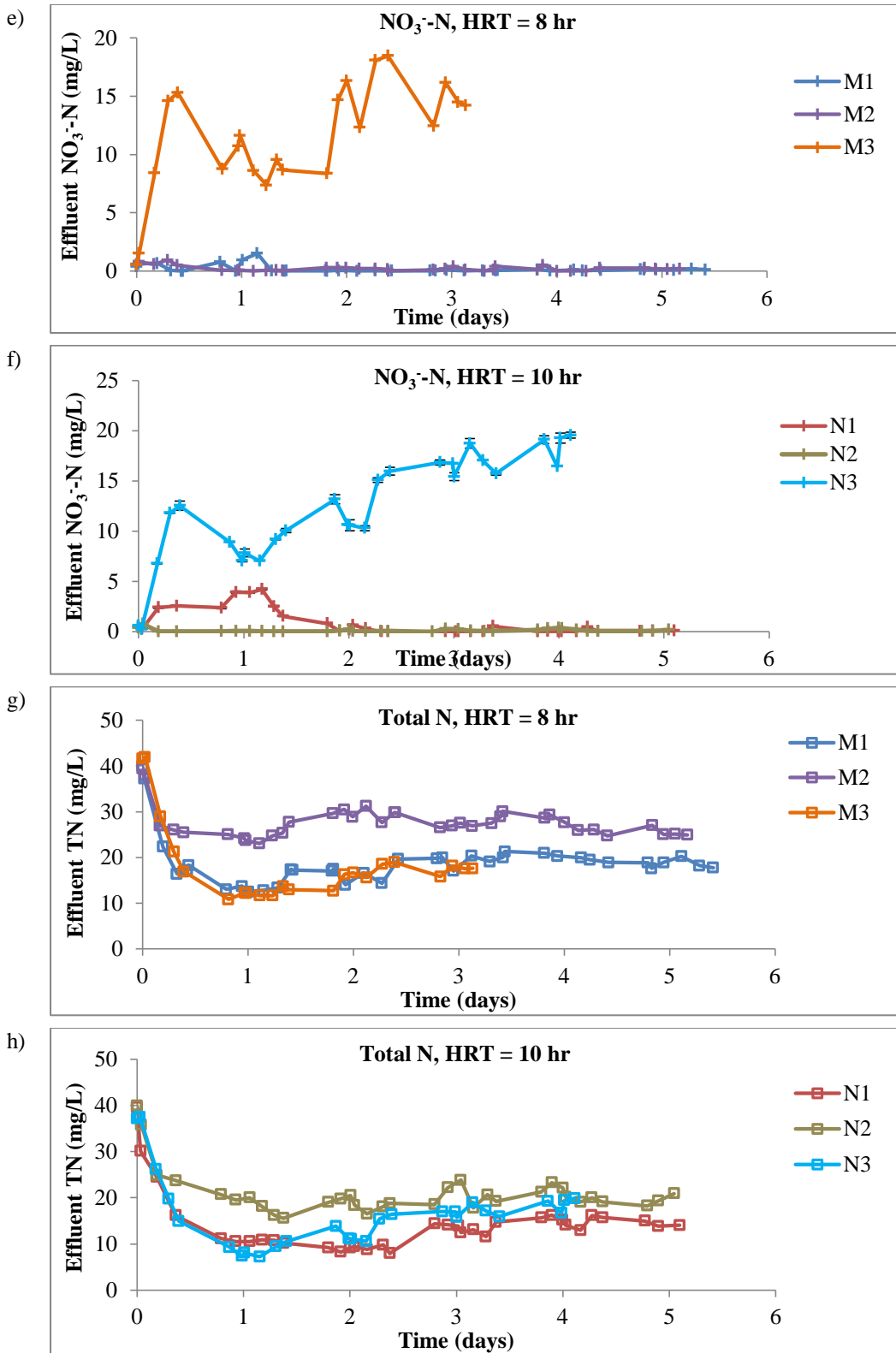


**Figure 7.4.** Temporal concentration profiles of  $\text{NH}_4^+ \text{-N}$  in the lumen-water of M2 and N2, and  $\text{NH}_4^+ \text{-N}$ ,  $\text{NO}_2^- \text{-N}$ ,  $\text{NO}_3^- \text{-N}$ , total nitrogen (TN) in the effluent of the AS-SHFMPs (M1, N1) and the control experiments (M2, M3, N2, N3).

**Table 7.3.** Summary of nitrogen removal performance in experimental sets M and N

Expt	Effluent $\text{NH}_4^+ - \text{N}$ conc. (mg/L)	$\text{NH}_4^+ - \text{N}$ removal efficiency (%)	Total inlet $\text{NH}_4^+ - \text{N}$ fed (mg)	Total $\text{NH}_4^+ - \text{N}$ removed by biomass (mg) *	TN removal efficiency (%)	Major nitrogenous component remained in effluent
M1	19.26	52	227.35	124.40	51	$\text{NH}_4^+ - \text{N}$
M2	27.18	32	217.15	63.06	32	$\text{NH}_4^+ - \text{N}$
M3	0.124	100	131.54	124.45	57	$\text{NO}_3^- - \text{N}$
N1	14.13	65	171.27	119.88	65	$\text{NH}_4^+ - \text{N}$
N2	19.4	52	169.52	76.63	52	$\text{NH}_4^+ - \text{N}$
N3	0.045	100	138.13	132.86	57	$\text{NO}_3^- - \text{N}$

\* Total  $\text{NH}_4^+ - \text{N}$  removed by biomass = (total inlet  $\text{NH}_4^+ - \text{N}$ ) – (total outlet  $\text{NH}_4^+ - \text{N}$ ) – (total  $\text{NH}_4^+ - \text{N}$  in lumen-water, if available)

As can be seen in Figure 7.4a and 7.4b, under fully aerated condition (experiments M3 and N3), the  $\text{NH}_4^+ - \text{N}$  concentration was quickly degraded and maintained around zero at both HRTs, resulting in  $\text{NH}_4^+ - \text{N}$  removal efficiency of 100%. The appearance of  $\text{NO}_2^- - \text{N}$  (Figure 7.4c and 7.4d) and high concentration of  $\text{NO}_3^- - \text{N}$  (up to 19 mg/L, Figure 7.4e and 7.4f) in the effluent suggested the occurrence of nitrification. Hence, it can be concluded that the 100% removal efficiency of  $\text{NH}_4^+ - \text{N}$  in M3 and N3 was achieved by biomass assimilation and nitrification. Due to the nitrification activity, the effluent total nitrogen concentrations were relatively high (around 15 mg/L (M3) and 17.4 mg/L (N3), Figure 7.4g and 7.4h), leading to a total nitrogen removal efficiency of 57% (Table 7.4). However, the majority component of total nitrogen in the effluent was  $\text{NO}_3^- - \text{N}$  (occupied more than 80% of effluent total nitrogen content), and it can be removed through biological denitrification. The denitrification process was not covered in this study.

Under non-aerated condition (experiments M2 and N2), part of the  $\text{NH}_4^+ - \text{N}$  concentration was also degraded. At the HRT of 8 hours, the steady state effluent  $\text{NH}_4^+ - \text{N}$  concentration was around 27.18 mg/L (Table 7.3). This resulted in a removal efficiency of 32%. However, it should be emphasized that there was a relatively high content of  $\text{NH}_4^+ - \text{N}$  found in the lumen-water of M2, approximately 50 mg/L on the final day of the run (Figure 7.4a), suggesting that part of the influent  $\text{NH}_4^+ - \text{N}$  had diffused to the lumen side of the membrane contactor. This phenomenon and its mechanism had been discussed in Section 6.3.2(a). Therefore, if the amount of  $\text{NH}_4^+ - \text{N}$  in the lumen-water was excluded, the actual amount of  $\text{NH}_4^+ - \text{N}$  that assimilated by activated sludge was only about 63.06 mg (Table 7.3), around 29% of total  $\text{NH}_4^+ - \text{N}$  fed. Similar trends for  $\text{NH}_4^+ - \text{N}$  concentration profiles were also observed in experiment N2. At longer HRT of 10 hours, steady state effluent  $\text{NH}_4^+ - \text{N}$  concentration was lower than that at HRT of 8 hours, approximately 19.4 mg/L. However this concentration did not reflect the actual  $\text{NH}_4^+ - \text{N}$  removal efficiency because around 53 mg/L  $\text{NH}_4^+ - \text{N}$  was also found in lumen-water of N2. As a consequence, the total amount of  $\text{NH}_4^+ - \text{N}$  degraded by sludge was 76.63 mg (Table 7.3), about 45% of total  $\text{NH}_4^+ - \text{N}$  fed. It should be noted that there was no nitrification activity in both experiments M2 and N2 as no effluent  $\text{NO}_2^- - \text{N}$  and  $\text{NO}_3^- - \text{N}$  concentrations were observed. This was because the two systems were operated under oxygen - deficient condition, which was certainly not favourable to the strict aerobic nitrifying bacteria (Gerardi 2006b). Hence, the total nitrogen remained in the effluent was mainly comprised of  $\text{NH}_4^+ - \text{N}$ .

With the support from photosynthetic oxygenation (experiments M1 and N1),  $\text{NH}_4^+ - \text{N}$  removal efficiencies in both HRTs were remarkably improved as compared to those under oxygen – deficient condition. At the HRT of 8 hours,  $\text{NH}_4^+ - \text{N}$  removal efficiency was 52%. The total amount of  $\text{NH}_4^+ - \text{N}$  processed was estimated around 124.45 mg (Table 7.3), 97% higher than that of M2. At longer HRT of 10 hours, effluent  $\text{NH}_4^+ - \text{N}$  concentration decreased to around 7.4 mg/L in the first 2.3 days. After that it increased and stabilized at around 14.13 mg/L, resulting in removal efficiency of 65%, significantly higher than that of M1 (52%). The total  $\text{NH}_4^+ - \text{N}$  removed by biomass was estimated at 119.88 mg, around 70% of total  $\text{NH}_4^+ - \text{N}$  fed in N1 and 57% higher than the total amount of  $\text{NH}_4^+ - \text{N}$  degraded by sludge in N2 (76.63 mg). It is worth noticing that no  $\text{NH}_4^+ - \text{N}$  was found in the microalgal cultures of M1 and N1. However, *C.vulgaris* growth was still sustained after the  $\text{NO}_3^- - \text{N}$  content in BBM was depleted (Figure 7.2). Thus, it can be ascertained that  $\text{NH}_4^+ - \text{N}$  in the wastewater might diffuse to the microalgal culture and be assimilated to support the *C.vulgaris* growth. This is a remarkable benefit of the AS-SHFMP system because part of the  $\text{NH}_4^+ - \text{N}$  in the wastewater can be consumed to produce clean microalgal biomass.

Results in Figure 7.4(c-f) also show that some nitrification of  $\text{NH}_4^+ - \text{N}$  occurred in the first two day of the AS-SHFMPs. This suggested that the generated oxygen from *C. vulgaris* photosynthesis had supported the nitrifiers. Higher nitrification activity was observed at the HRT of 10 hours, reflecting by higher effluent  $\text{NO}_2^- - \text{N}$  and  $\text{NO}_3^- - \text{N}$  concentrations in experiment N1, maximum 2.45 mg/L

and 4.23 mg/L respectively. However from day 2 onwards, there was very little oxidized-N present in the effluent. The effluent  $\text{NO}_2^- - \text{N}$  and  $\text{NO}_3^- - \text{N}$  concentrations only accounted for around 1% of total outlet nitrogen content at the HRT of 10 hours. It should be noted that the effluent  $\text{NH}_4^+ - \text{N}$  concentration in N1 also increased from 7.4 mg/L to around 14.13 mg/L from day 2.4 onwards. The reason for this trend could be because when the sludge mass increased, most of the oxygen produced by *C. vulgaris* was quickly consumed by the activated sludge to assimilate the organic matters (COD) and other nutrients. Hence from day 2 onwards, the nitrifiers may not have enough oxygen to oxidize  $\text{NH}_4^+ - \text{N}$  to  $\text{NO}_2^- - \text{N}$  and  $\text{NO}_3^- - \text{N}$ , resulting the decrease of  $\text{NO}_2^- - \text{N}$  and  $\text{NO}_3^- - \text{N}$  concentrations and the increase of  $\text{NH}_4^+ - \text{N}$  concentration in the effluent. As a consequence, the effluent total nitrogen in M1 and N1 was mainly composed of  $\text{NH}_4^+ - \text{N}$ .

As is well-known, nitrogen is an essential substance of all living organisms. All activated sludge treatment processes will remove a certain amount of net nitrogen for the production of new cell mass. Typically the nitrogen assimilation can remove 20 – 30% of the total influent nitrogen (Hong and Holbrook 1999). That explained part of the influent nitrogen was removed under non-aerated condition (experiments M2, N2). With the oxygen supply from *C. vulgaris*, the nitrogen removal efficiency was significantly enhanced. All the results taken together inferred that the ammonium input into the AS-SHFMP system was processed by biomass that consisted of activated sludge, most likely heterotrophs, nitrifiers, and



microalgae in the lumen side. It is also suggested that the largest N flux was by uptake for bacterial growth (and microalgal growth) rather than by nitrification.

To conclude, the results showcased the ability of the AS-SHFMP in  $\text{NH}_4^+$  – N removal over the oxygen-deprived system. Higher nitrogen removal efficiency was obtained in the AS-SHFMP with the HRT of 10 hours. Results also suggested that part of the ammonium input would be converted into clean and contamination-free *C. vulgaris* biomass.

### ***Phosphorus removal***

Phosphorus (P) is one of the macronutrient necessary for living cells (Comeau 2008), hence part of the phosphorus compounds in the wastewater will be assimilated for cell growth. Typically, phosphorus required for cell growth constitutes around 1 – 3% of the volatile fraction of the biomass produced (MLVSS) (Gerardi 2006f; Wentzel *et al.* 2008). Based on this information and the final MLSS, the amount of P required for sludge growth was calculated and presented in Table 7.4. Table 7.4 also summarizes the phosphorus removal performance in experimental sets M and N. Figure 7.5 shows the temporal profiles of effluent  $\text{PO}_4^{3-}$  – P concentration in experimental sets M and N.

As can be seen in Figure 7.5, identical trends were observed for effluent  $\text{PO}_4^{3-}$  – P concentration profiles in experiments M3 and N3. Under fully aeration condition, effluent  $\text{PO}_4^{3-}$  – P concentration quickly decreased and reached zero in the first 24 hours, suggesting that  $\text{PO}_4^{3-}$  – P was consumed to support the exponential growth phase of the activated sludge.

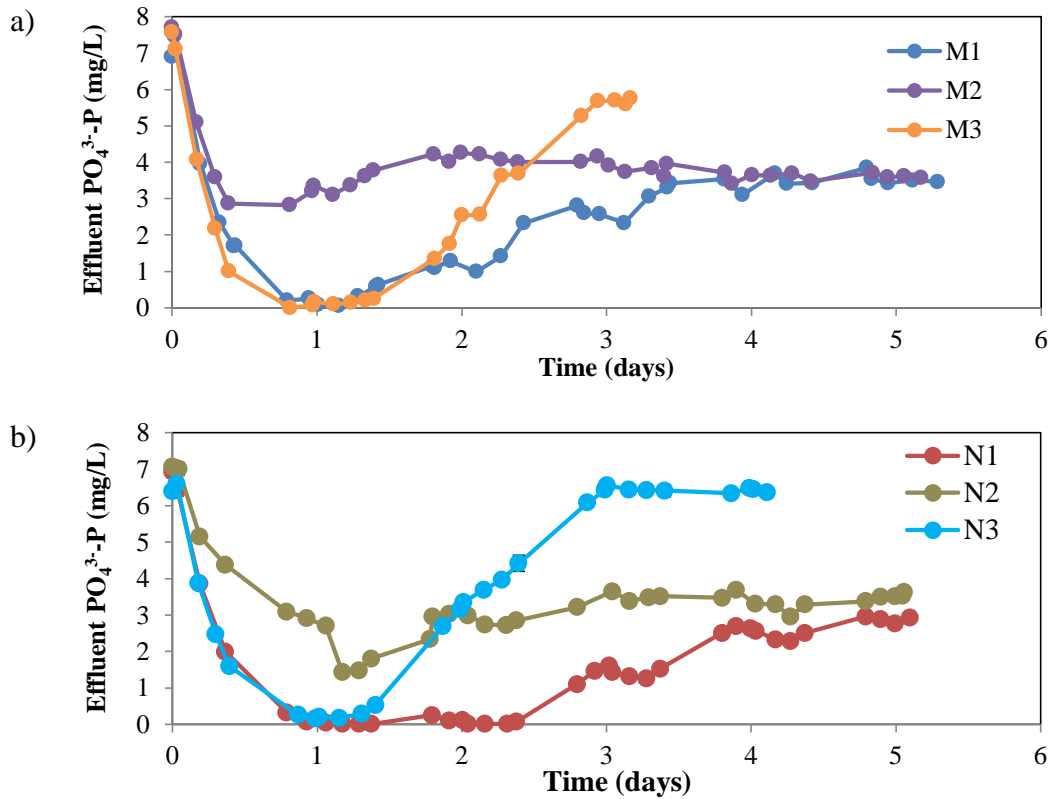


**Figure 7.5.** Temporal concentration profiles of effluent  $\text{PO}_4^{3-} - \text{P}$  in: (a) experimental set M, (b) experimental set N.

**Table 7.4.** Summary of phosphorus removal performance in experimental sets M and N

Expt	Effluent $\text{PO}_4^{3-} - \text{P}$ conc. (mg/L)	$\text{PO}_4^{3-} - \text{P}$ removal efficiency (%)	Final MLSS (g/L) *	Total inlet $\text{PO}_4^{3-} - \text{P}$ fed (mg)	Total $\text{PO}_4^{3-} - \text{P}$ removed (mg) **	P required for sludge growth (mg) ***
M1	3.44 (day 3.4 – 5.3)	57 (day 3.4 -5.3)	3.51	44.39	31.16	7.98 – 27.63
M2	3.68 (day 3.0 – 5.2)	55 (day 3.0 – 5.2)	3.24	43.43	22.88	7.37 – 25.50
M3	5.60 (day 2.9 – 3.1)	30 (day 2.9 – 3.1)	3.94	26.31	18.56	8.97 – 31.05
N1	2.63 (day 3.8 – 5.1)	67 (day 3.8 – 5.1)	3.85	34.25	27.95	8.76 – 30.32
N2	3.42 (day 3.0 – 5.1)	57 (day 3.0 – 5.1)	3.31	33.97	20	7.53 – 26.07
N3	6.45 (day 3.0 – 4.1)	19 (day 3.0 – 4.1)	2.95	27.63	14.96	6.72 – 23.25

\* Measured on the last day of experiments; \*\* Total  $\text{PO}_4^{3-} - \text{P}$  removed by activated sludge = (total inlet  $\text{PO}_4^{3-} - \text{P}$ ) – (total outlet  $\text{PO}_4^{3-} - \text{P}$ );

\*\*\* Estimated based on final MLVSS (assumed that MLVSS represented approximately 65–75% of MLSS (Bitton 2005a)) and phosphorus activated sludge content (approximately 1 – 3% of biomass, (Gerardi 2006f))

After that the effluent  $\text{PO}_4^{3-} - \text{P}$  concentrations in both cases started increasing and were steady at around 5.60 mg/L (M3) and 6.45 mg/L (N3). As a consequence, phosphorus removal efficiencies on the last day were around 30% (at HRT of 8 hours) and 19% (at HRT of 10 hours) (Table 7.4). The decrease in  $\text{PO}_4^{3-} - \text{P}$  removal efficiency on the last day could be because the population of microorganisms was approaching the carrying capacity or maximum number of organisms that the biological treatment unit can support (Gerardi 2006c). As a consequence, the sludge growth rate was slower, leading to less phosphorus required for their growth. Besides, the AS tanks were completely aerated, phosphorus accumulating organisms (PAOs) could not be stimulated and thus  $\text{PO}_4^{3-} - \text{P}$  could not be consumed in excess (Wentzel *et al.* 2008). The steady state phosphorus removal efficiencies in experiment M3 and N3 were consistent with the range of phosphorus removal obtained in a completely aerobic activated sludge system for many municipal wastewaters (15 – 25%, (Wentzel *et al.* 2008)). It is ascertained that the phosphorus content removed in aeration condition (M3, N3) was mainly for cell growth. This observation had been supported by the calculated  $\text{PO}_4^{3-} - \text{P}$  removed and estimated P required for activated sludge growth presented in Table 7.4. The higher loading rate of COD and nutrients under fully aeration condition at the HRT of 8 hours could have stimulated the sludge growth rate, resulting in higher  $\text{PO}_4^{3-} - \text{P}$  removal efficiency as compared to that under the HRT of 10 hours.

With the oxygen supply from photosynthetic oxygenation, the effluent  $\text{PO}_4^{3-} - \text{P}$  concentration trends in the first 24 hours in experiments M1 and N1 were similar

to those under aeration condition. As can be seen in Figure 7.5a, at the HRT of 8 hours  $\text{PO}_4^{3-} - \text{P}$  was quickly degraded to around zero to support the cell production. After 24 hours, effluent  $\text{PO}_4^{3-} - \text{P}$  concentration increased and were steady at around 3.44 mg/L from day 3.4 to day 5.3, resulting in a removal efficiency of 57% (Table 7.4). At the HRT of 10 hours, the effluent  $\text{PO}_4^{3-} - \text{P}$  concentration was maintained at a value less than 0.1 mg/L for more than a day (day 1 – day 2.31, Figure 7.5b). After that it was also increased and was steady at about 2.63 mg/L, resulting in a removal efficiency of 67% (Table 7.4). It might be that when the cell mass increased, more oxygen was required to degrade the organic matters and other nutrients (N and P). Most of the oxygen generated by *C. vulgaris* was used to support the complete COD removal (Figure 7.2) and 52 - 65%  $\text{NH}_4^+ - \text{N}$  removal (Table 7.3). Therefore, the remained oxygen may not be sufficient for a higher  $\text{PO}_4^{3-} - \text{P}$  removal. As a result, the  $\text{PO}_4^{3-} - \text{P}$  removal efficiency increased gradually and seemed stable at around 57 – 67%, highest as compared to those in experiments M2, M3, N2, N3, especially in the case of 10-hour HRT (Figure 7.5b). The estimated amount of  $\text{PO}_4^{3-} - \text{P}$  removed was in accordance with the estimated P amount required for cell growth, suggesting that phosphorus accumulation into the biomass was the main mechanism in this system. It should be noted that the operation of AS-SHFMP at 10-hour HRT (N1) allowed higher phosphorus removal efficiency as compared to that under 8-hour HRT (M1). This was because the AS flocs had more time to contact with the nutrients as well as the oxygen evolved from microalgal photosynthesis.

Based on the total amount of  $\text{PO}_4^{3-} - \text{P}$  fed to the AS tank and the calculated amount of  $\text{PO}_4^{3-} - \text{P}$  removed by activated sludge (Table 7.4), the percentage of amount of  $\text{PO}_4^{3-} - \text{P}$  removed in N1 (82%) was significantly higher than those under aerobic condition (N3, 54%) and oxygen-deficient condition (N2, 60%). This suggested that the photosynthetic oxygenation might have improved the  $\text{PO}_4^{3-} - \text{P}$  removal of the activated sludge over the extensive aeration condition or the oxygen-deficient condition.

In the absence of photosynthetic oxygenation and external aeration, microorganisms in activated sludge could have used the oxygen presented in the system during the startup phase to assimilate  $\text{PO}_4^{3-} - \text{P}$  for biomass production. Hence, effluent  $\text{PO}_4^{3-} - \text{P}$  concentrations were initially decreased to 2.8 mg/L (M2) and 1.4 mg/L (N2) in the first two days (Figure 7.5). After that, the effluent  $\text{PO}_4^{3-} - \text{P}$  concentration in M2 and N2 increased and were steady at around 3.68 mg/L (M2) and 3.42 mg/L (N2), resulting in similar average removal efficiencies of 55% and 57% (Table 7.4). The effluent  $\text{PO}_4^{3-} - \text{P}$  concentrations in M2 and N2 were significantly lower than those of M3, N3 and close to or slightly higher than those of M1 and N1. This suggested that the oxygen-deficient condition in the AS tanks of M2 and N2 could have stimulated the growth of the facultative anaerobes, and these microorganisms also required phosphorus to support cell growth. The MLSS results in Table 7.3 showed that MLSS still increased under oxygen-deficient condition, but was much lower than those under photosynthetic oxygenation after the same duration of experiment. The calculated amount of  $\text{PO}_4^{3-} - \text{P}$  removed in M2 and N2 fitted within the required range for cell growth.

From day 4 to day 5, the  $\text{PO}_4^{3-} - \text{P}$  removal efficiency in M2 was similar to that of M1. Only when the HRT was increased to 10 hours, phosphorus removal efficiency in the presence of photosynthetic oxygenation was improved and significantly higher than that in the absence of photosynthetic oxygenation (Figure 7.5b).

To conclude, the  $\text{PO}_4^{3-} - \text{P}$  removal efficiency in the AS-SHFMP was higher than those of fully aerated condition and oxygen-deficient condition. Phosphorus accumulation into the biomass was the main mechanism in this system. The assimilation of the phosphorus also depended on the HRT: the operation of the AS-SHFMP at the HRT of 10 hours yielded highest removal efficiency among those conditions tested.

#### ***7.3.1(d) Biofilm formation***

In wastewater treatment, biofilm formation on the membrane surface is inevitable especially when the membrane was in direct contact with a complex population of microorganisms in the activated sludge. To investigate the biofilm formation in the AS-SHFMP system and oxygen-deficient condition, the outer surface of hollow fiber membranes in experiments N1 and N2 were visually observed for biofilm condition after 5 days of operation (Figure 7.6).

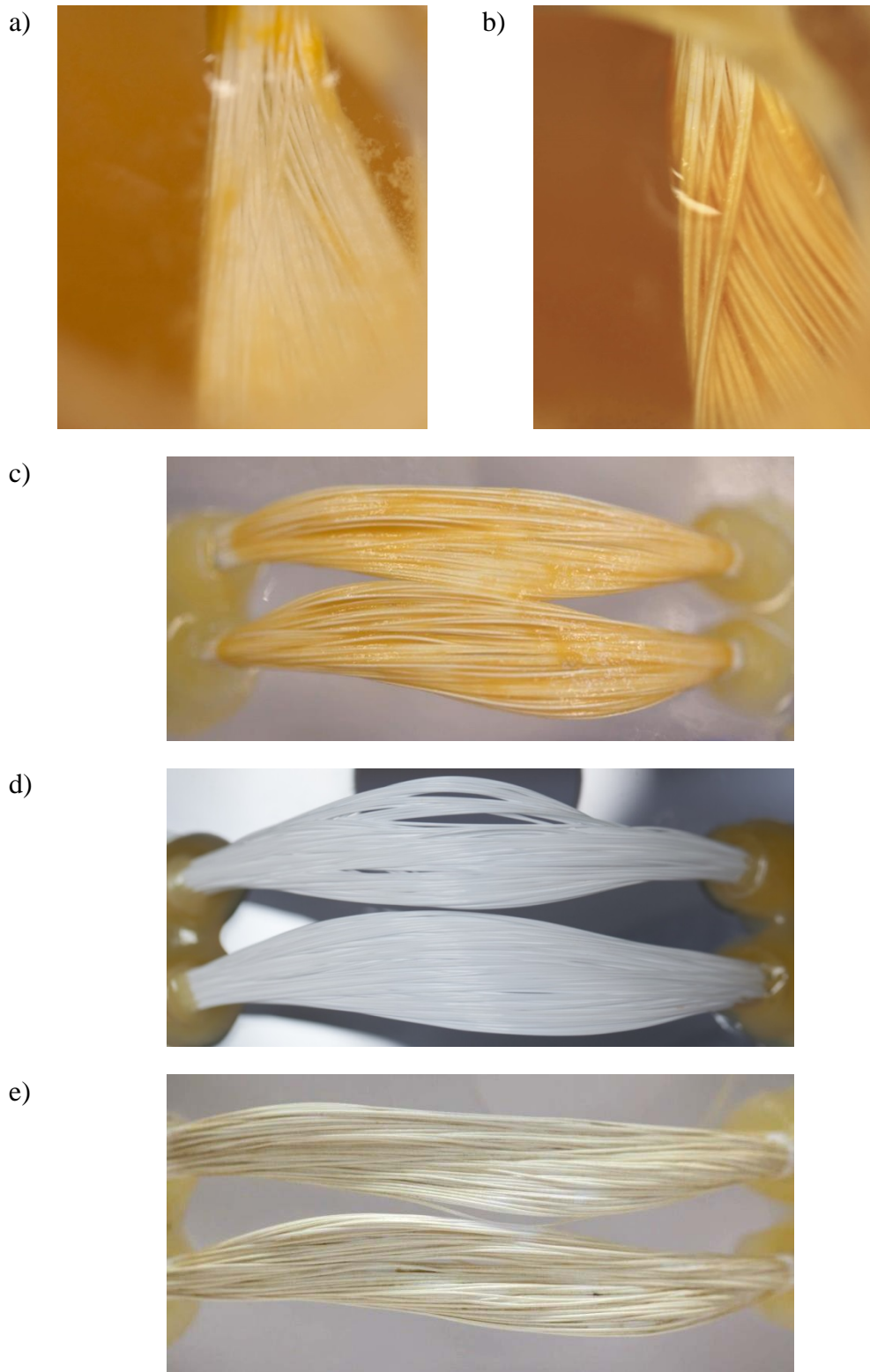


**Figure 7.6.** Hollow fiber membranes after 5-day run: (a) fibers in experiment N1 before washing, (b,c) fibers in experiment N2 before washing, (d) fibers in N1 after washing with 1M NaOH, (e) fibers in N2 after washing with 1M NaOH.

As can be seen in Figure 7.6a, under photosynthetic oxygenation the fibers were relatively clean after 5 days of experiment and their inherent white colour could still be visually recognized. In addition, most of the AS flocs attached on the fiber surface were easily removed by flushing with water. After removing these big AS flocs with water, the lumen side and shell side of fiber bundles were cleaned by 1M NaOH for a few hours to kill and remove all attached microbial cells, followed by the washing with pure water to eliminate excess NaOH until the pH dropped below 7. The fiber bundles were qualified as they were totally clean after the washing (Figure 7.6d) and were ready for the reuse in the next experiment.

On the contrary, the fiber bundles in the oxygen-deficient condition (N2) were severely attached by biofilm after the same duration of experiment. Unlike the fibers in N1, the fibers in N2 were covered by a yellow adhesive layer of biofilm (Figure 7.6 b, c), and this biofilm could not be removed by flushing with water. Even after 8 - hour washing with 1M NaOH, most of the areas on the fibers were still covered with firmly attached biofilm as shown in Figure 7.6e. Hence these fiber bundles were not reusable.

The difference in biofilm formation between the experiments N1 and N2 was originated from the difference in structural change of microbial community under different oxygen supply conditions. Under the oxygen-deficient condition, the biofilm was thicker and its specific resistance was higher than the biofilm formed under the oxygen-sufficient condition. This was due to the fact that at low dissolved oxygen (DO) concentration in the activated sludge, the dead cell number could be higher and hence the accumulation of the organic matters (e.g.



polysaccharides and proteins) produced from the lysis of dead cells would be more severe, which would dramatically change the biofilm structure. These organic matters are inherently adhesive (Ohashi and Harada 1994), leading to a more significant integration of flocs into the biofilm. As a consequence, the biofilm became thicker and denser as observed in the experiment N2. Our results were in agreement with the conclusion of Kim *et al.* (2006), where suggested that the rate of membrane fouling in MBR at the low DO concentration was much faster than that at the high DO concentration.

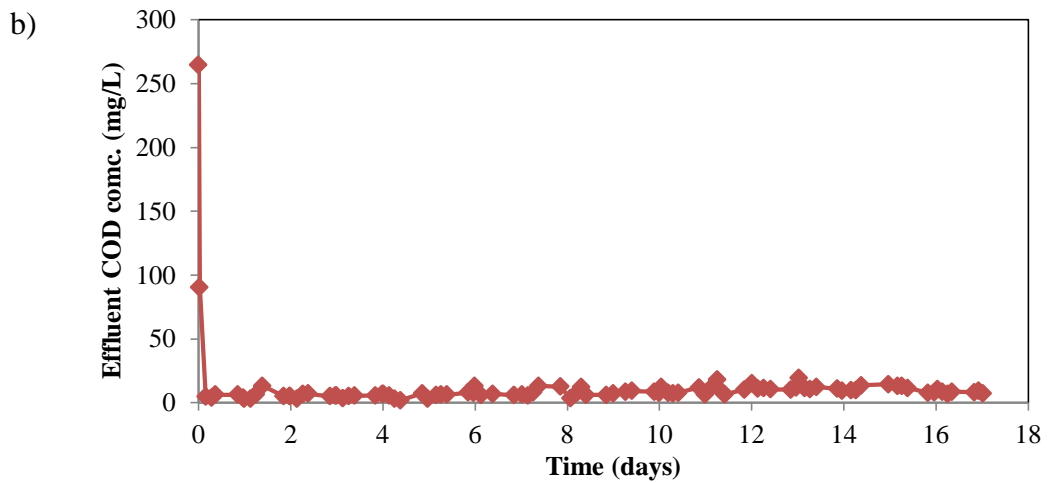
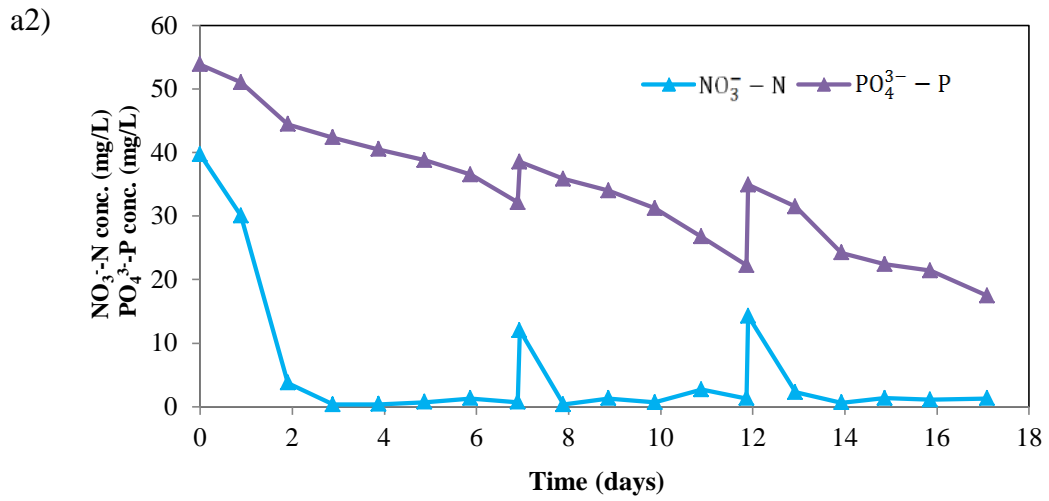
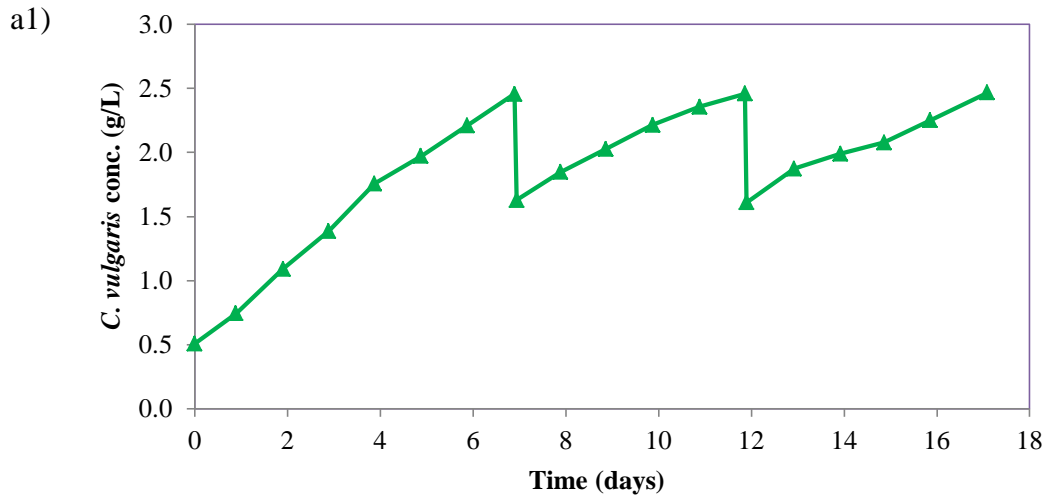
To conclude, the symbiotic AS-SHFMP system showcased its effectiveness in the aerobic wastewater treatment. With the oxygen supply from photosynthetic oxygenation the COD,  $\text{NH}_4^+ - \text{N}$  and  $\text{PO}_4^{3-} - \text{P}$  removal efficiencies were significantly higher than those under oxygen-deficient condition. Especially the COD degradation was successfully maintained at removal efficiency greater than 98% throughout the run, totally comparable with that of conventional activated sludge process. Microalgal biomass concentration was relatively high (2 g/L), and was free of contamination. The AS-SHFMP operation at the HRT of 10 hours exhibited better *C. vulgaris* growth as well as  $\text{NH}_4^+ - \text{N}$  and  $\text{PO}_4^{3-} - \text{P}$  biodegradation performance. Especially, the oxygen supply from microalgal photosynthesis helped to sustain the healthy growth of the activated sludge, which could help to prevent the significant formation of biofilm in the AS-SHFMP during 5-day operation.

Based on the obtained results the HRT of 10 hours was chosen to study the long-term operation of the AS-SHFMP. Besides, in order to sustain good performance

of the hollow fiber membranes in the long-term operation experiment, the fiber bundles in the activated sludge tank were replaced every 4 days for effective washing and reusability.

### **7.3.2 Long-term operation of the AS-SHFMP**

The operation of the AS-SHFMP system involves the kinetic growths of both microalgae and activated sludge. If microalgal growth rate decreases, the oxygen production will be reduced, and hence the COD and nutrient removal capacities of the activated sludge will be decelerated. On the other hand, microalgal photosynthesis also relies on the CO<sub>2</sub> produced by the activated sludge, the availability of other nutrients (N, P, etc.) and light. Therefore, the performance of the symbiotic AS-SHFMP system will be affected if one of the cultures does not function probably. In addition, hydrophobic hollow fiber membranes such as polypropylene are prone to biofilm especially when they are directly used with microbial cultures. In the long run, the biofilm become a mass transfer resistance to O<sub>2</sub> and CO<sub>2</sub> exchange, harmful to the symbiotic process. Hence in this follow up research, a 17 – day continuous operation of the AS-SHFMP at the HRT of 10 hours was conducted to validate if the waste removal capacity was stable and if not, how it could be mitigated. To prevent the negative effects of biofilm, the fiber bundles were exchanged every 3.5 – 4 days. Figure 7.7 shows the temporal profiles of *C. vulgaris*, COD and nutrients concentrations during the run.



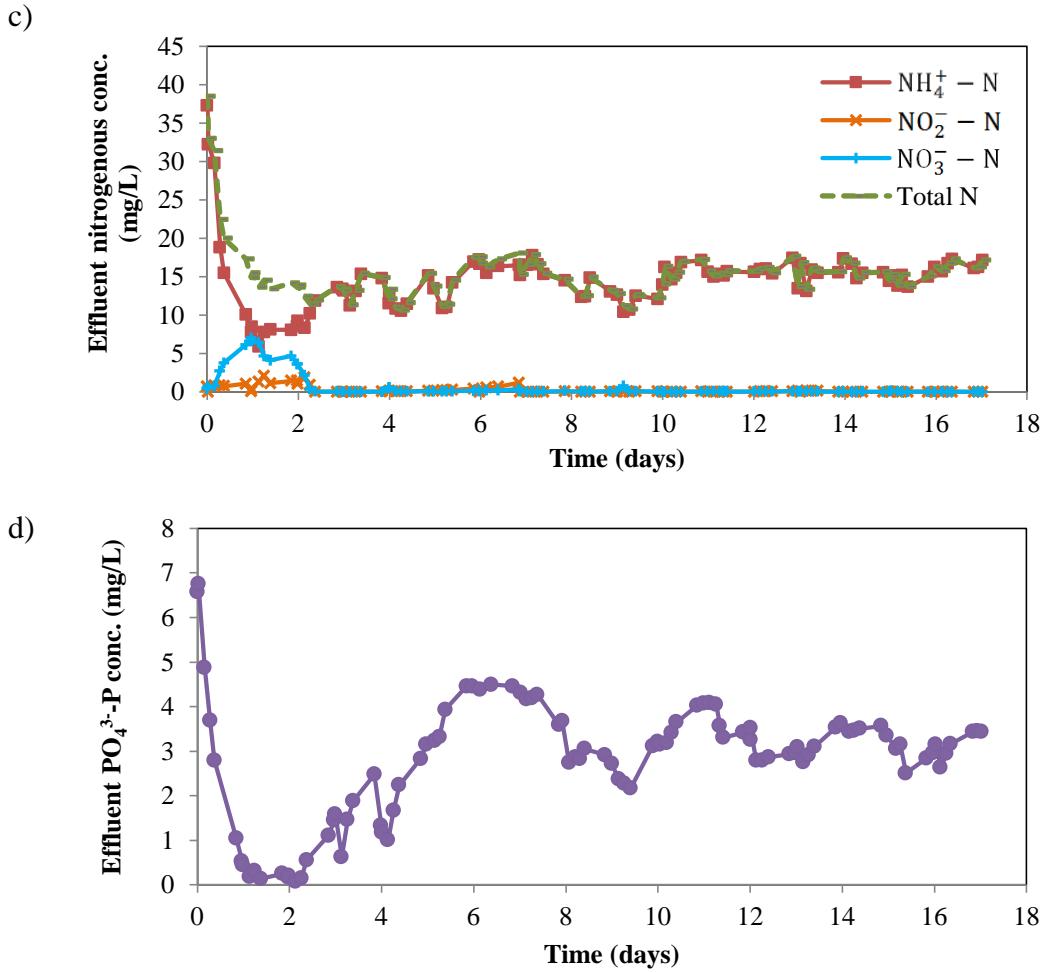


**Figure 7.7.** Long-term operation of the AS-SHFMP: temporal concentration profiles of (a1) *C. vulgaris*, (a2)  $\text{NO}_3^- - \text{N}$  and  $\text{PO}_4^{3-} - \text{P}$  in the microalgal culture; temporal concentration profiles of (b) COD, (c)  $\text{NH}_4^+ - \text{N}$ ,  $\text{NO}_2^- - \text{N}$ ,  $\text{NO}_3^- - \text{N}$  and (d)  $\text{PO}_4^{3-} - \text{P}$  in the effluent.

As can be seen in Figure 7.7, the trends in *C. vulgaris* growth, effluent COD,  $\text{NH}_4^+ - \text{N}$  and  $\text{PO}_4^{3-} - \text{P}$  concentration profiles in the first 5 days were identical to those obtained in experiment N1. The photosynthetic oxygenation of *C. vulgaris* successfully supported the complete COD biodegradation, maintaining the removal efficiency of COD around 98% throughout 17 days of operation (Figure 7.7b). This strongly suggested that effluent  $\text{BOD}_5$  concentration was most likely low, and can meet the desired  $\text{BOD}_5$  for the discharge. However, some

fluctuations were observed in the  $\text{NH}_4^+ - \text{N}$  and  $\text{PO}_4^{3-} - \text{P}$  removals. From day 5 to 7, although the effluent COD concentration was still remained steady at value lower than 13 mg/L, the effluent concentrations of  $\text{NH}_4^+ - \text{N}$  and  $\text{PO}_4^{3-} - \text{P}$  were increasing to around 16.5 mg/L and 4.4 mg/L, respectively (Figure 7.7c and 7.7d). In advance of the reduction in nutrients removal efficiency, the microalgal growth rate was found to decrease from day 4 to day 7 (Figure 7.7a1). As a result, the oxygen produced by photosynthesis was lessened and could be just sufficient to sustain the complete COD removal while not be able to maintain the removal capacities of  $\text{NH}_4^+ - \text{N}$  and especially  $\text{PO}_4^{3-} - \text{P}$ .

The reduction in *C. vulgaris* growth could be because of the fast depletion of nutrients in microalgal culture, which was most likely due to the high initial microalgae concentration used (500 mg/L). As can be seen in Figure 7.7a2, the  $\text{PO}_4^{3-} - \text{P}$  concentration in the *C. vulgaris* culture decreased to 32 mg/L (40% assimilated) while the  $\text{NO}_3^- - \text{N}$  content had been depleted since day 2.4. Although *C. vulgaris* could have obtained additional  $\text{NH}_4^+ - \text{N}$  from the shell side, the depletion of other nutrients or minerals might have also limited the cell growth. Hence when the *C. vulgaris* concentration approached 2.46 g/L on day 7, one-third of the microalgal culture (50 mL) was withdrawn and the same volume of fresh BBM was supplemented to the microalgae-flask. The addition of fresh BBM was to resume the volume of the microalgal culture as well as to supply the nutrients and minerals to *C. vulgaris*. The same fed-batch culture strategy was repeated on day 12 when the concentration was also at 2.46 g/L. The intermittent removed *C. vulgaris* culture could be harvested for biomass usage.

The addition of fresh BBM diluted the *C. vulgaris* concentration to 1.63 g/L.  $\text{NO}_3^- - \text{N}$  concentration in the microalgal culture increased to 12 mg/L and it was quickly consumed within the following day (Figure 7.7a2). The  $\text{PO}_4^{3-} - \text{P}$  concentration in the microalgal culture also increased to 38.5 mg/L (day 7) and 35 mg/L (day 12, Figure 7.7a2). After the addition of BBM, *C. vulgaris* growth was sustained and increased to the concentration of 2.46 mg/L after every 5 days (day 12 and day 17).

Immediately after the replacement of fresh BBM in *C. vulgaris* culture on day 7 and day 12, the effluent concentrations of  $\text{NH}_4^+ - \text{N}$  and  $\text{PO}_4^{3-} - \text{P}$  decreased. This implied that the oxygen production of microalgal photosynthesis was improved after the fed-batch culture and hence nutrient removal efficiencies were resumed. By using fed-batch strategy for microalgal culture, the removal efficiencies of  $\text{NH}_4^+ - \text{N}$  and  $\text{PO}_4^{3-} - \text{P}$  were maintained around 63% and 60%, respectively.

It should be noted that the nitrification activity was strongest in the first 2 days of operation when 80 – 85% of influent  $\text{NH}_4^+ - \text{N}$  was degraded (Figure 7.7c). The conversion of  $\text{NH}_4^+ - \text{N}$  into  $\text{NO}_2^- - \text{N}$  and  $\text{NO}_3^- - \text{N}$  accounted for 3% and 13% of total inlet nitrogen, respectively. From day 2.3 onwards, the effluent  $\text{NO}_2^- - \text{N}$  and  $\text{NO}_3^- - \text{N}$  concentrations were very low (around 0.5% and 0.6% of total outlet nitrogen content), and thus the resultant effluent total nitrogen concentration was relatively identical with effluent  $\text{NH}_4^+ - \text{N}$  concentration (Figure 7.7c). These inferred that the main nitrogen removal mechanism was activated sludge nitrogen assimilation, part of which may be assimilated by *C. vulgaris*.

The contamination test performed for the dense dark green *C. vulgaris* culture when the run was terminated showed that the culture was completely free of contaminations after 17 days of operation. As can be seen in Figure 7.8, there were only green colonies of *C. vulgaris* on nutrient agar plate; no colonies of other contaminants were observed even after incubating the agar plates at 30°C for a week. This confirmed that the polypropylene hollow fiber membranes had successfully done their jobs: facilitate the gaseous transfer between the two cultures and prevent the cross contamination of the cultures across the fibers, protecting the *C. vulgaris* culture from contamination.

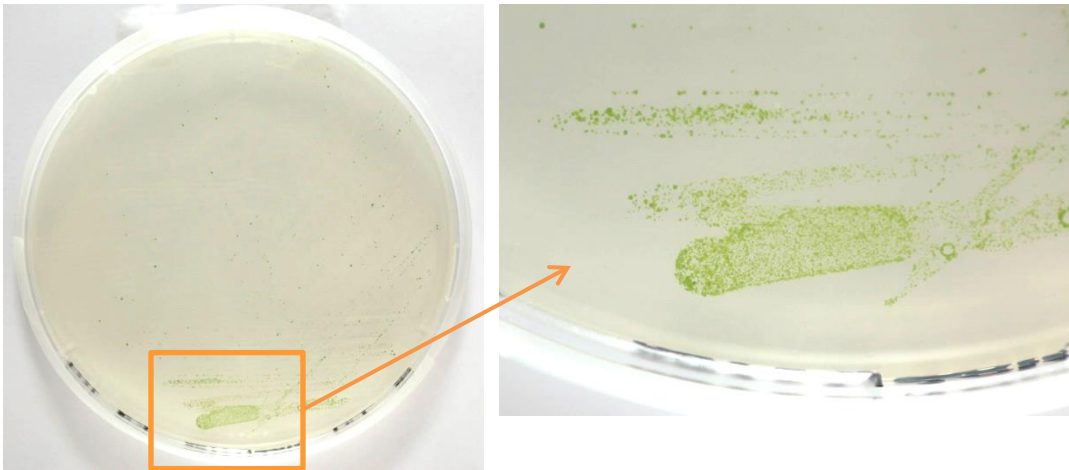


**Figure 7.8.** Nutrient agar plate of the *C. vulgaris* culture in the long-term operation experiment after one – week incubation at 30°C.

To conclude, the results from 17-day continuous operation suggested that long-term operation of the AS-SHFMP was feasible. The COD and nutrient removal capacities of the activated sludge essentially depended on the photosynthesis capacity of *C. vulgaris* and the quality of the hollow fiber membrane, hence by using fed-batch mode for a fixed volume of *C. vulgaris* culture and changing the

fiber bundles every 4 days to prevent the negative effects of biofilm, the photosynthetic oxygenation of *C. vulgaris* was sustained, and thus removal efficiencies of COD,  $\text{NH}_4^+ - \text{N}$  and  $\text{PO}_4^{3-} - \text{P}$  were maintained at 98%, 63% and 60% respectively. *C. vulgaris* concentration was relatively high (~ 2.5 g/L at day 17), especially it was isolated from the activated sludge and axenic, which was undoubtedly advantageous and flexible for the biomass harvesting and usage.

### **7.3.3 Comparison between AS-SHFMP and current co-culture symbiotic wastewater treatment processes**

Table 7.5 summarizes the COD and nutrient removal performances of the conventional activated sludge process and current symbiotic microalgal–bacterial processes treating different types of wastewaters.

In this study, the continuous operation of the AS-SHFMP at the HRT of 10 hours achieved the removal efficiencies of COD, nitrogen and phosphorus around 98%, 63% and 60%, respectively. Assumed the  $\text{BOD}_5/\text{COD}$  ratio after the biological treatment is 0.2 (Bitton 2005b),  $\text{BOD}_5$  removal efficiency of the AS-SHFMP could be greater than 99%. Thus the performance of the AS-SHFMP was more effective than that of the conventional activated sludge process treating municipal wastewater (Table 7.5).



**Table 7.5.** COD and nutrient removal performances of the AS-SHFMP, conventional activated sludge process and current symbiotic co-culture processes treating different types of wastewater

Reactor type	Source of wastewater	HRT	COD, N, P Removal (%)	Microalgal biomass (g/L)	Reference
AS-SHFMP	Synthetic wastewater (430 mg/L COD, 40 mg/L NH <sub>4</sub> <sup>+</sup> -N, 8 mg/L PO <sub>4</sub> <sup>3-</sup> -P)	10 hrs	98% COD, 63% NH <sub>4</sub> <sup>+</sup> -N, 60% PO <sub>4</sub> <sup>3-</sup> -P	2.5 g/L	This study
Conventional activated sludge process	Municipal wastewater	4 - 8 hrs	> 70% COD, > 90% BOD <sub>5</sub> , 35% N > 30% P	---	(Shieh and Nguyen 1999a)
Photo-bioreactor	Synthetic wastewater (150 mg/L COD, 8 mg/L NH <sub>4</sub> <sup>+</sup> -N)	6 days (batch mode)	85% COD 86.3% NH <sub>4</sub> <sup>+</sup> -N	---	(Roudsari <i>et al.</i> 2014)
HRAP	Primary settled wastewater (20 – 30.7 mg/L NH <sub>4</sub> <sup>+</sup> -N, 0.9 – 3.6 mg/L P)	5.5 – 9 days	47–79% NH <sub>4</sub> <sup>+</sup> -N, 20 – 49% P	---	(Sutherland <i>et al.</i> 2014a)
Biofilm algal-bacterial reactor	Domestic wastewater (91 mg/L TN, 7 mg/L PO <sub>4</sub> <sup>3-</sup> -P)	10 days	70% TN, 85% PO <sub>4</sub> <sup>3-</sup> -P	---	(Posadas <i>et al.</i> 2013)
Photo-bioreactor	Synthetic wastewater (20 mg/L NH <sub>4</sub> <sup>+</sup> -N, 4 mg/L TP)	6 days (batch mode)	86% NH <sub>4</sub> <sup>+</sup> -N, 93% TP	5.42 mg/L Chl- <i>a</i>	(Liang <i>et al.</i> 2013)
Opened sequencing batch reactor	Synthetic wastewater (50 mg/L NH <sub>4</sub> <sup>+</sup> -N)	18.5 hr react/ 24 hr cycle	100% NH <sub>4</sub> <sup>+</sup> -N (after less than 14 cycles)	29 mg/L Chl- <i>a</i>	(Karya <i>et al.</i> 2013)
HRAP	Municipal wastewater (56.6 mg/L NH <sub>4</sub> <sup>+</sup> -N)	4 days	88.3% NH <sub>4</sub> <sup>+</sup> -N (with CO <sub>2</sub> addition)	0.5 g/L	(Park and Craggs 2011)
Opened stirred tank photo-bioreactor	Municipal wastewater (103 – 133 mg/L COD, 15 – 19 mg/L NH <sub>4</sub> <sup>+</sup> -N, 4 – 5 mg/L PO <sub>4</sub> <sup>3-</sup> -P)	8 days (batch mode)	98% COD 100% NH <sub>4</sub> <sup>+</sup> -N, 54 – 76% PO <sub>4</sub> <sup>3-</sup> -P	1.84 g/L (algal-bacterial biomass)	(Su <i>et al.</i> 2011)

As compared to the current microalgal-bacterial wastewater treatment processes where microalgae and bacteria/activated sludge were cultured together in closed or opened systems, the COD and nutrient removal efficiencies of the AS-SHMP are more effective or at least comparable in consideration of source of wastewater (synthetic or real wastewater), quality of wastewater (COD and nutrient concentrations), mode of operation (batch, sequencing batch or continuous) and hydraulic retention time (in hours or days). For example, Roudsari and colleagues (2014) reported that the maximum removal efficiencies for COD and  $\text{NH}_4^+ - \text{N}$  were 85 and 86.3% in treating the synthetic anaerobic effluent of municipal wastewater. However, this synthetic wastewater only contained 150 mg/L COD and 8 mg/L  $\text{NH}_4^+ - \text{N}$ , which were much lower than the influent COD and  $\text{NH}_4^+ - \text{N}$  concentrations used in the AS-SHFMP. Besides, that synthetic wastewater was treated in a 6-day batch operation to obtain the mentioned removal efficiencies while the AS-SHFMP could achieve higher COD and  $\text{NH}_4^+ - \text{N}$  removal in continuous operation at HRT of 10 hours.

In comparison to the HRAP system where real municipal wastewater was treated, high  $\text{NH}_4^+ - \text{N}$  removal efficiency (88.3%) was only obtained with the addition of  $\text{CO}_2$  (Park and Craggs 2011), while there was no external supplementation of  $\text{O}_2$  and  $\text{CO}_2$  to the AS-SHFMP. In addition, although the long HRTs of 4 to 9 days were required for the operation of HRAPs (Park and Craggs 2011; Sutherland *et al.* 2014b), the nitrogen removal in the HARP is still limited (Karya *et al.* 2013). Park and Craggs (2011) observed that with an HRT of 8 days and an influent of  $56.6 \pm 9.6$  mg/L  $\text{NH}_4^+ - \text{N}$ , HRAP effluent still contained  $9.2 \pm$

6.1 mg/L  $\text{NH}_4^+ - \text{N}$ ; and the majority of nitrogen removal in the HARP systems was achieved by algal/bacteria assimilation. At shorter HRT (10-hour) in the AS-SHFMP, around 15 mg/L  $\text{NH}_4^+ - \text{N}$  still remained in the effluent, and the main nitrogen removal mechanism was also by the uptake for the activated sludge and microalgal growth rather than by nitrification. In an opened stirred tank photobioreactor operated in batch mode for 8 days, Su and colleagues (2011) concluded that  $\text{PO}_4^{3-} - \text{P}$  removal efficiency ranged from 54 – 76% (Table 7.5) with the main mechanism of phosphorus removal was the phosphorus accumulation into the biomass. These results were also in accordance with what observed in the AS-SHFMP.

Essentially, a major advantage of the AS-SHFMP that cannot be obtained in the conventional activated sludge process and current microalgal-bacterial wastewater treatment processes was the achievement of the axenic microalgal biomass, which was free of contaminations and other pollutants from the wastewater. The maximum microalgal biomass concentration obtained in the AS-SHFMP was 2.5 g/L, much higher than that obtained in the HRAP (0.5 g/L, Table 7.5). Besides, most of the biomass concentrations available in literature were referred to the algal-bacterial biomass (Muñoz *et al.* 2005a; Posadas *et al.* 2013; Su *et al.* 2011), or the microalgal biomass concentration was predicted through the chlorophyll-*a* content (Chl-*a*) (Karya *et al.* 2013; Liang *et al.* 2013) or by microscopic examination (de Godos *et al.* 2010b; González-Fernández *et al.* 2011b), hence might not be as straightforward as in the current study.

The AS-SHFMP exploits the photosynthetic oxygenation to aerobically treat the wastewater, hence the energy required for mechanical aeration can be reduced although mechanical mixing is still required to keep the AS flocs in suspension. Based on the data collected from six Danish wastewater treatment plants using the activated sludge process, Kiilerich *et al.* (2013) reported that around only 10% of total energy consumption is for mechanical mixing (using mixers) in the aeration tank while mechanical aeration (using diffusers) accounts for 42% of total energy. Thus, even if more energy for mixing is needed in the AS-SHFMP when the mechanical aeration is removed, it should not exceed the energy required for intense mechanical aeration.

Besides those mentioned advantages, some limitations of the developed AS-SHFMP system could be addressed as (i) the high initial capital investment cost for the constructions of the microalgae tank (microalgae photobioreactor), the installation of hollow fiber membrane bundles and the LED system, and (ii) the additional resistance to mass transfer due to the presence of the membrane between the two cultures. However, the latter can easily be negated through an increase in the number of membrane fibers and through proper cleaning and maintenance strategy for the fibers.

#### **7.4 Concluding Remarks**

A symbiotic AS-SHFMP was developed and operated with activated sludge and *C. vulgaris* for simultaneous activated sludge wastewater treatment and microalgal biomass production. With the support from photosynthetic oxygenation, the AS-SHFMP successfully removed 98% COD, 63%  $\text{NH}_4^+ - \text{N}$

and 60%  $\text{PO}_4^{3-} - \text{P}$  at the HRT of 10 hours in treating the synthetic wastewater. These results were comparable to those obtained in the conventional activated sludge process and other symbiotic microalgal-bacterial processes. In addition, it has also been demonstrated that long-term continuous operation of the AS-SHFMP was feasible and stable when fed-batch strategy was applied to *C. vulgaris* culture to additionally supply the nutrients for the microalgae. Although the hollow fiber membranes did not experience bad biofilm attachment after 5 days of operation, it was also advised to exchange the fiber bundles every 4 days to ensure good gaseous exchange performance. The periodical substitution of fiber bundles also benefits the reusability and the life span of the fibers.

Last but not least, one unique advantage of the AS-SHFMP over current symbiotic microalgal-bacterial processes was the provision of clean *C. vulgaris* biomass which was free of contaminants. The high quality microalgal biomass is advantageous and useful for the production of animal nutrition, animal feed, human nutrition, skin care products or even high value compounds of which the high quality and public acceptance are required.

These are promising results of a non-optimized AS-SHFMP system whereby the activated sludge and microalgae were coupled in the same system while still being physically separated. The application of the AS-SHFMP in the industry is promising especially when relatively small footprint is the main concern.

## Chapter 8

### Conclusions and Recommendations for Future Work

#### 8.1 Conclusions

This study successfully developed novel symbiotic hollow fiber membrane photobioreactor configurations capable of simultaneously performing aerobic biological wastewater treatment and microalgal biomass production. Results obtained in the symbiotic HFMP configuration supported the hypothesis: in an enclosed system without any external CO<sub>2</sub> and O<sub>2</sub> supply, polypropylene hollow fiber membranes provided excellent CO<sub>2</sub>/O<sub>2</sub> exchange, facilitating the symbiotic relationship between the bacterial and microalgal cultures while they were still physically separated. Bacterium *P. putida* aerobically degraded all of the glucose in the synthetic wastewater using the O<sub>2</sub> supply from the oxygenator *C. vulgaris*, while the *C. vulgaris* grew photo-autotrophically using the CO<sub>2</sub> produced by *P. putida*. The flow orientation of the microalgal culture and bacterial culture in the membrane contactor did remarkably affect the performance of the symbiotic HFMP. Results showed that the symbiotic HFMP performance was optimal when circulating bacterial culture in the shell side and microalgal culture in the lumen side of the membrane contactor: glucose in synthetic wastewater was almost completely degraded (98%) and microalgal biomass productivity was increased by 69% compared to the reversed flow orientation. This flow orientation also minimized the negative effect of bacterial biofilm on the membrane surface, beneficial for the lifespan of the hollow fiber membranes.

Results obtained in the symbiotic HFMP provided foundation for the design of the SHFMP configuration for retrofitting existing activated sludge tanks, especially those in current wastewater treatment plants where the land area for the construction of new microalgae photobioreactor and the hollow fiber membrane contactor might not be available. The most significant result emerged from the study was that the SHFMP could be operated at low volume ratio of microalgal culture to bacterial culture ( $VM/VB = 1 : 2.4$ ). Both batch and continuous operations of the SHFMP were successfully accomplished at this volume ratio. The small VM/VB ratio was indeed advantageous for practical application of the SHFMP because it can help to reduce the operational cost while still ensuring sufficient  $O_2$  supply for the biological wastewater treatment. Especially, the continuous operation at the HRT of 10.6 hours resulted in the 100% of glucose removal efficiency with the sole support from photosynthetic oxygenation. The successful continuous operation of the SHFMP made this configuration even more promising and applicable to the wastewater treatment process where the feed might be a continuous wastewater stream.

The fundamental results obtained in the SHFMP was further exploited in the coupling the activated sludge process with the SHFMP (AS-SHFMP) for the treatment of synthetic domestic wastewater. Once again, the symbiotic relationship between activated sludge and microalgae, which was definitely a more complex relationship, has successfully proved its effectiveness in supporting the aerobic biodegradation of the COD/BOD<sub>5</sub>, nitrogen and phosphorus compounds as well as photoautotrophic microalgal growth. Results showed that at

the hydraulic retention time of 10 hours, removal efficiencies of COD,  $\text{NH}_4^+\text{-N}$  and  $\text{PO}_4^{3-}\text{-P}$  were around 98%, 63% and 60%, respectively. These results were at least comparable to those obtained in the conventional activated sludge process as well as other symbiotic microalgal-bacterial processes in treating domestic or municipal wastewater. The AS-SHFMP was also operated for 17 days to examine its repeatability in biodegradation performance. It was demonstrated that when applying fed-batch strategy to microalgal culture to additionally supply the nutrients for microalgae, long-term continuous operation of the AS-SHFMP was feasible and stable.

One unique advantage of the symbiotic hollow fiber membrane photobioreactors was the generation of clean microalgal biomass which was free of contaminants. The microalgal biomass productivities obtained in the symbiotic HFMP and SHFMP configurations were comparable or higher than those obtained in other photobioreactors reported in literature. The *C. vulgaris* concentration in the AS-SHFMP can reach 2.5 g/L, which was significantly higher than those obtained in current HRAP systems. This high quality microalgal biomass is advantageous and useful for the production of animal nutrition, animal feed, human nutrition, skin care products or even high – value added compounds of which the high quality and public acceptance are strictly required.

Compared to current symbiotic microalgal – bacterial processes, the symbiotic hollow fiber membrane photobioreactor configurations in this research not only provided a self – oxygenated process but also a safer and more effective photosynthetic aeration to reduce the energy required for intense mechanical



aeration without the need of screening for the microalgal strains that are resistant to the pollutants in the wastewaters or for the compatible microalgal – bacterial consortium. The compact footprint of these systems also allowed the applicability and scalability in larger scales.

## **8.2 Recommendations for Future Works**

The promising results of the symbiotic hollow fiber membrane photobioreactor configurations for simultaneous activated sludge wastewater treatment and microalgal biomass production have opened several potential avenues for further exploration of this technology:

1. Results from a non-optimized AS-SHFMP system showed that the  $\text{NH}_4^+ - \text{N}$  and  $\text{PO}_4^{3-} - \text{P}$  removals performance was decent and comparable with those in the HRAP treatment systems and other symbiotic microalgal-bacterial processes in literature even at fairly short HRTs. The complete nutrient removal is complicated and difficult to achieve, however further studies can be carried out to optimize the AS-SHFMP operation and enhance the nitrogen and phosphorus removal efficiencies. For example, increase the hydraulic retention time, increase the number of fibers, or recirculation of treated effluent might be applied to improve the nutrient removal. Enhance phosphorus uptake by activated sludge could also be induced by subjecting the mixed liquor to a period of anaerobiosis prior to aeration (Hong and Holbrook 1999). Furthermore, several patented processes have been proposed to remove nitrogen and phosphorus simultaneously such as  $\text{A}^2/\text{O}$ , Phostrip, UCT/VIP (EPA 1997; Hong and Holbrook 1999). Hence, it is also

worth studying the integration of the AS-SHFMP and those processes to enhance the nutrient removal capacity.

2. The AS-SHFMP operation was studied in lab scale. In order to apply the symbiotic SHFMP in the wastewater treatment plant in Singapore, it is necessary to scale up the laboratory results and establish in pilot plants to treat real wastewater. A number of challenges might occur when dealing with real wastewater such as changes in viscosity, properties of wastewater which would affect the intertransfer of CO<sub>2</sub>/O<sub>2</sub>. Hence in-depth investigation of the effects of such operational parameters as mixing condition, flow velocity would be required. In addition, modification the hollow fiber membrane surface, using other microalgal strains might also be needed. The harvest and usage of clean microalgal biomass should also be taken into account. Data obtained from the larger scales should be subjected to economic feasibility analysis.
3. Due to the physical separation of the microalgal culture and bacterial culture, the symbiotic HFMP and SHFMP operations developed in this research would not be affected by hazardous or toxic pollutants whose toxicity could inhibit microalgal growth as in conventional symbiotic microalgal-bacterial processes. Therefore, apart from domestic wastewater treatment, it is interesting to explore the ability of the proposed models in the treatment of hazardous or toxic pollutants without the need to screen for microalgal strains resistant to those pollutants.

## REFERENCES

- Acién Fernández FG, González-López CV, Fernández Sevilla JM, Molina Grima E (2012) Conversion of CO<sub>2</sub> into biomass by microalgae: how realistic a contribution may it be to significant CO<sub>2</sub> removal? *Applied Microbiology and Biotechnology* 96(3):577-586.
- Acién FG, Fernández JM, Magán JJ, Molina E (2012) Production cost of a real microalgae production plant and strategies to reduce it. *Biotechnology Advances* 30(6):1344-1353.
- Aguirre A-M, Bassi A (2013) Investigation of biomass concentration, lipid production, and cellulose content in *Chlorella vulgaris* cultures using response surface methodology. *Biotechnology and Bioengineering* 110(8):2114-2122.
- Andersen RA, Berges JA, Harrison PJ, Watanabe MM (2005) *Appendix A—Recipes for Freshwater and Seawater Media*. In: Andersen RA (ed). *Algal Culturing Techniques*. Elsevier/Academic Press, pp 429 - 538.
- Anjos M, Fernandes BD, Vicente AA, Teixeira JA, Dragone G (2013) Optimization of CO<sub>2</sub> bio-mitigation by *Chlorella vulgaris*. *Bioresource Technology* 139(0):149-154.
- APHA (2012) *Standard methods for the examination of water and wastewater*, 22nd edn. American Public Health Association Inc., Washington DC
- Apt KE, Behrens PW (1999) Commercial developments in microalgal biotechnology. *Journal of Phycology* 35(2):215-226.
- Banin E, Brady KM, Greenberg EP (2006) Chelator-Induced Dispersal and Killing of *Pseudomonas aeruginosa* Cells in a Biofilm. *Applied and Environmental Microbiology* 72(3):2064-2069.
- Becker EW (1994) *Microalgae : biotechnology and microbiology*. Cambridge University Press, Cambridge ; New York.
- Becker W (2004) *Microalgae in Human and Animal Nutrition*. In: Richmond A (ed). *Handbook of Microalgal Culture : Biotechnology and Applied Phycology*. Blackwell Science, Oxford, UK ; Ames, Iowa, USA, pp 312 - 351.
- Behrens PW (2005) *Photobioreactors and Fermentors: The Light and Dark Sides of Growing Algae*. In: Andersen RA (ed). *Algal Culturing Techniques*. Elsevier/Academic Press, pp 189 - 203.
- Bérubé P (2010) *Chapter 9 Membrane Bioreactors: Theory and Applications to Wastewater Reuse*. In: Isabel CE, Andrea IS (eds). *Sustainability Science and Engineering*. vol Volume 2. Elsevier, pp 255-292.
- Bérubé PR, Afonso G, Taghipour F, Chan CCV (2006) Quantifying the shear at the surface of submerged hollow fiber membranes. *Journal of Membrane Science* 279(1-2):495-505.
- Bitton G (2005a) *Activated sludge process*. *Wastewater microbiology*. 3rd edn. John Wiley & Sons, Hoboken, N.J., pp 225 - 257.
- Bitton G (2005b) *Introduction to wastewater treatment*. *Wastewater microbiology*. 3rd edn. John Wiley & Sons, Hoboken, N.J., pp 213-223.
- Blanken W, Cuaresma M, Wijffels RH, Janssen M (2013) Cultivation of microalgae on artificial light comes at a cost. *Algal Research* 2(4):333-340.
- Boelee NC, Temmink H, Janssen M, Buisman CJN, Wijffels RH (2011) Nitrogen and phosphorus removal from municipal wastewater effluent using microalgal biofilms. *Water Research* 45(18):5925-5933.

- Borde X, Guieysse B, Delgado O, Muñoz R, Hatti-Kaul R, Nugier-Chauvin C, Patin H, Mattiasson B (2003) Synergistic relationships in algal-bacterial microcosms for the treatment of aromatic pollutants. *Bioresource Technology* 86(3):293-300.
- Brading MG, Boyle J, Lappin-Scott HM (1995) Biofilm formation in laminar flow using *Pseudomonas fluorescens* EX101. *Journal of Industrial Microbiology* 15(4):297-304.
- Brandi G, Sisti M, Amagliani G (2000) Evaluation of the environmental impact of microbial aerosols generated by wastewater treatment plants utilizing different aeration systems. *Journal of Applied Microbiology* 88(5):845-852.
- Brennan L, Owende P (2010) Biofuels from microalgae-A review of technologies for production, processing, and extractions of biofuels and co-products. *Renew Sust Energ Rev* 14(2):557-577.
- Cao YS (2011a) *General introduction*. Biological phosphorus removal activated sludge process in warm climates. IWA Publishing, London, pp 1-4.
- Cao YS (2011b) *Mass flow and balance of carbonaceous, nitrogenous and phosphorous matters in a large water reclamation plant in Singapore*. Mass flow and energy efficiency of municipal wastewater treatment plants. IWA Publishing, London, pp 1-19.
- Cao YS, Wah YL, Ang CM, Kandiah SR (2008) *General introduction*. Biological nitrogen removal activated sludge process in warm climates - Full-scale process investigation, scaled-down laboratory experimentation and mathematical modeling. IWA Publishing, London, pp 1-8.
- Carvalho A, Silva S, Baptista J, Malcata FX (2011) Light requirements in microalgal photobioreactors: an overview of biophotonic aspects. *Applied Microbiology and Biotechnology* 89(5):1275-1288.
- Carvalho AP, Malcata FX (2001) Transfer of Carbon Dioxide within Cultures of Microalgae: Plain Bubbling versus Hollow-Fiber Modules. *Biotechnology Progress* 17(2):265-272.
- Carvalho AP, Meireles LA, Malcata FX (2006) Microalgal Reactors: A Review of Enclosed System Designs and Performances. *Biotechnology Progress* 22(6):1490-1506.
- Casey E, Glennon B, Hamer G (1999) Review of membrane aerated biofilm reactors. *Resources, Conservation and Recycling* 27(1-2):203-215.
- Chavan A, Mukherji S (2008) Treatment of hydrocarbon-rich wastewater using oil degrading bacteria and phototrophic microorganisms in rotating biological contactor: Effect of N:P ratio. *Journal of Hazardous Materials* 154(1-3):63-72.
- Chavan A, Mukherji S (2010) Effect of co-contaminant phenol on performance of a laboratory-scale RBC with algal-bacterial biofilm treating petroleum hydrocarbon-rich wastewater. *Journal of Chemical Technology & Biotechnology* 85(6):851-859.
- Cheng L, Zhang L, Chen H, Gao C (2006) Carbon dioxide removal from air by microalgae cultured in a membrane-photobioreactor. *Separation and Purification Technology* 50(3):324-329.
- Chisti Y (2007) Biodiesel from microalgae. *Biotechnology Advances* 25(3):294-306.
- Chisti Y (2008) Biodiesel from microalgae beats bioethanol. *Trends in Biotechnology* 26(3):126-131.
- Chiu S-Y, Kao C-Y, Chen C-H, Kuan T-C, Ong S-C, Lin C-S (2008) Reduction of CO<sub>2</sub> by a high-density culture of *Chlorella* sp. in a semicontinuous photobioreactor. *Bioresource Technology* 99(9):3389-3396.
- Chiu S-Y, Tsai M-T, Kao C-Y, Ong S-C, Lin C-S (2009) The air-lift photobioreactors with flow patterning for high-density cultures of microalgae and carbon dioxide removal. *Engineering in Life Sciences* 9(3):254-260.

- Cole JJ (1982) Interactions between bacteria and algae in aquatic ecosystems. *Annual Review of Ecology and Systematics* 13:291-314.
- Comeau Y (2008) *Microbial Metabolism*. In: Henze M, van Loosdrecht MCM, Ekama GA, Brdjanovic D (eds). *Biological wastewater treatment : principles, modelling and design*. IWA Pub., London :, pp 9-32.
- Costerton JW, Lewandowski Z, Caldwell DE, Korber DR, Lappin-Scott HM (1995) Microbial Biofilms. *Annual Review of Microbiology* 49(1):711-745.
- Côté P, Bersillon J-L, Huyard A (1989) Bubble-free aeration using membranes: mass transfer analysis. *Journal of Membrane Science* 47(1-2):91-106.
- Craggs RJ, Heubeck S, Lundquist TJ, Benemann JR (2011) Algal biofuels from wastewater treatment high rate algal ponds. *Water science and technology : a journal of the International Association on Water Pollution Research* 63(4):660-5.
- de Godos I, Blanco S, García-Encina PA, Becares E, Muñoz R (2010a) Influence of flue gas sparging on the performance of high rate algae ponds treating agro-industrial wastewaters. *Journal of Hazardous Materials* 179(1-3):1049-1054.
- de Godos I, González C, Becares E, García-Encina P, Muñoz R (2009) Simultaneous nutrients and carbon removal during pretreated swine slurry degradation in a tubular biofilm photobioreactor. *Applied Microbiology and Biotechnology* 82(1):187-194.
- de Godos I, Vargas VA, Blanco S, González MCG, Soto R, García-Encina PA, Becares E, Muñoz R (2010b) A comparative evaluation of microalgae for the degradation of piggery wastewater under photosynthetic oxygenation. *Bioresource Technology* 101(14):5150-5158.
- Doan QC, Moheimani NR, Mastrangelo AJ, Lewis DM (2012) Microalgal biomass for bioethanol fermentation: Implications for hypersaline systems with an industrial focus. *Biomass and Bioenergy* 46(0):79-88.
- Duan J, Higuchi M, Krishna R, Kiyonaga T, Tsutsumi Y, Sato Y, Kubota Y, Takata M, Kitagawa S (2014) High CO<sub>2</sub>/N<sub>2</sub>/O<sub>2</sub>/CO separation in a chemically robust porous coordination polymer with low binding energy. *Chemical Science* 5(2):660-666.
- Ekama GA, Wentzel MC (2008) *Nitrogen Removal*. In: Henze M, Loosdrecht MCM, Ekama GA, Brdjanovic D (eds). *Biological wastewater treatment : principles, modelling and design*. IWA Pub., London :, pp 87-137.
- EPA (1997) *Waste Water Treatment Manuals: Primary, Secondary and Tertiary Treatment*. Environmental Protection Agency, Ireland
- Fan L-H, Zhang Y-T, Zhang L, Chen H-L (2008) Evaluation of a membrane-sparged helical tubular photobioreactor for carbon dioxide biofixation by *Chlorella vulgaris*. *Journal of Membrane Science* 325(1):336-345.
- Fan LH, Zhang YT, Cheng LH, Zhang L, Tang DS, Chen HL (2007) Optimization of Carbon Dioxide Fixation by *Chlorella vulgaris* Cultivated in a Membrane-Photobioreactor. *Chemical Engineering & Technology* 30(8):1094-1099.
- Feng Y, Li C, Zhang D (2011) Lipid production of *Chlorella vulgaris* cultured in artificial wastewater medium. *Bioresource Technology* 102(1):101-105.
- Ferreira BS, Fernandes HL, Reis A, Mateus M (1998) Microporous hollow fibres for carbon dioxide absorption: Mass transfer model fitting and the supplying of carbon dioxide to microalgal cultures. *Journal of Chemical Technology & Biotechnology* 71(1):61-70.
- Fukami K, Nishijima T, Ishida Y (1997) Stimulative and inhibitory effects of bacteria on the growth of microalgae. *Hydrobiologia* 358(1):185-191.
- Gabelman A, Hwang S-T (1999) Hollow fiber membrane contactors. *Journal of Membrane Science* 159(1-2):61-106.

- Gerardi MH (2006a) *Bacteria*. In: Gerardi MH (ed). Wastewater Bacteria. John Wiley & Sons, Inc., pp 19 - 31.
- Gerardi MH (2006b) *Bacterial Groups*. In: Gerardi MH (ed). Wastewater Bacteria. John Wiley & Sons, Inc., pp 33 - 40.
- Gerardi MH (2006c) *Bacterial Growth*. In: Gerardi MH (ed). Wastewater Bacteria. John Wiley & Sons, Inc., pp 65 - 73.
- Gerardi MH (2006d) *Microbial Ecology*. In: Gerardi MH (ed). Wastewater Bacteria. John Wiley & Sons, Inc., pp 11-18.
- Gerardi MH (2006e) *Nitrifying Bacteria*. In: Gerardi MH (ed). Wastewater Bacteria. John Wiley & Sons, Inc., pp 77 - 89.
- Gerardi MH (2006f) *Poly-P Bacteria*. In: Gerardi MH (ed). Wastewater Bacteria. John Wiley & Sons, Inc., pp 103-116.
- Ghirardi ML, Zhang L, Lee JW, Flynn T, Seibert M, Greenbaum E, Melis A (2000) Microalgae: a green source of renewable H<sub>2</sub>. *Trends in Biotechnology* 18(12):506-511.
- González-Fernández C, Molinuevo-Salces B, García-González MC (2011a) Nitrogen transformations under different conditions in open ponds by means of microalgae-bacteria consortium treating pig slurry. *Bioresource Technology* 102(2):960-966.
- González-Fernández C, Riaño-Irazábal B, Molinuevo-Salces B, Blanco S, García-González MC (2011b) Effect of operational conditions on the degradation of organic matter and development of microalgae-bacteria consortia when treating swine slurry. *Applied Microbiology and Biotechnology* 90(3):1147-1153.
- González C, Marciniak J, Villaverde S, León C, García PA, Muñoz R (2008) Efficient nutrient removal from swine manure in a tubular biofilm photo-bioreactor using algae-bacteria consortia *Water Sci Technol* 58(1):95-102.
- Gouveia L (2011) *Microalgae and Biofuels Production*. Microalgae as a feedstock for biofuels. Springer, Heidelberg ; New York, pp 2 - 20.
- Green FB, Lundquist TJ, Oswald WJ (1995) Energetics of advanced integrated wastewater pond systems. *Water Science & Technology* 31(12):9-20.
- Grobbelaar JU (2004) *Algal Nutrition - Mineral Nutrition*. In: Richmond A (ed). Handbook of Microalgal Culture. Blackwell Publishing Ltd, pp 97 - 115.
- Hamoda MF (2006) Air Pollutants Emissions from Waste Treatment and Disposal Facilities. *Journal of Environmental Science and Health, Part A* 41(1):77-85.
- Harun R, Singh M, Forde GM, Danquah MK (2010) Bioprocess engineering of microalgae to produce a variety of consumer products. *Renewable and Sustainable Energy Reviews* 14(3):1037-1047.
- Henze M, Comeau Y (2008) *Wastewater Characterization*. In: Henze M, Loosdrecht MCMv, Ekama GA, Brdjanovic D (eds). Biological wastewater treatment : principles, modelling and design. IWA Pub., London :, pp 33-52.
- Hong S-N, Holbrook RD (1999) *Nutrient (Nitrogen and Phosphorus) Removal*. In: Liu DHF, Lipták BB (eds). Environmental Engineers' Handbook. CRC Press LLC, Boca Raton, Fla. :, pp 805-818.
- Hu Q, Sommerfeld M, Jarvis E, Ghirardi M, Posewitz M, Seibert M, Darzins A (2008) Microalgal triacylglycerols as feedstocks for biofuel production: perspectives and advances. *Plant J* 54(4):621-39.
- Hwang B-K, Lee W-N, Yeon K-M, Park P-K, Lee C-H, Chang i-S, Drews A, Kraume M (2008) Correlating TMP Increases with Microbial Characteristics in the Bio-Cake on the Membrane Surface in a Membrane Bioreactor. *Environmental Science & Technology* 42(11):3963-3968.
- Illman AM, Scragg AH, Shales SW (2000) Increase in Chlorella strains calorific values when grown in low nitrogen medium. *Enzyme Microb Technol* 27(8):631-635.

- Irving T, Allen D (2011) Species and material considerations in the formation and development of microalgal biofilms. *Applied Microbiology and Biotechnology* 92(2):283-294.
- Jahn A, Griebe T, Nielsen PH (1999) Composition of *Pseudomonas putida* biofilms: Accumulation of protein in the biofilm matrix. *Biofouling* 14(1):49-57.
- Jiménez C, Cossi, amp, x, o BR, Niell FX (2003) Relationship between physicochemical variables and productivity in open ponds for the production of *Spirulina*: a predictive model of algal yield. *Aquaculture* 221(1-4):331-345.
- Johnson M, Wen Z (2009) Development of an attached microalgal growth system for biofuel production. *Applied Microbiology and Biotechnology* 85(3):525-534.
- Johnson M, Wen Z (2010) Development of an attached microalgal growth system for biofuel production. *Applied Microbiology and Biotechnology* 85(3):525-534.
- Kalontarov M, Doud DFR, Jung EE, Angenent LT, Erickson D (2014) Hollow fibre membrane arrays for CO<sub>2</sub> delivery in microalgae photobioreactors. *RSC Advances* 4(3):1460-1468.
- Kanezashi M, Yamamoto A, Yoshioka T, Tsuru T (2010) Characteristics of ammonia permeation through porous silica membranes. *AIChE Journal* 56(5):1204-1212.
- Karya NGAI, van der Steen NP, Lens PNL (2013) Photo-oxygenation to support nitrification in an algal-bacterial consortium treating artificial wastewater. *Bioresource Technology* 134(0):244-250.
- Keller J, Hartley K (2003) Greenhouse gas production in wastewater treatment: process selection is the major factor. *Water science and technology : a journal of the International Association on Water Pollution Research* 47(12):43-8.
- Kiilerich B, Utility W, Yang E (2013) Energy saving potential of mixing. *World Pumps* 2013(6):24-29.
- Kim H-Y, Yeon KM, Lee CH, Lee S, Swaminathan T (2006) Biofilm Structure and Extracellular Polymeric Substances in Low and High Dissolved Oxygen Membrane Bioreactors. *Separation Science and Technology* 41(7):1213-1230.
- Kim HW, Marcus AK, Shin JH, Rittmann BE (2011) Advanced Control for Photoautotrophic Growth and CO<sub>2</sub>-Utilization Efficiency Using a Membrane Carbonation Photobioreactor (MCPBR). *Environmental Science & Technology* 45(11):5032-5038.
- Kraume M, Drews A (2010) Membrane Bioreactors in Waste Water Treatment - Status and Trends. *Chemical Engineering & Technology* 33(8):1251-1259.
- Kumar A, Ergas S, Yuan X, Sahu A, Zhang QO, Dewulf J, Malcata FX, van Langenhove H (2010a) Enhanced CO<sub>2</sub> fixation and biofuel production via microalgae: recent developments and future directions. *Trends in Biotechnology* 28(7):371-380.
- Kumar A, Yuan X, Sahu AK, Dewulf J, Ergas SJ, Van Langenhove H (2010b) A hollow fiber membrane photo-bioreactor for CO<sub>2</sub> sequestration from combustion gas coupled with wastewater treatment: a process engineering approach. *Journal of Chemical Technology & Biotechnology* 85(3):387-394.
- Kunjapur AM, Eldridge RB (2010) Photobioreactor Design for Commercial Biofuel Production from Microalgae. *Industrial & Engineering Chemistry Research* 49(8):3516-3526.
- Lawrence JR, Korber DR, Hoyle BD, Costerton JW, Caldwell DE (1991) Optical sectioning of microbial biofilms. *J Bacteriol* 173(20):6558-67.
- Le-Clech P (2010) Membrane bioreactors and their uses in wastewater treatments. *Appl Microbiol Biotechnol* 88(6):1253-60.
- Lee Y-K (2001) Microalgal mass culture systems and methods: Their limitation and potential. *Journal of Applied Phycology* 13(4):307-315.

- Lehr F, Posten C (2009) Closed photo-bioreactors as tools for biofuel production. *Current Opinion in Biotechnology* 20(3):280-285.
- Li Y, Horsman M, Wang B, Wu N, Lan C (2008) Effects of nitrogen sources on cell growth and lipid accumulation of green alga *Neochloris oleoabundans*. *Applied Microbiology and Biotechnology* 81(4):629-636.
- Li Y, Loh K-C (2006) Activated carbon impregnated polysulfone hollow fiber membrane for cell immobilization and cometabolic biotransformation of 4-chlorophenol in the presence of phenol. *Journal of Membrane Science* 276(1-2):81-90.
- Li Y, Loh K-C (2007) Continuous phenol biodegradation at high concentrations in an immobilized-cell hollow fiber membrane bioreactor. *Journal of Applied Polymer Science* 105(4):1732-1739.
- Liang Z, Liu Y, Ge F, Xu Y, Tao N, Peng F, Wong M (2013) Efficiency assessment and pH effect in removing nitrogen and phosphorus by algae-bacteria combined system of *Chlorella vulgaris* and *Bacillus licheniformis*. *Chemosphere* 92(10):1383-1389.
- Liu C, Huang PM (2000) Kinetics of phosphate adsorption on iron oxides formed under the influence of citrate. *Canadian Journal of Soil Science* 80(3):445-454.
- Liu Z-Y, Wang G-C, Zhou B-C (2008) Effect of iron on growth and lipid accumulation in *Chlorella vulgaris*. *Bioresource Technology* 99(11):4717-4722.
- Loh K-C, Wang S-J (1998) Enhancement of biodegradation of phenol and a nongrowth substrate 4-chlorophenol by medium augmentation with conventional carbon sources. *Biodegradation* 8(5):329-338.
- Loosdrecht MCMv (2008) *Innovative Nitrogen Removal*. In: Henze M, Loosdrecht MCMv, Ekama GA, Brdjanovic D (eds). *Biological wastewater treatment : principles, modelling and design*. IWA Pub., London :, pp 139-154.
- Lv J-M, Cheng L-H, Xu X-H, Zhang L, Chen H-L (2010) Enhanced lipid production of *Chlorella vulgaris* by adjustment of cultivation conditions. *Bioresource Technology* 101(17):6797-6804.
- Markou G, Nerantzis E (2013) Microalgae for high-value compounds and biofuels production: A review with focus on cultivation under stress conditions. *Biotechnology Advances* 31(8):1532-1542.
- Mata TM, Martins AA, Caetano NS (2010) Microalgae for biodiesel production and other applications: A review. *Renewable and Sustainable Energy Reviews* 14(1):217-232.
- Memon AR, Andresen J, Habib M, Jaffar M (2014) Simulated sugar factory wastewater remediation kinetics using algal-bacterial raceway reactor promoted by Polyacrylate polyalcohol. *Bioresource Technology* 157(0):37-43.
- Metcalf, Eddy (1991) *Wastewater engineering : treatment, disposal, and reuse*, 3rd ed. / revised by George Tchobanoglous, Franklin L. Burton. edn. McGraw-Hill, New York.
- Molina-Grima E, Belarbi EH, Ación Fernández FG, Robles Medina A, Chisti Y (2003) Recovery of microalgal biomass and metabolites: process options and economics. *Biotechnology Advances* 20(7-8):491-515.
- Molina E, Fernández J, Ación FG, Chisti Y (2001) Tubular photobioreactor design for algal cultures. *Journal of Biotechnology* 92(2):113-131.
- Moller S, Pedersen AR, Poulsen LK, Arvin E, Molin S (1996) Activity and three-dimensional distribution of toluene-degrading *Pseudomonas putida* in a multispecies biofilm assessed by quantitative in situ hybridization and scanning confocal laser microscopy. *Appl Environ Microbiol* 62(12):4632-40.
- Monteith HD, Sahely HR, MacLean HL, Bagley DM (2005) A rational procedure for estimation of greenhouse-gas emissions from municipal wastewater treatment plants. *Water Environ Res* 77(4):390-403.



- Muñoz R, Alvarez MT, Muñoz A, Terrazas E, Guieysse B, Mattiasson B (2006) Sequential removal of heavy metals ions and organic pollutants using an algal-bacterial consortium. *Chemosphere* 63(6):903-911.
- Muñoz R, Guieysse B (2006) Algal-bacterial processes for the treatment of hazardous contaminants: A review. *Water Research* 40(15):2799-2815.
- Muñoz R, Guieysse B, Mattiasson B (2003a) Phenanthrene biodegradation by an algal-bacterial consortium in two-phase partitioning bioreactors. *Applied Microbiology and Biotechnology* 61(3):261-267.
- Muñoz R, Jacinto M, Guieysse B, Mattiasson B (2005a) Combined carbon and nitrogen removal from acetonitrile using algal-bacterial bioreactors. *Applied Microbiology and Biotechnology* 67(5):699-707.
- Muñoz R, Köllner C, Guieysse B (2009) Biofilm photobioreactors for the treatment of industrial wastewaters. *Journal of Hazardous Materials* 161(1):29-34.
- Muñoz R, Köllner C, Guieysse B, Mattiasson B (2003b) Salicylate biodegradation by various algal-bacterial consortia under photosynthetic oxygenation. *Biotechnology Letters* 25(22):1905-1911.
- Muñoz R, Köllner C, Guieysse B, Mattiasson B (2004) Photosynthetically oxygenated salicylate biodegradation in a continuous stirred tank photobioreactor. *Biotechnology and Bioengineering* 87(6):797-803.
- Muñoz R, Rolvering C, Guieysse B, Mattiasson B (2005b) Photosynthetically oxygenated acetonitrile biodegradation by an algal-bacterial microcosm: A pilot-scale study. *Water Sci Technol* 51(12):261-265.
- Nguyen T, Roddick F, Fan L (2012) Biofouling of Water Treatment Membranes: A Review of the Underlying Causes, Monitoring Techniques and Control Measures. *Membranes* 2(4):804-840.
- Norsker N-H, Barbosa MJ, Vermuë MH, Wijffels RH (2010) Microalgal production -- A close look at the economics. *Biotechnology Advances* 29(1):24-27.
- Ohashi A, Harada H (1994) Adhesion strength of biofilm developed in an attached-growth reactor. *Water Science and Technology* 46 29 (10-11 ):281-288.
- Olguín EJ (2012) Dual purpose microalgae-bacteria-based systems that treat wastewater and produce biodiesel and chemical products within a Biorefinery. *Biotechnology Advances* 30(5):1031-1046.
- Olivieri G, Salatino P, Marzocchella A (2014) Advances in photobioreactors for intensive microalgal production: configurations, operating strategies and applications. *Journal of Chemical Technology & Biotechnology* 89(2):178-195.
- Oswald WJ (1962) The Coming Industry of Controlled Photosynthesis. *American Journal of Public Health* 52(2):235-242.
- Oswald WJ (1991) Introduction to advanced integrated wastewater ponding systems. *Water Science & Technology* 24(5):1-7.
- Oswald WJ (2003) My sixty years in applied algology. *Journal of Applied Phycology* 15(2):99-106.
- Oswald WJ, Gotaas HB (1957) Photosynthesis in Sewage Treatment. *Transactions of the American Society of Civil Engineers* 122:73-105.
- Oswald WJ, Gotaas HB, Ludwig HF, Lynch V (1953) Algae Symbiosis in Oxidation Ponds. II. Growth Characteristics of *Chlorella pyrenoidosa* Cultured in Sewage. *Sewage and Industrial Wastes* 25:1:26-37.
- Owen WF (1982) *Energy in wastewater treatment*. : Prentice-Hall, Englewood Cliffs, N.J.
- Park JB, Craggs RJ (2011) Nutrient removal in wastewater treatment high rate algal ponds with carbon dioxide addition. *Water science and technology : a journal of the International Association on Water Pollution Research* 63(8):1758-64.

- Park JBK, Craggs RJ, Shilton AN (2011) Wastewater treatment high rate algal ponds for biofuel production. *Bioresource Technology* 102(1):35-42.
- Pedersen AR, Møller S, Molin S, Arvin E (1997) Activity of toluene-degrading *Pseudomonas putida* in the early growth phase of a biofilm for waste gas treatment. *Biotechnology and Bioengineering* 54(2):131-141.
- Pegallapati AK, Nirmalakhandan N (2013) Internally illuminated photobioreactor for algal cultivation under carbon dioxide-supplementation: Performance evaluation. *Renewable Energy* 56(0):129-135.
- Peng L, Lan CQ, Zhang Z (2013) Evolution, detrimental effects, and removal of oxygen in microalga cultures: A review. *Environmental Progress & Sustainable Energy* 32(4):982-988.
- Pinto G, Pollio A, Previtera L, Stanzione M, Temussi F (2003) Removal of low molecular weight phenols from olive oil mill wastewater using microalgae. *Biotechnology Letters* 25(19):1657-1659.
- Posadas E, Bochon S, Coca M, García-González MC, García-Encina PA, Muñoz R (2014) Microalgae-based agro-industrial wastewater treatment: a preliminary screening of biodegradability. *Journal of Applied Phycology*:1-11.
- Posadas E, Garcia-Encina PA, Soltau A, Dominguez A, Diaz I, Munoz R (2013) Carbon and nutrient removal from centrates and domestic wastewater using algal-bacterial biofilm bioreactors. *Bioresour Technol* 139:50-8.
- Posten C (2009) Design principles of photo-bioreactors for cultivation of microalgae. *Engineering in Life Sciences* 9(3):165-177.
- Pulz O, Gross W (2004) Valuable products from biotechnology of microalgae. *Applied Microbiology and Biotechnology* 65(6):635-648.
- Qiu G, Ting Y-P (2013) Osmotic membrane bioreactor for wastewater treatment and the effect of salt accumulation on system performance and microbial community dynamics. *Bioresource Technology* 150(0):287-297.
- Ras M, Lardon L, Bruno S, Bernet N, Steyer J-P (2011) Experimental study on a coupled process of production and anaerobic digestion of *Chlorella vulgaris*. *Bioresource Technology* 102(1):200-206.
- Rawat I, Ranjith Kumar R, Mutanda T, Bux F (2011) Dual role of microalgae: Phycoremediation of domestic wastewater and biomass production for sustainable biofuels production. *Applied Energy* 88(10):3411-3424.
- Reardon DJ (1995) Turning Down the Power. *Civil Engineering—ASCE* 65(8):54-56.
- Reboloso Fuentes MM, Acién Fernández GG, Sánchez Pérez JA, Guil Guerrero JL (2000) Biomass nutrient profiles of the microalga *Porphyridium cruentum*. *Food Chemistry* 70(3):345-353.
- Reuter LH (1999) *Conventional Sewage Treatment Plants*. In: Liu DHF, Lipták BB (eds). *Environmental Engineers' Handbook*. CRC Press LLC, Boca Raton, Fla. :, pp 682-690.
- Rodolfi L, Chini Zittelli G, Bassi N, Padovani G, Biondi N, Bonini G, Tredici MR (2009) Microalgae for oil: Strain selection, induction of lipid synthesis and outdoor mass cultivation in a low-cost photobioreactor. *Biotechnology and Bioengineering* 102(1):100-112.
- Roudsari F, Mehrnia M, Asadi A, Moayedi Z, Ranjbar R (2014) Effect of Microalgae/Activated Sludge Ratio on Cooperative Treatment of Anaerobic Effluent of Municipal Wastewater. *Applied Biochemistry and Biotechnology* 172(1):131-140.
- Rupprecht J (2009) From systems biology to fuel--*Chlamydomonas reinhardtii* as a model for a systems biology approach to improve biohydrogen production. *Journal of Biotechnology* 142(1):10-20.

- Safonova E, Kvitko KV, Iankevitch MI, Surgko LF, Afti IA, Reisser W (2004) Biotreatment of Industrial Wastewater by Selected Algal-Bacterial Consortia. *Engineering in Life Sciences* 4(4):347-353.
- Santiago AF, Calijuri ML, Assemany PP, Calijuri MdC, Reis AJDd (2013) Algal biomass production and wastewater treatment in high rate algal ponds receiving disinfected effluent. *Environmental Technology* 34(13-14):1877-1885.
- Scholz M (2006) *Chapter 18 - Activated sludge processes*. In: Scholz M (ed). *Wetland Systems to Control Urban Runoff*. Elsevier, Amsterdam, pp 115-129.
- Schumacher G, Blume T, Sekoulov I (2003) Bacteria reduction and nutrient removal in small wastewater treatment plants by an algal biofilm. *Water science and technology : a journal of the International Association on Water Pollution Research* 47(11):195-202.
- Scott SA, Davey MP, Dennis JS, Horst I, Howe CJ, Lea-Smith DJ, Smith AG (2010) Biodiesel from algae: challenges and prospects. *Curr Opin Biotechnol*.
- Semmens M (2008) Alternative MBR configurations: using membranes for gas transfer. *Desalination* 231(1-3):236-242.
- Semmens MJ, Foster DM, Cussler EL (1990) Ammonia removal from water using microporous hollow fibers. *Journal of Membrane Science* 51(1-2):127-140.
- Shieh WK, Nguyen VT (1999a) *Activated-Sludge Processes*. In: Liu DHF, Lipták BB (eds). *Environmental Engineers' Handbook*. CRC Press LLC, Boca Raton, Fla. :, pp 705-715.
- Shieh WK, Nguyen VT (1999b) *Wastewater Microbiology*. In: Liu DHF, Lipták BB (eds). *Environmental Engineers' Handbook*. CRC Press LLC, Boca Raton, Fla. :, pp 690-696.
- Sialve B, Bernet N, Bernard O (2009) Anaerobic digestion of microalgae as a necessary step to make microalgal biodiesel sustainable. *Biotechnology Advances* 27(4):409-416.
- Spolaore P, Joannis-Cassan C, Duran E, Isambert A (2006) Commercial applications of microalgae. *Journal of Bioscience and Bioengineering* 101(2):87-96.
- Stenstrom MK, Rosso D (2008) *Aeration and Mixing*. In: Henze M, Loosdrecht MCMv, Ekama GA, Brdjanovic D (eds). *Biological wastewater treatment : principles, modelling and design*. IWA Pub., London :, pp 245-272.
- Su Y, Mennerich A, Urban B (2011) Municipal wastewater treatment and biomass accumulation with a wastewater-born and settleable algal-bacterial culture. *Water Res* 45(11):3351-8.
- Subashchandrabose SR, Ramakrishnan B, Megharaj M, Venkateswarlu K, Naidu R (2011) Consortia of cyanobacteria/microalgae and bacteria: Biotechnological potential. *Biotechnology Advances* 29(6):896-907.
- Sutherland D, Howard-Williams C, Turnbull M, Broady P, Craggs R (2014a) Seasonal variation in light utilisation, biomass production and nutrient removal by wastewater microalgae in a full-scale high-rate algal pond. *Journal of Applied Phycology* 26(3):1317-1329.
- Sutherland DL, Turnbull MH, Craggs RJ (2014b) Increased pond depth improves algal productivity and nutrient removal in wastewater treatment high rate algal ponds. *Water Research* 53(0):271-281.
- Tamer E, Amin MA, Ossama ET, Bo M, Benoit G (2006) Biological treatment of industrial wastes in a photobioreactor. *Water Sci Technol* 53(11):117-125.
- Tan X, Tan SP, Teo WK, Li K (2006) Polyvinylidene fluoride (PVDF) hollow fibre membranes for ammonia removal from water. *Journal of Membrane Science* 271(1-2):59-68.

- Tang X, He LY, Tao XQ, Dang Z, Guo CL, Lu GN, Yi XY (2010) Construction of an artificial microalgal-bacterial consortium that efficiently degrades crude oil. *Journal of Hazardous Materials* 181(1-3):1158-1162.
- Tolker-Nielsen T, Molin S (2000) Spatial Organization of Microbial Biofilm Communities. *Microb Ecol* 40(2):75-84.
- Tomaselli L (2004) *The Microalgal Cell*. In: Richmond A (ed). *Handbook of Microalgal Culture*. Blackwell Publishing Ltd, pp 1-19.
- Tresse O, Lescob S, Rho D (2003) Dynamics of living and dead bacterial cells within a mixed-species biofilm during toluene degradation in a biotrickling filter. *Journal of Applied Microbiology* 94(5):849-854.
- Valdés FJ, Hernández MR, Catalá L, Marquilla A (2012) Estimation of CO<sub>2</sub> stripping/CO<sub>2</sub> microalgae consumption ratios in a bubble column photobioreactor using the analysis of the pH profiles. Application to *Nannochloropsis oculata* microalgae culture. *Bioresource Technology* 119:1-6.
- Wang B, Lan CQ, Horsman M (2012) Closed photobioreactors for production of microalgal biomasses. *Biotechnology Advances* 30(4):904-912.
- Wang L, Min M, Li Y, Chen P, Chen Y, Liu Y, Wang Y, Ruan R (2009) Cultivation of Green Algae *Chlorella* sp. in Different Wastewaters from Municipal Wastewater Treatment Plant. *Applied Biochemistry and Biotechnology* 162(4):1174-86.
- Wentzel MC, Comeau Y, Ekama GA, Loosdrecht MCMv, Brdjanovic D (2008) *Enhanced Biological Phosphorus Removal*. In: Henze M, Loosdrecht MCMv, Ekama GA, Brdjanovic D (eds). *Biological wastewater treatment : principles, modelling and design*. IWA Pub., London :, pp 155-220.
- Wiesmann U, Choi IS, Dombrowski E-M (2007) *Wastewater Characterization and Regulations*. *Fundamentals of biological wastewater treatment*. Wiley-VCH, Weinheim, pp 25 - 42.
- Yamaguchi K (1996) Recent advances in microalgal bioscience in Japan, with special reference to utilization of biomass and metabolites: a review. *Journal of Applied Phycology* 8(6):487-502.
- Yang M-C, Cussler EL (1986) Designing hollow-fiber contactors. *AIChE Journal* 32(11):1910-1916.
- Yen H-W, Hu IC, Chen C-Y, Ho S-H, Lee D-J, Chang J-S (2013) Microalgae-based biorefinery – From biofuels to natural products. *Bioresource Technology* 135(0):166-174.
- Yoo C, Jun SY, Lee JY, Ahn CY, Oh HM (2010) Selection of microalgae for lipid production under high levels carbon dioxide. *Bioresource Technology* 101:S71-S74.
- Zhang K, Kurano N, Miyachi S (2002) Optimized aeration by carbon dioxide gas for microalgal production and mass transfer characterization in a vertical flat-plate photobioreactor. *Bioprocess and Biosystems Engineering* 25(2):97-101.
- Zhong W, Li Y, Sun K, Jin J, Li X, Zhang F, Chen J (2011) Aerobic degradation of methyl tert-butyl ether in a closed symbiotic system containing a mixed culture of *Chlorella ellipsoidea* and *Methylibium petroleiphilum* PM1. *Journal of Hazardous Materials* 185(2-3):1249-1255.

## **LIST OF CONFERENCE PRESENTATIONS**

1. Loh Kai-Chee, Vu T.K. Linh, Symbiotic hollow fiber membrane photobioreactor for microalgae growth & activated sludge wastewater treatment, GSK Symposium 2011.
2. Loh Kai-Chee and Vu T.K. Linh, Symbiotic hollow fiber membrane photobioreactor for microalgae growth and activated sludge wastewater treatment. 14<sup>th</sup> Asia Pacific Confederation of Chemical Engineering Congress (APCCChE 2012).
3. Vu T.K. Linh, Loh Kai-Chee, Symbiotic hollow fiber membrane photobioreactor for microalgae growth and bacterial wastewater treatment, AIChE 2012 – 2012 AIChE Annual Meeting, Conference Proceedings.
4. Vu T.K. Linh, Loh Kai-Chee, Development of symbiotic hollow fiber membrane photobioreactor for microalgal growth and bacterial wastewater treatment, World Biotechnology Congress 2013.
5. Vu T.K. Linh, Prashant Praveen, Loh Kai-Chee, Submerged hollow fiber membrane bioreactor for symbiotic microalgal growth and bacterial wastewater treatment, AIChE 2013 – 2013 AIChE Annual Meeting, Conference Proceedings.

## **LIST OF PUBLICATIONS**

1. Vu T.K. Linh, Loh Kai-Chee, Symbiotic hollow fiber membrane photobioreactor for microalgae growth and bacterial wastewater treatment (In preparation).
2. Vu T.K. Linh, Loh Kai-Chee, Submerged hollow fiber membrane photobioreactor for retrofitting existing activated sludge tank (In preparation).
3. Vu T.K. Linh, Loh Kai-Chee, Coupling the submerged hollow fiber membrane photobioreactor to activated sludge wastewater treatment process (In preparation).